LOCALLY-SIMILAR SOLUTIONS OF SECOND-ORDER BOUNDARY-LAYER EQUATIONS

By
SRICHAND RAISINGHANI

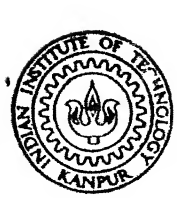

DEPARTMENT OF AERONAUTICAL ENGINEERING
INDIAN INSTITUTE OF TECHNOLOGY KANPUR

JULY 1973

LOCALLY-SIMILAR SOLUTIONS OF SECOND-ORDER BOUNDARY-LAYER EQUATIONS

A Thesis Submitted
In Partial Fulfilment of the Requirements
for the Degree of
DOCTOR OF PHILOSOPHY

By
SRICHAND RAISINGHANI

to the

DEPARTMENT OF AERONAUTICAL ENGINEERING
INDIAN INSTITUTE OF TECHNOLOGY KANPUR

JULY 1973

Dedicated to

the departed soul of my

Dear Mother

CERTIFICATE

This is to certify that the present work LOCALLY-SIMILAR SOLUTIONS OF SECOND-ORDER BOUNDARY-LAYER EQUATIONS has been carried out under my supervision and has not been submitted elsewhere for the award of a degree.

Noor Afzal

(Noor Afzal)
Assistant Professor
Department of Aeronautical Engineering
Indian Institute of Technology
Kanpur-16, India

ACKNOWLEDGEMENTS

It has been my privilege to work under the supervision of Dr. Noor Afzal, with whom my relations have been mainly personal and not mere professional contacts. This thesis is an out come of his unlimited efforts and untiring interest. I take this opportunity to thank him with gratitude for his manifold help at all stages of this work.

I wish to place on record my gratefulness to Dr. M.M. Oberai who has generously given his valuable time for some fruitful discussions, leading to several critical but constructive suggestions.

It is a pleasure to thank my venerable teachers Drs. P.N. Murthy, N.C. Nigam and A.C. Jain for their encouragement and concern about the author's welfare at all times.

I am ever grateful to my father who has suffered a lot to educate me upto this level and also to my mother who alas! is not alive to see this day. My heartiest and affectionate gratitude to our family friend Dr. L.C. Kakkar who has always been a source of inspiration to me.

The cooperation of the computer centre staff, in particular that of Messers K.S. Singh and Pawan Kumar, is highly appreciated.

Finally, I would like to express my sincere and heartfelt thanks to my wife, Kavita, who has shared with me the ecstacies and agonies of writing a Ph.D. dissertation.

Srichand Raisinghani

TABLE OF CONTENTS

LIST OF TABLES

LIST OF FIGURES

NOMENCLATURE

a, the nose radius of a blunted wedge;

a_m, coefficients of the power series ($m = 0$-4) for the displacement speed on a blunted wedge, defined by (4.30);

A_m multiplicative constants in front of the eigenvalue terms in the first-order asymptotic series for the skin friction;

b_m, c_m, d_m, quantities defined by (4.41);

B_i, quantities defined by (3.9) and (3.26) for $i = l,t,d,v,H$;

B_m, the multiplicative constants in front of the eigenvalue terms in the second-order asymptotic series for the skin friction;

B_d^*, B_l^*, asymptotic form of B_d and B_l for a blunted wedge, defined by (5.65) and (5.57) respectively;

$B_{d_m}^*, B_{l_m}^*$, coefficients of the power series B_d^* and B_l^*;

$B_1(\Psi_1)$, the Bernoulli function defined as $= P_1 + (U_1^2 + V_1^2)/2$;

C_f, skin friction coefficient;

$\hat{C}_f$, C_f after Euler transformation;

C_h, $\overline{C}_h$, heat transfer coefficient for self-similar flows (with dissipation) defined by (3.42) and (3.60) for liquids and gases respectively;

C_q heat transfer coefficient for a blunted wedge, defined by (4.73);

$\hat{C}_q$ C_q after Euler transformation;

e, thermal expansion parameter defined as $(\partial \log \rho / \partial \log T)_p$;

e_1, quantity defined by (4.81);

E, Eckert number defined by (3.25);

E_m, Quantities defined by (4.33);

f, F, the first and the second-order modified stream functions defined by (3.3) and (3.7) respectively;

f_m, F_m, coefficient functions of the power series for f and F;

$\bar{f}_m, \bar{F}_m$, coefficient functions of the asymptotic series ($\sigma \to \infty$) for f and F;

$F_m^{*(i)}$, coefficient functions of the power series for the second-order skin friction contribution: i = l, for longitudinal curvature and i = d, for displacement speed;

g, G, the first and the second-order modified temperatures defined by (3.20) and (3.21) respectively;

g_1, G_1, functions governing heat transfer in liquids due to the prescribed wall temperature (Chapter 3);

$\bar{g}_1, \bar{G}_1$, functions defined for gases, corresponding to g_1, and G_1;

g_m, G_m, coefficient functions of power series for g and G for nonsimilar flows (Chapter 4);

$G_m^{*(i)}$, coefficient functions of the power series for the second-order heat transfer contribution: i = l,d;

h, enthalpy of the fluid;

h_1, h_2, the first and second-order enthalpy in the inner flow;

$H_1(\Psi)$, stagnation enthalpy function defined by $T_1 + (U_1^2 + V_1^2)/2$;

H_1, H_2, the first and second-order enthalpy in outer flow;

j, a number defined as zero for two-dimensional flow and unity for axisymmetric flow;

k, thermal conductivity of fluid;

K, the longitudinal curvature of the body;

L, operator defined by (5.19);

L_1, L_2, L_3, L_4, operators defined by (5.59), (5.60), (5.61) and (5.62) respectively;

L^*, operator defined by (4.84);

L^+, operator defined by (5.12);

$M_n(\eta)$, coefficient functions of the asymptotic series for F;

n, coordinate normal to the body;

N, stretched normal coordinate defined as $nR^{1/2}$;

$N_n(\eta)$, eigenfunctions of the first-order velocity boundary-layer equation;

p, pressure of fluid (Chapter 2 and 3); a number denoting the location of singularity of the series solution (Chapter 4);

p_1, p_2, the first and second-order pressures in inner flow;

P_1, P_2, the first and second-order pressures in outer flow;

$P_n(\eta)$, eigenfunctions of the second-order velocity boundary-layer equation;

Pr, Prandtl number of the fluid defined as $= \mu C_p/k$;

q_w, heat transfer at the wall

q_1, q_2, the first and second-order heat transfer coefficients;

$\hat{q}_1, \hat{q}_2$, q_1 and q_2 after Euler transformations;

$Q_n(\eta)$, coefficient functions of the asymptotic series for F;

r radius of the body in axisymmetric flow;

r_1, $\bar{r}_1$, the first-order recovery factor for liquids and gases respectively;

r_2, $\bar{r}_2$, the second-order recovery factor for liquids and gases respectively;

r_f, total recovery factor

R, the characteristic Reynolds number of the flow;

$\bar{R}$, the gas constant;

$R_n(\eta)$, coefficients functions of the asymptotic series for F;

s, coordinate along the body;

S_n, partial sum of n terms of a series;

$S_{mn}(\eta)$, coefficient functions of the asymptotic series for F;

t, temperature of the fluid;

t_1, t_2, the first and second-order temperature in inner flow;

T_1, T_2, the first and second-order temperature in outer flow;

T_r, recovery temperature;

T_w, wall temperature;

$\underset{\sim}{U}$, velocity vector with components u and v in s and n directions respectively;

u_1, u_2, the first and second-order velocities in s-direction in inner flow;

U_1, U_2, the first and second order velocities in s-direction in outer flow;

$U_1(s,0)$, the first-order outer velocity at the wall;

$U_2(s,0)$, the second-order outer velocity (displacement speed) at the wall;

v_1, v_2, the first and second-order velocity in n-direction in the inner flow;

$V_2(s,0)$, second-order outer velocity in n-direction at the wall;

$\underset{\sim}{x}$, distance vector;

x, the real part of Z (Cf. Figure 4.1.);

y, the imaginary part of Z (Cf. Figure 4.1);

z, modified streamwise variable defined as $= \xi^2/(1+\xi^2)$, used in Euler transformation;

Z, complex variable after conformal mapping (Cf.Figure 4.1);

Greek Symbols:

α, defined as $\lim_{\eta \to \infty} (\eta - f)$;

α_m, defined as $\alpha_0 = \lim_{\eta \to \infty} (\eta - f_0)$ and $\alpha_m = \lim_{\eta \to \infty} (-f_m)$ for $m \geq 1$;

β, the Falkner-Skan pressure gradient parameter;

β_m, the coefficients in the expansion of the principal velocity function;

γ_m, eigenvalues for the second-order momentum transfer problem;

δ, δ^*, the first-order displacement thickness;

δ_m^*, the coefficients of the power series for δ^*;

Δ, Δ^*, the second-order displacement thickness;

$\Delta_{1_m}^*, \Delta_{d_m}^*$, the coefficients of the power series for Δ^*;

ζ, complex variable before conformal mapping (cf. Figure 4.1);

η, boundary-layer variable defined as $= U_1 r^j N/\sqrt{(2\sigma)}$

θ, angle between axis of axisymmetric body and the tangent to meridian curve at any point (cf. Figure 2.1);

λ_n, eigenvalues for the first-order momentum transfer problem;

Λ, wall temperature parameter;

Λ_i, parameters due to longitudinal curvature, transverse curvature and displacement speed respectively for $i = l,t,d$;

Λ_{B_i}, principal functions arising in the second-order problems, defined by (3.10) and (3.24);

μ, viscosity of the fluid;

ν, kinematic viscosity defined as $=\mu/\rho$;

ξ, the imaginary part of ζ (cf. Figure 4.1);

ρ, density of the fluid;

σ, boundary-layer variable defined as $= \int_0^\infty U_1 r^{2j}\, ds$;

τ_w, skin friction at the wall;

τ_1, τ_2, the first and the second-order contributions to the skin friction coefficient;

$\hat{\tau}_1, \hat{\tau}_2$, τ_1 and τ_2 after Euler transformation;

ϕ, real velocity potential for inviscid flow past a blunted wedge;

Φ, complex flow potential for flow past a blunted wedge;

χ, the real part of ζ (cf. Figure 4.1);

Ψ, stream function of the flow;

ψ_1, ψ_2 the first and second-order stream functions in the inner (boundary-layer) flow;

Ψ_1, Ψ_2, the first and the second-order stream functions in outer flow;

Superscripts:

$\hat{}$, Eulerized form of a series;

$'$, differentiation with respect to η;

d, displacement speed;

H, enthalpy gradient;

l, longitudinal curvature;

t, transverse curvature;

v, external vorticity;

Subscripts:

n, partial derivative with respect to n (Chapter 2); denotes number = 1,2,...(Chapters 4 and 5);

N, partial derivative with respect to N;

m, denotes number = 0,1,2,3,...(Chapters 4 and 5);

s, partial derivative with respect to s;

$\bar{\sigma}$, partial derivative with respect to $\bar{\sigma}$;

∞, free stream (Chapter 2); far downstream i.e. $s = \bar{\sigma} = \infty$ (Chapters 4 and 5).

LOCALLY-SIMILAR SOLUTIONS OF SECOND-ORDER BOUNDARY-LAYER EQUATIONS

A Thesis Submitted
In Partial Fulfilment of the Requirements
For the Degree of
DOCTOR OF PHILOSOPHY

by

Srichand Raisinghani

to the

Department of Aeronautical Engineering
Indian Institute of Technology, Kanpur

SYNOPSIS

The present investigation deals with the study of the second-order laminar boundary-layer equations. The three aspects of the problem studied are: (i) general self-similar solutions including dissipation, (ii) locally-similar solutions near a stagnation point using Görtler method with an application to a blunted wedge and (iii) locally-similar solutions valid at large distances in the downstream direction with an application to a blunted wedge.

In the first problem, we investigate a general structure of the self-similarity for the second-order boundary-layer equations with dissipation. The second-order boundary-layer equations associated with longitudinal curvature, transverse curvature, displacement speed, external vorticity and enthalpy gradient are obtained from the Navier-Stokes equations by using the method of matched asymptotic expansions. As regards the thermal boundary condition on the wall we study both cases:

that of the prescribed wall temperature and of the insulated wall. For the latter case, the classical concept of the recovery factor is extended to the second-order flows. The self-similar governing equations are integrated numerically and results are critically discussed; in particular, the present work explains the mathematical as well as physical aspects of the singularities observed in the second-order boundary-layer equations (See Afzal and Oberai 1972, Werle and Davis 1970). In the formulation of the thermal problem, the thermal expansion parameter [defined as $(\partial \log \rho / \partial \log T)_p$, where ρ is the density, T is the temperature and p is the pressure] is negligibly small and hence the compressibility term is neglected. This is valid for most of the liquids. However, for the flow of perfect gases, the magnitude of the thermal expansion parameter is unity and thus the compressibility term is to be retained. For such cases, a general formulation of the second-order boundary-layer equations is given by Van Dyke (1962). Self-similar solutions to Van Dyke's equations are also obtained.

Once the general structure of the self-similar solutions is understood, the next logical step is to develop nonsimilar solutions. The second problem deals with locally-similar solutions for a uniform flow past two-dimensional bodies where only displacement and longitudinal curvature effects are present. The method is illustrated by solving the problem of a blunted

wedge [if ($\beta_\infty \pi$) denotes the wedge angle then parabola and flat plate normal to flow direction are special cases of the blunted wedge with $\beta_\infty = 0$ and 1 respectively]. The displacement problem is global in the sense that it alone requires the determination of the outer flow due to displacement. The perturbed Euler equation is solved and the displacement speed, $U_2(\sigma, 0)$, is obtained as a function of streamwise coordinate, σ. First five terms for the second-order skin friction and heat transfer in a Görtler series expansion in σ are calculated. The convergence of the series is poor for large σ. The region of validity is extended in the downstream direction by Eulerization of the series. Non-linear Shanks transformation has also been employed, where necessary, for further accelerating the convergence. It is found that the Eulerized results for the skin friction and heat transfer give accurate results (within 2 percent) even as $\sigma \to \infty$. Further, a comparison of the present results for the special case of a parabola, with the exact solutions of the Navier-Stokes equations of Davis (1972), Dennis and Walsh (1971) and Botta, Dijkstra and Veldman (1972) show a good agreement (within one percent) upto Reynolds number as low as one thousand.

The series solutions of the kind mentioned above have, in general, a restricted region of validity in downstream direction and, therefore, it seems desirable to have alternate solutions valid for large σ; this forms the subject matter of the third problem. Solutions are constructed for the second-order boundary-layer equations for $\sigma \to \infty$ by expanding the variables

in terms of its eigenfunctions with certain unspecified multiplicative coefficients, to be determined from the prescribed initial conditions. The eigenvalues and eigenfunctions for various second-order effects are obtained by solving the associated homogenous problems, the governing equations of which have a form similar to the well-known Sturm-Liouville equation. For the first-order boundary-layer equations, such studies have been made by Libby and his coworkers (refer Libby 1970). The solutions for the second-order effects are displayed graphically and discussed for a variety of flow situations. The results provide a further insight into the singularities of the second-order solutions. The results of the first problem explain the location of isolated singularities whereas those of the last problem show two distinct domains of stable and unstable solutions separated by the first critical value (corresponding to the above mentioned singularities for various second-order effects) of the parameter. Thus, it is shown that if the second-order parameters assume a value less than the critical value, any departure from strict similarity grows in the downstream direction and as such the flow is, in some sense, unstable. The application of the above procedure is illustrated by considering a uniform flow past a blunted wedge. The initial condition is prescribed in terms of the Eulerized series solution obtained earlier (second problem). In addition to eigenfunctions, we include terms due to variation of the second-order parameters with σ. The multiplicative coefficient of the first eigenfunction

is determined for each of the second-order effects, by joining the present series ($\sigma \to \infty$) with the Eulerized Görtler series. The resulting asymptotic solution for large σ, in conjunction with the Eulerized Görtler series may be used to assess the accuracy of the corresponding results obtained by numerical or approximate methods, where the error bounds are unknown or uncertain.

CHAPTER 1

INTRODUCTION

Recently a lot of interest has been shown in the so-called higher order approximations of the boundary-layer theory (specially the second-order). There are various reasons for undertaking such studies. For example, the leading term in the asymptotic expansion of the Navier-Stokes equations for large Reynolds number represents the classical boundary-layer equations of Prandtl. It is well-known that the Navier-Stokes equations are elliptic whereas the classical boundary-layer equations are parabolic and thereby do not permit the upstream influence. It is of interest to study how the higher order terms in an asymptotic expansion reassert the elliptic nature of the Navier-Stokes equations, suppressed in the classical boundary-layer equations. The practical utility of such higher order corrections lies in the fact that they are found to give good results even under distinctly nonasymptotic situations; Lagerstrom and Cole (1955) have shown that the second approximation in some cases may predict correct skin friction upto Reynolds number as low as ten.

There is another motivation for studying the higher order approximations. Prandtl's boundary-layer theory does not account for what Rott and Lenard (1959) call the secondary effects. Physically these effects can arise due to longitudinal

curvature, transverse curvature, displacement speed, external vorticity, external enthalpy gradient, velocity slip and temperature jump. These effects are of order $R^{-1/2}$ as compared to the Prandtl's boundary-layer and become significant at moderately large values of Reynolds number.

Van Dyke (1962) gave a systematic formulation of the scheme for calculating the higher order corrections to the classical boundary-layer (first-order). The technique used is that of matched asymptotic expansions developed by Kaplun, Lagerstrom and their colleagues. This method divides the flow into inner and outer regions which are to be matched in an overlapping domain. An interesting feature of perturbation technique is that the resulting second-order equations are linear and, thus, the analysis can be further simplified by subdividing them into various simpler problems, each having a clear physical interpretation.

The theory so formulated by Van Dyke (1962) has been studied by various authors and an excellent review has been given by Van Dyke (1969) and as such will not be repeated here. Among the articles published thereafter, the following three are most relevant for the present study: Afzal (1969), Werle and Davis (1970) and Afzal and Oberai (1972). These authors have proposed a more general form of the self-similar solutions for the second-order equations of Van Dyke by identifying three new parameters, one each for the longitudinal curvature, transverse

curvature and displacement speed. Werle and Davis(1969) studied the problem of momentum transfer while Afzal (1969) and Afzal and Oberai (1972), have also included the study of the heat transfer but without the viscous dissipation terms. These authors reported that for some critical values of the second-order parameters, the second-order solutions show several singularities (infinite discontinuities), but the general pattern of the singularities was not investigated. The present work (Chapter 3) elaborates the mathematical as well as physical aspects of such singularities. It is shown that the singularities occur whenever the parameters take the value equal to the eigenvalue for the corresponding homogeneous problem.

The problem of heat transfer from two-dimensional and axisymmetric geometries has considerable practical interest. Afzal and Oberai (1972) in their study of heat transfer have neglected the viscous dissipation. However, there are situations where the dissipation terms may not be negligible e.g. the case where the product of the Prandtl number σ and Eckert number E is of the order unity i.e. $\sigma E \sim O(1)$. One such situation arises with liquids of moderately large Prandtl number (of the order of 50 or so). The formulation of Van Dyke (1962) for the thermal problem is applicable to perfect gases as the formulation takes care of the equation of state, i.e. $P = \rho \bar{R} T$ where P is the pressure, ρ the density, $\bar{R}$ the gas constant and T the temperature. Thus, for the flow of liquids, a new formulation is needed and is described in Chapter 2.

One of the problems studied in the present work deals with the second-order effects on heat transfer including dissipation for both liquids (employing the formulation of Chapter 2) and gases with constant density (using the formulation of Van Dyke). As regards the thermal boundary condition on the wall we study both cases: that of the prescribed (arbitrary) wall temperature and of the adiabatic wall (no heat transfer at the wall). For the latter case, the classical concept of the recovery factor is extended to the second-order flows. A general self-similar analysis of the heat transfer with dissipation for both liquids and gases is presented in Chapter 3. The equations so obtained for various second-order effects are integrated numerically for various values of parameters by Runge-Kutta-Gill method with a step size $\Delta\eta = 0.5$ on IBM-7044 Computer at IIT Kanpur. The results are displayed graphically and a critical estimate of contributions due to various second-order effects, attributed to longitudinal curvature, transverse curvature, displacement speed, external vorticity and enthalpy gradient, is presented.

Once the general structure of self-similarity for the second-order boundary-layer equations has been understood, the next logical step is to develop the methods for studying the nonsimilar solutions. To deal with nonsimilar flows, various methods are available in literature, e.g. numerical techniques (like finite difference, finite elements etc.), momentum

integral methods and series solutions using some sort of local similarity. The numerical methods like finite difference employed for studying the full partial differential equations are expensive and need special experience. Further, in a given problem a fresh calculation is needed for each set of data so that the effects of the parameters on the solution are not obvious. The momentum integral methods are approximate methods and, in general, it is difficult to estimate the accuracy. The methods for studying the locally-similar flows (starting from the stagnation point or leading edge) have been constructed by Blassius (1908), Görtler (1957) and Meksyn (1961). The technique of Meksyn was further developed by Merk (1959) and Bush (1964) and will be cited as MMB method. It is well-known that the Blassius method suffers from the disadvantage of poor convergence of the series for a slender body shape (cf.e.g. Schlichting 1968). The Görtler and the MMB methods are attempts to overcome the above mentioned drawback of the Blassius method. In the Görtler and MMB methods, the leading term (governed by the well-known Falkner-Skan equation) satisfies the outer boundary conditions exactly while the other terms of the locally-similar expansion give corrections that arise from the inner part of the boundary-layer. The difference in the Görtler and the MMB methods lies in the choice of the expansion parameter. In the Görtler method, the expansion parameter is

$$\sigma = \int_0^s U_1(s,o)\, ds$$

while in the MMB method, it is $d\beta/d\chi$ where

$$\beta = 2d \ln U_1/d \ln \sigma \quad \text{and} \quad \chi = \ln \sqrt{\sigma}$$

In the MMB method, the numerical solution involves terms like $\partial f_r/\partial\beta$, $\partial^2 f_r/\partial\beta\partial\chi$ for $r = 0,1,2...$(here f_o is the similar solution). Thus, the calculations tend to be tedius and laborious. Considering all the aforementioned methods, it seems that a compromise between the accuracy and the computational labour involved is achieved by Görtler type series solution and is used here for the study of the nonsimilar flows considered next.

In the present work we apply the above method to study the locally similar solutions of uniform flow past two-dimensional bodies. In such flows, the second-order effects are those of longitudinal curvature and displacement. Both momentum and heat transfer are studied. Using the Görtler method, solutions are obtained by expanding the flow variables in terms of the streamwise coordinate, σ. It seems desirable that the solutions for the general case be obtained by constructing the universal functions which when multiplied by the appropriate parameters of a given problem, yield the required results. However, it was observed that such a procedure leads to unmanageable number of equations and, therefore, no attempt has been made to tabulate the universal functions. Instead, the procedure is fully illustrated for a particular problem, namely flow past a blunted wedge.

We assume a steady laminar flow, at moderately large Reynolds number, past a semi-infinite, symmetric blunted wedge (shown in Figure 4.1) with constant wall temperature. If $(\beta_\infty \pi)$ be the included angle of the blunted wedge, two well-known special cases of the blunted wedge are parabola ($\beta_\infty = 0$) and flat plate normal to flow direction ($\beta_\infty = 1$). For a blunted wedge, the first-order momentum transfer has been studied by Chen, Libby, Rott and Van Dyke (1969) while the corresponding heat transfer is studied by Chen (1970). The second-order effects for a parabola ($\beta_\infty = 0$) have been studied by Van Dyke (1964a) by estimating the leading term in the Blassius series expansion and as such the second-order contributions are evaluated at the stagnation point only.

Of the two second-order effects, that due to the longitudinal curvature is a local effect as it depends only on the first-order boundary-layer quantities while the displacement effect is global in the sense that it requires the evaluation of the outer velocity, $U_2(s,o)$ and thus, represents the elliptic nature of the original Navier-Stokes equations. In the present work, we obtain the required displacement speed, $U_2(s,o)$, by solving the perturbed Euler equation with appropriate boundary conditions at far upstream and on the body surface. However, there is an alternate procedure to find the correction in the outer flow due to displacement thickness. The Euler equation is solved for a fictitious body with appropriate boundary conditions. The profile of the fictitious body is obtained by

a suitable fit to the original body plus its displacement thickness (cf. e.g. Davis and Flugge-Lotz 1964).

Once the expressions for displacement speed and longitudinal curvature are known, we obtain the governing equations for the first five terms of a series in σ, for both skin friction and heat transfer. These equations are integrated numerically for various values of wedge angles. However, the convergence of the series is poor for large σ. This happens, often, due to the presence of a singularity in the complex-plane and as such the radius of convergence is limited due to a mathematical singularity rather than a physical one. In such cases, it is possible to enlarge the radius of convergence by either removing the singularity or pushing it farther downstream. One of the most powerful techniques for such purposes is Eulerization which is employed when the location of the singularities is either known or can be guessed. Further, if there is only one singularity and its location is known, the Eulerization extends the radius of convergence to infinity. We have found the location of the singularity for our case so that the power series of skin friction and heat transfer is Eulerized to extend the validity range farther downstream. It is sometimes possible to further accelerate the convergence of a series by either applying the Shanks non-linear transformation or using extrapolation. These have been employed, where necessary. It is found that the Eulerization, combined with extrapolation, gives accurate results (within two percent) for the skin friction and

heat transfer even as $\sigma' \to \infty$. Further, a comparison of the present results for the special case of a parabola ($\beta_\infty = 0$), with the exact solutions of the Navier-Stokes equations of Davis (1972), Dennis and Walsh (1971) and Botta, Dijkstra and Veldman (1972). shows a good agreement (within one percent) upto Reynolds number as low as one thousand.

The series solutions of the kind mentioned above have, in general, a restricted region of validity in the downstream direction and, therefore, it seems desirable to have alternate solutions valid for large σ'. This forms the subject matter of Chapter 5. We consider boundary-layer flows which are nearly similar, i.e. such that they are nearly described by solutions with one independent variable η. The limiting similar solutions corresponding to the prescribed pressure gradient parameter and second-order parameters are assumed to be known for $\sigma' \to \infty$. Corrections are sought in terms of the inverse powers of σ' so as to extend the validity range of the solutions in the upstream direction. Alternately, such a problem may be posed as an initial value problem: an initial profile deviating slightly from the similar profile is prescribed at a given streamwise station, σ'_i and we wish to know how the similar solution is approached as $\sigma' \to \infty$. Thus, we wish to confirm, in a mathematical sense, our intuitive expectation that the deviations of the initial profile from similarity will decay with increasing streamwise distance.

As already mentioned, various numerical and momentum integral methods are available to deal with nonsimilar boundary-layer flows and may be used to obtain boundary-layer developement downstream of a specified initial profile. However, we prefer an analytical method to formulate the problem outlined in the preceding paragraph. This method avoids the complexity of the numerical methods and is more accurate than the momentum integral methods. According to the method employed here, the variables are expanded in terms of a complete set of eigenfunctions multiplied by unspecified coefficients: these coefficients are to be determined from the initial condition. Although exact in principal, the method yields approximate solutions due to truncation of the series after a few terms. Such an approach has been used by Libby and Fox (1963) and Chen and Libby (1968) for the first-order boundary-layer flows. Further, Libby (1970) has given a review of the method (subsequently referred as Libby method) and its applications to a variety of problems.

Following Libby method, the second-order nonsimilar boundary-layer solutions for the momentum transfer problem are constructed for large values of the streamwise coordinate, σ'. An initial profile (upto second-order) deviating slightly from the limiting similar profile ($\sigma' \to \infty$) is assumed to be known at a given station σ'_i. The solutions are linearized about the limiting similar solution and successive nonsimilar correction terms are obtained. The analysis leads to eigenvalue problem, the governing equations of which have a form similar to the

well-known Sturn-Liouville equation and, therefore, it is possible to predict, in certain cases, that the eigenvalues are real and discrete; in particular, for Falkner-Skan flows, the eigenvalues are known to be real and discrete for the upper branch solutions in the usual range of β, i.e. $-.1988... < \beta \leq 2$ (see Chen and Libby 1968). The solutions for the second-order effects associated with the longitudinal curvature, transverse curvature, displacement and external vorticity are obtained for a variety of parameters and are presented graphically.

The results of the above analysis provide a further insight into the singularities of the second-order solutions. The results of the first problem, described earlier, fix the location of the isolated singularities whereas those of the last problem show two distinct domains of stable and unstable solutions separated by the first critical value (corresponding to the singularities for various second-order effects mentioned in the first problem) of the parameter. Thus, it is shown that if the second-order parameters assume a value less than the critical value, any departure from strict similarity grows in the downstream direction and as such the flow is, in some sense, unstable.

The application of the above procedure is illustrated by considering a uniform flow past a blunted wedge. The boundary layer on a blunted wedge corresponds to a two-dimensional stagnation point flow ($\beta = 1$) at the start ($\sigma = o$) and then

accelerates to approach a constant $\beta \neq 1$ (depending on the wedge angle) as $\sigma \to \infty$. Thus the initial and the final solutions are similar while at the intermediate stations, the flow is non-similar. A Görtler series solution, starting from the stagnation point, is already known from the second problem studied here. This series solution, extended sufficiently downstream by Eulerization, is used to prescribe the initial condition for the present problem for constructing the asymptotic solutions to give the approach to the far downstream ($\sigma \to \infty$) similar solution. In addition to the eigenfunctions, we also include terms arising due to variation of the second-order parameters with σ. The multiplicative coefficient of the first eigenfunction is determined for each of the second-order effects, by joining the present series ($\sigma \to \infty$) with the Eulerized Görtler series. The resulting solution provides in a certain sense a proof of convergence for the Görtler series solution. Further, the resulting asymptotic solution for large σ, in conjunction with the Eulerized Görtler series may be used to assess the accuracy of the corresponding results obtained by certain numerical or approximate methods, where the error bounds are unknown or uncertain.

It seems appropriate here to make a brief mention of the second-order theories other than that of Van Dyke (1962). Lenard (1961), Maslen (1963) and Honda and Kiyokawa (1969) have independently given the second-order boundary-layer theory, the

first two authors obtaining solutions valid near the stagnation point while the latter authors formulated the problem in the stream function coordinates. More recently, an alternate approach to incorporate the second-order effects due to longitudinal curvature, displacement and transverse curvature in the first-order boundary-layer equations itself has been given by Van Dyke (1969), Davis, Werle and Wornom (1970) and Davis, Whitehead and Wornom (1971). Werle and Wornom (1972) have applied this theory to study the longitudinal curvature and displacement effects for a circular cylinder in the incompressible flow. The single set of equations are suitable for numerical methods such as finite difference and finite element. However, since the second-order effects have not been linearly separated out, one has to solve the equations separately for each value of the parameter. Thus, for the present work where we study the contribution of the various second-order parameters to the individual second-order effects, Van Dyke's (1962) formulation is preferred.

CHAPTER 2

FUNDAMENTAL EQUATIONS AND RELATIONS

2.1 Introduction:

We describe here a procedure for obtaining the second-order incompressible boundary-layer equations, containing terms due to longitudinal curvature, transverse curvature, displacement speed, external vorticity and stagnation enthalpy gradient. Van Dyke (1962) has provided one such formulation for the momentum and heat transfer in constant density flow of a perfect gas. However, for liquids, the thermal problem of Van Dyke needs some modifications (as explained in Section 2.3). The main aim of this chapter is to present such a modified analysis for liquids.

The governing equations for the second-order boundary-layer problem are obtained from the Navier-Stokes equations, using the method of matched asymptotic expansions, with inverse powers of the square root of Reynolds number $R^{-1/2}$ as the expansion parameter. This method divides the flow in two regions which are described by two different limit processes: an outer limit (defined as $R \to \infty$ with physical normal coordinate n fixed) valid everywhere except in a narrow region of order $R^{-1/2}$ near the wall and an inner limit (defined as $R \to \infty$ with stretched physical normal coordinate $nR^{1/2}$ fixed) valid in the region of

order $R^{-1/2}$ near the wall. The repeated application of these limit processes yields outer and inner expansions which are matched in an overlapping region to obtain the missing boundary conditions.

The coordinate system employed in the present work is described in Section 2.2. The Navier-Stokes equations are given in Section 2.3. A unified analysis for liquids and gases is presented in Section 2.4 and the final governing equations of the second-order boundary-layer problem are listed separately for liquids and gases in Section 2.5. These equations are the starting point for subsequent chapters and are studied for variety of flow situations. In the last Section 2.6, we also include a note on the displacement thickness which is needed in the subsequent chapters.

2.2 Coordinate System:

The orthogonal coordinate system (s, n) used for the present problem is shown in Figure 2.1. Here s is the distance along the surface measured from the stagnation point or the leading edge and n is the distance normal to the surface. The velocity components in s and n directions are, respectively u and v. The longitudinal curvature of the body (reckoned positive for a convex surface) is denoted by k(s). In axisymmetric flow, $\theta(s)$ is the angle that the tangent to the meridian curve makes with the axis of the body and r(s) denotes the normal distance from the axis. The three quantities k, θ and s are connected

through the following relations:

$$\sin\theta = dr/ds, \qquad \cos\theta = -K^{-1}\, d^2r/ds^2.$$

The length element dl in space is given by

$$dl^2 = (1+Kn)^2\, ds^2 + dn^2 + (r+n\cos\theta)^{2j}\, d\phi^2$$

where for the axisymmetric flow, j is unity and ϕ is the azimuthal angle while for the plane flow, j is zero and ϕ is the linear distance normal to the plane of flow.

2.3 Equations of Motion:

The Navier-Stokes equations for a steady, plane or axisymmetric flow of an incompressible fluid in nondimensional form (distances $\underline{x}(s, n)$ are nondimensionalized with respect to the characteristic length L of the body, velocity $\underline{U}(u, v)$ by reference velocity U_c, pressure by ρU_c^2 and temperature T by U_c^2/C_p) are

$$\text{div}\ \underline{U} = 0, \tag{2.1}$$

$$\underline{U}.\text{grad}\ \underline{U} + \text{grad}\ P = -R^{-1}\ \text{curl curl}\ \underline{U}, \tag{2.2}$$

$$\underline{U}.\text{grad}\ T - (PrR)^{-1}\nabla^2 T = R^{-1}\,\text{grad}\ \underline{U}.\text{def}\ \underline{U} - e\underline{U}.\text{grad}\ P \tag{2.3}$$

Here we have defined the Reynolds number $R = \rho U_c L/\mu$ and the Prandtl number $Pr = \mu C_p/k$ where μ is the coefficient of viscosity, ρ the density, k the thermal conductivity and C_p the specific heat.

The quantity e, defined as $(\partial \log \rho/\partial \log T)_p$, is the thermal expansion parameter. It may be noted that for a perfect gas its

value is minus unity ($e=-1$) while for liquid, it is negligibly small ($e\simeq 0$). The formulation of the thermal problem of Van Dyke (1962) corresponds to $e=-1$. In this case, the last term of the energy equation (2.3) can be eliminated with the help of the momentum equation (2.2) to obtain the equation

$$\underset{\sim}{U}.\text{grad}\,(T+U^2/2)-R^{-1}\nabla^2(Pr^{-1}T+U^2/2) = R^{-1}(\text{grad}\,\underset{\sim}{U}).(\text{grad}\,\underset{\sim}{U})^*($$

used by Van Dyke (1962). However in the case of liquids, by putting $e=0$ in the equation (2.5) one obtains the following equation:

$$\underset{\sim}{U}.\text{grad}\,T-R^{-1}\nabla^2(Pr^{-1}T) = R^{-1}\,\text{grad}\,\underset{\sim}{U}.\text{def}\,\underset{\sim}{U}. \qquad (2.5)$$

Since equation (2.5) does not follow from equation (2.4) as a special case, we have to reformulate higher order problem for equation (2.5), valid for liquids. We choose to formulate the problem for arbitrary value of e such that the governing equations for two special cases of gas and liquid will follow by choosing, respectively $e=-1$ and 0.

The boundary conditions for the equations (2.1)-(2.3) are

$$\underset{\sim}{U} = 0 \qquad \text{at } n = 0, \qquad (2.6)$$

$$T = T_w(s) \qquad \text{or } \partial T/\partial n = 0 \qquad \text{at } n = 0 \qquad (2.7)$$

where (2.6) is the well-known no slip condition for impermeable surface. In (2.7), only one of the two conditions on the surface is required. The first prescribes the wall temperature $T_w(s)$ and the second implies an adiabatic wall (no heat transfer at the wall). As regards the upstream condition, the oncoming stream may be nonuniform (but prescribed, independent of Reynolds number) and have gradients of velocity (vorticity) and temperature.

2.4 Formulation of the Second-Order Boundary-Layer Problem:

We now obtain the asymptotic behaviour of Navier-Stokes equations for large values of Reynolds number using the technique of the matched asymptotic expansions. Application of the outer and the inner limits to the Navier-Stokes equations yields two sets of equations which are matched in the overlapping region by using the well-known matching principle.

2.4.1 Outer Expansion:

We write the outer expansion of the variables in equation (2.1)-(2.3) by considering the outer (Euler) limit defined as $R \to \infty$ with $\underset{\sim}{x}$ fixed. The appropriate sequence of gauge functions for unseparated flows past analytic bodies consists of the inverse power of square root of Reynolds number (Van Dyke 1962). The outer expansions may be written as

$$\begin{aligned}
\underset{\sim}{U}(\underset{\sim}{x}; R) &= \underset{\sim}{U}_1(\underset{\sim}{x}) + R^{-1/2}\underset{\sim}{U}_2(\underset{\sim}{x}) + \ldots, \\
P(\underset{\sim}{x}; R) &= P_1(\underset{\sim}{x}) + R^{-1/2}P_2(\underset{\sim}{x}) + \ldots, \\
T(\underset{\sim}{x}; R) &= T_1(\underset{\sim}{x}) + R^{-1/2}T_2(\underset{\sim}{x}) + \ldots, \\
\Psi(\underset{\sim}{x}; R) &= \Psi_1(\underset{\sim}{x}) + R^{-1/2}\Psi_2(\underset{\sim}{x}) + \ldots.
\end{aligned} \tag{2.8}$$

Here Ψ is the stream function, defined by

$$(r+n\cos\theta)^j U = \partial\Psi/\partial n, \quad (1+Kn)(r+n\cos\theta)^j V = -\partial\Psi/\partial s.$$

On substituting the expansions (2.8) into the governing equations (2.1)-(2.3) and collecting the coefficients of the like powers of $R^{-1/2}$ gives the problems for the successive orders. The first order equations are

The first order equations are

$$\text{div } \underset{\sim}{U}_1 = 0, \tag{2.9a}$$

$$\underset{\sim}{U}_1 \cdot \text{grad } \underset{\sim}{U}_1 + \text{grad } P_1 = 0, \tag{2.9b}$$

$$\underset{\sim}{U}_1 \cdot \text{grad } (T_1 + eP_1) = 0. \tag{2.9c}$$

These are the well-known inviscid Euler equations. The integration of these equations along a stream line leads to

$$P_1 + \underset{\sim}{U}_1^2/2 = B_1(\Psi_1), \tag{2.10a}$$

$$T_1 - e\underset{\sim}{U}_1^2/2 = H_1(\Psi_1). \tag{2.10b}$$

The Bernoulli function $B_1(\Psi_1)$ and temperature function $H_1(\Psi_1)$ are to be evaluated from the upstream conditions. Equations (2.10a,b) show that the total pressure and temperature are conserved along the first-order stream line ($\Psi_1 = \text{constant}$) defined as

$$(r + n\cos\theta)^j U_1 = \partial\Psi_1/\partial n,$$

$$(1 + Kn)(r + n\cos\theta)^j V_1 = -\partial\Psi_1/\partial s.$$

The second-order equations are

$$\text{div } \underset{\sim}{U}_2 = 0, \tag{2.11a}$$

$$\underset{\sim}{U}_1 \cdot \text{grad } \underset{\sim}{U}_2 + \underset{\sim}{U}_2 \cdot \text{grad } \underset{\sim}{U}_1 + \text{grad } P_2 = 0, \tag{2.11b}$$

$$\underset{\sim}{U}_1 \cdot \text{grad } (T_2 + eP_2) + \underset{\sim}{U}_2 \cdot \text{grad } (T_1 + eP_1) = 0. \tag{2.11c}$$

These equations are the perturbed Euler equations which represent the displacement of the outer flow due to the first-order boundary-layer. The first integral of equations (2.11b) and

(2.11c) gives

$$P_2 + \underset{\sim}{U}_1 \cdot \underset{\sim}{U}_2 = \Psi_2 B_1'(\Psi_1) + B_2(\Psi_1), \tag{2.12a}$$

$$T_2 - e\underset{\sim}{U}_1 \cdot \underset{\sim}{U}_2 = \Psi_2 H_1'(\Psi_1) + H_2(\Psi_1). \tag{2.12b}$$

where Ψ_2 is the second-order stream function for the outer flow and is defined by

$$(r + n\cos\theta)^j U_2 = \partial\Psi_2/\partial n,$$

$$(1 + Kn)(r + n\cos\theta)^j V_2 = -\partial\Psi_2/\partial s.$$

As the oncoming stream is prescribed, independent of Reynolds number, we have $B_2 = H_2 = 0$.

It is well-known that the outer equations do not satisfy the no slip boundary condition due to the loss of the highest order derivative of the Navier-Stokes equations at large Reynolds number. These equations are, therefore, not valid within a distance of order $R^{-1/2}$ near the wall. It is clear that a different inner limiting process valid near the wall, in a region of order $R^{-1/2}$, is needed.

2.4.2 Inner Expansion:

To study the behavior of the flow near the wall in the region of order $R^{-1/2}$, we introduce the stretched inner (Prandtl) variable

$$N = R^{1/2} n$$

and study the limit $R \to \infty$ with N fixed. The inner expansions

are of the following form:

$$
\begin{aligned}
u(s,n;R) &= u_1(s,N) + R^{-1/2}u_2(s,N) + \dots , \\
v(s,n;R) &= R^{-1/2}v_1(s,N) + R^{-1}v_2(s,N) + \dots , \\
P(s,n;R) &= p_1(s,N) + R^{-1/2}p_2(s,N) + \dots , \\
T(s,n;R) &= t_1(s,N) + R^{-1/2}t_2(s,N) + \dots , \\
\Psi(s,n;R) &= R^{-1/2}\psi_1(s,N) + R^{-1}\psi_2(s,N) + \dots .
\end{aligned}
\tag{2.13}
$$

Substituting the above expansions in the governing equations and collecting the coefficients of the like powers of $R^{-1/2}$, we obtain the problems of successive orders. The terms independent of $R^{-1/2}$ give the following first-order equations:

$$(r^j u_1)_s + (r^j v_1)_N = 0, \tag{2.14a}$$

$$u_1 u_{1s} + v_1 u_{1N} - u_{1NN} + p_{1s} = 0, \tag{2.14b}$$

$$p_{1N} = 0, \tag{2.14c}$$

$$u_1 t_{1s} + v_1 t_{1N} - Pr^{-1} t_{1NN} = u_{1N}^2 - e u_1 p_{1s} \tag{2.14d}$$

with the corresponding boundary conditions

$$u_1(s,0) = 0 \ , \quad v_1(s,0) = 0, \tag{2.15a,b}$$

$$t_1(s,0) = T_w(s) \text{ or } t_{1N} = 0. \tag{2.15c}$$

Here subscripts s and N denote the partial differentiation. These are the well-known classical equations of Prandtl boundary layer. Again, the terms of order $R^{-1/2}$ give the second-order boundary-layer equations as

$$[r^j(u_2 + Nu_1 \, j \cos\theta/r)]_s + r^j [v_2 + (K + j\cos\theta/r)Nv_1]_N = 0 \quad (2.16a)$$

$$u_2u_{1s} + v_2u_{1N} + u_1u_{2s} + v_1u_{2N} - u_{2NN} + p_{2s}$$

$$= K[(Nu_{1N})_N - v_1(Nu_1)_N] + j\cos\theta/r \, u_{1N}, \quad (2.16b)$$

$$p_{2N} = Ku_1^2, \quad (2.16c)$$

$$u_2t_{1s} + v_2t_{1N} + u_1t_{2s} + v_1t_{2N} - Pr^{-1}t_{2NN}$$

$$= (K + j\cos\theta/r)\, Pr^{-1}t_{1N} - 2Ku_1u_{1N} + 2u_{1N}u_{2N}$$

$$+ KNu_1t_{1s} - eKNu_1 \, p_{1s} + e(u_1p_{2s} + v_1p_{2s} + u_2p_{1s} + v_2p_{1N}) \quad (2.1$$

with the boundary conditions

$$u_2(s, 0) = 0, \qquad v_2(s, 0) = 0 \quad (2.17a,b)$$

$$t_2(s, 0) = 0 \quad \text{or} \quad t_{2N}(s, 0) = 0. \quad (2.17c)$$

2.4.3 Matching:

The outer expansion violates the boundary conditions on the velocity and temperature at the wall while the inner expansion does not satisfy the boundary condition far away from the wall. Therefore, the validity of the inner expansion is restricted to a region of order $R^{-1/2}$ near the wall whereas the outer expansion is valid only outside the region of $O(R^{-1/2})$. Thus neither expansion has sufficient boundary conditions and the missing boundary conditions have to be determined to make the problem determinate. This is done by matching the inner and the outer expansions in the overlapping region by the well-known matching principle (Kaplun 1957, Van Dyke 1964b)

written as follows:

Inner limit of the (outer expansion)

= Outer limit of the (inner expansion). (2.18)

This matching principle is applied to all the variables and corresponding matching conditions are obtained. Since the procedure is identical for all the variables, we illustrate it for one typical variable say $\phi(s, n; R)$. The outer expansion is given by

$$\phi(s, n; R) = \Phi_1(s, n) + R^{-1/2}\Phi_2(s, n) + R^{-1}\Phi_3(s, n) + \dots . \quad (2.19)$$

To find its inner limit, we write the equation (2.19) in terms of the inner variables (s, N) and take the limit $R \to \infty$ with inner variables fixed. Thus,

$$\phi(s, NR^{-1/2}; R \to \infty) = \Phi_1(s, 0) + R^{-1/2}[\Phi_2(s, 0) + N\Phi_{1n}(s, 0)] + R^{-1}\left[\Phi_3(s, 0) + N\Phi_{2n}(s, 0) + \frac{N^2}{2}\Phi_{1nn}(s, 0)\right] + \dots . \quad (2.20$$

The outer limit of the inner expansion is found by rewriting the inner expansion in terms of the outer variables (s, n) and taking the limit $R \to \infty$ with (s, n) fixed. This gives,

$$\phi(s, nR^{1/2}; R \to \infty) = \phi_1(s, N \to \infty) + R^{-1/2}\phi_2(s, N \to \infty) + R^{-1}\phi_3(s, N \to \infty) + \dots . \quad (2.21)$$

Using the matching principle (2.18) to compare equations (2.20) and (2.21), we obtain the following matching conditions:

$$\left.\begin{aligned} \phi_1(s, N) &= \Phi_1(s, 0) , \\ \phi_2(s, N) &\sim N\Phi_{1n}(s, 0) + \Phi_2(s, 0). \end{aligned}\right\} N \to \infty \quad (2.22a)$$

Using equation (2.22a) along with relations (2.10a,b), the matching conditions for the first-order boundary-layer problem may be written as follows:

$$V_1(s,0) = 0, \tag{2.23a}$$

$$u_1(s,N) = U_1(s,0), \tag{2.23b}$$

$$\left.\begin{aligned} p_1(s,N) &= P_1(s,0) = B_1(0) - U_1^2(s,0)/2, \\ t_1(s,N) &= T_1(s,0) = H_1(0) + eU_1^2(s,0)/2. \end{aligned}\right\} N \to \infty \tag{2.23c,d}$$

Equation (2.23a) represents the boundary condition at the wall for the first-order outer problem: the condition $U_1(s,0) = 0$ has to be given up.

The matching conditions for the second-order boundary-layer problem are obtained by using equation (2.22b) alongwith (2.13). Thus,

$$u_2(s,N) \sim U_2(s,0) + NU_{1n}(s,0) = U_2(s,0) + N[r^j B_1'(0) - KU_1(s,0)] \tag{2.24a}$$

$$p_2(s,N) \sim P_2(s,0) + NP_{1n}(s,0) = B_1'(0)\Psi_2(s,0) - U_1(s,0)\,U_2(s,0) + KNU_1^2(s,0) \tag{2.24b}$$

$$t_2(s,N) \sim T_2(s,0) + N\,T_{1n}(s,0) = H_1'(0)\Psi_2(s,0) + e\,U_1(s,0)\,U_2(s,0) + NU_1(s,0)\,[r^j H_1'(0) - e\,r^j B_1'(0) + e\,KU_1(s,0)] \tag{2.24c}$$

$$\left.\begin{aligned} &u_2(s,N) \sim U_2(s,0) + NU_{1n}(s,0) = U_2(s,0) + N[r^j B_1'(0) - KU_1(s,0)] \\ &p_2(s,N) \sim P_2(s,0) + NP_{1n}(s,0) = B_1'(0)\Psi_2(s,0) - U_1(s,0)\,U_2(s,0) + KNU_1^2(s,0) \\ &t_2(s,N) \sim T_2(s,0) + N\,T_{1n}(s,0) = H_1'(0)\Psi_2(s,0) + e\,U_1(s,0)\,U_2(s,0) + NU_1(s,0)\,[r^j H_1'(0) - e\,r^j B_1'(0) + e\,KU_1(s,0)] \end{aligned}\right\} N \to \infty$$

$$\psi_1(s,N) \sim \Psi_2(s,0) + N\Psi_{1n}(s,0). \tag{2.24d}$$

In the above equations (2.24a-c), the extreme right hand side expressions are obtained with the help of equations (2.10) and (2.12). The matching condition (2.24d) can be rewritten in the following forms:

$$\Psi_2(s,0) = \lim_{N\to\infty} (\psi_1 - N\psi_{1N}), \tag{2.25}$$

$$V_2(s,0) = \lim_{N\to\infty} (v_1 - Nv_{1N}). \tag{2.26}$$

This is an important matching condition for the second-order outer flow and represents the effect of displacement of the inviscid (outer) flow by the boundary-layer (inner) flow. The quantities on the right hand side of the expressions $\Psi_2(s,0)$ and $V_2(s,0)$ can be evaluated from the first-order boundary-layer solution. A physical interpretation of these equations is that the effect of the classical boundary-layer upon the outer flow is equivalent to surface distribution of sources.

2.5 Summary of the Governing Equations:

2.5.1 Equations for the outer flow:

First Order (Euler Flow): The governing equation of the first-order outer stream function Ψ_1, obtained from equations (2.9) and (2.10) is

$$\left[\frac{\partial}{\partial s}\left(r^{-j}(1+Kn)^{-1} \frac{\partial}{\partial s}\right) + \frac{\partial}{\partial n}\left(r^{-j}(1+Kn) \frac{\partial}{\partial n}\right)\right]\Psi_1 = r^j(1+Kn)\, B_1'(\Psi_1) \tag{2.27a}$$

with the corresponding matching and boundary conditions given by

$$\Psi_1(s,0) = 0, \quad \Psi_1 = \Psi_{1\infty} \text{ far upstream} \tag{2.27b,c}$$

where $B_1'(\Psi_1)$ and $\Psi_{1\infty}$ are known from the upstream conditions.

The integration of equation (2.11a) subjected to the boundary conditions (2.11b,c) gives the velocity components $U_1(s, n)$ and $V_1(s, n)$ and, in particular, $U_1(s, 0)$ needed in the matching conditions for the first-order boundary-layer problem. Further, using U_1 and V_1, pressure distribution P_1 can be determined by the Bernoulli equation (2.10a).

Second Order (Displacement Flow): The governing equation of the second-order outer stream function Ψ_2 are obtained from equations (2.11) and (2.12) and can be written as:

$$\left[\frac{\partial}{\partial s}\left(r^{-j}(1+Kn)^{-1}\right)\frac{\partial}{\partial s}+\frac{\partial}{\partial n}\left(r^{-j}(1+Kn)\frac{\partial}{\partial n}\right]\Psi_2 = r^{j}(1+Kn)\,B_1''(\Psi_1)\Psi_2\,, \qquad (2.28a)$$

with the corresponding boundary and matching conditions as:

$$\Psi_2(s, 0) = \lim_{N\to\infty}(\psi_1 - N\psi_{1N}),$$

$$\Psi_2(s, n) = 0 \text{ far upstream.} \qquad (2.28b,c)$$

where ψ_1 is obtained from the first-order boundary-layer solution. The solution of the problem (2.28) yields $U_2(s, n)$ and $V_2(s, n)$ whereby we can evaluate $U_2(s, 0)$ required for the matching conditions of the second-order boundary-layer problem. Using U_2 and V_2 alongwith equation (2.12), we can evaluate the pressure distribution P_2.

2.5.2 Boundary-Layer Equations:

We now write down the governing equations of the first and second-order boundary-layer problem for both liquids and gases. Since the continuity and momentum transfer (velocity

boundary-layer) equations are same for both the cases (liquids and gases), we write them once only. The energy (thermal boundary-layer) equation for the liquids and gases is obtained by putting respectively e = 0 and 1 in the general form of the energy equation, boundary conditions and matching conditions obtained earlier in § 2.4 and are given separately for these two cases.

Momentum Transfer:

First-order:

$$(r^j u_1)_s + (r^j v_1)_N = 0, \tag{2.29a}$$

$$u_1 u_{1s} + v_1 u_{1n} - u_{1NN} = U_1(s,0)\, U_{1s}(s,0), \tag{2.29b}$$

$$u_1(s,0) = v_1(s,0) = 0, \tag{2.29c}$$

$$u_1(s,N) = U_1(s,0) \quad \text{as } N \to \infty . \tag{2.29d}$$

Second-order:

$$[r^j(u_2 + Nu_1\, j\cos\theta/r)]_s + r^j[v_2 + (K + j\cos\theta/r)Nv_1]_N = 0, \tag{2.30a}$$

$$\begin{aligned} u_1 u_{2s} + u_2 u_{1s} + v_1 u_{2n} + v_2 u_{1N} - u_{2NN} &= K[Nu_1 u_{1s} - u_1 v_1 \\ &\quad - NU_1(s,0)\, U_{1s}(s,0) + u_{1N}] - [KNU_1^2(s,0) \\ &\quad + K\int_N^\infty (U_1^2(s,0) - u_1^2)\, dN]_s + u_{1N}\, j\cos\theta/r \\ &\quad - r^j B_1'(0)\,[\lim_{N\to\infty}(v_1 - Nv_1)] + [U_1(s,0)\, U_2(s,0)]_s , \end{aligned} \tag{2.30b}$$

$$u_2(s,0) = 0 = v_2(s,0), \tag{2.30c}$$

$$u_2(s,N) \backsim - NKU_1(s,0) + r^j NB_1'(0) + U_2(s,0) \text{ as } N \to \infty . \tag{2.30d}$$

Energy equation for liquids (e = 0):

First-order:

$$u_1 t_{1s} + v_1 t_{1N} - Pr^{-1} t_{1NN} - u_{1N}^2 = 0, \tag{2.31a}$$

$$t_1(s,0) = T_w(s) \text{ or } t_{1N} = 0, \tag{2.31b}$$

$$t_1(s,N) = H_1(0) \ , \quad \text{as } N \to \infty \ . \tag{2.31c}$$

Second-order:

$$u_1 t_{2s} + u_2 t_{1s} + v_1 t_{2N} + v_2 t_{1N} - Pr^{-1} t_{2NN} - 2u_{1N} u_{2N}$$
$$= K[Nu_1 t_{1s} + Pr^{-1} t_{1N} - 2u_1 u_{1N}] + Pr^{-1} t_{1N} j \cos\theta/r, \tag{2.32a}$$

$$t_2(s,0) = 0 \quad \text{or } t_{2N}(s,0) = 0, \tag{2.32b}$$

$$t_2(s,N) \backsim [\Psi_2(s,0) + r^j N U_1(s,0)] \ H_1'(0) \quad \text{as } N \to \infty \ . \tag{2.32c}$$

Energy equation for gases (e = -1):

First-order:

$$u_1 h_{1s} + v_1 h_{1N} - Pr^{-1} h_{1NN} = 0 \tag{2.33a}$$

$$h_1(s,0) = t_w(s) \tag{2.33b}$$

$$h_1(s,N) = H_1(0) \quad \text{as } N \to \infty \ . \tag{2.33c}$$

Second-order:

$$u_1 h_{2s} + u_2 h_{1s} + v_1 h_{2N} + v_2 h_{1N} - Pr^{-1} h_{2NN}$$
$$= K[Nu_1 h_{1s} + Pr^{-1} h_{1N}] + Pr^{-1} h_{1N} j \cos\theta/r, \tag{2.34a}$$

$$h_2(s,0) = 0, \tag{2.34b}$$

$$h_2(s,N) \backsim [\Psi_2(s,0) + r^j N U_1(s,0)] \ H_1'(0) \quad \text{as } N \to \infty \ . \tag{2.34c}$$

It may be noted that the above form of the energy equations for gases is preferred in order to conform it with that of Van Dyke (1962). It is obtained by substituting e = -1 in the

energy equations (2.14d) and (2.16d), which is then manipulated with the help of the momentum equations to obtain the above form.

2.6 Displacement Thickness:

Before closing this chapter we define and obtain expressions for δ and Δ - the first and second-order displacement thickness. The displacement thickness δ is defined by the relation:

$$\int_{\delta}^{n_\infty} U r^j dn = \int_{0}^{n_\infty} u r^j dn \qquad (2.35)$$

where n_∞ is the value of n arbitrarily chosen to be beyond the outer limit of the inner layer. The displacement thickness may be expanded as:

$$\delta(s; R^{-1/2}) = R^{-1/2}\delta\ (s) + R^{-1}\Delta\ (s) \ldots \ . \qquad (2.36)$$

Now, we let $R \to \infty$ as n_∞ remains fixed and rewrite equation (2.35) in the following form:

$$\delta + R^{-1/2}\Delta + \ldots$$
$$\int_{0} U(s, R^{-1/2}N)\, r^j\, dN$$
$$= \int_{0}^{\infty} [U(s, R^{-1/2}N) - u(s, N)]\, r^j\, dN \qquad (2.37)$$

The expansions for $u(s, N)$ and $U(s, R^{-1/2}N)$ are given by respectively, equations (2.8) and (2.13). Also we have to expand r^j as

$$r^j = r_0^j + R^{-1/2} N\, j \cos\theta \qquad (2.38)$$

Further, the expression for $U(s, R^{-1/2}N)$ is expanded in a Taylor series about $R^{-1/2}N = 0$ so that we have

$$U(s, R^{-1/2}N) \sim U_1(s, 0) + R^{-1/2}\,[NU_{1n}(s, 0) + U_2(s, 0)] + \ldots \ . \qquad (2.39)$$

Substituting the above mentioned expansions in equation (2.37)

and integrating the left hand side, we obtain:

$$U_1(s,0)\, r_o^j \delta + R^{-1/2}\left[U_1(s,0)\, r_o^j \Delta + \frac{\delta^2}{2} r_o^j U_{1n}(s,0) + \delta\, U_2(s,0)\, r_o^j + \frac{\delta^2}{2} U_1(s,0)\, j \cos\theta\right] = \int_0^\infty \left[\{U_1(s,0) - U_1(s,N)\} r_o^j + R^{-1/2}\left\{[NU_{1n}(s,0) + U_2(s,0) - u_2(s,N)]\, r_o^j + N[U_1(s,0) - u_1(s,N)]\, j \cos\theta\right\}\right] dN \qquad (2.40)$$

Now collection of the coefficients of the like powers of $R^{-1/2}$ yields the following expressions for the first and the second-order displacement thickness:

$$\delta = \int_0^\infty \left[1 - \frac{u_1(s,N)}{U_1(s,N)}\right] dN\,, \qquad (2.41)$$

$$\Delta = -\frac{1}{2}\frac{U_{1n}(s,0)}{U_1(s,0)}\delta^2 - \frac{j\cos\theta}{r_o^j}\left[\frac{\delta^2}{2} - \int_0^\infty N\left\{1 - \frac{u_1(s,N)}{U_1(s,0)}\right\} dN\right] - \frac{U_2(s,0)}{U_1(s,0)}\left[\delta - \int_0^\infty \left\{1 - \frac{u_2(s,N) - NU_{1n}(s,0)}{U_2(s,0)}\right\} dN\right] \qquad (2.42)$$

CHAPTER 3

SELF-SIMILAR SOLUTIONS OF THE SECOND-ORDER BOUNDARY-LAYER EQUATIONS INCLUDING DISSIPATION TERMS

3.1 Introduction:

We now study the self-similar solutions of the second-order boundary-layer equations including the dissipation terms, viz. the equations (2.29)-(2.34) given in §2.5.2 of Chapter 2. In these equations, the terms involving K arise due to longitudinal curvature, $j \cos\theta/r$ due to transverse curvature, $B_1'(0)$ due to external vorticity, $H_1'(0)$ due to stagnation enthalpy gradient and the remaining terms due to displacement speed. These effects are of order $R^{-1/2}$ as compared to the classical boundary-layer theory and become significant when R is only moderately large.

The above mentioned second-order problems have been studied by various authors and an excellent review is given by Van Dyke (1969). Recently, Afzal (1969, 1972) and Werle and Davis (1970) have proposed a more general class of similarity as compared to the earlier works and have shown that the description of the second-order problem needs three principal functions, namely those due to longitudinal curvature, transverse curvature and displacement speed. Afzal and Oberai(1972) have studied the momentum and heat-transfer in the second-order

boundary-layer flows without the viscous dissipation terms while Werle and Davis (1970) have studied only the momentum transfer. Afzal and Oberai (1972) have shown that for a given pressure gradient parameter, the solutions to the second-order equations show a sequence of infinite discontinuities for certain critical values of the second-order parameters while Werle and Davis (1970) have reported only one such discontinuity. However, these authors have not given a detailed account of the occurrence of such discontinuities. We investigate here (§3.3) the general pattern of these infinite discontinuities and suggest their relevance to the design of body shapes so as to achieve some desired aerodynamic properties.

The main aim of this chapter is to study the general self-similar structure of the second-order boundary-layer equations when the viscous dissipation terms are included. The contribution due to the viscous dissipation may be significant whenever the product of the Prandtl number and Eckert number is of the order of unity. We may expect one such situation for liquids of moderately large Prandtl number. We consider here steady, laminar flow with constant density, past a two-dimensional or axisymmetric body. The study includes both types of the thermal boundary conditions at the wall: (i) specified wall temperature and (ii) an insulated wall (no heat transfer at the wall). For the latter case, the classical concept of the recovery factor is extended to the second-order flows. The terms in the heat transfer and recovery factor due to

longitudinal curvature, transverse curvature, displacement speed, external vorticity and stagnation enthalpy gradient are calculated for various values of the parameters arising in the problem and the results are displayed graphically.

We first describe in §3.2, the momentum transfer problem and then in §3.3, discuss the occurrence of the infinite discontinuities. The subject matter described thereafter is subdivided into two parts. In part I (§§3.4-3.7), we study the thermal problem for liquids while part II (§§3.8-3.11) is concerned with the corresponding thermal problem for the constant density flow of gases.

3.2 Momentum Transfer Problem:

The momentum transfer problem is governed by equations (2.29) and (2.30) given in §2.5.2. In view of the reasons given in Chapter 1, we choose the Görtler variables to study the boundary-layer equations for nonsimilar flow situations. The Görtler variables are defined as

$$\sigma = \int_0^s U_1(s,0)\, r^{2j}\, ds \quad , \qquad \eta = r^j (2\sigma)^{-1} U_1(s,0)\, N. \tag{3.1}$$

The equation of continuity (2.29a) for the first-order boundary-layer is identically satisfied by introducing the first-order stream function ψ_1 such that

$$\psi_{1N} = r^j u_1, \qquad \psi_{1s} = -r^j v_1 . \tag{3.2}$$

It is found convenient to write the stream function ψ_1 in the following form:

$$\psi_1 = \sqrt{(2\sigma)}\, f(\sigma,\eta) \tag{3.3}$$

Introducing the above expression (3.3) in the first-order momentum transfer equation (2.29), we get,

$$f''' + ff'' + \Lambda_{U_1}(1-f'^2) - 2\sigma(f'f'_\sigma - f''f_\sigma) = 0, \qquad (3.4a)$$

$$f(\sigma, 0) + 2\sigma f_\sigma(\sigma, 0) = 0, \qquad (3.4b)$$

$$f'(\sigma, 0) = 0 \quad , \quad f(\sigma, \infty) = 1. \qquad (3.4c,d)$$

Here prime (') denotes the differentiation with respect to η. The quantity Λ_{U_1} is the principal velocity function defined by

$$\Lambda_{U_1} = [2\sigma/U_1(s, 0)]\,[dU_1(s, 0)/d\sigma]. \qquad (3.5)$$

The function Λ_{U_1} is an important parameter for the boundary-layer problem. It has relevance for nonsimilar as well as similar flows. For the latter case, it remains constant in the streamwise direction and can be identified as the familiar Falkner-Skan pressure gradient parameter denoted by β. However, for nonsimilar flows, Λ_{U_1} varies in the streamwise direction (see, e.g. the blunted wedge problem considered in Chapter 4). In general, Λ_{U_1} can be determined, if the first-order outer velocity, $U_1(s, 0)$, is known either from the solution of the outer flow or by curve fitting to the experimental data.

The continuity equation (2.30a) for the second-order flows is satisfied by defining the second-order stream function ψ_2 as

$$r^j[u_2 + jNu_1 \cos\theta/r] = \psi_{2N}, \quad r^j[v_2 + (K + j\cos\theta/r)\,Nv_1] = -\psi_{2s}. \qquad (3.6)$$

If we express the second-order stream function in the following form

$$\psi_2 = \sqrt{(2\sigma)}\, F(\sigma, \eta) \qquad (3.7)$$

the second-order momentum transfer problem (2.30) reduces to

$$F''' + fF'' - 2\Lambda_{U_1} f'F' + f''F - 2\sigma (f'_\sigma F' - f''F_\sigma + f'F_\sigma - f_\sigma F'')$$
$$= B_1 [-\eta(1+\Lambda_{U_1})f''' + (\Lambda_{B_1} + \Lambda_{U_1} - 1)(f'' + ff' + 2\sigma f'f_\sigma + 4\sigma \int_\eta^\infty f'_\sigma f' d\eta)$$
$$+ (\Lambda_{B_1} + 2\Lambda_{U_1})(\eta\Lambda_{U_1} + \alpha + 2\sigma\alpha_\sigma)]/(1+\Lambda_{U_1})$$
$$+ B_t[-\eta(2\Lambda_{U_1} + f''') + f'' + ff' - \Lambda_{B_t} f'^2 + 2\sigma f_\sigma f']$$
$$- B_v(\alpha + 2\sigma\alpha_\sigma) - B_d(2\Lambda_{U_1} + \Lambda_{B_d}), \qquad (3.8a)$$

$$F(\sigma, 0) + 2\sigma F_\sigma(\sigma, 0) = 0, \quad F'(\sigma, 0) = 0, \qquad (3.8b,c)$$

$$F'(o, \infty) = \eta(-B_1 + B_t + B_v) + B_d . \qquad (3.8d)$$

In the above equations, we have defined the following quantities for convenience of writing:

$$\alpha = \lim_{\eta \to \infty} (\eta - f), \quad B_1 = \sqrt{(2\sigma)}\, K/r^j U_1(s, 0), \qquad (3.9a,b)$$

$$B_t = \sqrt{(2\sigma)}\, j \cos\theta / r^{2j} U_1(s, 0), \quad B_d = U_2(s, 0)/U_1(s, 0), \qquad (3.9c,d)$$

$$B_v = \sqrt{(2\sigma)}\, B_1'(0)/U_1^2(s, 0) . \qquad (3.9e)$$

Further, the quantities Λ_{B_1}, Λ_{B_t} and Λ_{B_d} are respectively the principal functions corresponding to longitudinal curvature, transverse curvature, and displacement speed and are defined by

$$\Lambda_{B_i} = (2\sigma/B_i)(dB_i/d\sigma), \quad i = 1,t,d \qquad (3.10)$$

It is noted that the external vorticity does not give rise to a new principal function since

$$\Lambda_{B_v} = (2\sigma/B_v)(dB_v/d\sigma) = 1 - 2\Lambda_{U_1} . \qquad (3.10a)$$

Again, the Λ_B's are constant for similar flows while for non-similar flows, they vary in the streamwise direction (see, e.g. the blunted wedge problem in Chapter 4).

In the present chapter, since we are interested in studying the general self-similar solutions, the modified stream functions $f(\sigma,\eta)$ and $F(\sigma,\eta)$ are assumed to be of the following form:

$$f(\sigma,\eta) = f(\eta), \tag{3.11a}$$

$$F(\sigma,\eta) = \sum_i B_i F^{(i)}(\eta), \quad i = 1,t,d,v \tag{3.11b}$$

In writing the equation (3.11b), we have exploited the linearity of the second-order problem and decomposed the contributions of various second-order effects which have a clear physical interpretation.

Substitution of (3.11a) in (3.4) yields the following ordinary differential equation for the first-order boundary-layer:

$$\begin{aligned} &f''' + ff'' + \beta(1 - f'^2) = 0, \\ &f(0) = 0 = f'(0), \quad f'(\infty) = 1 \end{aligned} \tag{3.12}$$

which is the well-known Falkner-Skan equation. Here the principal velocity function Λ_{U_1} is constant and is denoted by β.

The second-order boundary-layer equations, obtained by substitution of (3.11b) in (3.8), reduce to the following system of ordinary differential equations:

$$\begin{aligned} &F'''^{(i)} + fF''^{(i)} - (2\beta + \lambda_i) f'F'^{(i)} + (1 + \lambda_i) f''F^{(i)} = L_i, \\ &F^{(i)}(0) = 0 = F'^{(i)}(0), \; F^{(i)}(\eta) = C_i \text{ as } \eta \to \infty \end{aligned} \quad i = 1,t,d,v \tag{3.13}$$

where λ_i, L_i and C_i are given in Table 3.1. Here again, the principal functions Λ_{B_1}, Λ_{B_t} and Λ_{B_d} are constant and are respectively denoted by Λ_1, Λ_t and Λ_d.

Table 3.1: Values of λ's, L's and C's in the second-order boundary-layer equations.

Second-order effect	i	λ_i	L_i	C_i
Longitudinal curvature	1	Λ_1	$-\eta f''' + [(\Lambda_1 + \beta - 1)(f'' + ff') + (2\beta + \Lambda_1)(\beta\eta + \alpha)]/(1+\beta)$	$-\eta$ (3.14)
Transverse curvature	t	Λ_t	$-\eta(2\beta + f''') + f'' + ff' - \Lambda_t \eta f'^2$	η (3.15)
Displacement speed	d	Λ_d	$-2\beta - \Lambda_d$	-1 (3.16)
External vorticity	v	$1-2\beta-\alpha$		η (3.17)

Solutions to the momentum transfer equations (3.11) have been adequately described by Werle and Davis (1970) and Afzal and Oberai (1972). Afzal and Oberai (1972) have shown that for a given β, the solution of the second-order equations contain a large number of singularities for some critical values of the parameters Λ_1, Λ_t and Λ_d; Werle and Davis (1970) also pointed out the first, of these singularities. Since no attempt is made by these authors to elaborate on the observed infinite discontinuities, we investigate, the general pattern of the singularities and point out their mathematical as well as physical significance in the next section.

3.3 Investigation of the Singular Behaviour of the Second-Order Solutions for Some Critical Values of the Second-Order Parameters:

First of all, we wish to establish that the singularities in the second-order solutions occur whenever the parameters Λ_1, Λ_t and Λ_d assume a value equal to the eigenvalue of the corresponding second-order homogeneous problem given by

$$L(M, \Lambda_i) \equiv M''' + fM'' - (2\beta + \Lambda_i) f'M' + (1 + \Lambda_i) f''M = 0,$$
$$M(0) = M'(0) = M'(\infty) = 0. \qquad (3.18)$$

The operator (3.18) is similar to the one encountered by Chen and Libby (1968) in connection with the asymptotic studies of the first-order boundary-layer theory. Chen and Libby (1968) have estimated the first twenty eigenvalues corresponding to $\beta_\infty = 0.5$ and the first eigenvalue corresponding to several other values of β.

The contribution of the longitudinal curvature, transverse curvature and displacement speed to the skin friction for two typical values of $\beta = 0.5$ and 1.0 is shown as a function of the corresponding second-order parameter in Figures, 3.1, 3.2 and 3.3. The eigenvalues of the associated homogeneous operator (3.18) are taken from Chen and Libby (1968) and are indicated by an arrow on the Λ_i-axis in the above mentioned figures (E_n, n = 1,2,3,4 denote the first four eigenvalues for $\beta = 0.5$ and D_1, the first eigenvalue for $\beta = 1.0$). Figures 3.1-3.3 show that for positive values of the parameters Λ_1, Λ_t and Λ_d, the corresponding second-order contributions to the skin friction

are well-behaved. However, for the negative values of the parameters, a large number of singularities occur; the location of these singularities is seen to be near the values of the parameters Λ_l, Λ_t and Λ_d such that it is equal to the eigenvalue of the operator (3.18) indicated by arrows. This behaviour is further supported by the close form solution for the displacement speed problem, which is given by

$$F^{(d)} = [(\beta - 1)\eta f' + f]/\beta \qquad (3.19)$$

for $\Lambda_d = \beta - 2$. Solution (3.19) shows that for $\beta = 0$, there is an infinite discontinuity at $\Lambda_d = -2$; Chen and Libby (1968) have shown that for $\beta = 0$, the first eigenvalue of the operator (3.18) is indeed -2. Thus, the general pattern of the singularities in the second-order solutions can be predicted: the location of the isolated singularities is given by the values of the second-order parameters Λ_l, Λ_t and Λ_d such that they are equal to the eigenvalue of the corresponding homogeneous operator 3.18.

Further, it is well-known (cf. e.g. Courant and Hilbert 1953) that the unique solution to the nonhomogeneous boundary value problem exists only if the corresponding homogeneous operator with homogeneous boundary conditions possesses trivial solution. However, if the homogeneous operator has an eigen solution, then, the nonhomogeneous problem does not have a unique solution; the bounded nonunique solution exists only if the eigenfunctions are orthogonal to the nonhomogeneous terms of the given differential equation. In the present study, the

solutions at the eigenvalues become unbounded (in other words, do not exist) and, therefore, suggest that the associated eigenvalues are not orthogonal to the nonhomogeneous terms of the differential equations.

We suggest that the above observations may be used as a caution while designing the profiles of aerodynamic bodies. In order that the contributions due to second-order effects to the skin friction remain bounded, the profile should be chosen such that the values of the second-order parameters Λ_1, Λ_t and Λ_d are not in the neighbourhood of the above mentioned eigenvalues. It seems that, when the values of these parameters Λ_1, Λ_t and Λ_d approach a value equal to eigenvalues, the skin friction etc. become very large and as such the second-order boundary-layer theory of Van Dyke (1962a) breaks down.

We now cite an analogy (from solid mechanics) with the linear oscillations of a spring-mass system under an applied periodic force. Although the analogy may seem rather far-fetched, nevertheless it serves well in understanding the significance of the singularities discussed above. For a spring-mass system, it is well-known that when the frequency of the applied force approaches the natural frequency of the system, the amplitude of oscillations increases leading to the phenomenon called resonance (infinite amplitude). In designing such systems, sufficient care is taken to separate the two frequencies so that the operating frequencies are kept distinct from the natural frequencies. Further, the linear theory breaks down in the

neighbourhood of resonance and a nonlinear theory is needed (cf. e.g. Cole 1968, Narasimha 1968). Analogously we suggest that in the neighbourhood where the second-order parameters Λ_1, Λ_t and Λ_d assume a value close to the eigenvalues of the associated homogeneous operator (3.18), a nonlinear boundary-layer theory seems in order.

Part I: Heat Transfer in Liquids

3.4 Thermal Boundary-Layer Equations for Self-similar Solutions:

The governing thermal boundary-layer equations (2.31) and (2.32) are given in §2.5 of Chapter 2. We shall again use the Görtler variables (σ, η) defined by (3.1). First, to obtain the general nonsimilar equations for the thermal boundary-layer, we write the first and second-order temperatures, t_1 and t_2, in the following form:

$$t_1 = [T_w - H_1(0)]\ g(\sigma,\eta) + H_1(0) \tag{3.20}$$

$$t_2 = [T_w - H_1(0)]\ G(\sigma,\eta) \tag{3.21}$$

Introducing (3.20) in (2.31), we obtain the first-order thermal boundary-layer equation in the following form:

$$\begin{aligned} &Pr^{-1} g'' + fg' - \Lambda_{T_w - H_1} f' g - 2\sigma (f' g_\sigma - f_\sigma g') = -Ef''^2, \\ &g(\sigma, 0) = 1, \quad g(\sigma, \infty) = 0. \end{aligned} \tag{3.22}$$

Substitution of (3.21) in (2.32) yields the second-order thermal boundary layer equations. Thus,

$$\begin{aligned} &Pr^{-1} G'' + fG' - \Lambda_{T_w - H_1} f' G - 2\sigma (f' G_\sigma - f_\sigma G') = \Lambda_{T_w - H_1} F' g \\ &\quad - Fg' - 2\sigma (F' g_\sigma - F_\sigma g') - 2Ef''F'' \\ &\quad + B_1 [-Pr^{-1}(\eta g')' + Ef''(\eta f'' + 2f')] \\ &\quad + B_t [-Pr^{-1}(\eta g')' + Ef''(\eta f'' + 2f')], \\ &G(\sigma, 0) = 0, \quad G(\sigma, \eta) = B_H(\eta - \alpha) \text{ as } \eta \to \infty. \end{aligned} \tag{3.23}$$

In the above equations, $\Lambda_{T_w-H_1}$ is the thermal principal function defined as

$$\Lambda_{T_w-H_1} = 2\sigma/[T_w-H_1(0)]\ \partial[T_w-H_1(0)]/\partial\sigma. \qquad (3.24)$$

The thermal principal function, $\Lambda_{T_w-H_1}$, will be constant for self-similar flows whereas for nonsimilar flows, it varies along the streamwise direction. For convenience of writing, we have introduced Eckert number, E, and a quantity B_H defined as

$$E = U_1^2(s,0)/[T_w - H_1(0)], \qquad (3.25)$$

$$B_H = \sqrt{(2\sigma)}\, H_1'(0)/[T_w - H_1(0)]\ . \qquad (3.26)$$

Since we are interested in studying the self-similar solutions, we assume that the functions g and G are of the following form:

$$g(\sigma,\eta) = g_1(\eta) + Eg_2(\eta)\ , \qquad (3.27)$$

$$G(\sigma,\eta) = \sum_i B_i[G_1^{(i)}(\eta) + E\,G_2^{(i)}(\eta)],\ i=l,t,d,v,H \qquad (3.28)$$

while $\Lambda_{T_w-H_1}$ is constant, denoted by Λ. In writing the above equations, we have exploited the linearity of the energy equations and separated the heat transfer due to the prescribed wall temperature $[g_1'(0)$ and $G_1'(0)]$ and viscous dissipation $[g_2'(0)$ and $G_2'(0)]$. Thus the heat transfer problem can be solved independent of the Eckert number. Further, in writing (3.28), we have again subdivided the second-order problem into various physically meaningful problems; as was done for the momentum transfer case. Finally, it can be easily shown that Λ is the index of power law for wall temperature variation: $T_w = T_\infty + C\sigma^{-\Lambda/2}$, where C is a constant.

Substitution of (3.27) and (3.28) in (3.22) and (3.23) yields the following ordinary differential equations of the thermal boundary-layer problem:

First-Order:

$$\begin{aligned} &Pr^{-1} g_1'' - f g_1' \quad \Lambda f' g_1 = 0, \\ &g_1(0) = 1, \quad g_1(\infty) = 0. \end{aligned} \tag{3.29}$$

$$\begin{aligned} &Pr^{-1} g_2'' - f g_2' - 2\beta f' g_2 = -f''^2, \\ &g_2(0) = 0 = g_2(\infty). \end{aligned} \tag{3.30}$$

Second-Order:

$$\begin{aligned} &Pr^{-1} G_1''(i) + f G_1'(i) - (\Lambda + \lambda_i) f' G_1^{(i)} + (1 + \lambda_i) F^{(i)} g_1' \\ &\qquad - \Lambda F'(i) g_1 = M_i, \\ &G_1^{(i)}(0) = 0, \; G_1^{(i)}(\eta) = d_i \quad \text{as} \quad \eta \to \infty. \end{aligned} \tag{3.31}$$

$$\begin{aligned} &Pr^{-1} G_2''(i) + f G_2'(i) - (2\beta + \lambda_i) f' G_2^{(i)} + (1 + \lambda_i) F^{(i)} g_2' \\ &\qquad - 2\beta F'(i) g_2 + 2 f'' F''(i) = N_i, \\ &G_2^{(i)}(0) = 0 = G_2^{(i)}(\infty). \end{aligned} \tag{3.32}$$

where λ_i, M_i, N_i and d_i for various second-order effects (denoted by superscript $i = l, t, d, v, H$) are given in Table 3.2.

It may be noted that even when the dissipation terms are included, the similarity is obtained when the Eckert number, E, is constant; this leads to $\Lambda = 2\beta$. This condition implies that the wall temperature cannot be prescribed arbitrarily; it will depend on the value of the pressure gradient parameter for the given problem.

Table 3.2: The values of λ's, d's, M's and N's in the second-order thermal boundary-layer equations for liquids.

Second-order effect	i	λ_i	M_i	d_i	N_i
Longitudinal curvature	l	Λ_l	$-Pr^{-1}(\eta g_1')'$	0	$-Pr^{-1}(\eta g_2')'+f''(2f'-\eta f'')$
Transverse curvature	t	Λ_t	$-Pr^{-1}(\eta g_1')'$	0	$-Pr^{-1}(\eta g_2')'+f''(2f'-\eta f'')$
Displacement speed	d	Λ_d	0	0	0
External vorticity	v	$1-2\beta$	0	0	0
Temperature gradient in on-coming stream	H	$1-\Lambda$	0	$\eta-\alpha$	0

3.5 Heat Transfer and Recovery Factor:

The total heat transfer rate at the wall is given by

$$q = -k(\partial T/\partial n)_{n=0} \qquad (3.33)$$

where k is the thermal conductivity of the liquid. Substituting the expansion of T from (2.13) and using relations (3.1), (3.20), (3.21), (3.27) and (3.28), the above expression for q may be written as

$$q = -Pr^{-1} r^j U_1(s,0) R^{-1/2}(T_w - H_1)(2\sigma)^{-1/2}(q_1 + R^{-1/2} q_2 + \ldots)$$

with

$$q_1 = g_1'(0) + E g_2'(0)$$

$$q_2 = \sum_i B_i [G_1'^{(i)}(0) + E G_2'^{(i)}(0)], \quad i = l, t, d, v, H \qquad (3.34)$$

As mentioned earlier, the full similarity of heat transfer problem with dissipation exists only for $\Lambda = 2\beta$ which corresponds to constant Eckert number.

The temperature of an insulated wall T_r (also known as the recovery temperature) is defined as the wall temperature for which the total heat transfer rate q is zero. The expression (3.34) with q = 0 gives the following expression for the recovery temperature:

$$T_r = H_1(0) - U_1^2(s,0)\, g_2'(0)/g_1'(0) + U_1^2(s,0)\, R^{-1/2} \sum_i B_i [\{g_2'(0)\, G_1'^{(i)}(0) - g_1'(0)\, G_2'^{(i)}(0)\}/g_1'^2(0)] - R^{-1/2} B_{\bar{H}} U_1^2(s,0)\, G_1'^{(H)}(0)/g_1'(0) \quad , \; i = l,t,d,v \qquad (3.35)$$

where $B_{\bar{H}} = \sqrt{(2\sigma)} H_1'(0)/U_1^2(s,0)$. A move convenient way to study the recovery temperature is to express it in nondimensional form, called the recovery factor and defined as

$$r_f = 2[T_r - H_1(0)]/U_1^2(s,0) \qquad (3.36)$$

It may be noted that the recovery temperature and recovery factor are functions of Reynolds number R and also call for the following expansions as $R \to \infty$:

$$T_r = T_{r_1} + R^{-1/2}\, T_{r_2} + \cdots . \qquad (3.37)$$

$$r_f = r_1 + R^{-1/2} r_2 + \cdots .$$

with $$r_2 = \sum_i B_i\, r_2^{(i)} \quad , \; i = l,t,d,v,\bar{H} \qquad (3.38)$$

Substituting (3.35) in (3.36) and using (3.38), we obtain the following expressions for the first and second-order recovery factor:

$$r_1 = -2g_2'(0)/g_1'(0) \tag{3.39}$$

$$r_2^{(i)} = 2\,[g_2'(0)\,G_1'^{(i)}(0) - g_1'(0)\,G_2'^{(i)}(0)]/g_1'^2(0), \quad i = l, t, d, v \tag{3.40a}$$

$$r_2^{(H)} = 2\,[G_1'(0)/g_1'(0)] \tag{3.40b}$$

Introducing the recovery temperature (3.35) into the expression (3.34) for the total heat transfer rate q and with $\Lambda = 2\beta$, we obtain the following expression for q:

$$q = -Pr^{-1} r^j (2\sigma)^{-1/2} R^{-1/2} U_1(s,0)\,[T_w - T_r]\,[g_1'(0) + R^{-1/2} \sum_{i=l,..v} B_i G_1'^{(i)}(0)] \tag{3.41}$$

This shows when the wall temperature, T_w, equals the recovery temperature, T_r, there is no heat transfer at the wall.

For convenience of discussion, we define the coefficient of heat transfer, C_h, as

$$C_h \equiv q(2\sigma)^{1/2} Pr\, R^{1/2}/[r^j U_1(s,0)(T_w - T_r)] = -g_1'(0) - R^{-1/2} \sum_i B_i G_1'^{(i)}(0), \quad i = l,t,d,v. \tag{3.42}$$

3.6 Exact solution for the Displacement Speed Problem:

The displacement speed problem for jointly self-similar case, i.e. $\Lambda_d = 0$, has the following close form solution:

$$F^{(d)} = (\eta f' + f)/2, \tag{3.43a}$$

$$G_1^{(d)} = \eta g_1'/2, \tag{3.43b}$$

$$G_2^{(d)} = 2g_2 + \eta g_2'/2. \tag{3.43c}$$

Using the above solution, the second-order contribution to recovery factor can be expressed in terms of the first-order recovery factor by the following relation:

$$r_2^{(d)} = 2r_1, \tag{3.44}$$

3.7 Discussion:

The heat-transfer at the wall and recovery factor are obtained by integrating equations (3.29)-(3.32) along with those of momentum transfer, namely (3.12) and (3.13). The numerical integration was performed by using Runge-Kutta-Gill method on IBM-7044 Computer at Indian Institute of Technology, Kanpur. The step size used was $\Delta\eta = .05$ and all the calculations were carried out in double precision to minimise the round off errors. The equations were integrated for full similarity with dissipation which corresponds to $\Lambda = 2\beta$. Contributions of longitudinal curvature, transverse curvature, displacement speed, external vorticity and temperature gradient (in on coming stream) to heat transfer, $G_1'(0)$, and recovery factor, r_2 are displayed graphically. It may be noted that the heat transfer $G_1'(0)$ [due to prescribed wall temperature], $G_2'(0)$ [due to viscous dissipation] and recovery factor, r_2, are related to each other so that given any two of these quantities, the third can be determined. Therefore, we present results only for two of these quantities, namely heat transfer, $G_1'(0)$, and recovery factor, r_2, in the range $-.1988... \leq \beta \leq 2.0$, $0.5 \leq Pr \leq 5.0$ and $-2.0 \leq \Lambda_1, \Lambda_t, \Lambda_d \leq 5.0$. We shall first discuss below each of the second-order effect separately and then a comparative study of these effects will be given for a representative case.

The second-order contribution due to longitudinal curvature to heat transfer $G_1'(0)$ is shown in Figure 3.4. A large

number of infinite discontinuities are observed for $\Lambda_1 < 0$ while for $\Lambda_1 \geq 0$, the heat transfer is well behaved. Such types of discontinuities for $\Lambda_1 < 0$ are also reported by Afzal and Oberai (1972). An elaborate discussion of such discontinuities was given in §3.3 and, therefore, it is unnecessary to discuss results for negative values of Λ_1. For $\Lambda_1 \geq 0$, Figure 3.4 shows that for given Λ_1 and Pr, the heat transfer $G_1'(0)$ decreases as β increases. Further, the heat transfer $G_1'(0)$ increases as Λ_1 (alternately Pr) increases for a given Pr (given Λ_1) and β. Since the sign of the second-order heat transfer $G_1'(0)$ is opposite to that of the first order heat transfer $g_1'(0)$, the positive longitudinal curvature (convex surface) will decrease the total heat transfer. The second-order recovery factor r_2 due to longitudinal curvature is plotted in Figure 3.5 which shows that the recovery factor r_2 decreases (in magnitude) as β increases. Further, the recovery factor increases (in magnitude) as Λ_1) (alternately Pr) increases for a given Pr (given Λ_1) and β. As the first and second-order recovery factors are of opposite signs, the overall recovery factor decreases on a convex surface.

The effect of the transverse curvature on the second-order heat transfer $G_1'(0)$ and recovery factor r_2 are, respectively shown in Figures 3.6 and 3.7. Again we observe several infinite discontinuities for $\Lambda_t < 0$ which are of similar nature as for the case of the longitudinal curvature and, therefore, no additional comment is needed. For $\Lambda_t \geq 0$, we observe from Figure 3.6 that the heat transfer $G_1'(0)$ decreases (in magnitude) as β increases.

Further, as Λ_t (alternately Pr) increases for a given Pr (given Λ_t) and β, the heat transfer $G_1'(0)$ increases in magnitude. The sign of heat transfer $G_1'(0)$ being negative (which is same as that of the first-order heat transfer), the total heat transfer will increase for positive transverse curvature. Figure 3.7 shows that the recovery factor r_2 decreases as β increases. For a given Pr and β, the recovery factor r_2 increases as Λ_t increases. Further, the recovery factor r_2 is positive for $Pr > 1$ and negative for $Pr < 1$ which leads to the conclusion that the total recovery factor for positive transverse curvature will increase for $Pr > 1$ and decrease for $Pr < 1$.

The solutions to the displacement speed problem for the heat transfer $G_1'(0)$ and recovery factor r_2 are shown in Figures 3.8 and 3.9 respectively. Here again we discuss the results for $\Lambda_d \geq 0$ only for reasons mentioned earlier. Figure 3.8 shows that for $\Lambda_d \geq 0$, the heat transfer $G_1'(0)$ increases (in magnitude) as Λ_d (alternately Pr) increases for a given Pr (given Λ_d) and β. Further, the sign of the heat transfer $G_1'(0)$ being negative, the total heat transfer will increase for positive displacement speed. From Figure 3.9, we observe that the recovery factor r_2 increases as Λ_d (alternately Pr) increases for a given Pr (given Λ_d) and β. Exact solution for the case of $\Lambda_d = 0$ given by (3.44) shows that the second-order recovery factor r_2 can be expressed in terms of the first-order recovery factor r_1 which varies very slightly with β and, therefore, the recovery factor r_2 is also seen to be almost constant for the whole range of β.

Further, the total recovery factor will increase in the presence of the positive displacement speed, since both the first and second-order recovery factors have the same sign.

The second-order contribution of external vorticity to the heat transfer $G_1'(0)$ is shown in Figure 3.10. It is interesting to compare these results with those of Afzal and Oberai (1972). For $\Lambda = 0$ and 1, Afzal and Oberai (1972) have shown that the heat transfer due to vorticity for a given Pr contains an infinite discontinuity for some critical value of β. However, in the present work, for the case of $\Lambda = 2\beta$, we do not observe any such infinite discontinuity. Thus, in contrast to the results of Afzal and Oberai (1972), we note that if we consider the case of the prescribed wall temperature such that full similarity (with dissipation included) is preserved (i.e. $\Lambda = 2\beta$), then the heat transfer $G_1'(0)$ due to vorticity is well-behaved. Figure 3.10 shows that for a given Pr, the heat transfer $G_1'(0)$ decreases (in magnitude) as β increases. Since the sign of the first and second-order contributions to heat transfer is same, the total heat transfer increases in the presence of external vorticity. The second-order recovery factor r_2 due to external vorticity is shown in Figure 3.11 and we observe that the recovery factor r_2 is well-behaved in the sense that no singularity of the type mentioned earlier is encountered. For a given β, the recovery factor r_2 increases as Pr increases while for a fixed Pr, the recovery

factor r_2 decreases as β increases. Since both the first and second-order recovery factors are positive, the overall recovery factor increases due to external vorticity.

For the temperature gradient (in on-coming stream) problem, the heat transfer $G_1'(0)$ is same as reported by Afzal and Oberai (1972) while G_2 is identically zero. The second-order recovery factor r_2 due to temperature gradient is shown in Figure 3.12 . As Pr (alternately, β) increases for a given β (given Pr), the recovery factor r_2 decreases. The sign of the first and second-order recovery factors being same, we conclude that the overall recovery factor will increase in the presence of temperature gradient in the on-coming stream.

In the above discussion, we considered the individual second-order effects. We shall now show a comparison of the second-order results with the first-order in order to indicate the relative importance of the second-order solutions. For the example considered here, we choose the same values of the various parameters as will be done for the case of gases in §3.11, so that the two cases of liquid and gas can also be compared with each other. We choose $\beta = 0.5$, Pr = 0.7, Λ_l, Λ_t and $\Lambda_d = 0$ (jointly self-similar case): the corresponding heat transfer coefficient, C_h, defined by (3.42), is given by

$$C_h = 0.6665 - .2716\, B_l R^{-1/2} + 0.5683\, B_t R^{-1/2} + 0.3332\, B_d R^{-1/2} + .0.5023\, B_v R^{-1/2} + O(R^{-1}) \qquad (3.45)$$

If we choose $B_l R^{-1/2}$, $B_t R^{-1/2}$ etc. to be 0.1, we find that the second-order contributions due to longitudinal curvature is about 4%, transverse curvature 8%, displacement speed 5% and external vorticity 7.5% when compared to the first-order contribution. Further, as parameters $B_l R^{-1/2}$ etc. increase, the relative magnitude of the second-order effects increases; when $B_l R^{-1/2}$ etc. become of the order unity, the expression (3.45) shows that the second-order contributions are as important as the first-order itself and as such the second-order theory dose not hold good. Therefore, the above results may be used only when the parameters $B_l R^{-1/2}$ etc are less than order unity. The corresponding result for the recovery factor gives the following expression:

$$r_f = 0.8356 - 3.840\ B_l R^{-1/2} - .0758\ B_t R^{-1/2} + 1.6713\ B_d R^{-1/2} + 2.594\ B_v R^{-1/2} + 1.789\ B_H R^{-1/2} + O(R^{-1}) \qquad (3.46)$$

Here, as compared to the first-order, the contribution due to longitudinal curvature is 45%, transverse curvature 1%, displacement speed 4%, external vorticity 21% and temperature gradient (in oncoming stream) 21%. It may be seen from equation (3.46) that we have to restrict $B_l R^{-1/2}$ etc. to values less than 0.2; thus for an insulated wall the parameters $B_l R^{-1/2}$ etc. are restricted to a much lower value as compared to the case of a prescribed wall temperature. However, these comparisons are for the particular case considered here and no general conclusions may be drawn from the limited discussion given above.

PART II HEAT TRANSFER IN GASES

3.8 Thermal Boundary-Layer Equations for Self-Similar Solutions:

The thermal boundary-layer equations for gases are given by (2.33) and (2.34) as listed in §2.5 of Chapter 2. The procedure of obtaining the equations for self-similar solutions is essentially similar to that described for liquids in Part I. We, therefore, mention here only the important steps leading to the final set of ordinary differential equations. The first and second-order temperatures are assumed to be of the following form:

$$t_1 + u_1^2/2 = [T_w - H_1(0)]\, g(\sigma,\eta) + H_1(0), \tag{3.47}$$

$$t_2 + u_1 u_2 = [T_w - H_1(0)]\, G(\sigma,\eta). \tag{3.48}$$

Substituting the above expressions in (2.33) and (2.34), the governing thermal boundary-layer equations are reduced to the following forms:

First-Order:

$$\Pr^{-1}\bar{g}'' + f\bar{g}' - \Lambda_{T_w-H_1} f'\bar{g} - 2\sigma(f'\bar{g}_\sigma - f_\sigma \bar{g}') = E(\Pr^{-1}-1)(f'f'')',$$
$$\bar{g}(\sigma,0) = 1, \quad \bar{g}(\sigma,\infty) = 0. \tag{3.49}$$

Second-Order:

$$\begin{aligned}\Pr^{-1}\bar{G}'' + f\bar{G}' &- \Lambda_{T_w-H_1} f'\bar{G} - 2\sigma(f'\bar{G}_\sigma - f_\sigma \bar{G}') = \Lambda_{T_w-H_1} F'\bar{g} \\ &- F\bar{g}' + 2\sigma(F'\bar{g}_\sigma - F_\sigma \bar{g}') - E(\Pr^{-1}-1)(f'F')'' \\ &- B_t[\Pr^{-1}(\eta\bar{g}')' + E(\Pr^{-1}-1)\{\eta(f'f'')' + 3f'f''\}] \\ &+ B_1[-\Pr^{-1}(\eta\bar{g}')' + E\{(\Pr^{-1}-1)\eta(f'f'')' + (\Pr^{-1}+1)f'f''\}]\end{aligned}$$
$$\bar{G}(\sigma,0) = 0, \quad \bar{G}(\sigma,\eta) = B_H(\eta-\alpha) \quad \text{as} \quad \eta \to \infty \tag{3.50}$$

Here Λ_{T_w-H} , B_1, B_t, B_H and E are same as defined in Part I and no further comment is needed.

To obtain the self-similar equations, we assume that $\bar{g}$ and $\bar{G}$ are of the same form as was assumed for liquids, viz.

$$\bar{g}(\sigma,\eta) = \bar{g}_1(\eta) + E\bar{g}_2(\eta), \tag{3.51}$$

$$\bar{G}(\sigma,\eta) = \sum_i B_i[\bar{G}_1^{(i)}(\eta) + \bar{G}_2^{(i)}(\eta)], \quad i = 1,t,d,v,H \tag{3.52}$$

Substituting the above forms of $\bar{g}$ and $\bar{G}$ in (3.49) and (3.50), we obtain the following system of ordinary differential equations for the first-order and the second-order heat transfer for gases:

First-Order:

$$Pr^{-1}\bar{g}_1'' + f\bar{g}_1' - \Lambda f'\bar{g}_1 = 0,$$

$$\bar{g}_1(0) = 1, \ \bar{g}_1(\infty) = 0. \tag{3.53}$$

$$Pr^{-1}\bar{g}_2'' + f\bar{g}_2' - 2\beta f'\bar{g}_2 = (Pr^{-1}-1)(f'f'')',$$

$$\bar{g}_2(0) = 0 = \bar{g}_2(\infty). \tag{3.54}$$

Second-Order:

$$Pr^{-1}\bar{G}_1''^{(i)} + f\bar{G}_1'^{(i)} - (\Lambda+\lambda_i)f'\bar{G}^{(i)} + (1+\lambda_i)F^{(i)}\bar{g}_1' - \Lambda F'^{(i)}\bar{g}_1 = Q_i,$$

$$\bar{G}_1^{(i)}(0) = 0, \ \bar{G}_1^{(i)}(\eta) = b_i \ \text{ as } \eta \to \infty. \tag{3.55}$$

$$Pr^{-1}\bar{G}_2''^{(i)} + f\bar{G}_2'^{(i)} - (2\beta+\lambda_i)f'\bar{G}_2^{(i)} + (1+\lambda_i)F^{(i)}\bar{g}_2' - 2\beta F'^{(i)}\bar{g}_2 - (Pr^{-1}-1)(f'F'^{(i)})'' = R_i, \tag{3.56}$$

$$\bar{G}_2(0) = 0 = \bar{G}_2(\infty). \tag{3.56}$$

where λ_i, Q_i, b_i and R_i for various second-order effects are given in Table 3.3.

Table 3.3: The values of λ's, Q's, b's and R's in the second-order thermal boundary-layer equations for gases.

Second-order effect	i	λ_i	Q_i	b_i	N_i
Longitudinal curvature	l	Λ_l	$-Pr^{-1}(\eta\bar{g}_1')'$	0	$-Pr^{-1}(\eta\bar{g}_2')'+(Pr^{-1}+1)f'f''$ $+(Pr^{-1}-1)\eta(f'f'')'$
Transverse curvature	t	Λ_t	$-Pr^{-1}(\eta\bar{g}_1')'$	0	$-Pr^{-1}(\eta\bar{g}_2')'+(Pr^{-1}-1)$ $[-\eta(f'f'')'-3f'f'']$
Displacement speed	d	Λ_d	0	0	0
External vorticity	v	$1-2\beta$	0	0	0
External enthalpy gradient	H	$1-\Lambda$	0	$\eta-\alpha$	0

Again we remark that the full similarity with dissipation is obtained with $\Lambda = 2\beta$. Further, it may be noted that the thermal boundary-layer equations corresponding to the prescribed wall temperature (i.e, for $\bar{g}_1$ and $\bar{G}_1^{(i)}$) are the same as obtained earlier for liquids (i.e. for g_1 and $G_1^{(i)}$) in Part I, thus the solution for $\bar{G}_1^{(i)}$ is the same as that for $G_1^{(i)}$ given in Part I.

3.9 Heat Transfer and Recovery Factor:

Following the same procedure as in §3.5 for liquids, we write down the expression for total heat transfer at the wall. Thus,

$$q = -Pr^{-1}r^{j}\, U_1(s,0)\, R^{-1/2}[T_w - H_1(0)](2\sigma)^{-1/2}$$
$$[\bar{g}_1'(0) + E\bar{g}_2'(0) + R^{-1/2} \sum B_i \{\bar{G}_1'^{(i)}(0) + E\bar{G}_2'^{(i)}(0)\}],$$
$$i = l,t,d,v,H \qquad (3.57)$$

Putting $q = 0$ in (3.57) and using (3.36), we obtain the following expression for the recovery factors:

$$\bar{r}_1 = 1 - 2\bar{g}_2'(0)/\bar{g}_1'(0) \qquad (3.58)$$

$$\bar{r}_2^{(i)} = 2[\bar{g}_2'(0)\,\bar{G}_1'^{(i)}(0) - \bar{g}_1'(0)\,\bar{G}_2'^{(i)}(0)]/\bar{g}_1'^{2}(0),$$
$$i = l,t,d,v \qquad (3.59a)$$

$$\bar{r}_2^{(H)} = 2\bar{G}_1'(0)/\bar{g}_1'(0). \qquad (3.59b)$$

The heat transfer coefficient, with $\Lambda = 2\beta$, is defined as

$$\bar{C}_h \equiv q(2\sigma)^{1/2} Pr\, R^{1/2}[r^{j}U_1(s,0)\,(T_w - T_r)]$$
$$= -\bar{g}_1'(0) - R^{-1/2} \sum_{i=l,..v} B_i\, \bar{G}_1'^{(i)}(0) \qquad (3.60)$$

3.10 Exact Solution for the Displacement Speed Problem:

As in the case of liquids, here again we can express the solution of the displacement speed problem for $\Lambda_d = 0$ in terms of the first-order solution. Thus,

$$F^{(d)} = (\eta f' + f)/2,$$
$$\bar{G}_1^{(d)} = \eta\,\bar{g}_1'/2, \qquad (3.61)$$
$$\bar{G}_2^{(d)} = 4\bar{g}_2 + \eta\,\bar{g}_2'/2.$$

Using the above solution, we can again express the second-order recovery factor in terms of the first-order recovery factor as

$$\bar{r}_2^{(d)} = 2\bar{r}_1. \qquad (3.62)$$

3.11 Discussion:

The heat transfer at the wall and recovery factor are obtained in the same way as described in §3.7 of Part I. As mentioned earlier, the solution for $\bar{G}_1$ is identical with that of G_1 obtained for liquids and, therefore, it is unnecessary to discuss it here. We shall present results for the second-order recovery factor $\bar{r}_2$ only and discuss the contributions of individual second-order effects.

The contribution of the longitudinal curvature to the recovery factor $\bar{r}_2$ is shown in Figure 3.13. For a given Pr and $\Lambda_1 \geq 0$, we observe that the recovery factor $\bar{r}_2$ decreases (in magnitude) as β increases. Further, for $\Lambda_1 = 0$ and $Pr \geq .7$, the second-order recovery factor $\bar{r}_2$ is seen to be negative and its sign is, therefore, opposite to that of the first-order recovery factor and we conclude that in presence of the convex longitudinal curvature, the total recovery factor decreases as Pr increases.

The second-order effect of transverse curvature on the recovery factor $\bar{r}_2$ is shown in Figure 3.14. For fixed $\Lambda_t \geq 0$, the recovery factor $\bar{r}_2$ is positive for $Pr > 1$ and negative for $Pr < 1$. Thus we conclude that positive transverse curvature will increase the overall recovery factor r_f for $Pr > 1$ and decrease for $Pr < 1$.

The effect of displacement on the second-order recovery factor $\bar{r}_2$ is shown in Figure 3.15. For $\Lambda_d \geq 0$, the recovery factor $\bar{r}_2$ is positive for $Pr > 1$ and negative for $Pr < 1$.

Since the first-order recovery factor r_1 is positive, the second-order recovery factor $\bar{r}_2$ will add to the first-order recovery factor r_1 for Pr > 1 whereas the total recovery factor r_f will decrease for Pr < 1.

The second-order contribution due to external vorticity to recovery factor r_2, as function of β with Pr as the parameter is shown in Figure 3.16. For a given Pr, the second-order contributions are larger for negative β as compared to those for positive β. The recovery factor $\bar{r}_2$ is positive for Pr > 1 and negative for Pr < 1. As compared to the first-order recovery factor r_1, the sign of the second-order recovery factor $\bar{r}_2$ is same for Pr > 1 and hence, the total recovery factor r_f increases (for Pr < 1, the total recovery factor r_f decreases).

For the stagnation enthalpy problem, the second-order recovery factor $\bar{r}_2$ is identical to r_2, obtained for liquids in Part I (shown in Figure 3.12); no further comments are needed.

As in Part I, we present now a comparison of the first-order with the second-order solutions. We consider a practical case of stagnation region of an axisymmetric body flying in air. Thus, $\beta = 0.5$, Pr = 0.7, Λ_1, Λ_t and $\Lambda_d = 0$ (jointly self-similar case). We note that the same set of parameters were used for the case of liquids also. Further, the solution for $\bar{G}_1$ being the same as that for G_1 discussed in Part I, we

shall present here results for the recovery factor $\bar{r}_2$ only. For the case mentioned above, the total recovery factor r_f is given by

$$r_f = 0.8356 - 0.1670\ B_1 R^{-1/2} - 0.0758\ B_t R^{-1/2} - .3286\ B_d R^{-1/2} - 0.8031\ B_v R^{-1/2} - 0.351\ B_H R^{-1/2} + O(R^{-1}) \qquad (3.63)$$

If we again choose $B_1 R^{-1/2}$ etc. to be 0.1, we find that as compared to the first-order, the second-order contribution due to longitudinal curvature is about 2%, transverse curvature 1%, displacement speed 4%, external vorticity 10% and external enthalpy gradient 4%. Equation (3.63) suggests that to obtain meaningful results for the second-order effects, $B_1 R^{-1/2}$ etc. are to be restricted to values less than order unity.

The main results of Part I and Part II are contained in references [3] and [4] respectively.

CHAPTER 4

LOCALLY-SIMILAR SOLUTIONS TO THE SECOND-ORDER BOUNDARY-LAYER EQUATIONS FOR TWO-DIMENSIONAL FLOWS

4.1 Introduction:

In the previous chapter, we studied the self-similar solutions of the boundary-layer equations. In various engineering problems, however, there are flow situations where the similarity conditions are not met and, therefore, one has to deal with the nonsimilar flows. Nevertheless, the self-similar solutions are of considerable interest since they represent the leading term of the locally-similar expansion. In literature various methods are available to deal with the nonsimilar flows; a brief discussion of these methods, with relative merits and demerits, is given in Chapter 1 and as mentioned there, we adopt here the Görtler series method to construct the locally-similar solutions of the second-order boundary-layer flows. In this method, the stream function and temperature are represented by a power series having streamwise coordinate σ as the expansion parameter. Likewise, the pressure gradient parameter and the second-order parameters are also expanded in terms of σ. The method is applied to uniform flow past two-dimensional bodies where the second-order contributors present are longitudinal curvature and displacement speed. Although the

treatment of the problem, in its essence, is quite general, detailed solutions are presented only for a blunted wedge geometry.

We consider, in detail, the boundary-layer solutions for a steady uniform flow (free of vorticity) past a semi-infinite, symmetric blunted wedge of included angle $\beta_\infty \pi$ such that $0 \leq \beta_\infty \leq 1$ (see Figure 4.1). Parabola ($\beta_\infty = 0$) and flat plate normal to flow direction ($\beta_\infty = 1$) are the two special degenerate cases of the blunted wedge. The boundary-layer flow on a blunted wedge starts from a two-dimensional stagnation point, then accelerates in the downstream direction and finally approaches that past a wedge of included angle $\beta_\infty \pi$. Thus, at the stagnation point ($\sigma = 0$) and far downstream ($\sigma \to \infty$), the flow is similar while in the intermediate region, it has to be regarded as nonsimilar. The first-order velocity boundary-layer on a blunted wedge has been studied by Chen et.al. (1969) while the thermal boundary-layer was considered by Chen (1970). Further, the leading term (corresponding to the stagnation point) of the second-order contribution for a parabola has been obtained by Van Dyke (1964a).

The Görtler series method is used to obtain skin friction and heat transfer distribution on a blunted wedge. Out of the two second-order effects present, the longitudinal curvature effect is local in nature and depends only on the

first-order boundary-layer quantities. However, the displacement effect requires the evaluation of the second-order outer velocity $U_2(s, 0)$ and thus has an upstream influence; it is in this spirit that displacement effect is said to be global in nature and exhibits the elliptic nature of the original Navier-Stokes equations. Methods for obtaining $U_2(s, 0)$ are discussed in Chapter 1 and as mentioned there, we solve the perturbed Euler equation with appropriate boundary conditions to get the expression of $U_2(s, 0)$ for a blunted wedge. The first five terms of the power series for skin-friction and heat transfer are evaluated for both the second-order contributors. Since the radius of convergence of the series is limited, we Eulerize the series to extend its range of validity to infinity. The results for large streamwise distances are further improved by accelerating the convergence of the series by using either Shanks non-linear transformation or a polynomial fit to the partial sums of the series. The results of skin-friction and heat transfer distribution for various values of wedge angles are displayed graphically. The skin friction distribution so obtained for the case of a parabola ($\beta_\infty = 0$) is compared with that obtained via exact numerical solutions of the Navier-Stokes equations, by Davis (1972), Dennis and Walsh (1971) and Botta et.al. (1972) and the discrepancy is found to be less than two percent for Reynolds number as low as 10^3.

4.2 Governing Equations of the Boundary-Layer Flow:

Consider an incompressible uniform flow past a semi-infinite two-dimensional body with prescribed wall temperature. The first-order and the second-order velocity and thermal (without dissipation terms) boundary-layer equations may be written as follows (notations employed are same as used in Chapter 2):

First-Order Boundary Layer Equations:

Continuity:
$$u_{1s} + v_{1N} = 0 \tag{4.1a}$$

Momentum:
$$u_1 u_{1s} + v_1 u_{1N} - u_{1NN} = U_1(s,0)U_{1s}(s,0) \tag{4.1b}$$

Energy:
$$u_1 h_{1s} + v_1 h_{1N} - Pr^{-1} h_{1NN} = 0 \tag{4.1c}$$

Boundary conditions:
$$u_1(s,0) = 0 = v_1(s,0),\ h_1(s,0) = T_w \tag{4.1d}$$

Matching conditions:
$$\left.\begin{aligned} u_1(s,N) &= U_1(s,0) \\ h_1(s,N) &= H_1(0) \end{aligned}\right\} \quad N \to \infty \tag{4.1e}$$

Second-Order Boundary-Layer Equations:

Continuity:
$$u_{2s} + v_{2N} = -K(Nv_1)_N \tag{4.2a}$$

Momentum:
$$\begin{aligned} -u_{2NN} = K[&Nu_1u_{1s} - NU_1(s,0)U_{1s}(s,0) \\ &+u_{1N}-u_1v_1]-[KNU_1^2(s,0) \\ &+K\int_N^\infty U_1^2(s,0)-u_1^2\, dN]_s \\ &+[U_1(s,0)U_2(s,0)]_s \end{aligned} \tag{4.2b}$$

Energy:
$$\begin{aligned} u_1 h_{2s} + v_1 h_{2N} + u_2 h_{1s} + v_2 h_{1N} \\ -Pr^{-1} h_{2NN} = K(NU_1 h_{1s} + Pr^{-1} h_{1N}) \end{aligned} \tag{4.2c}$$

Boundary conditions:
$$u_2(s,0) = 0 = v_2(s,0),\ h_2(s,0) = 0 \tag{4.2d}$$

Matching conditions:
$$\left.\begin{aligned} u_2(s,N) &\sim -KNU_1(s,0) + U_2(s,0), \\ h_2(s,N) &= H_1'(0)\,\Psi_1(s,N) \end{aligned}\right\} N \to \infty \tag{4.2e}$$

It may be noted that the momentum transfer equations are same as those given by Narasimha and Ojha (1967).

4.3 Nonsimilar Solutions to the Momentum Transfer Problem:

We shall use the Görtler type variables, defined as,

$$\sigma = \int_0^s U_1(s,0)\,ds \ , \quad \eta = (2\sigma)^{-1/2} U_1(s,0)\,N. \qquad (4.3)$$

The first and second-order stream functions ψ_1 and ψ_2 are introduced so that the equations of continuity (4.1a) and (4.2a) are automatically satisfied. Thus,

$$u_1 = \psi_{1N} \ , \quad v_1 = -\psi_{1s} \qquad (4.4)$$

$$u_2 = \psi_{2N} \ , \quad v_2 + KNv_1 = -\psi_{2s} \qquad (4.5)$$

We assume the following forms for the first and second-order stream functions

$$\psi_1 = (2\sigma)^{1/2} f(\sigma,\eta) \qquad (4.6)$$

$$\psi_2 = (2\sigma)^{1/2} F(\sigma,\eta) \qquad (4.7)$$

so that the momentum equations (4.1b) and (4.2b) are reduced to the following forms:

First-order velocity boundary-layer equations:

$$f''' + ff'' + \Lambda_{U_1}(1-f'^2) - 2\sigma\,(f'f_\sigma - f_\sigma f'') = 0, \qquad (4.8a)$$

$$f(\sigma,0) + 2\sigma f_\sigma(\sigma,0) = 0, \qquad (4.8b)$$

$$f'(\sigma,0) = 0, \quad f'(\sigma,\infty) = 1. \qquad (4.8c,d)$$

Here Λ_{U_1} is same as defined earlier by (3.5).

Second-order velocity boundary-layer equations:

$$\begin{aligned} F''' + fF'' - 2\Lambda_{U_1} f'F' + f'F' - 2\sigma\,(f_\sigma F' - f'F_\sigma + f'F_\sigma - f_\sigma F'') \\ = B_1[-\eta(1+\Lambda_{U_1})f''' + (\Lambda_{B_1}+\Lambda_{U_1}-1)(f'' + ff' + 2\sigma f' f_\sigma \\ + 4\sigma \int_\eta^\infty f' f'_\sigma\,d\eta) + (2\Lambda_{U_1}+\Lambda_{B_1})(\Lambda_{U_1} + \alpha + 2\sigma\alpha_\sigma)]/(1+\Lambda_{U_1}) \\ - B_d(2\Lambda_{U_1} + \Lambda_{B_d}), \end{aligned} \qquad (4.9a)$$

$$F(\sigma, 0) + 2\sigma F_{\sigma}(\sigma, 0) = 0, \tag{4.9b}$$

$$F'(\sigma, 0) = 0, \quad F'(\sigma, \eta) \sim -B_1 \eta + B_d \text{ as } \eta \to \infty \tag{4.9c,d}$$

Here the quantities B_1 and B_d are given by, respectively (3.9b) and (3.9d) with $j = 0$ while Λ_{B_1} and Λ_{B_d} are defined by (3.10). It may be emphasized again that the generalized local pressure gradient parameter Λ_{U_1}, longitudinal curvature parameter Λ_{B_1}, and displacement speed parameter Λ_{B_d} are functions of streamwise coordinate σ and the form of these parameters varies for different flow conditions and geometric configurations. We assume the following general form of these parameters

$$\Lambda_{U_1} = \sum_{m=0} \beta_m \sigma^{pm} \tag{4.10a}$$

$$\Lambda_{B_1} = \sum_{m=0} \Lambda_{1_m} \sigma^{qm} \tag{4.10b}$$

$$\Lambda_{B_d} = \sum_{m=0} \Lambda_{d_m} \sigma^{lm} \tag{4.10c}$$

where p, q and l are positive or negative numbers. To study the locally-similar solutions of the second-order problem (2.8)-(2.9), we assume, in addition to (4.10), the following power series for $f(\sigma,\eta)$ and $F(\sigma,\eta)$:

$$f(\sigma,\eta) = \sum_{m=0} f_m(\eta)\, \sigma^{pm} \tag{4.11}$$

$$F(\sigma,\eta) = \sum_{m=0} \left[B_1 F_m^{(1)}(\eta) + B_d F_m^{(d)}(\eta)\right] \sigma^{pm} \tag{4.12}$$

Substituting the above expansions (4.10)-(4.12) in

equations (4.8)-(4.9) and collecting coefficients of the like powers of σ, we obtain the equations for the successive approximations. It may seem desirable to reduce the coefficient functions $F_i(\eta;\ \beta_o;\Lambda_{l_o};\Lambda_{d_o};\ \beta_1,\beta_2\cdots;\Lambda_{l_1},\Lambda_{l_2}\cdots;\ \Lambda_{d_1},\Lambda_{d_2}\cdots)$ to linear combination of (universal) functions that do not depend on β_i,Λ_{l_i} and Λ_{d_i} $(i = 1,2,\ldots n)$. However, it was realized that the velocity boundary-layer alone gives rise to 89 equations as against the original 16 equations while for the thermal boundary-layer; the number of equations becomes even larger. It would be a formidable job to handle such a large number of equations and tabulate the results.. Here we shall be content with solving the fewer original equations for the problem at hand and no attempt will be made to tabulate the universal functions. Instead, we illustrate the procedure in detail for a particular problem, described in the next section.

4.4 Velocity Boundary-Layer on a Blunted Wedge:

We describe here the procedure for studying the locally-similar solutions of the velocity boundary-layer due to uniform (zero vorticity), steady, laminar flow past a blunted wedge shown in Figure 4.1. Let the wedge half-angle be $\beta_\infty\pi/2$ $(0 \leq \beta_\infty \leq 1)$ and its nose radius unity. In the physical plane $Z = x+iy$, the coordinates (s, n) are used to denote respectively distances along the surface of the body and normal to it.

4.4.1 First-Order Problem:

First of all, we have to obtain solutions to the first-order outer problem; in particular we are interested in inviscid flow velocity, $U_1(s, 0)$. For this purpose, conformal mapping is used which transforms a sharp wedge in the physical plane $Z = x+iy$ into the imaginary axis $\chi = 0$ of a plane $\zeta = \chi+i\xi$. The transformation is

$$Z = (1 - \beta_\infty)\, \zeta^{(2-\beta_\infty)}/(2 - \beta_\infty). \tag{4.13}$$

As shown in Figure 4.1, this transformation maps the blunted wedge of include angle $\beta_\infty\pi$ into the line $\chi = 1$. The length element $ds = (dx^2+dy^2)^{1/2}$ in Z-plane is mapped to $dh = (d\chi^2+d\xi^2)^{1/2}$ in ζ-plane by

$$\frac{ds}{dh} = \left|\frac{dZ}{d\zeta}\right| = (1-\beta_\infty)(\chi^2+\xi^2)^{(1-\beta_\infty)/2} \tag{4.14}$$

so that along the surface of the blunted wedge ($\chi = 1$) we have

$$ds = (1-\beta_\infty)(1+\xi^2)^{(1-\beta_\infty)/2}\, d\xi\ . \tag{4.15}$$

The complex flow potential is given by

$$\Phi = -\frac{1}{2}(1-\beta_\infty)(\zeta-1)^2 \tag{4.16}$$

from which we obtain the following expressions for the real velocity potential, ϕ and the stream function, Ψ_1

$$\phi = -\frac{1}{2}(1-\beta_\infty)\left[(\chi-1)^2-\xi^2\right] \tag{4.17}$$

$$\Psi_1 = -(1-\beta_\infty)\,\xi\,(\chi-1) \tag{4.18}$$

The first-order outer velocity along the surface of the blunted wedge, as obtained from (4.17), is given by

$$U_1(s,0) \equiv \left.\frac{\partial \phi}{\partial s}\right|_{\chi=1} = \left.\frac{\partial \phi}{\partial \xi}\cdot\frac{d\xi}{ds}\right|_{\chi=1} = \xi(1+\xi^2)^{-(1-\beta_\infty)/2} \qquad (4.19)$$

In the Görtler method, since the real potential along the surface of the body is used as the streamwise coordinate (denoted by σ), we obtain σ by evaluating (4.17) at $\chi = 1$; thus,

$$\sigma = \phi|_{\chi=1} = (1-\beta_\infty)\,\xi^2/2. \qquad (4.20)$$

The generalized local pressure gradient parameter, Λ_{U_1} for the blunted wedge is now obtained by using (3.5); we have

$$\Lambda_{U_1} \equiv [2\sigma/U_1(s,0)]\; dU_1(\sigma,0)/d\sigma$$

$$= (1-\beta_\infty+2\beta_\infty\sigma)\,(1-\beta_\infty+2\sigma)^{-1} \qquad (4.21)$$

which can be expanded for small σ to yield

$$\Lambda_{U_1} = \sum_{m=0} \beta_m \sigma^m = \beta_0 + \sum_{m=1} (-2)^m (1-\beta_\infty)^{1-m}\,\sigma^m \text{ with } \beta_0 = 1. \qquad (4.22)$$

The solution of the first-order boundary-layer equation (4.8) is expressed as a power series in σ with coefficients depending on η only; thus,

$$f(\sigma,\eta) = \sum_{m=0} f_m(\eta)\,\sigma^m \qquad (4.23)$$

Substituting (4.22) and (4.23) in (4.8) and collecting coefficients of the like powers of σ, we obtain the following recursive system of ordinary differential equations:

$$f_0''' + f_0 f_0'' + \beta_0(1-f_0'^2) = 0 \qquad (4.24a)$$

$$f_m''' + f_0 f_m'' - (2\beta_0+m) f_0' f_m' + (2m+1) f_0'' f_m = \beta_m (f_0'^2 - 1)$$

$$+ \sum_{j=1}^{m-1} \sum_{i=1}^{m-j} \beta_j f_i' f_{m-i-j}' + f_0 \sum_{j=1}^{m-1} \beta_j f_{m-j}' + \sum_{j=1}^{m-1} \{\beta_0 + 2(m-j)\}$$

$$f_j' f_{m-j}' - \sum_{j=1}^{m-1} (1+2j) f_j f_{m-j}'', \quad (m = 1.2.3.\ldots) \qquad (4.24b)$$

with the boundary conditions,

$$f_o(0) = f_o'(0) = 0, \quad f_o'(\infty) = 1,$$

$$f_m(0) = f_m'(0) = 0, \quad f_m'(\infty) = 0 \quad (m=1,2,3\ldots) \qquad (4.24c)$$

Here equation (4.24a) is the well-known Falkner-Skan equation and except for it, all the other equations of the above system are linear. It may be noted here that for $\beta_\infty = 1$, the expansion (4.21) reduces to $\Lambda_{U_1} = 1$ so that all β_∞'s ($m \geq 1$) are zero; consequently the expansion of $f(\sigma, \eta)$ will have only the leading term $f_o(\eta)$ and the other terms $f_m(\eta)$ for $m \geq 1$ are absent. This flow situation corresponds to the stagnation flow (Hiemenz flow) whose solution may be obtained from (4.24a).

The solution for $0 \leq \beta_\infty < 1$ is obtained by solving the set of equations (4.24). Görtler (1957) has tabulated the results for the first six f's in (4.23), by splitting them into linear combination of universal functions so as to make the solution independent of β_m's ($m \geq 1$) and depend on β_o only; the tabulated results are available for $\beta_o = 0$ and 1. For the present case, we are interested in the solutions for $\beta_o = 1$ only. With β's known from (4.22), the first-order solution is known in the series form (4.23) upto first six terms. This solution is needed to evaluate the displacement effect,

4.4.2 Second-Order Problem:

Of the two second-order effects present, we first consider that due to the displacement. In order to study the displacement speed problem, we need to know the second-order outer velocity, U_2.

To evaluate it, we have to first solve the second-order outer flow problem (2.28) which may be expressed in the transformed coordinates (χ, ξ) as

$$(\partial^2\Psi_2/\partial\chi^2) + (\partial^2\Psi_2/\partial\xi^2) = 0 \qquad (4.25a)$$

with the boundary conditions

$$\Psi_2(\xi, 1) = \lim_{N\to\infty} (\psi_1 - N\psi_{1N}) = \sqrt{1-\beta_\infty}\ \xi \lim_{\eta\to\infty} [f(\xi,\eta)-\eta] \qquad (4.25b)$$

$$\Psi_2 = 0 \text{ far upstream.}$$

Here equation (4.25a) is the Laplace equation in transformed coordinates, and the boundary condition (4.25b) specifies that the value of Ψ_2 on the surface of the blunted wedge ($\chi = 1$) is governed by the first-order boundary-layer quantities while the boundary conditions (4.25c) implies that the second-order outer velocity vanishes far upstream. Before proceeding to solve the above equation, we evaluate the right hand side of the boundary condition (4.25b) as follows:

Using (4.23), we rewrite the boundary condition (4.25b) as,

$$\Psi_2(\xi, 1)\,(1-\beta_\infty)^{1/2} \left[\lim_{\eta\to\infty} \sum_{m=1} \{(1/2)(1-\beta_\infty) f_m(\eta)\xi^{2m}\} - \alpha_o\right] \qquad (4.26)$$

where $\alpha_o = \lim_{\eta\to\infty} |\eta - f_o(\eta)|$

Here $f_m(\eta)$ as $\eta\to\infty$ are obtained from the first-order boundary-layer solutions. Using the asymptotic forms of the universal functions along with β's given by (4.22), we get

$$f_1(\infty) = -.367830,$$

$$f_2(\infty) = -.276744 + .633740\ (1-\beta_\infty)^{-1},$$

$$f_3(\infty) = -.227944 + .929008\ (1-\beta_\infty)^{-1} - 1.127664\ (1-\beta_\infty)^{-2},$$

$$f_4(\infty) = -.204192 + 1.147280\,(1-\beta_\infty)^{-1} - 2.414976\,(1-\beta_\infty)^{-2} + 2.047952\,(1-\beta_\infty)^{-3},$$

$$f_5(\infty) = -.196640 + 1.381760\,(1-\beta_\infty)^{-1} - 3.956864\,(1-\beta_\infty)^{-2} + 5.703264\,(1-\beta_\infty)^{-3} - 3.772288\,(1-\beta_\infty)^{-4},$$

$$\alpha_o = .647901. \qquad (4.27)$$

Substitution of (4.27) in (4.26) yields the expression for $\Psi_2(\xi, 1)$ in a series form whose coefficients are multiplied by $\xi^{2m+1}(m = 0,1,2,3,\ldots)$. However, it is observed that the series converges for ξ less than unity due to a singularity at $\xi = \pm i$. It is possible to enlarge the radius of convergence by applying Euler transformation (see §4.5 for detailed discussion) The series (4.26) is recast in powers of a new variable $z=\xi^2/(1+\xi^2)$ Since $\Psi_2(\xi,1)$ is an odd function of ξ whereas z is even, we extract ξ from the series before introducing the z variable. The resulting series for $\Psi_2(\xi,1)$ in terms of z variable is given by

$$\Psi_2(\xi, 1) = \sqrt{(1-\beta_\infty)}\,\xi\,\{.647901 + .183915\,(1-\beta_\infty)\,z + [.025480\,(1-\beta_\infty) + .069186\,(1-\beta_\infty)^2]z^2 + [.008003\,(1-\beta_\infty) + .022246\,(1-\beta_\infty)^2 + .028493\,(1-\beta_\infty)^3]z^3 + [.003487\,(1-\beta_\infty) + .010116\,(1-\beta_\infty)^2 + .013774\,(1-\beta_\infty)^3 + .01272\,(1-\beta_\infty)^4]z^4 + [.001819(1-\beta_\infty) + .005505\,(1-\beta_\infty)^2 + .007790(1-\beta_\infty)^3 + .007868\,(1-\beta_\infty)^4 + .006145\,(1-\beta_\infty)^5]z^5 + \ldots\} \qquad (4.28)$$

Now we shall solve the second-order outer flow problem governed by (4.25a) with boundary conditions (4.25c) and (4.28). Instead of solving the equation formally, we shall write down the solution for $\Psi_2(\xi,\chi)$ by inspection. The terms in (4.28) are replaced by functions of ξ and χ so that they satisfy

the equation (4.25a) and the boundary conditions (4.25c) and (4.28). In order to satisfy the Laplace's equation (4.25a), all the terms in $\Psi_2(\xi,\chi)$ must be harmonic functions and further they should reduce to the form (4.28) at $\chi = 1$ and also have proper behaviour far upstream. The first term in (4.28) is ξ, which is already harmonic and satisfies the boundary conditions on the body surface and upstream; we retain it as such. Other terms in (4.28) are, however, not harmonic. These are replaced by proper harmonic functions which, at $\chi = 1$ should reduce to the original terms of equation (4.28). The final solution, thus obtained, is given by,

$$\begin{aligned}\Psi_2(\xi,\chi) = -(1-\beta_\infty)^{1/2}\{ &.647901\,\xi + .183915\,(1-\beta_\infty)\,[\xi - \xi/(\xi^2+\chi^2)] \\ &+ [.025480\,(1-\beta_\infty) + .069186\,(1-\beta_\infty)^2]\,[\xi - 2\xi/(\xi^2+\chi^2) \\ &+ \xi\chi/(\xi^2+\chi^2)^2] + [.008003\,(1-\beta_\infty) + .022246\,(1-\beta_\infty)^2 \\ &+ .028493\,(1-\beta_\infty)^3]\,[\xi - 3\xi/(\xi^2+\chi^2) + 11\xi\chi/4(\xi^2+\chi^2)^2 \\ &+ \xi^3 - 3\xi\chi^2/4(\xi^2+\chi^2)^3] + [.003487\,(1-\beta_\infty) + .010116\,(1-\beta_\infty)^2 \\ &+ .013774\,(1-\beta_\infty)^3 + .01272\,(1-\beta_\infty)^4]\,[\xi - 4\xi/(\xi^2+\chi^2) \\ &+ 41\xi\chi/8(\xi^2+\chi^2)^2 + 7(\xi^2-3\xi\chi^2)/8(\xi^2+\chi^2)^3 \\ &+ \xi\chi(\xi^2-\chi^2)/2(\xi^2+\chi^2)^4] + [.001819\,(1-\beta_\infty) + .005505\,(1-\beta_\infty)^2 \\ &+ .007790\,(1-\beta_\infty)^3 + .007868\,(1-\beta_\infty)^4 + .006145\,(1-\beta_\infty)^5] \\ &[\xi - 5\xi/(\xi^2+\chi^2) + 515\xi\chi/64(\xi^2+\chi^2)^2 + 125(\xi^3-3\xi\chi^2)/ \\ &64(\xi^2+\chi^2)^3 - 17\xi\chi(\xi^2-\chi^2)/8(\xi^2+\chi^2)^4 \\ &- (\xi^5 - 10\xi^3\chi^2 + 5\xi\chi^4)/16(\xi^2+\chi^2)^5] + \ldots\} \qquad (4.29)\end{aligned}$$

Now we can obtain the displacement speed $U_2(2,0)$ from (4.29). Thus,

$$U_2(s,0) = (1-\beta_\infty)^{-1}\left[(\xi^2+\chi^2)^{(1-\beta_\infty)/2}\,\partial\Psi_2/\partial\chi\right]_{\chi=1}$$
$$= -\sqrt{(1-\beta_\infty)}\;\xi(1+\xi^2)^{(\beta_\infty-5)/2}\left[a_0+a_1z+a_2z^2+a_3z^3+a_4z^4+\ldots\right]$$

where

$$a_0 = .402486 + .095203\,(1-\beta_\infty) + .034238\,(1-\beta_\infty)^2 + .012279\,(1-\beta_\infty)^3 + .003360\,(1-\beta_\infty)^4,$$
$$a_1 = .125430 + .343291\,(1-\beta_\infty) + .087384\,(1-\beta_\infty)^2 + .028978\,(1-\beta_\infty)^3 + .007681\,(1-\beta_\infty)^4,$$
$$a_2 = .062571 + .176210\,(1-\beta_\infty) + .229807\,(1-\beta_\infty)^2 + .055989\,(1-\beta_\infty)^3 + .013826\,(1-\beta_\infty)^4,$$
$$a_3 = .035172 + .102948\,(1-\beta_\infty) + .141352\,(1-\beta_\infty)^2 + .133568\,(1-\beta_\infty)^3 + .02458\,(1-\beta_\infty)^4,$$
$$a_4 = .01819 + .005505\,(1-\beta_\infty) + .0779\,(1-\beta_\infty)^2 + .07868\,(1-\beta_\infty)^3 + .06145\,(1-\beta_\infty)^4. \qquad (4.30)$$

The series in the square bracket is divergent for $\xi > 1$ $(z > \frac{1}{2})$. To ensure that the series is convergent for the whole range of ξ (i.e. upto $z = 1$), different factors of the type $(1+\xi^2)^m$ (where m was varied) were extracted and convergence was tested for each case; these observations suggested that extracting out a factor $\xi(1+\xi^2)^{(\beta_\infty-2)/2}$ resulted in the best convergent series for the complete range of β_∞ $(0 \le \beta_\infty < 1)$. It may be noted that we have excluded the case $\beta_\infty = 1$, since in this case the boundary condition (4.28) reduces to $\Psi_2(\xi,1) = 0$ so that the Laplace's equation is identically satisfied by $\Psi_2(\xi,\chi) = 0$ leading to $U_2(s,0) = 0$.

Using the expression (4.29) of $U_2(s,0)$ along with (4.19) for $U_1(s,0)$, we obtain the following expression for B_d $(=U_2(s,0)/U_1(s,0))$:

$$B_d = -\sqrt{(1-\beta_\infty)}\,(1+\xi^2)^{-1/2}\,[a_o + (a_1 - 3a_o/2)z + (a_2 - 3a_1/2 + 3a_o/8)z^2 + (a_3 - 3a_2/2 + 3a_1/8 + a_o/16)z^3 + (a_4 - 3a_3/2 + 3a_2/8 + a_1/16 + 3a_o/128)z^4 + \ldots] \tag{4.31}$$

Finally, the displacement speed parameter, Λ_{B_d}, defined by

$$\Lambda_{B_d} = (2\sigma/B_d)\,(dB_d/d\sigma) \tag{4.32}$$

is evaluated and written as

$$\Lambda_{B_d} = \Lambda_{d_1}\sigma + \Lambda_{d_2}\sigma^2 + \Lambda_{d_3}\sigma^3 + \Lambda_{d_4}\sigma^4 + \ldots,$$

with

$$\Lambda_{d_1} = 4(1-\beta_\infty)^{-1}\,E_1,$$

$$\Lambda_{d_2} = 8(1-\beta_\infty)^{-2}\,(2E_2 - E_1^2)$$

$$\Lambda_{d_3} = 16(1-\beta_\infty)^{-3}\,[3E_3 - 2E_1E_2 + E_1(E_1^2 - E_2)],$$

$$\Lambda_{d_4} = 32(1-\beta_\infty)^{-4}\,[4E_4 - 3E_1E_3 + 2E_2\,(E_1^2 - E_2) + E_1\,(2E_1E_2 - E_1^3 - E_3)]$$

where

$$E_1 = (a_1 - 2a_o)/a_o,$$

$$E_2 = (a_2 - 3a_1 + 3a_o)/a_o$$

$$E_3 = (a_3 - 4a_2 + 6a_1 - 4a_o)/a_o,$$

$$E_4 = (a_4 - 5a_2 + 10a_2 - 10a_1 + 5a_o)/a_o. \tag{4.33}$$

The other second-order effect present is that due to the longitudinal curvature and will be considered now. The expression for the longitudinal curvature K and B_1 are given by

$$K = [1+2(1-\beta_\infty)^{-1}\,\sigma]^{-(3-\beta_\infty)/2},\quad B_1 = (2\sigma)^{-1/2}\,K/U_1(s,0) \tag{4.34,35}$$

Now the longitudinal curvature parameter Λ_{B_1} is given by

$$\Lambda_{B_1} \equiv \Lambda_{1_1}\sigma + \Lambda_{1_2}\sigma^2 + \Lambda_{1_3}\sigma^3 + \Lambda_{1_4}\sigma^4 + \ldots \text{ say}$$

$$= -4\sigma(1-\beta_\infty + 2\sigma)^{-1} = -4(1-\beta_\infty)^{-1} \sum_{m=1} [-2/(1-\beta_\infty)]^{m-1} \sigma^m \tag{4.37}$$

Again we note that as expected, for $\beta_\infty = 1$ the expression (4.34) gives $K = 0$, meaning thereby that there is no contribution due to the longitudinal curvature for $\beta_\infty = 1$. Thus, the above results are used for $0 \leq \beta_\infty < 1$.

In order to study the second-order momentum transfer problem, we assume, in addition to expansions (4.33) and (4.37), the following expansion for F:

$$F(\sigma, \eta) = B_1 \sum_{m=0} F_i^{(1)}(\eta)\, \sigma^m + B_d \sum_{m=0} F_i^{(d)}(\eta)\, \sigma^m \tag{4.38}$$

In writing down, the above expansion, we have decomposed the contributions due to longitudinal curvature and displacement speed. Substitution of the expansions (4.33), (4.37) and (4.38) in equation (4.9) and collection of the coefficients of the like powers of σ (after terms multiplied by B_d and B_1 have been separated) yields the recursive system of governing equations for the displacement speed and longitudinal curvature problems. The first five equations for both the second-order effects in the range $0 \leq \beta_\infty < 1$ are written as follows (superscripts 1 and d are suppressed):

Displacement Speed:

$$F_o''' + f_o F_o'' - 2\beta_o f_o' F_o' + f_o'' F_o = -2,$$

$$F_o(0) = 0 = F_o'(0), \quad F_o'(\infty) = 1. \tag{4.39a}$$

$$F_m''' + f_o F_m'' - 2\beta_o\, f_o' F_m' + f_m'' F_o + \sum_{i=1}^{m} [(2i+1)(F_i f_{m-i}'' + f_i F_{m-i}'') - (2\beta_o+2i) f_i' F_{m-i}' - 2i F_i' f_{m-i}'] + \sum_{i=1}^{m}\sum_{j=0}^{m-i} [\Lambda_{d_i} f_j'' F_{m-i-j} - (2\beta_i + \Lambda_{d_i}) f_j' F_{m-i-j}'] = -\Lambda_{d_m} - 2\beta_m,$$

$$F_m(0) = 0 = F_m'(0), \quad F_m'(\infty) = 0 \quad (m = 1,2,3,4). \tag{4.39b}$$

Longitudinal Curvature:

$$F_o''' + f_o F_o'' - 2\beta_o\, f_o' F_o' + f_o'' F_o = \eta(1 - f_o'') + \alpha_o,$$

$$F_o(0) = 0 = F_o'(0), \quad F_o'(\eta) \to -\eta \text{ as } \eta \to \infty. \tag{4.40a}$$

$$F_m''' + f_o F_m'' - 2\beta_o\, f_o' F_m' + f_m'' F_o + \sum_{i=1}^{m} [(2i+1)(F_i f_{m-i}'' + f_i F_{m-i}'') - (2\beta_o+2i) f_i' F_{m-i}' - 2i F_i' f_{m-i}'] + \sum_{i=1}^{m}\sum_{j=0}^{m-i} [\Lambda_{l_i} f_j'' F_{m-i-j} - (2\beta_i + \Lambda_{l_i}) f_j' F_{m-i-j}'] = \eta(\beta_m - f_m''') + (2m+1)\alpha_m + \sum_{i=1}^{m} c_i (f_{m-i}'' + \alpha_{m-i} + \eta\beta_{m-i}) + \sum_{i=1}^{m-1} (2i\,\alpha_i\, c_{m-i} + c_i\, b_{m-i}) + \sum_{i=1}^{m}\sum_{j=0}^{m-i} c_i f_j f_{m-i-j}' + \sum_{i=1}^{m-1}\sum_{j=1}^{m-i} 2j\, c_i f_j f_{m-i-j}'$$

$$F_m(0) = 0 = F_m'(0), \quad F_m'(\infty) = 0 \qquad (m = 1,2,3,4) \tag{4.40b}$$

Here $c_1 = (\beta_\infty - 3)/(1-\beta_\infty)$,

$c_2 = [(\beta_\infty-3)/2(1-\beta_\infty)]\,[\beta_1 + 4/(1-\beta_\infty)]$,

$c_3 = [\beta_\infty-3)/2(1-\beta_\infty)]\,[-\beta_2 + \beta_1^2/2 + 2\beta_1/(1-\beta_\infty) + 8/(1-\beta_\infty)^2]$,

$c_4 = [\beta_\infty-3)/2(1-\beta_\infty)]\,[-\beta_3 + \beta_1\beta_2 - \beta_1^3/4 + (2\beta_2 - \beta_1^2)/(1-\beta_\infty) - 4\beta_1/(1-\beta_\infty)^2 - 16/(1-\beta_\infty)^3]$,

$$b_1 = \frac{1}{4}\left[\beta_1 d_o - 2d_1\right],$$

$$b_2 = \frac{1}{12}\left[-8d_2 + 2\beta_1 d_1 + (4\beta_2 - \beta_1^2)\, d_o\right],$$

$$b_3 = \frac{1}{64}\left[-48d_3 + 8\beta_1 d_2 + 2(6\beta_2 - \beta_1^2)d_1 + (\beta_1^3 - 10\beta_1\beta_2 + 24\beta_2)d_o\right],$$

where,

$$d_j = f_j'' + (2j+1)\,\alpha_j + \eta\beta_j + \sum_{i=0}^{j} (2i+1)\, f_i f'_{j-i}, \quad (j = 0,1,2,3)$$

$$\alpha_m = \lim_{\eta\to\infty}\left[-f_m(\eta)\right] \quad (m = 1,2,3,4). \tag{4.41}$$

4.4.3 Velocity boundary-layer characteristics:

In order to study and describe the detailed behaviour of the boundary-layer, it is convenient to define few boundary-layer characteristics. The quantities of particular interest which have to be determined are the velocity profile, displacement thickness and skin friction. We now obtain expressions for these quantities for both the first-order and the second-order boundary-layer flows on a blunted wedge.

Velocity profile:

The first-order dimensionless velocity profile is given by

$$f'(\sigma,\eta) = \sum_{m=0} f'_m(\eta)\, \sigma^m. \tag{4.42}$$

The second-order velocity profiles corresponding to the displacement effect and longitudinal curvature effect are given by

$$F'^{(d)}(\sigma,\eta) = B_d \sum_{m=0} F'^{(d)}_m(\eta)\, \sigma^m \tag{4.43a}$$

$$F'^{(1)}(\sigma,\eta) = B_1 \sum_{m=0} F'^{(1)}_m(\eta)\, \sigma^m \tag{4.43b}$$

$$\Delta^* \equiv (2\sigma)^{1/2} U_1(s,0)\,\Delta = B_1(\Delta_1 - \delta^{*2}/2) + B_d(\Delta_d - \delta^*) \qquad (4.47)$$

where

$$\Delta_1 - \delta^{*2}/2 = \int_0^\infty [-\eta - F'^{(1)}(\eta)]\, d\eta - \delta^{*2}/2 \equiv \Delta_1^* \qquad (4.47a)$$

$$\Delta_d - \delta^* = \int_0^\infty [1 - F'^{(d)}(\eta)]\, d\eta - \delta^* \equiv \Delta_d^* \qquad (4.47b)$$

We assume the following power series for Δ^*:

$$\Delta^* = \sum_{m=0} [B_1 \Delta_{1_m}^* + B_d \Delta_{d_m}^*]\, \sigma^m \qquad (4.48)$$

Using expressions (4.47) and (4.48) in conjunction with (4.42) and (4.43), and collecting the coefficients of the like powers of σ, we obtain the following expressions for the coefficient functions of the power series of Δ^*:

Longitudinal Curvature:

$$\Delta_{1_0}^* = \delta_0^{*2}/2 - \lim_{\eta\to\infty} [\eta^2/2 + F_0^{(1)}(\eta)],$$

$$\Delta_{1_1}^* = \delta_0^*\delta_1^* - \lim_{\eta\to\infty} F_1^{(1)}(\eta),$$

$$\Delta_{1_2}^* = \delta_0^*\delta_2^* + \delta_1^{*2}/2 - \lim_{\eta\to\infty} F_2^{(1)}(\eta),$$

$$\Delta_{1_3}^* = \delta_0^*\delta_3^* + \delta_1^*\delta_2^* - \lim_{\eta\to\infty} F_3^{(1)}(\eta),$$

$$\Delta_{1_4}^* = \delta_0^*\delta_4^* + \delta_1^*\delta_3^* + \delta_2^{*2}/2 - \lim_{\eta\to\infty} F_4^{(1)}(\eta). \qquad (4.49)$$

Displacement speed:

$$\Delta_{d_m}^* = \lim_{\eta\to\infty} [f_m(\eta) - F_m^{(d)}(\eta)], \quad m = 0,1,2,3,4. \qquad (4.50)$$

Skin friction:

The total skin friction at the wall, τ_w, is given by the following expression:

$$\tau_w = (\partial u/\partial n)_{n=0} = R^{-1/2}\tau_{w_1} + R^{-1}\tau_{w_2} + \dots . \quad (4.51)$$

Substituting the inner expansion (2.13) in (4.51) and using (4.4) to (4.7), (4.11) and (4.12), we obtain the following expression for τ_w:

$$\tau_w = 2(2\sigma)^{-1/2} U_1^2(s,0)\, R^{-1/2}\Big\{ \sum_{m=0} f_m''(0)\sigma^m + R^{-1/2} \sum_{m=0} [B_1 F_m''^{(1)}(0) + B_d F_m''^{(d)}(0)]\sigma^m \Big\} . \quad (4.52)$$

For convenience, we define the skin friction coefficient by

$$C_f \equiv R^{1/2}(2\sigma)^{1/2}\tau_w/2U_1^2(s,0) = \tau_1 + R^{-1/2}\tau_2 + \dots . \quad (4.53)$$

where τ_1 and τ_2 are the first and second-order skin friction coefficients. Using (4.52) and (4.53), the expressions for τ_1 and τ_2 are readily obtained and may be written as

$$\tau_1 = \sum_{m=0} f_m''(0)\sigma^m, \quad (4.54)$$

$$\tau_2 = \tau_2^{(1)} + \tau_2^{(d)}$$

with

$$\tau_2^{(1)} = B_1 \sum_{m=0} F_m''^{(1)}(0)\sigma^m \quad (4.55a)$$

$$\tau_2^{(d)} = B_d \sum_{m=0} F_m''^{(d)}(0)\sigma^m \quad (4.55b)$$

Here $\tau_2^{(1)}$ and $\tau_2^{(d)}$ represent the overall contribution of the longitudinal curvature and displacement speed to the skin friction coefficient C_f. For the blunted wedge, using expressions (4.31) and (4.35), we may express the quantities B_d and B_1 by a power series in σ . Thus,

$$B_d = \sum_{m=0} B_{d_m}\sigma^m = -(1-\beta_\infty)^{1/2} a_0 [1 + 2(1-\beta_\infty)^{-1} E_1\sigma + 4(1-\beta_\infty)^{-2} E_2\sigma^2 + 8(1-\beta_\infty)^{-3} E_3\sigma^3 + 16(1-\beta_\infty)^{-4} E_4\sigma^4 + \dots] \quad (4.56)$$

$$B_1 = \sum_{m=0} B_{1_m} \sigma^m = (1-\beta_\infty)^{1/2} \left[1-2(1-\beta_\infty)^{-1} \sigma \right.$$

$$\left. + 4(1-\beta_\infty)^{-2} \sigma^2 - 8(1-\beta_\infty)^{-3}\sigma^3 + 16(1-\beta_\infty)^{-4}\sigma^4 + \ldots \right] \quad (4.57)$$

Introducing the above expressions in (4.45), we obtain the following expressions for $\tau_2^{(1)}$ and $\tau_2^{(d)}$;

$$\tau_2^{(1)} = \sum_{m=0} F_m^{*(1)} \sigma^m$$

$$\text{with} \quad F_m^{*(1)} = \sum_{n=0}^{m} B_{1_n} F_{m-n}^{''(1)}(0) \quad (4.58)$$

$$\tau_2^{(d)} = \sum_{m=0} F_m^{*(d)} \sigma^m$$

$$\text{with} \quad F_m^{*(d)} = \sum_{n=0}^{m} B_{d_n} F_{m-n}^{''(d)}(0). \quad (4.59)$$

Here B_{1_n}'s and B_{d_n}'s are obtainable from (4.46) and (4.47).

4.5 Heat Transfer Problem:

In the preceding sections, we considered the nonsimilar solutions of the momentum transfer problem (§4.3) and studied explicitly the example of a blunted wedge (§4.4). We now consider the corresponding thermal problem here and in the next section (§4.6) we shall study the example of the thermal boundary-layer on a blunted wedge.

The thermal boundary-layer equations (4.1c) and (4.2c) may be rewritten in (σ,η) variables with the help of the following transformations for the first and second-order enthalpy:

$$h_1 = [T_w - H_1(0)]\, g(\sigma,\eta) + H_1(0), \quad (4.60)$$

$$h_2 = [T_w - H_1(0)]\, G(\sigma,\eta). \quad (4.61)$$

Using the above expressions along with (4.11) and (4.12), the thermal boundary-layer equations are reduced to the following form:

First-Order:

$$Pr^{-1}g'' + fg' - 2\sigma\,(f'g_\sigma - f_\sigma g') = 0,$$
$$g(\sigma, 0) = 1,\ g(\sigma, \infty) = 0. \tag{4.62}$$

Second-Order:

$$Pr^{-1}G'' + fG' - 2\sigma\,(f'G_\sigma - f_\sigma G') = -Fg' + 2\sigma\,(F'g_\sigma - F_\sigma g') - Pr^{-1}B_1(\eta g')',$$
$$G(\sigma, 0) = 0,\ G(\sigma, \infty) = 0. \tag{4.63}$$

In order to study the locally-similar solutions of (4.52) and (4.53), we assume the following power series for $g(\sigma,\eta)$ and $G(\sigma,\eta)$:

$$g(\sigma,\eta) = \sum_{m=0} g_m(\eta)\ \sigma^{pm} \tag{4.64}$$

$$G(\sigma,\eta) = \sum_{m=0} \left[B_1\ G_m^{(l)}(\eta) + B_d\ G_m^{(d)}(\eta)\right]\ \sigma^{pm} \tag{4.65}$$

Substituting the above series of $g(\sigma,\eta)$ and $G(\sigma,\eta)$ in equations (4.62) and (4.63) and collecting the coefficients of the like powers of σ, we obtain the equations for the successive approximations. However, as commented earlier for the momentum transfer problem, we shall not attempt to obtain the solutions to these equations in terms of the universal functions; instead, the procedure is fully illustrated in the next section by considering the problem of heat transfer on a blunted wedge.

4.6 Thermal Boundary-Layer on a Blunted Wedge:

The momentum transfer on a blunted wedge was studied in §4.4; the corresponding heat transfer problem is considered here. Although we shall study the constant wall temperature case, the method may be readily extended to the case of a variable wall temperature.

4.6.1 First-order problem:

Following the procedure outlined in the preceding section, we assume the following power series form for $g(\sigma,\eta)$:

$$g(\sigma,\eta) = \sum_{m=0} g_m(\eta)\sigma^m \tag{4.66}$$

Substituting (4.66) in (4.62) and collecting the coefficients of the like powers of σ , we obtain the following recursive system of ordinary differential equations:

$$\begin{aligned} &Pr^{-1}g_o'' + f_o g_o' = 0, \\ &g_o(0) = 1,\ g(\infty) = 0. \end{aligned} \tag{4.67a}$$

$$\begin{aligned} Pr^{-1}g_m'' + f_o\, g_m' - 2m\, f_o' g_m = &- \sum_{i=1}^{m} (2i+1) f_i g_{m-1}' \\ &+ \sum_{i=1}^{m-1} 2(m-i) f_i' g_{m-i}, \end{aligned}$$

$$g_m(0) = 0,\quad g_m(\infty) = 0 \qquad (m = 1,2,3,\ldots) \tag{4.67b}$$

Equation (4.67a) will yield the well-known similar solution for the two-dimensional problem and has been studied quite extensively in literature. Further, for Prandtl number unity, the problem (4.67) reduces to the one corresponding to the cross-flow

problem studied by Görtler (1957) and as such the solution may be written directly with the help of the universal functions tabulated by Görtler (1957). This fact has been used by Chen (1970) while studying the first-order heat-transfer on a blunted wedge. However, Prandtl number unity is not of much interest. For air, Prandtl number is close to 0.7 and we shall choose this value for the present study. As such, the equations (4.67) has been solved by numerical integration to obtain solutions needed for the study of the second-order problem.

4.6.2 Second order problem:

For the second-order problem, we assume the following expansion for $G(\sigma,\eta)$:

$$G(\sigma,\eta) = \sum_{m=0} \left[B_1 G_m^{(1)}(\eta) + B_d G_m^{(d)}(\eta)\right] \sigma^m . \qquad (4.68)$$

Here we have separated the contributions due to displacement and longitudinal curvature. Substituting the expression (4.68) in equation (4.63) and collecting coefficients of various powers of σ, we obtain the following recursive systems of ordinary differential equations for the displacement and longitudinal curvature problems:

Displacement speed:

$$\begin{aligned} Pr^{-1}G_m'' + f_o G_m' - 2m f_o' G_m &= 2m g_m F_o' - g_m' F_o + \sum_{i=1}^{m-1} 2i\left[G_i f_{m-i}' + g_i F_{m-i}'\right] \\ &\quad - \sum_{i=1}^{m} \left[(2i+1)(f_i G_{m-i}' - F_i g_{m-i}') + \Lambda_{d_i}(F_o g_{m-i}' - f_o' G_{m-i})\right] \\ &\quad + \sum_{i=1}^{m-1}\sum_{j=1}^{m-i} \Lambda_{d_i}(f_j' G_{m-i-j} - F_j' g_{m-i-j}), \end{aligned}$$

$$G_m(0) = 0 = G_m(\infty). \qquad (m = 0,1,2,3,4) \qquad (4.69)$$

Longitudinal curvature:

$$Pr^{-1} G_m'' + f_o G_m' - 2m f_o' G_m = -Pr^{-1}(\eta g_m')' + 2m g_m F_o' - g_m' F_o + \sum_{i=1}^{m-1} 2i \left[G_i f_{m-i}' + g_i F_{m-i}' \right] - \sum_{i=1}^{m} \left[(2i+1) (f_i G_{m-i}' - F_i g_{m-i}') + \Lambda_{1_i} (F_o g_{m-i}' - f_o' G_{m-i}) \right] + \sum_{i=1}^{m-1} \sum_{j=1}^{m-i} \Lambda_{1_i} (f_j G_{m-i-j} - F_j g_{m-i-j}'),$$

$$G_m(0) = 0 = G_m(\infty). \qquad (m = 0,1,2,3,4). \qquad (4.70)$$

4.6.3 Thermal-boundary-layer characteristics:

We now obtain expressions for two important thermal boundary-layer characteristics, namely temperature profile and heat transfer at the wall.

Temperature profile:

The first-order and the second-order temperature profiles are given by (4.66) and (4.68) and are repeated here for ready reference.

First-order:

$$g(\sigma,\eta) = \sum_{m=0} g_m(\eta)\sigma^m \qquad (4.56)$$

Second-order:

$$G^{(1)}(\sigma,\eta) = B_1 \sum_{m=0} G_m^{(1)}(\eta)\, \sigma^m \qquad (4.58a)$$

$$G^{(d)}(\sigma,\eta) = B_d \sum_{m=0} G^{(d)}(\eta)\, \sigma^m \qquad (4.58b)$$

Heat transfer:

The local heat transfer at the wall, q_w, is defined as,

$$q_w = -k\, (\partial T/\partial n)_{n=0} \qquad (4.71)$$

Substituting the inner expansion (2.13) for T in (4.71) and using (4.66) and (4.68) we obtain the following expression for q_w:

$$q_w = -Pr^{-1} R^{-1/2} U_1(s,0) [T_w - H_1(0)] (2\sigma)^{-1/2} \left[\sum_{m=0} g_m'(0)\sigma^m + R^{-1/2} \sum_{m=0} \{ B_1 G_m'^{(1)}(0) + B_d G_m'^{(d)}(0) \} \sigma^m \right] \tag{4.72}$$

For convenience, we define the heat transfer coefficient by

$$C_q \equiv -R^{1/2} Pr (2\sigma)^{1/2} q_w [T_w - H_1(0)]^{-1} / U_1(s,0) = q_1 + R^{-1/2} q_2 + \dots . \tag{4.73}$$

where q_1 and q_2 are, respectively, the first-order and the second-order heat transfer coefficients. Comparison of (4.72) and (4.73) leads to the following expressions for q_1 and q_2:

$$q_1 = \sum_{m=0} g_m'(0) \sigma^m, \tag{4.74}$$

$$q_2 = q_2^{(1)} + q_2^{(d)}$$

with

$$q_2^{(1)} = B_1 \sum_{m=0} G_m'^{(1)}(0) \sigma^m, \tag{4.75a}$$

$$q_2^{(d)} = B_d \sum_{m=0} G_m'^{(d)}(0) \sigma^m. \tag{4.75b}$$

Here $q_2^{(1)}$ and $q_2^{(d)}$ represent the overall contribution of the longitudinal curvature and displacement speed to the heat transfer coefficient C_q. Introducing power series for B_d (4.56) and B_1 (4.57) in (4.75), we rewrite the expressions for $q_2^{(1)}$ and $q_2^{(d)}$ in the following form:

$$q_2^{(1)} = \sum_{m=0} G_m^{*(1)} \sigma^m \quad \text{with } G_m^{*(1)} = \sum_{n=0}^{m} B_{1_n} G_{m-n}'^{(1)}(0). \tag{4.76}$$

$$q_2^{(d)} = \sum_{m=0} G_m^{*(d)} \sigma^m \quad \text{with } G_m^{*(d)} = \sum_{n=0}^{m} B_{d_n} G_{m-n}'^{(d)}(0).$$

4.7 Extending Range of Validity of the Series Solutions in the Downstream Direction:

The range of validity of the series solutions, studied in the preceding sections, is restricted in the downstream direction because of the limited radius of convergence of the series. We now discuss various methods which have been used to extend the range of validity of the solutions in the downstream direction. It is well-known that in many applied mechanics problems, a power-series expansion has a small radius of convergence because of a singularity in the complex plane, usually on the negative axis, although the expansion has a physical significance only for the real positive values of the expansion parameter. In such cases, if we know the location of the singularity, it is usually possible to enlarge the radius of convergence by transferring the singularity farther away, possibly to infinity. Depending on the knowledge of the location and nature of the singularity, various transformations are available to extract maximum information from a slowly convergent or even a divergent series. Bellman (1955) and Van Dyke (1964b) have given several interesting examples of such transformations.

Euler transformation is one of the most powerful and commonly employed techniques for enlarging the radius of convergence of a power-series expansion. According to this method, if there is only one singularity and its location is

known, then it is possible to transfer the singularity to infinity so that the transformed series has an infinite radius of convergence. For a power-series having one of the coordinates (say $\bar{\sigma}$) as the expansion parameters, it is usually found that its radius of convergence is limited because of a singularity on the negative axis (say at $\bar{\sigma} = -p$) although from physical point of view, only the positive values of $\bar{\sigma}$ are relevant. Such artificial limitation can be overcome by a simple conformal mapping whereby the singularity is shifted to infinity - the technique is known as the Euler transformation which consists of introducing a new variable z defined as,

$$z = \bar{\sigma}/(\bar{\sigma} + p) \tag{4.78}$$

The transformed series in z has the radius of convergence $z = 1$ which corresponds to $\bar{\sigma} \to \infty$. Thus, the transformed series assures convergence for all values of $\bar{\sigma}$, and the utility of series solutions is considerably improved. As a first step we have, therefore, to estimate the value of p.

The power-series expansion in the case of a blunted wedge have $\bar{\sigma}$ as the expansion parameter. Using (4.20), the expression (4.19) for the inviscid first-order velocity $U_1(s, 0)$ may be written in the following form:

$$U_1(s, 0) = (2\bar{\sigma})^{1/2} (1-\beta_\infty)^{-1} \left[1 + 2\bar{\sigma}/(1-\beta_\infty)\right]^{-(1-\beta_\infty)/2} \tag{4.79}$$

The above expression shows that $U_1(s, 0)$ is singular at $\bar{\sigma} = -(1-\beta_\infty)/2$. This suggests that the first-order series-solutions will also exhibit a singularity at $\bar{\sigma} = -(1-\beta_\infty)/2$.

This expectation is further supported from the trend of the ratio of the successive coefficients $f_1, f_2 \ldots f_5$ of the first order series solutions (e.g.4.54), which seems to approach constant value equal to $(1-\beta_\infty)/2$ for a fixed β_∞ (cf. §4.8). Thus, we obtain the following form of the Euler transformation:

$$z = \sigma/(\sigma + (1-\beta_\infty)/2) \qquad (4.80)$$

We suggest that the above form of the Euler transformation is suitable for the second-order series solutions for the longitudinal curvature (4.34) and the displacement speed (4.30); both the expressions are singular at $\sigma = (1-\beta_\infty)/2$. Again, the ratio of the successive coefficients of the second-order series solutions [e.g. F^*_m/F^*_{m+1}, m = 0-4 in (4.58) and (4.59)] is found to approach a constant value equal to $(1-\beta_\infty)/2$ and, therefore, suggest that the radius of convergence is limited by a singularity at $\sigma = -(1-\beta_\infty)/2$(see §4.8). We have used the same Euler transformation (4.80) for both the momentum transfer and heat transfer problems since the above comments regarding the radius of convergence of the series solutions hold good for the heat-transfer problem as well.

The Eulerized series though convergent upto $z = 1$ (i.e. $\sigma \to \infty$), the convergence is found to be rather slow leading to considerable error for large values of σ. To extract further information from such a slowly convergent series, it is sometimes possible to accelerate the convergence by applying Shanks non-linear transformation. Shanks (1955) has given several examples to show how a

lot of additional information can be obtained from a few terms of a given series. The Shanks method consists of applying the following non-linear transformation to the partial sums of the series (cf. e.g. Van Dyke 1964b): denoting n-th, partial sum by S_n, we write,

$$e_1(S_n) = (S_{n+1}\, S_{n-1} - S_n^2)/(S_{n+1} + S_{n-1} - 2S_n) \,. \qquad (4.81)$$

The process may be repeated by using $e_1(S_n)$'s as the S_n's for the next iteration.

Another technique is to fit a polynomial in 1/n (n denotes the number of terms) to the last few partial sums of the series and thus extrapolate the sum of the series for $n \to \infty$. Using the last three partial sums of a series containing n number of terms, the polynomial fit will predict the sum of the series given by the following expression:

$$S = (n-2)^2/2\; S_{n-2} - (n-1)^2\; S_{n-1} + n^2/2\; S_n. \qquad (4.82)$$

In particular, for n = 6 (for the first-order problem where the first six terms of the series are known)

$$S = 8S_4 - 25\; S_5 + 18S_6 \qquad (4.82a)$$

and for n = 5 (second-order problem)

$$S = 4.5\; S_3 - 16\; S_4 + 12.5\; S_5. \qquad (4.82b)$$

For the present case, it will be shown in §4.8 that the latter method gives better results as compared to the Shanks non-linear transformation.

4.7.1 Eulerized skin-friction and heat transfer:

Since the series solutions for the skin friction and heat transfer are of the same kind, we illustrate the Eulerization procedure for a general case. Consider a power-series expansion for some variable ϕ to be of the following form:

$$\phi = \phi_0 + \phi_1\sigma + \phi_2\sigma^2 + \phi_3\sigma^3 + \phi_4\sigma^4 + \phi_5\sigma^5 + \ldots . \quad (4.83)$$

Introducing the variable z (4.80) in the above series and denoting the resulting Eulerized series by ϕ, we obtain the following expression for ϕ in the operator form:

$$\hat{\phi} = L^*(\phi_m, z) \equiv \phi_0 + p\phi_1 z + (p\phi_1 + p^2\phi_2)z^2 + (p\phi_1 + 2p^2\phi_2 + p^3\phi_3)z^3$$
$$+ (p\phi_1 + 3p^2\phi_2 + 3p^3\phi_3 + p^4\phi_4)z^4 + (p\phi_1 + 4p^2\phi_2 + 6p^3\phi_3 + 4p^4\phi_4$$
$$+ 5p^5\phi_5)\, z^5 + \ldots . \quad (4.84)$$

where $p = (1-\beta_\infty)/2$.

Using the above result along with the definition of the operator L^* given by (4.84), we may readily obtain Eulerized series solutions for the skin-friction and heat transfer.

First-order:

Eulerization of (4.54) and (4.74) yields the following Eulerized series solutions for the first-order skin friction and heat transfer:

$$\hat{\tau}_1 = L^*[f_m''(0), z] \quad (4.85)$$

$$\hat{q}_1 = L^*[g_m'(0), z] \qquad (m = 0\text{-}5) \quad (4.86)$$

Longitudinal Curvature:

Eulerizing (4.58) and (4.76), we obtain the following Eulerized series solutions for the overall contribution of the longitudinal curvature to skin friction and heat transfer:

$$\hat{\tau}_2^{(l)} = L^*[F_m^{*(l)}, z] \tag{4.87}$$

$$\hat{q}_2^{(l)} = L^*[G_m^{*(l)}, z] \qquad (m = 0\text{-}4) \tag{4.88}$$

Displacement Speed:

Eulerizing (4.59) and (4.77), we obtain the following Eulerized series solutions for the overall contribution of the displacement speed to skin friction and heat transfer:

$$\hat{\tau}_2^{(d)} = L^*[F_m^{*(d)}, z] \tag{4.89}$$

$$\hat{q}_2^{(d)} = L^*[G_m^{*(d)}, z] \qquad (m = 0\text{-}4) \tag{4.90}$$

To extract further information from the Eulerized series solutions, both the methods described earlier, i.e. that of Shanks non-linear transformation and extrapolation, were used. The results thus improved are described in §4.8 and it will be pointed out how much improvement is achieved by the two techniques of accelerating the convergence of the Eulerized series. The total Eulerized skin friction and heat transfer coefficients, combined with extrapolation, may be expressed in the following form:

$$\hat{C}_f = \hat{\tau}_1 + R^{-1/2} (\hat{\tau}_2^{(d)} + \hat{\tau}_2^{(l)}), \tag{4.91}$$

$$\hat{C}_q = \hat{q}_1 + R^{-1/2} (\hat{q}_2^{(a)} + \hat{q}_2^{(l)}). \tag{4.92}$$

4.8 Numerical Results and Discussion:

The recursive system of differential equations for the first and second-order momentum and heat transfer problems are solved by numerical integration, using Runge-Kutta-Gill method. The solutions are obtained for various values of wedge angles ($\beta_\infty \pi$) in the range $0 \leq \beta_\infty \leq 1$.

We first describe the results for the first-order problem. As mentioned earlier (§4.6) Chen (1970) has studied the first-order heat transfer for $\beta_\infty = 0.5$ and Pr = 1, by utilizing the universal functions of the cross flow problem, tabulated by Görtler (1957). However, when Pr is different from unity, these solutions are to be obtained numerically. In the present calculations we take the value of Pr = 0.7 as it is the value for air and hence of more practical interest.

For the first-order boundary-layer, the first six terms in momentum and heat transfer are computed from the solutions of equations (4.24) and (4.67). It may be noted that the first two equations (for both momentum and heat transfer problems) in the above system are independent of β_∞ and hence the solutions of these two equations will only be valid in the immediate neighbourhood of the stagnation point. The velocity profiles for three representative values of β_∞, namely $\beta_\infty = 0$, 0.5 and 0.8 are shown in Figures 4.2a,b and c. The first six coefficients of the skin friction τ_1 (i.e. $f_m''(0)$, m = 0-5) and displacement thickness δ^* (i.e. δ_m^*, m = 0-5)versus β_∞ are shown in Figure 4.3. The first two coefficients of skin friction $[f_1''(0)$ and $f_2''(0)]$

and displacement thickness (δ_1^* and δ_2^*) are independent of β_∞ (so are their governing equations) while others increase monotonically as β_∞ increases. For a fixed value of β_∞, Figure 4.3 shows that the ratio of the successive coefficients ($f_n''(0)/f_{n+1}''(0)$, $\delta_n^*/\delta_{n+1}^*$, n = 0-4) tends to a constant value, equal to $(1-\beta_\infty)/2$ and supports what was anticipated in §4.7. Thus the series solutions (4.45) and (4.54) is expected to have a radius a convergence of $(1-\beta_\infty)/2$ and are useful only for $\sigma < (1-\beta_\infty)/2$. However, the region of validity of the results is extended in the downstream direction by Eulerizing the series with $p = (1-\beta_\infty)/2$. If there is no other singularity, in the complex-plane, then the Eulerization will lead to results which are valid every where on the blunted wedge. To test the Eulerized results for various values of β_∞, we consider the limit as $z \to 1$ (corresponding to $\sigma \to \infty$) where the properties of the boundary-layer should approach those of a wedge (given by well-known Falkner-Skan equation with corresponding value of β_∞). The Eulerized series of the skin friction (4.85) for z = 1, shows that the successive partial sums do approach a value equal to that given by Falkner-Skan equation for all β_∞ (see Table 4.1). The difference between the last partial sum and the exact value is about 15 percent for $\beta_\infty = 0$, 0.6 percent for $\beta_\infty = 0.5$ and almost zero for $\beta_\infty = 1.0$. To further improve the convergence of the Eulerized series, two methods were tried. First the non-linear transformation of Shanks was applied but the results, although improved, were still in error by about 7 percent for $\beta_\infty = 0$. Then a polynomial

fit in 1/n to the last three partial sums was used and the results (cited as improved Eulerized) have shown a marked improvement (error is about 1.3 percent for $\beta_\infty = 0$). A comparative study of the Eulerized and improved Eulerized results for $z = 1$ with those of Falkner-Skan solutions of the corresponding β_∞, obtained by Smith (1954) is shown in Table 4.1 below:

Table 4.1: The Eulerized first-order skin friction results at $z = 1$.

β_∞	Eulerized $\hat{\tau}_1$	Improved Eulerized $\hat{\tau}_1$	A.M.O. Smith (1954)
0.0	0.5410	0.4636	0.469600
0.1	0.6298	0.5815	0.587035
0.2	0.7129	0.6840	0.686708
0.3	0.7909	0.7743	0.774755
0.4	0.8643	0.8553	0.854421
0.5	0.9336	0.9289	0.927680
0.6	0.9992	0.9970	0.995836
0.7	1.0616	1.0606	1.0598078
0.8	1.1211	1.1207	1.120267

The improved Eulerized results for the skin friction τ_1 versus z for various values of β_∞ are shown in Figure 4.4 and we note that the skin friction decreases monotonically for increasing streamwise distance for $0 \leq \beta_\infty < 1$, and remains constant for $\beta_\infty = 1$.

For the first-order heat transfer problem the temperature profile for some representative values of β_∞ (= 0, 0.5 and 0.8) are shown in Figures 4.5a,b and c. The results for the coefficients of the heat transfer at wall $g_m'(0)$ versus β_∞ for n = 0-5 are plotted in Figure 4.6. Except for the first two coefficients, i.e. $g_0'(0)$ and $g_1'(0)$ which remain constant, other coefficients increase monotonically as β_∞ increases. Further, for a given β_∞, the ratio of the successive coefficients, i.e. $g_m'(0)/g_{m+1}'(0)$ for m = 0-5, is found to approach $(1-\beta_\infty)/2$, implying thereby that the radius of convergence of the series for heat transfer rate is same as that for the skin friction. The Eulerized and improved Eulerized results for heat transfer at z = 1 are tested and a comparative study is shown in Table 4.2.

Table 4.2: Eulerized first-order heat transfer results at z = 1.

β_∞	Eulerized q_1	Improved Eulerized q_1	Evans (1967)
0.0	0.4143	0.4029	0.41391
0.1	0.4275	0.4238	0.43140
0.2	0.4391	0.4399	0.44438
0.3	0.4494	0.4523	0.45470
0.4	0.4585	0.4621	0.46323
0.5	0.4665	0.4700	0.47049
0.6	0.4737	0.4766	0.47680
0.7	0.4801	0.4823	0.48235
0.8	0.4859	0.4872	0.48732

The above table shows that for any value of β_∞, the improved Eulerised results compare well (within 2 percent) with the corresponding solutions for a wedge, given by Evans (1967). Figure 4.7 shows the improved Eulerized heat transfer q_1 versus z for various values of β_∞. The figure shows that for $\beta_\infty = 1$, the heat transfer is same for all z while for other value of β_∞ it decreases monotonically as z increases. Further, this rate of decrease of heat transfer increases as β_∞ decreases.

We now describe the second-order results for the displacement effect, obtained from the solutions of the first five equations in each of the systems (4.39) and (4.69); these results are displayed in Figures 4.8 to 4.14. In Figures 4.8a,b and c the coefficients of the power series (4.43a) for the velocity profile are presented for $\beta_\infty = 0$, 0.5 and 0.8 respectively. In Figure 4.9 the coefficients $F_m^{"(d)}(0)$ of the skin friction series (4.55) are plotted versus β_∞ and the corresponding results ($\Delta_{d_m}^*$ versus β_∞) for the displacement thickness (4.50) are shown in Figure 4.10. To get a better insight in the structure of the displacement speed solutions, the coefficients $F_m^{*(d)}$ of the power-series (4.59) for the overall displacement speed contribution $\tau_2^{(d)}$ to the skin friction are also plotted as a function of β_∞ in Figure 4.9. It may be seen from Figure 4.9 that the first coefficient $F_0^{*(d)}$ of (4.59) decreases as β_∞ increases; the skin friction at the stagnation point ($\sigma = 0$) decreases as β_∞ increases and is zero for $\beta_\infty = 1$. Further, the other coefficients $F_m^{*(d)}$ show a monotonic increase with β_∞.

Using the series (4.59) and the coefficients $F_m^{*(d)}$ from Figure 4.9, we can compute the total contribution of the displacement effect to the skin friction. Further, for a fixed β_∞, Figure 4.9 shows that the successive ratio $F_m^{*(d)}/F_{m+1}^{*(d)}$ (m = 0-4) approaches the value $(1-\beta_\infty)/2$. Therefore, for improving the convergence of the results, Eulerization with $p = (1-\beta_\infty)/2$ is employed. The Eulerized skin friction contribution due to the displacement effect $\hat{\tau}_2^{(d)}$ is plotted versus z for various values of β_∞ as is shown in Figure 4.11. For a given β_∞, the second-order contribution to the skin friction is negative near the stagnation point ($\sigma = z = 0$) and changes sign for $z > 0.65$ and becomes zero for $z = 1$. This behaviour of the skin friction is similar to that of the displacement speed. For the particular case of $\beta_\infty = 1$ (plane stagnation point flow) the displacement speed is zero and so is the contribution to the skin friction etc.

To study the contribution of displacement to heat transfer, the coefficients for the temperature profiles (4.58b) are shown in Figures 4.12a,b and c for $\beta_\infty = 0$, 0.5 and 0.8. The first five coefficients of the power series (4.75), i.e. $G_m'^{(d)}(0)$ for m = 0-4 versus β_∞ are shown in Figure 4.13. The overall contribution of displacement effect $q_2^{(d)}$ to heat transfer is given by power series (4.77) whose first five coefficients are also displayed in the same figure; the first coefficient $G_o^{*(d)}$ of series (4.77) decreases as β_∞ increases, which means that the contribution of the displacement speed near $\sigma = 0$ (stagnation point) decreases as β_∞ increases, while the other coefficients

show an increase as β_∞ increases. The radius of convergence of series (4.77) remains the same as in the momentum transfer problem so that the results can be used for $\sigma < (1-\beta_\infty)/2$. The Eulerized results for the series (4.77), given by (4.90), are shown in Figure 4.14 for various values of β_∞. The quantitative behaviour of the heat transfer $\hat{q}_2^{(d)}$ contribution is similar to that of the skin friction $\hat{\tau}_2^{(d)}$ and, hence no further comments are needed.

For the longitudinal curvature problem, governed by equations (4.40) and (4.70), the results of numerical integration of the first five equations for the momentum and heat transfer problems are shown in Figures 4.15 - 4.21. The velocity profiles for $\beta_\infty = 0$, 0.5 and 0.8 are shown in Figures 4.15a, b and c. The first five coefficients of the series for the skin friction, (i.e. $F_m''^{(1)}(0)$ given by (4.55a), and for the displacement thickness, i.e. $\Delta_{1_m}^*$ given by (4.49), are plotted versus β_∞ as shown in Figures 4.16 and 4.17 respectively. The overall contribution of the longitudinal curvature to the skin friction $\tau_2^{(1)}$, given by (4.58) is also shown in Figure 4.16 - the first five coefficients $F_m''^{(1)}$ of the series are plotted as a function of β_∞. For a given β_∞, the Figure 4.16 shows thatthe ratio of the successive coefficients ($F_m^{*(1)}/F_{m+1}^{*(1)}$, m = 0-4) tends to $(1-\beta_\infty)/2$ and hence the radius of convergence of this series is the same as that mentioned earlier. The Eulerized skin friction due to the longitudinal curvature $\hat{\tau}_2^{(1)}$, given by (4.87), is shown in Figure 4.18 for various values of β_∞. For a given β_∞, this figure shows

that the longitudinal curvature contribution to skin friction is negative and decreases (in magnitude) as streamwise distance z increases upto 0.65. For $z > 0.65$ the sign becomes positive but the magnitude is very small and is zero for $z = 1$.

The temperature profile for the second-order contribution of longitudinal curvature are plotted in Figures 4.19a,b and c for the heat transfer rate at the wall, of the series (4.75a) and (4.76) are shown in Figures 4.20a and 4.20b. The Eulerized results for the heat transfer $\hat{q}_2^{(1)}$ versus z for various values of β_∞ are shown in Figure 4.21. The qualitative behaviour of the heat transfer results is the same as that of the skin friction and hence no further comments are needed.

So far we have discussed the results for each of the individual effects. We now describe the Eulerized results for the total skin friction $\hat{C}_f$ and heat transfer $\hat{C}_q$ and discuss their validity with respect to the streamwise coordinate z or σ and Reynolds number. For clarity of presentation, the skin friction on the blunted wedge for various values of β_∞ are spread over two figures, namely 4.22a and 4.22b and values of Reynolds number are ∞, 10^4, 10^3 and 10^2. Figure 4.22 shows that for a given β_∞ the skin friction decreases monotonically as z increases for $R \geq 10^3$. However for lower Reynolds number e.g. $R = 100$ and $\beta > 0.2$, the skin friction is found to increase initially with increasing z and then decreases to approach the Falkner-Skan value at $z = 1$. A comparison of the present results at $z = 1$, with those of Smith's Falkner-Skan solutions is given

The present skin friction results for a parabola ($\beta_\infty = 0$) are compared with the exact numerical solutions of the Navier-Stokes equations, obtained independently by Botta et.al.(1971), Davis (1972) and Dennis et.al. (1972). A comparison of the present results for the skin friction at the nose of the parabola with those obtained by the above mentioned authors and that by Van Dyke (1964) is given in Table 4.3 below:

Table 4.3: Skin friction at the nose of the parabola ($\beta_\infty = 0$).

$R = U/\nu$	Present results	Davis (1972)	Dennis et.al. (1971)	Botta et.al. (1972)	Van Dyke (1964)
10^2	1.316	1.427	1.424	1.428	1.314
10^3	1.616	1.626	1.625	1.624	1.607
10^4	1.684	1.710		1.706	1.700
10^5	1.712			1.734	1.730

Figure 4.23 shows a comparison between the present results and those of Davis (1972) for the distribution of the skin-friction over a parabola at various Reynolds number. Upto Reynolds number as low as 10^3, the difference in the two results is only about one percent. Even at $R = 10^2$, our results are lower by about 7 percent, most of the difference in the two being near the stagnation region. Further, Davis has also given, what he calls the 'parabolic approximations'

and it is pointed out by Davis that the difference between the exact results and parabolic approximations is mainly due to the displacement effects. We have also shown our corresponding parabolic approximation results by excluding the contribution of the displacement effect to the skin friction. It may be seen from Figure 4.23 that the two results for the 'parabolic approximations' compare well (within two percent) even for Reynolds number as low as 100. This suggests that we have probably over estimated the displacement contribution to the skin friction. In Figure 4.24, we have compared the skin friction results with those of Dennis and Welsh (1971) for $R = \infty$ and 100. Also we have plotted the results of Smith and Clutter (1963) for $R = \infty$. It may be seen that for $R = \infty$, our results are close to those of Smith and Clutter whereas the values obtained by Dennis and Walsh are somewhat higher for large values of the streamwise distance z. For R = 100 also our values are lower than those of Dennis and Welsh. This behaviour is consistent with that observed from Figure 4.23 (comparison with Davis) as might be expected in view of the fact that the results of Davis (1972), Dennis et.al. (1972) and Botta et.al. (1971) compare quite well among themselves.

The Eulerized total heat transfer coefficient $\hat{C}_q$ for various values of β_∞ and $R = \infty$, 10^4, 10^3 and 10^2 is plotted as a function of the streamwise coordinate z in Figures 4.25a and 4.25b. The effect of variation of β_∞ and R on the heat transfer distribution is qualitatively similar to that described

earlier for the corresponding skin friction results and as such no further comment is needed. A test of the present results at $z = 1$ ($\delta \to \infty$) with those of Evans (1967) for the corresponding β_∞ (see Table 4.2) shows an agreement within two percent.

In view of the above discussion, we suggest that the present results for the skin friction and heat transfer distribution on a blunted wedge may be used with little error (within two percent) for Reynolds number upto 10^3; for still lower Reynolds number, however, one has to be more cautious.

CHAPTER 5

NONSIMILAR SECOND-ORDER BOUNDARY-LAYER SOLUTIONS VALID FAR DOWNSTREAM

5.1 Introduction:

In the present chapter, we study the locally-similar solutions valid for large values of streamwise coordinate σ. Apart from the fact that these solutions are of interest in themselves, they are also useful in assessing the validity of the Görtler and Blassius type series solutions (obtained for small σ) for large σ.

Various methods, with varying degree of complexity and accuracy, are available for studying the present problem. The finite difference and difference differential schemes are available to calculate the development of the boundary-layer downstream of a specified initial velocity profile. Although exact in principal, these methods are unattractive for a parametric study due to the large amount of calculations involved. An analytical approach is preferred. To obtain solutions for $\sigma \to \infty$, variables are expanded in a complete set of eigenfunctions leaving unspecified multiplicative constants, which are to be determined from the prescribed initial conditions. In principle, this analytical method is exact but in practice, the eigenfunction representation is truncated after a few terms to yield an approximate solution. This approach has been used for the first-order boundary-layer flows by

Libby and his several colleagues and a good review has recently been made by Libby (1970). In their study, the required set of eigenfunctions are determined from the linearized equation (obtained by linearizing about the limiting similar solution). This linearized equation is, in some sense, similar to the well-known Sturm-Liouville equation for which the eigenvalues are known to be real and discrete.

Such a procedure is used here to study the second-order momentum transfer problem for large values of σ. We first consider the initial value problem for each of the second-order effects, namely the longitudinal curvature, transverse curvature, displacement and external vorticity. We let the pressure-gradient parameter Λ_{U_1}, longitudinal curvature parameter Λ_{B_l}, transverse curvature parameter Λ_{B_t} and displacement speed parameter Λ_{B_d} be constant. Since we are primarily interested here in studying the eigenvalue problem, the restriction of choosing constant parameters simplifies the problem considerably without affecting its general nature. At a streamwise station an initial velocity profile (upto second-order) differing slightly from the limiting similar profile for the specified parameters is assumed. We are interested in studying the downstream behaviour of the solution so as to find how the limiting similar solution is approached as $\sigma \to \infty$. The results obtained for a variety of parameters are displayed

graphically. A critical discussion of the results is given; in particular, the effect of parameter variation on the stability of the flow is examined and the implications of the singular behaviour of the solutions to the design of body shapes having desired aerodynamic characteristics is pointed out.

The application of the above formulation is illustrated for a blunted wedge, where only the longitudinal curvature and displacement effects are present. Additional terms due to the variation of the parameters $(\Lambda_{U_1}, \Lambda_{B_1}, \Lambda_{B_d})$ with σ are to be included. The multiplicative constants of the eigenfunctions are determined by joining the presently obtained asymptotic series (for $\sigma \to \infty$) with the Eulerized Görtler series for the blunted wedge obtained in Chapter 4 . Thus, the asymptotic solution for $\sigma \to \infty$ provides a test for the assessment of the Eulerized series solutions obtained for the nose region. Further, these two forms can be used to estimate the accuracy of numerical methods having uncertain error bounds.

The material presented in the sequel is divided into two parts. In the first part (§§5.2-5.4) the general initial value problem is treated, while in the second part (§§5.5-5.7) we have studied the detailed solutions for a blunted wedge.

PART I: Second-order initial value problem

We consider flow past a two-dimensional or axisymmetric body shown in Figure 2.1. The governing equations for the momentum transfer problem to be studied here are given in terms

of the modified stream functions $f(\sigma,\eta)$ and $F(\sigma,\eta)$ by (3.4) and (3.8). For completeness, we shall first consider briefly the first-order problem.

5.2 First-Order Problem:

The first-order boundary-layer equation is

$$f''' + ff'' + \Lambda_{U_1}(1-f'^2) - 2\sigma(f'f'_\sigma - f_\sigma f'') = 0,$$

$$f(0) = 0 = f'(0), \quad f'(\infty) = 1. \tag{5.1}$$

We consider a flow with Λ_{U_1} = constant = β_∞ (say) and with initial condition prescribed as

$$f(\sigma_i,\eta) = f^*(\eta), \tag{5.2}$$

such that $f^*(\eta)$ deviates slightly from the similar solution $f_\infty(\eta)$ corresponding to Falkner-Skan solution for β_∞, known at $\sigma \to \infty$. Following Chen and Libby (1968), the solution for $f(\sigma,\eta)$ is assumed of the form

$$f(\sigma,\eta) \sim f_\infty(\eta) + f_1(\sigma,\eta) + f_2(\sigma,\eta) + \ldots . \tag{5.3}$$

where $f_\infty >> f_1 >> f_2$ and so on. Substituting (5.3) in (5.1) and properly ordering various terms, we obtain the equations for successive approximations. Obviously, the equation for $f_\infty(\eta)$ is the well-known Falkner-Skan equation, viz:

$$f_\infty''' + f_\infty f_\infty'' + \beta_\infty(1-f_\infty'^2) = 0,$$

$$f_\infty(0) = 0 = f_\infty'(0), \quad f_\infty'(\infty) = 1. \tag{5.4}$$

The auxiliary condition imposed is that approach of f' to unity as $\eta \to \infty$ must be exponential. The equation for f_1 is

found to be,

$$Lf_1 \equiv f_1''' + f_\infty f_1'' - 2\beta_\infty f_\infty' f_1' + f_\infty'' f_1 - 2\sigma (f_\infty' f_{1\sigma}' - f_\infty'' f_{1\sigma}) = 0,$$

$$f_1(\sigma, 0) = f_1'(\sigma, 0) = f_1'(\sigma, \infty) = 0, \qquad (5.5)$$

with the initial condition

$$f_1(\sigma_i, \eta) = f^*(\eta) - f_\infty(\eta).$$

The equations for f_2, f_3 etc. are of the form

$$Lf_n = T_n,$$

$$f_n(0) = f_n'(0) = f_n'(\infty) = 0,$$

$$f_n(\sigma_i, \eta) = 0.$$

Here T_n is a function of f_1, $f_2 \cdots f_{n-1}$. Using the method of separation of variables to solve the equation (5.5), we write

$$f_1(\sigma, \eta) \sim S(\sigma)\, N(\eta).$$

Introducing λ_n as the separation constant, we find that $S(\sigma) \sim \sigma^{-\lambda_n/2}$ while $N_n(\eta)$ is governed by the following eigenvalue problem:

$$N_n''' + f_\infty N_n'' + (\lambda_n - 2\beta_\infty) f_\infty' N_n' + (1-\lambda_n) f_\infty'' N_n = 0,$$

$$N_n(0) = N_n'(0) = N_n'(\infty) = 0. \qquad (5.6)$$

In addition, we have to impose the auxiliary condition that N' approaches zero, exponentially as $\eta \to \infty$. It is this condition which leads to discrete eigenvalues. It is observed that for $\beta_\infty > -.1988\ldots$, f_∞' satisfies the equation (5.6) but is not its eigenfunction (since the boundary condition $N_n'(0) = 0$ is not satisfied). Therefore, we reduce the order of the

equation (5.6) to two by introducing $H_n = (N_n/f_\infty')'$. Thus we obtain

$$(\bar{p}H_n')' + (\bar{q}-t\lambda_n)H_n = 0, \tag{5.7}$$

where

$$\bar{p} = f_\infty'^3 \exp\left(\int_0^\eta f_\infty \, d\eta\right),$$

$$t = f_\infty' \bar{p},$$

$$\bar{q} = f_\infty'^2 \exp\left(\int_0^\eta f_\infty \, d\eta\right) \left[\beta_\infty (3 - f_\infty'^2) + f_\infty f_\infty''\right].$$

The boundary conditions are

$$H_n'(0) - \left[\beta_\infty / f_\infty''(0)\right] H_n(0) = H_n(\infty) = 0,$$

with H_n approaching zero exponentially as $\eta \to \infty$. Equation (5.7) is in Sturm-Liouville form and differs from the standard form in some details. Using (5.7), it may be shown that for $\beta_\infty \geq 0$, the eigenvalues of the equation (5.7) are real and positive (cf. Chen and Libby, 1968). Further, it is seen that the $H_n(\eta)$ are orthogonal in the sense

$$\int_0^\infty t H_n H_m \, d\eta = \delta_{nm} C_m, \tag{5.8}$$

where C_m is the square of the norm. Similarly, for the socalled upper branch solutions for $-.1988\ldots < \beta_\infty < 0$, realness of λ_n and orthogonality of H_n functions is established directly while the fact that the minimum λ_n (denoted by λ_1) is indeed positive is established after it is numerically found to be so. For the lower branch solutions, equation (5.7) becomes a non-standard Sturn-Liouville problem and a careful study indicates existence of infinite set of both positive and negative eigenvalues. The

numerical values of the eigenvalues may be obtained by a quasi-linearization technique proposed by Libby and Chen (1968).

In view of the above discussion, we conclude that the solution for f_1 expressed as

$$f_1(\sigma,\eta) = \sum_{n=1}^{\infty} A_n \sigma^{-\lambda_n/2} N_n(\eta) \qquad (5.9)$$

is meaningful only for the upper branch solutions for $\beta_\infty > -.1988...$ when λ_n are positive. Here the A_n is arbitrary constant and is to be determined from the initial profile by using the relation (5.8), leading to the following expression for A_n:

$$A_n = C_n^{-1} \int_0^\infty t\,(N_n/f_\infty')'\,[(f^*-f_\infty)/f_\infty']'\,d\eta\,. \qquad (5.9a)$$

Substitution of (5.9) in (5.3) yields the solution of (5.1) in the following form:

$$f(\sigma,\eta) = f_\infty(\eta) + A_1 N_1(\eta)\,\sigma^{-\lambda_1/2} + A_2 N_2(\eta)\sigma^{-\lambda_2/2} + \ldots + T_1 + T_2 + \ldots. \qquad (5.10)$$

5.3 Second-Order Problem:

The second-order boundary-layer problem is subdivided to study separately the effects of the longitudinal curvature, transverse curvature, displacement and external vorticity. The initial value problem for the second-order momentum transfer may be formulated in many ways depending on how the initial profile is prescribed. One special way is to specify the initial profile at a streamwise station σ_i in such a manner that the

first-order solution is similar, i.e. $f(\sigma_i, \eta) = f_\infty(\eta)$, while the second-order profile $F(\sigma_i, \eta)$ deviates slightly from the limiting similar solution $F_\infty(\eta)$. However, in general we let both the first-order and the second-order initial profiles deviate slightly from the similar profile. We shall formulate the problem for the latter case and study the approach of the solution to limiting similar solution as $\sigma \to \infty$. We describe the problem separately for each of the second-order effects.

5.3.1 Longitudinal curvature:

The second-order boundary-layer equation for the longitudinal curvature problem, in terms of the modified stream function $F^{(1)}(\sigma, \eta)$, is

$$
\begin{aligned}
L^+(F^{(1)}, \Lambda_{B_1}) &= -\eta f''' + [(\Lambda_{B_1} + \Lambda_{U_1} - 1)(f'' + ff' + 2\sigma f' f_\sigma \\
&\quad + 4\sigma \int_\eta^\infty f' f'_\sigma \, d\eta) + (2\Lambda_{U_1} + \Lambda_{B_1}) \\
&\quad (\alpha + 2\sigma \alpha_\sigma + \Lambda_{U_1})]/(1 + \Lambda_{U_1}), \\
(1 + \Lambda_{B_1}) F(\sigma, 0) &+ 2\sigma F_\sigma(\sigma, 0) = 0, \\
F'(\sigma, 0) &= 0, \quad F'(\sigma, \eta) \backsim -\eta \quad \text{as } \eta \to \infty.
\end{aligned}
\tag{5.11}
$$

Here we have defined the operator L^+ as

$$
\begin{aligned}
L^+(Y, \epsilon) \equiv\ & Y''' + fY'' - (2\Lambda_{U_1} + \epsilon) f'Y' + (1 + \epsilon) f''Y \\
& -2\sigma (f'_\sigma Y' - f''Y_\sigma + f'Y'_\sigma - f_\sigma Y'').
\end{aligned}
\tag{5.12}
$$

As in the first-order problem, we assume Λ_{B_1} to be constant (denoted by Λ_1) alongwith $\Lambda_{U_1} = \beta_\infty$. The initial condition imposed is

such that $F^*(\eta)$ is slightly different from $F_\infty^{(1)}(\eta)$. In the subsequent matter, superscript 1 of F is dropped for convenience of writing.

The solution of the equation (5.11) is assumed to be of the form,

$$F(\sigma,\eta) \sim F_\infty(\eta) + F_1(\sigma,\eta) + F_2(\sigma,\eta) + \ldots, \qquad (5.13)$$

where $F_{n+1} << F_n$, in accordance with the imposed initial condition (5.12). Substitution of (5.13) in (5.11) and ordering terms, we obtain the equations for F_1 F_2 etc. Alternately, the form of F may be written by inspection. Here we adopt the latter approach to write,

$$\begin{aligned} F(\sigma,\eta) \sim F_\infty(\eta) &+ \sum_{n=1} A_n M_n(\eta)\sigma^{-\lambda_n/2} + \sum_{n=1} B_n P_n(\eta)\sigma^{-\gamma_n/2} \\ &+ \sum_n A_n^2 Q_n(\eta)\sigma^{-\lambda_n} + \sum_n \sum_m A_n A_m (1-\delta_{mn}) R_{mn}(\eta)\sigma^{-(\lambda_n+\lambda_m)/2} \\ &+ \sum_n \sum_m A_n B_m S_{mn}(\eta)\sigma^{-(\lambda_n+\gamma_m)/2} + \ldots. \qquad (5.14) \end{aligned}$$

Here $F_\infty(\eta)$ is the similar solution for specified β_∞ and Λ_1. The first correction term $M_n(\eta)$ arises due to the nonsimilarity of the first-order solution $N_n(\eta)$ itself. As mentioned in §5.2, there exists a discrete set of eigenvalues λ_n for the first-order problem and this introduces the multiplying factor of $\sigma^{-\lambda_n/2}$ for $M_n(\eta)$. The next correction term $P_n(\eta)$ is due to the eigenfunctions of the second-order longitudinal curvature problem, multiplied by the factors $\sigma^{-\gamma_n/2}$ where γ_n are the corresponding eigenvalues. Other correction terms arise due to product of the eigenfunction terms of the first-order with

powers $\sigma^{-\lambda_n}$ and $\sigma^{-(\lambda_n+\lambda_m)/2}$. Then follow terms like $S_{mn}(\eta)$ with factors which are powers of σ resulting from the multiplication of the previously mentioned series, i.e. $\sigma^{-(\lambda_n+\lambda_m)/2}$ and so on in indefinite proliferation. It may be noted that the terms in (5.14) have not been ordered according to the magnitude of the power of σ; such ordering is done after specifying the values of the pressure gradient parameter β_∞ and longitudinal curvature parameter Λ_1. The multiplicative constants B_n are to be determined from the upstream data for the longitudinal curvature problem while the constants A_n are known from the first-order problem.

Substitution of (5.14) in (5.11) and collection of coefficients of the like powers of σ yields the following sequence of equations:

$$L(F_\infty, \Lambda_1) = (1+\beta_\infty)^{-1}\left[-\eta(1+\beta_\infty) f_\infty''' + (\Lambda_1+\beta_\infty - 1)(f_\infty'' + f_\infty f_\infty') + (2\beta_\infty + \alpha_0)\right],$$

$$F_\infty(0) = 0 = F_\infty'(0), \quad F_\infty'(\eta) \sim -\eta \text{ as } \eta \to \infty. \tag{5.15}$$

$$L(P_n, \Lambda_1-\gamma_n) = 0, \tag{5.16}$$

$$P_n(0) = P_n'(0) = P_n'(\infty) = 0.$$

$$\begin{aligned} L(M_n,\Lambda_1-\lambda_n) = {} & -(1+\Lambda_1)F_\infty N_n'' + (2\beta_\infty+\Lambda_1-\lambda_n) F_\infty' N_n' - (1-\lambda_n)F_\infty'' N_n \\ & +(1+\beta_\infty)^{-1}\Big[-\eta(1+\beta_\infty)N_n''' +(\Lambda_1-\beta_\infty-1)\left[N_n''+f_\infty N_n'\right. \\ & +(1-\lambda_n) f_\infty' N_n - \lambda_n(\lambda_n-\beta_\infty-1)^{-1}\{N_n'' + f_\infty N_n' \\ & \left.+(1-\lambda_n)(f_\infty' N_n - N_n(\eta\to\infty))\}\right] + (2\beta_\infty+\Lambda_1) \\ & (\lambda_n-1)\, N_n(\eta\to\infty)\Big], \end{aligned}$$

$$L(Q_n, \Lambda_1 - 2\lambda_n) = (\lambda_n - \Lambda_1 - 1)\, N_n'' M_n + (2\beta_\infty + \Lambda_1 - 2\lambda_n) N_n' M_n'$$
$$-(1-\lambda_n)\, N_n M_n'' + (1+\beta_\infty)^{-1} \left[N_n N_n' - \lambda_n N_n' N_n \right.$$
$$\left. - \int_\eta^\infty \lambda_n N_n'^2 \, d\eta \right],$$
$$Q_n(0) = Q_n'(0) = Q_n'(\infty) = 0. \qquad (5.18)$$

Here L is the differential operator defined as

$$L(Y, \epsilon) \equiv Y''' + f_\infty Y'' - (2\beta_\infty + \epsilon) f_\infty' Y' + (1+\epsilon) f_\infty'' Y \qquad (5.19)$$

The first equation (5.15) is the familiar equation which yields self-similar solutions. The next equation (5.16) is a homogeneous equation with homogeneous boundary conditions, leading to an eigenvalue problem. If we put $\gamma_n - \Lambda_1 = \lambda_n^*$ in equation (5.16), it reduces to

$$P_n''' + f_\infty P_n'' - (2\beta_\infty - \lambda_n^*) f_\infty' P_n' + (1 - \lambda_n^*) f_\infty'' P_n = 0,$$
$$P_n(0) = P_n'(0) = P_n'(\infty) = 0. \qquad (5.16a)$$

The form of the above equation is identical with the equation (5.6) for $N_n(\eta)$ whose solution is already known. The rest of the equations for $M_n(\eta)$, $Q_n(\eta)$ etc. are to be solved by numerical integration.

5.3.2 Transverse curvature:

The governing equation of the transverse curvature problem is given by

$$L^+ (F^{(t)}, \Lambda_{B_t}) = -(2\Lambda_{U_1} + f''') + f'' + ff' - \Lambda_{B_t} \eta f'^2 + 2\sigma f' f_\sigma,$$
$$(1 + \Lambda_{B_t}) F^{(t)}(\sigma, 0) + 2\sigma F_\sigma^{(t)}(\sigma, 0) = 0,$$
$$F'^{(t)}(\sigma, 0) = 0, \quad F'^{(t)}(\sigma, \eta) \sim \eta \quad \text{as } \eta \to \infty. \qquad (5.20)$$

Initial condition:

$$F^{(t)}(\sigma_i, \eta) = F^*(\eta)$$

The transverse curvature parameter is assumed to be constant and denoted by Λ_t alongwith $\Lambda_{U_1} = \beta_\infty$. Following the arguments used earlier for the longitudinal curvature problem, we assume the following expansion for $F^{(t)}(\sigma,\eta)$:

$$F(\sigma,\eta) \sim F_\infty(\eta) + \sum_{n=1} A_n M_n(\eta)\sigma^{-\lambda_n/2} + \sum_{n=1} B_n P_n(\eta)\sigma^{-\gamma_n/2} + \sum_{n=1} A_n^2 Q_n(\eta)\,\sigma^{-\lambda_n} + \ldots . \tag{5.21}$$

Here we have dropped the superscript t from F. Substituting (5.21) in (5.20) and collecting various powers of σ, the resulting equations are written in the operator form as given below,

$$L(F_\infty, \Lambda_t) = -\eta(2\beta_\infty + f_\infty''') + f_\infty'' + f_\infty f_\infty' - \Lambda_t \eta f_\infty'^2,$$
$$F_\infty(0) = 0 = F_\infty'(0), \quad F_\infty'(\eta) \sim \eta \ \text{ as } \eta \to \infty. \tag{5.22}$$

$$L(P_n, \Lambda_t - \gamma_n) = 0,$$
$$P_n(0) = P_n'(0) = P_n'(\infty) = 0. \tag{5.23}$$

$$L(M_n, \Lambda_t - \lambda_n) = -(1+\Lambda_t)F_\infty N_n'' + (2\beta_\infty + \Lambda_t - \lambda_n) F_\infty' N_n' - (1-\lambda_n) F_\infty'' N_n - \eta N_n''' + N_n'' + (f_\infty - 2\Lambda_t \eta f_\infty')N_n' + (1-\lambda_n) f_\infty' N_n,$$
$$M_n(0) = M_n'(0) = M_n'(\infty) = 0. \tag{5.24}$$

$$L(Q_n, \Lambda_t - 2\lambda_n) = -(1+\Lambda_t-\lambda_n) N_n'' M_n + (2\beta_\infty + \Lambda_t - 2\lambda_n) N_n' M_n' - (1-\lambda_n) N_n M_n'' + (1-\lambda_n) N_n N_n' - \Lambda_t \eta N_n'^2,$$

Equation (5.22) yields the limiting similar solution. With the substitution of $\gamma_n - \Lambda_t = \lambda_n^*$, the equation (5.23) reduces to (5.6) whose solutions are known. Other equations are to be solved by numerical integration.

5.3.3 Displacement speed:

The second-order boundary-layer equation due to displacement is written as

$$L^+ (F^{(d)}, \Lambda_{B_d}) = -\Lambda_{B_d} - 2\Lambda_{U_1},$$

$$(1+\Lambda_{B_d})\, F^{(d)}(\sigma, 0) + 2\sigma F^{(d)}_{\sigma}(\sigma, 0) = 0,$$

$$F'^{(d)}(\sigma, 0) = 0, \quad F'^{(d)}(\sigma, \infty) = 1. \tag{5.26}$$

Initial condition:

$$F^{(d)}(\sigma_i, \eta) = F^*(\eta)$$

Here again Λ_{B_d} = constant $= \Lambda_d$ (say) and $\Lambda_{U_1} = \beta_\infty$. As in the case of the longitudinal curvature, we assume the following expansion for $F(\sigma, \eta)$ after superscript d has been dropped for convenience, thus

$$F(\sigma, \eta) \sim F_\infty(\eta) + \sum_{n=1} A_n M_n(\eta)\, \sigma^{-\lambda_n/2} + \sum_{n=1} B_n P_n(\eta) \sigma^{-\gamma_n/2}$$

$$+ \sum_{n=1} A_n^2\, Q_n(\eta)\, \sigma^{-\lambda_n} + \ldots . \tag{5.27}$$

Substituting the above expansion in equation (5.26), we obtain the following set of equations in the operator form:

$$L(F_\infty, \Lambda_d) = -\Lambda_d - 2\beta_\infty,$$

$$F_\infty(0) = 0 = F'_\infty(0), \quad F'_\infty(\infty) = 1. \tag{5.28}$$

$$L(P_n, \Lambda_d - \gamma_n) = 0,$$

$$P_n(0) = P_n'(0) = P_n'(\infty) = 0. \tag{5.29}$$

$$L(M_n, \Lambda_d - \lambda_n) = -(1+\Lambda_d)F_\infty N_n'' + (2\beta_\infty + \Lambda_d - \lambda_n)F_\infty' N_n' - (1-\lambda_n) F_\infty'' N_n,$$

$$M_n(0) = M_n'(0) = M_n'(\infty) = 0. \tag{5.30}$$

$$L(Q_n, \Lambda_d - 2\lambda_n) = -(1+\Lambda_d-\lambda_n) N_n'' M_n + (2\beta_\infty+\Lambda_d-2\lambda_n)N_n'M_n' - (1-\lambda_n) N_n M_n'',$$

$$Q_n(0) = Q_n'(0) = Q_n'(\infty) = 0. \tag{5.31}$$

Equation (5.27) yields the limiting similar solution for the displacement effect. Again we can substitute $\gamma_n + \Lambda_d = \lambda_n^*$ in the equation (5.29) to reduce it to the form (5.6) for which the solutions are known. The other equqtions for M_n, Q_n etc. are integrated numerically. However, for the special case of $\Lambda_d = 0$, the equation (5.30) for $M_n(\eta)$ has an exact solution in terms of the first-order eigenfunctions $N_n(\eta)$ given by

$$M_n(\eta) = [\, N_n'(\eta) + N_n(\eta)]/2. \tag{5.32}$$

5.3.4 External vorticity:

The second-order boundary-layer equation for the external vorticity is given by

$$L^+(F^{(v)}, 1-2\Lambda_{U_1}) = -\alpha - 2\sigma\, \alpha_\sigma,$$

$$2(1-\Lambda_{U_1})\, F^{(v)}(\sigma, 0) + 2\sigma\, F_\sigma^{(v)}(\sigma, 0) = 0,$$

$$F'^{(v)}(\sigma, 0) = 0, \quad F'^{(v)}(\sigma, \eta) \sim \eta \quad \text{as } \eta \to \infty. \tag{5.33}$$

Initial condition:

$$F^{(v)}(\sigma_i, \eta) = F^*(\eta)$$

Here again, we assume $\Lambda_{U_1} = \beta_\infty$ = constant and drop the superscript v from F. As for the other second-order effects, here again we assume the following form for F:

$$F(\sigma, \eta) \backsim F_\infty(\eta) + \sum_{n=1} A_n M_n(\eta) \sigma^{-\lambda_n/2} + \sum_{n=1} B_n P_n(\eta) \sigma^{-\gamma_n/2} + \sum_{n=1} A_n^2 Q_n(\eta) \sigma^{-\lambda_n} + \ldots . \tag{5.34}$$

Substitution of (5.34) in (5.33) yields the following system of equations:

$$L(F_\infty, 1-2\beta_\infty) = -\lim_{\eta \to \infty} (\eta - f_\infty(\eta))$$
$$F_\infty(0) = 0 = F_\infty'(0), \quad F_\infty'(\eta) \backsim \eta \text{ as } \eta \to \infty. \tag{5.35}$$

$$L(P_n, 1-2\beta_\infty - \gamma_n) = 0,$$
$$P_n(0) = P_n'(0) = P_n'(\infty) = 0. \tag{5.36}$$

$$L(M_n, 1-2\beta_\infty - \lambda_n) = -(2-2\beta_\infty) F_\infty N_n'' + (1-\lambda_n) F_\infty' N_n' - (1-\lambda_n) F_\infty'' N_n + (1-\lambda_n) N_n(\eta \to \infty),$$
$$M_n(0) = M_n'(0) = M_n'(\infty) = 0. \tag{5.37}$$

$$L(Q_n, 1-2\beta_\infty - 2\lambda_n) = -(2-2\beta_\infty-\lambda_n) N_n'' M_n + (1-2\lambda_n) N_n' M_n' - (1-\lambda_n) N_n M_n'',$$
$$Q_n(0) = Q_n'(0) = Q_n'(\infty) = 0. \tag{5.38}$$

The limiting similar solution due to external vorticity is given by equation (5.31). Substituting $\gamma_n - 1 + 2\beta_\infty = \lambda_n^*$ in

5.4 Numerical Results and Discussion:

For each of the second-order problems along with the first-order problem, detailed solutions have been obtained for two representative values of β_∞, namely 0 and 1/2. The effect of variation of the second-order parameters, arising due to longitudinal curvature, transverse curvature and displacement speed on the corresponding solutions is examined for $-2 \leq \Lambda_{1,t,d} \leq 4$. For completeness, we first discuss briefly the first-order solutions for $\beta_\infty = 0$ and 1/2.

The solution of the first-order problem can be expressed as,

$$f(\sigma,\eta) \sim f_\infty(\eta) + A_1 N_1(\eta)\, \sigma^{-\lambda_1/2} + A_2 N_2(\eta) \sigma^{-\lambda_2/2} + \ldots . \quad (5.39)$$

The eigenvalues λ_n and eigenfunctions $N_n(\eta)$ are determined by solving equation (5.6) with the auxiliary condition specified earlier. Libby and Fox (1963) have listed the first ten eigenvalues for the above equation for $\beta_\infty = 0$ while Chen and Libby (1968) have provided the first twenty eigenvalues for $\beta_\infty = 1/2$. The important question that arises is where to truncate the series (5.39) for the purpose of studying its effect on the second-order solutions. This question is linked with the prescribed initial condition; for a very small departure of the initial profile from the similar one, only a few terms may provide a satisfactory answer. Since, we are interested here in small deviations of the initial profile so as to linearize the solutions about the limiting similar solution, it is decided to include terms upto $\sigma^{-\lambda_2/2}$. This will be consistently followed in the second-order

series representation for $F(\sigma,\eta)$ also. The required first two eigenvalues and the corresponding squares of norms for $\beta_\infty = 0$ and 1/2 are given in Table 5.1.

Table 5.1: The eigenvalues and squares of norms for $\beta_\infty = 0$ and 1/2.

β	n	λ_n	C_n
0	1	2.0	2.2672
	2	3.774	1.1447
1/2	1	3.092	2.066
	2	4.959	1.011

The multiplicative constants A_1 and A_2 are estimated from relation (5.9a). The eigenfunctions $N_n(\eta)$ are shown in Figure 5.1. It may be noted that all the eigenvalues are positive so that the initial profile which deviating slightly from the similarity profile, approaches asymptotically the similarity profile as $\sigma \to \infty$. We now proceed to examine the corresponding second-order boundary layer results and see if such a behaviour is exhibited.

The solution for the second-order problem is expressed as

$$F^{(i)}(\sigma,\eta) \sim F_\infty^{(i)}(\eta) + \sum_n A_n M_n^{(i)}(\eta)\sigma^{-\lambda_n/2} + \sum_n B_n P_n^{(i)}(\eta)\sigma^{-\gamma_n/2} + \sum_n A_n^2 Q_n^{(i)}(\eta)\,\sigma^{-\lambda_n} + \ldots . \qquad (i = 1,t,d,v) \qquad (5.40)$$

Two important points to be considered in regard to the above solution are: to choose a criterion for truncating the series and to order the terms according to the powers of σ. For the first question, we mentioned earlier while discussing the first-order problem, that we shall retain terms upto $\sigma^{-\lambda_2/2}$ only so as to make $f(\sigma,\eta)$ and $F(\sigma,\eta)$ consistent in some sense. Thus, in the following discussion we shall show only those terms which have the magnitude of power of σ less than $\lambda_2/2$. Now to answer the second question, we remark that, in general, it is not possible to order the terms without specifying the parameters $\beta_\infty, \Lambda_l, \Lambda_t$ and Λ_d. This is due to the dependence of λ_n on β_∞ and of γ_n on $\Lambda_l, \Lambda_t, \Lambda_d$ and β_∞. We now discuss each of the second-order effect separately to show some typical properly ordered solutions for $F^{(i)}(\sigma,\eta)$ for various values of the parameters.

5.4.1 Longitudinal curvature:

The longitudinal curvature problem is governed by the equations (5.15)-(5.18). The eigenvalue problem (5.16) involves the eigenvalues γ_n which is determined by using the relation

$$\gamma_n = \Lambda_l + \lambda_n \tag{5.41}$$

and in particular

$$\gamma_1 = \Lambda_l + \lambda_1 , \quad \gamma_2 = \Lambda_l + \lambda_2 . \tag{5.41a,b}$$

Depending on the longitudinal curvature of the body and hence, the value of Λ_l, the terms in (5.40) can be ordered according to the powers of σ; five such distinct cases (a-e) given below

(a) $\Lambda_1 > (\lambda_2-\lambda_1)$

$$F(\sigma,\eta) \sim F_\infty(\eta) + A_1M_1(\eta)\sigma^{-\lambda_1/2} + A_2M_2(\eta)\sigma^{-\lambda_2/2} + O(\sigma^{-\lambda_2/2}) \tag{5.42}$$

(b) $(\lambda_2-\lambda_1) > \Lambda_1 > 0$

$$F(\sigma,\eta) \sim F_\infty(\eta) + A_1M_1(\eta)\sigma^{-\lambda_1/2} + B_1P_1(\eta)\sigma^{-\gamma_1/2} + A_2M_2(\eta)\sigma^{-\lambda_2/2} + O(\sigma^{-\lambda_2/2}). \tag{5.43}$$

(c) $0 > \Lambda_1 > -(\lambda_2-\lambda_1)$

$$F(\sigma,\eta) \sim F_\infty(\eta) + B_1P_1(\eta)\sigma^{-\gamma_1/2} + A_1M_1(\eta)\sigma^{-\lambda_1/2} + B_2P_2(\eta)\sigma^{-\gamma_2/2} + A_2M_2(\eta)\sigma^{-\lambda_2/2} + O(\sigma^{-\lambda_2/2}) \tag{5.44}$$

(d) $-(\lambda_2-\lambda_1) > \Lambda_1 > -\lambda_1$

$$F(\sigma,\eta) \sim F_\infty(\eta) + B_1P_1(\eta)\sigma^{-\gamma_1/2} + B_2P_2(\eta)\sigma^{-\gamma_2/2} + A_1M_1(\eta)\sigma^{-\lambda_1/2} + A_2M_2(\eta)\sigma^{-\lambda_2/2} + O(\sigma^{-\lambda_2/2}) \tag{5.45}$$

(e) $\Lambda_1 < -\lambda_1$

$$F(\sigma,\eta) \sim B_1P_1(\eta)\sigma^{-\gamma_1/2} + F_\infty(\eta) + B_2P_2(\eta)\sigma^{-\gamma_2/2} + A_1M_1(\eta)\sigma^{-\lambda_1/2} + A_2M_2(\eta)\sigma^{-\lambda_2/2} + O(\sigma^{-\lambda_2/2}) \tag{5.46}$$

It may be noted that we have intentionally omitted the equality sign from all the above shown limits for Λ_1; the reasons for doing so will become apparent later where we discuss the solutions corresponding to the values of Λ_1 given by equality sign in the above mentioned limits.

We first discuss the last case (e), since it has certain implications about the nature of the longitudinal curvature of the body. For this case, the first eigenvalue λ_1 is negative so that the corresponding term due to the first eigenfunction $P_1(\eta)$ is multiplied by positive power of σ. Thus, for $\Lambda_1 < \lambda_1$, the solution is unstable in the sense that any departure from similarity (at a given initial station) will grow indefinitely in the downstream direction as $\sigma \to \infty$. If, however, the initial condition is prescribed such that $B_1 = 0$, then the equation (5.46) shows that the solution is again stable, in the sense defined above, till Λ_1 is decreased so much that $\Lambda_1 < -\lambda_2$ so that γ_2 becomes negative and again makes the solution unstable. Similar arguments may be applied to show that for various prescribed initial conditions, $-\Lambda_1 = \lambda_1, \lambda_2, \lambda_3$ etc. are the critical values. For a general initial condition, however, it is the value $\Lambda_1 = -\lambda_1$ itself that is the most critical and solutions will be unstable for $\Lambda_1 < -\lambda_1$. We recall here an earlier discussion of §3.3; it was shown for the longitudinal curvature problem that the self-similar solution, $F_\infty(\eta)$ in the present notations, has several infinite discontinuities whenever Λ_1 takes a value equal to the eigenvalue λ_n for a given β (β_∞ in present notation). That the locally similar solutions are indeed singular at these critical values of Λ_1, is further reinforced from the present analysis which shows that the flow becomes unstable for the values of Λ_1 corresponding to the singular points. In §3.3, while discussing the design of aerodynamic shapes, it was

suggested that the curvature of the body is to be so prescribed that $\Lambda_1 \neq \lambda_n$. Within the linear theory, the present analysis, puts a further restriction on the selection of the value for Λ_1. It seems desirable that the values of Λ_1, such that $\Lambda_1 < -\lambda_1$, should be avoided to ensure that any slight departure from the similarity profile will not cause the skin friction to grow indefinitely in the downstream direction.

For the values of Λ_1 shown in other cases (a-d), the solution (5.40) is stable in the sense that the slightly non-similar initial profile does approach the limiting similar profile as $\sigma \to \infty$. The governing equations (5.15)-(5.17) are integrated numerically for various values of Λ_1 and β_∞. Results are presented for two representative values of $\beta_\infty = 0$ and $1/2$ and Λ_1 in the range $-2 \leq \Lambda_1 \leq 4$. The solution of the equation (5.16) and (5.17) is obtained for n = 1 and 2. Figure 5.1 shows the eigenfunctions $P_1(\eta)$ and $P_2(\eta)$ for both $\beta_\infty = 0$ and $1/2$. The corresponding eigenvalues γ_1 and γ_2 for a given Λ_1 are given by the equation (5.46).

The solutions of the first two equations of the system (5.17) are shown in Figures 5.2 and 5.3 for two values of β_∞ i.e. 0 and $1/2$. Figure 5.2 shows $M_1^{''(1)}(0)$ vs. Λ_1 obtained from solution of the equation 5.17 for n = 1. It may be seen that several discontinuities occur for both the values of β_∞ at certain critical values of the longitudinal curvature parameter Λ_1. First discontinuity occurs at $\Lambda_1 = 0$. This

behaviour of the equqtion (5.17) is easily explained by considering the operator of the equation which, on substitution of $\Lambda_1 = 0$, reduces to the first-order eigenvalue operator (5.6) corresponds to λ_1. Thus, M_1 becomes the eigenfunction of the operator of the equation (5.17) and leads to the discontinuity (nonunique solution) in the numerical integration of the equation. The next discontinuity occurs at $\Lambda_1 = \lambda_1 - \lambda_2$. Again, substitution of the value reduces the operator of (5.17) to the first-order eigenvalue operator (5.6) corresponding to λ_2 and hence, the singular behaviour. There will be many more such discontinuities whenever Λ_1 takes a value equal to $\lambda_1 - \lambda_n$, for $n \geq 1$. The solutions for M_1 are also found to be singular whenever $\Lambda_1 = -\lambda_n$. This happens due to the singular behaviour of the corresponding equation (5.15) as was explained in Chapter 3 (§3.3). Thus, for these values, the Right hand side of equation (5.17), involving the solution of (5.15), blows up.

The solution of the equation (5.17) for n = 2 is shown in Figure 5.3 in the form of $M_2''^{(1)}(0)$ versus Λ_1. Here again, several discontinuities are observed whenever $\Lambda_1 = \lambda_2 - \lambda_n$ or $\Lambda_1 = -\lambda_n$ $(n \geq 1)$ for the reasons mentioned in the preceding paragraph. We may note that the first singularity occurs here for positive values of Λ_1 which has never been observed before. Therefore, there exist both positive and negative critical values of Λ_1 such that the second-order longitudinal curvature solution becomes unstable in the sense that any departure from

similarity at a given streamwise station grows in the increasing streamwise distance.

As mentioned earlier, the equality sign was purposely omitted while writing the limits on Λ_1 for different cases (a-e). It is now clear that for those limiting values of Λ_1 with equality sign, the flow is unstable because the solutions M_1 and M_2 are themselves found to be singular at these values. To what we said earlier about choosing the values of Λ_1 for aerodynamic shapes, it may be added that besides the restriction $\Lambda_1 > -\lambda_1$, the isolated critical values of Λ_1 (given in the preceding paragraphs) are also to be excluded.

5.4.2 Transverse curvature:

The transverse curvature problem is, governed by equations (5.22)-(5.25). The value of γ_n is determined by using the relation,

$$\gamma_n = \Lambda_t + \lambda_n \quad (n = 1,2,\ldots) \tag{5.67}$$

As in the case of the longitudinal curvature, we may order the terms in (5.40) depending on the value of Λ_t and obtain the five distinct cases given by equations (5.42)-(5.46) after replacing Λ_1 by Λ_t. For any given Λ_t, the nature of the solutions being similar to that for the longitudinal curvature described in §5.5.1, no further comments are needed.

The solutions of equation (5.24) for n = 1 and 2 are presented in Figures 5.4 and 5.5. The variation of $M_1^{''(t)}(0)$ and $M_2^{''(t)}(0)$ with Λ_t for both $\beta_\infty = 0$ and 1/2 is shown,

respectively, in Figures 5.4 and 5.5. Again, several singularities are observed for the critical values of Λ_t which are equal to the critical values of Λ_1 given in §5.5.1 and, therefore, no further comment is needed.

5.4.3 Displacement speed:

Solutions to the displacement speed problem are obtained by numerical integration of the equations (5.28)-(5.30). The value of γ_n is again obtained by using the relation

$$\gamma_n = \Lambda_d + \lambda_n \quad (n = 1,2,\ldots). \tag{5.48}$$

The terms in the expansion of $F^{(d)}(\sigma,\eta)$ are ordered according to the value of Λ_d as given by the equations (5.42)-(5.46). The comments given earlier regarding the stability of the flow for various values of the second-order parameters Λ_1, Λ_t hold good for the displacement effect also and need no elaboration.

The solution of the first equation (n=1) of the system (5.30) is shown in Figure 5.6 for two values of β_∞, namely $\beta_\infty = 0$ and 1/2. Again, we observe from Figure 5.6, that $M_1''(0)$ has several singularities for $\Lambda_d = \lambda_1 - \lambda_n$ $(n > 1)$. These infinite discontinuities occur at the same values of the displacement speed parameter Λ_d as observed for the longitudinal and transverse curvature problems but for one exception: at $\Lambda_d = 0$, the solution is finite and is marked by '*' in the Figure 5.6. For the last case $(\Lambda_d = 0)$, the operator of the equation (5.30) is reduced to the first-order eigenvalue operator, suggesting thereby that inspite of λ_1 (at $\Lambda_d = 0$) being an eigenvalue, the function

$M_1(\eta)$ is not singular. The particular integral of (5.30), viz.

$$M_1^*(\eta) = \left(N_1'(\eta) + N_1(\eta)\right)/2$$

satisfies all the boundary conditions, as does the complimentary function

$$M_1^{**}(\eta) = A N_1(\eta)$$

Consequently, we obtain the following expression for the complete solution of $M_1(\eta)$:

$$M_1(\eta) = A. M_1^{**}(\eta) + M_1^*(\eta) \qquad (5.49)$$

where A is an arbitrary constant. One way to evaluate the constant is to join smoothly the two solutions for $\Lambda_d = 0^+$ and 0^-.

The solutions for function $M_2''(0)$ as a function of Λ_d are shown in Figure 5.7 for the values of $\beta_\infty = 0$ and $1/2$. Again we observe that the solutions of the equations (5.30) for $n = 2$ are not unique whenever $\Lambda_d = \lambda_2 - \lambda_n$ $(n > 2)$. In Figure 5.7, for $\Lambda_d = 0$, we have again indicated the corresponding value of $M_2''(0)$ by '*'. The nature of the solutions is similar to that of M_1 and hence no further comments are needed.

5.4.4 External vorticity:

The second-order external vorticity problem does not contain any new parameter. Solutions to equations (5.28)-(5.30) are obtained for $\beta_\infty = 0$ and $1/2$ by numerical integration. The value of γ_n is obtained by the relation

$$\gamma_n = 1 - 2\beta_\infty + \lambda_n \quad (n = 1, 2, \ldots) \qquad (5.50)$$

The terms in the expansion of $F^{v}(\sigma,\eta)$ can be ordered for a given β_∞. It may be noted that for $\beta_\infty = 1/2$, equation (5.30) is reduced to the form same as that for the first-order eigenvalue problem so that the solution of $M_n(\eta)$ becomes singular for all values of n so that the flow is unstable in the sense defined earlier. For $\beta_\infty = 0$, the terms in (5.27) are correctly ordered in the following manner:

$$F^{(v)}(\sigma,\eta) \sim F_\infty(\eta) + A_1 M_1(\eta)\ \sigma^{-\lambda_1/2} + B_1 P_1(\eta)\sigma^{-\gamma_1/2} + A_2 M_2(\eta)\sigma^{-\lambda_2/2} + O(\sigma^{-\lambda_2/2}) + \ldots \quad (5.51)$$

The operator of equation (5.30) for n = 1 and $\beta_\infty = 0$ (with corresponding $\lambda_1 = 2$) is reduced to the following form:

$$L(M_1, -1) \equiv M_1''' + f_\infty M_1'' + f_\infty' M_1' \quad (5.52)$$

This leads to solution $M_1''(0) \equiv 0$ in the numerical integration of equation (5.30) for $\beta_\infty = 0$ and n = 1. The solution of (5.30) for $\beta_\infty = 0$ and n = 2 is found to be $M_2''(0) = -2.591$. Substituting the values of M_1 and M_2 thus obtained in (5.51), it may seen how $F^{(v)}$ approaches to the limiting similar solution for $\beta_\infty = 0$.

Part II: <u>Skin friction on a blunted wedge for large streamwise distances</u>:

The general analysis of Part I essentially deals with the evaluation of the eigenvalues and the corresponding eigenfunctions which are to be included in the expansion of the variable that represents the solution to an initial value

problem of the type studied in the preceding sections. However, in many problems of practical interest, the parameters $\Lambda_{U_1}, \Lambda_{B_1}$ etc. are, in general, functions of σ and, therefore, the expansion must include additional terms (besides eigenfunctions) to account for the variation of $\Lambda_{U_1}, \Lambda_{B_1}$ etc. with σ. We now obtain detailed solutions for one such problem: uniform flow past a blunted wedge shown in Figure 4.1, and study the momentum transfer problem for large σ. The corresponding solutions for small values of σ were studied in §4.4 of Chapter 4 and the Eulerized form of these solutions is used to impose the initial condition for the present problem. Thus, we shall show how the Eulerized series solution for nose region approaches the limiting similar solution at $\sigma \to \infty$. The quantity of particular interest is the skin friction coefficient defined by (4.53) and as such we focus our attention on $f''(\sigma,0)$ and $F''(\sigma, 0)$ defined by (4.54) and (4.55) respectively.

5.5 First-Order Problem:

The first-order boundary-layer equation in terms of the modified stream function $f(\sigma,\eta)$ is given by (5.1). The initial condition (5.2) is prescribed in the following form:

$$f''(\sigma_i, 0) = \hat{\tau}_1 \qquad (5.50)$$

where $\hat{\tau}_1$, defined by (4.85), is the Eulerized Görtler series solution obtained in Chapter 4. The pressure gradient parameter Λ_{U_1} for the blunted wedge given by (4.21), viz.

$$\Lambda_{U_1} = (1-\beta_\infty + 2\beta_\infty \sigma)/(1-\beta_\infty + 2\sigma),$$

is expanded for large values of σ to yield the following expansion:

$$\Lambda^*_{U_1} = \beta_\infty + \sum_{n=1} (\beta_\infty - 1)^{n+1} (2\sigma)^{-n} . \qquad (5.51)$$

Using (5.10), the solution of (5.1) is expressed in the following form:

$$f(\sigma, \eta) = f_\infty(\eta) + \bar{f}_1(\eta)\, \sigma^{-1} + A_1 N_1(\eta)\sigma^{-\lambda_1/2} + \bar{f}_2(\eta)\sigma^{-2} + A_2 N_2(\eta)\sigma^{-\lambda_2/2} + \ldots . \qquad (5.52)$$

Here the additional terms of the type $\bar{f}_n(\eta)\sigma^{-n}$ are 'forced' by the pressure gradient parameter $\Lambda^*_{U_1}$, since it varies with σ in the manner given by (5.51). It is noted that the relative position of the terms in (5.52) will depend on the value of β_∞: In (5.52), we have shown correct order of the terms for $0 < \beta_\infty < 1$.

Substitution of (5.52) in (5.1) and collection of the coefficients of the like powers of σ yields the following system of equations (bar on f_n's is suppressed for convenience):

$$f_1''' + f_\infty f_1'' + 2(1-\beta_\infty)\, f_\infty' f_1' - f_\infty'' f_1 = -(1-\beta_\infty)^2(1-f_\infty'^2)/2,$$
$$f_1(0) = f_1'(0) = f_1'(\infty) = 0. \qquad (5.53)$$
$$f_2''' + f_\infty f_2'' + 2(1-\beta_\infty)\, f_\infty f_2' - 3f_\infty'' f_2 = f_1 f_1'' - (2-\beta_\infty)\, f_1'^2 + (1-\beta_\infty)^2 f_\infty' f_1' - (1-\beta_\infty)^3(1-f_\infty'^2)/4,$$
$$f_2(0) = f_2'(0) = f_2'(\infty) = 0. \qquad (5.54)$$

The equations for $f_\infty(\eta)$ and $N_n(\eta)$ are same as those given by (5.4) and (5.7) respectively. The solution of (5.53), expressed in terms of the solution of the equation (5.4), is of the following form:

$$f_1(\eta) = (1-\beta_\infty)^2 (4\beta_\infty)^{-1} (\eta f'_\infty - f_\infty). \qquad (5.55)$$

The solution of (5.54) has to be obtained by numerical integration. The multiplicative constants A_1, A_2 etc. in (5.52) have to be determined by making use of the initial condition (5.50) whereby we join (5.52) to the Görtler series solution obtained in Chapter 4.

5.6 Second-Order Problem:

The second-order boundary-layer equation for the longitudinal curvature is given by (5.11) and is repeated here (superscript 1 is dropped) for convenience,

$$L^+(F, \Lambda_{B_1}) = -\eta f''' + [(\Lambda_{B_1} + \Lambda_{U_1} - 1)(f'' + ff' + 2\sigma f' f_\sigma + 4\sigma \int_\eta^\infty f' f_\sigma \, d\eta) + (2\Lambda_{U_1} + \Lambda_{B_1})(\alpha + 2\sigma \alpha_\sigma + \Lambda_{U_1})]/(1+\Lambda_{U_1}),$$

$$(1+\Lambda_{B_1})F(\sigma, 0) + 2\sigma F_\sigma(\sigma, 0) = 0 = F'(\sigma, 0), F'(\sigma, \eta) \underset{\text{as } \eta \to \infty}{\sim} -\eta, \qquad (5.56)$$

The operator L^+ is defined by (5.12). We may note that $\Lambda^*_{U_1}$ and $\Lambda^*_{B_1}$ are function of σ here. The initial condition is prescribed by fixing the initial profile at any given station σ_i in terms of the Eulerized Görtler series for the longitudinal curvature, obtained earlier in Chapter 4. Since we are primarily interested in the skin friction coefficient, the initial condition has the following form:

$$B_1^* F''^{(1)}(\sigma_i, 0) = \tau_2^{(1)} \qquad (5.56a)$$

where $\tau_2^{(1)}$ is given by (4.87). The quantity B_1, defined by (4.36), is expanded for large values of σ to yield the

following expression for B_1, denoted by B_1^*:

$$B_1^* = (1-\beta_\infty)^{3/2}\,(2\sigma)^{-1} - (1-\beta_\infty)^{5/2}\,(2\sigma)^{-2} + \ldots \quad (5.57a)$$

Using (4.37), we obtain the following expression for the longitudinal curvature parameter for large values of σ:

$$\Lambda_{B_1}^* = -2 + \sum_{n=1} (-2)\,(\beta_\infty - 1)^n\,(2\sigma)^{-n} = \Lambda_{1_o}^* + \Lambda_{1_1}^* \sigma^{-1} + \Lambda_{1_2}^* \sigma^{-2} + \ldots \text{ say} \quad (5.57b)$$

The above form of the expansion suggests that the expansion of $F^{(1)}(\sigma,\eta)$ will contain a series of functions $\bar{F}_n(\eta)$ multiplied by inverse integral powers of σ. Including such additional terms in the expansion (5.14) of $F(\sigma,\eta)$, we write the solution of (5.56) in the following form:

$$\begin{aligned} F(\sigma,\eta) \sim F_\infty(\eta) &+ B_1 P_1(\eta)\sigma^{-\gamma_1/2} + \bar{F}_1(\eta)\sigma^{-1} + B_2 P_2(\eta)\sigma^{-\gamma_2/2} \\ &+ A_1 M_1(\eta)\sigma^{-\lambda_1/2} + \bar{F}_2(\eta)\sigma^{-2} \\ &+ A_2 M_2(\eta)\sigma^{-\lambda_2/2} + \ldots \end{aligned} \quad (5.58)$$

Here terms in σ^{-1} and σ^{-2} arise due to variation of Λ_{B_1} with σ. The relative position of the terms in (5.58) will depend on the value of β_∞; in (5.58) the terms have been ordered correctly for $\beta_\infty = 1/2$. The value of γ_n is determined from the relation (5.41).

Substituting (5.58) in (5.56) and collecting the like powers of σ, we obtain the following system of equations for the longitudinal curvature problem (again, bar on F_n's is suppressed):

$$L_1(F_\infty, \Lambda^*_{B_1};\ \beta_\infty) \equiv F_\infty''' + f_\infty F_\infty'' - (2\beta_\infty + \Lambda^*_{1_0})\ f_\infty' F_\infty'$$
$$+ (1+\Lambda^*_{1_0})\ f_\infty'' F_\infty = -\eta f_\infty''' + 2(\beta_\infty - 1)(\beta_\infty + 1)^{-1}\ (\alpha_0 + \eta\beta_\infty)$$
$$+ (\beta_\infty - 3)(\beta_\infty + 1)^{-1}(f_\infty'' + f_\infty f_\infty'),$$
$$F_\infty(0) = 0 = F_\infty'(0),\ F'(\eta) \backsim -\eta \quad \text{as } \eta \to \infty. \tag{5.59}$$

$$L_2(F_1, \Lambda^*_{B_1};\ \beta_\infty) \equiv F_1''' + f_\infty F_1'' + (2 - 2\beta_\infty - \Lambda^*_{1_0})\ f_\infty' F_1'$$
$$+ (\Lambda^*_{1_0} - 1)\ f_\infty'' F_1 - f_1 F_\infty'' + (2\beta_\infty + \Lambda^*_{1_0} - 2)\ f_1' F_\infty'$$
$$+ (1+\Lambda^*_{1_0})\ f_1'' F_\infty - [(\beta_\infty - 1)^2 + \Lambda^*_{1_1}]\ f_\infty' F_\infty' + \Lambda^*_{1_1} f_\infty'' F_\infty$$
$$= -\eta f_1''' + 2(\beta_\infty - 1)(\beta_\infty + 1)^{-1}\ [-\alpha_1 + \eta(\beta_\infty - 1)^2/2]$$
$$+ (\beta_\infty - 3)(\beta_\infty + 1)^{-1}\ [f_1'' - f_\infty' f_1 + f_\infty f_1'$$
$$+ \eta f_\infty'^2/2 - (1+\beta_\infty)^{-1}(f_\infty''' + f_\infty f_\infty' + \alpha_0 + \eta\beta_\infty)/2]$$
$$+ (\beta_\infty - 3)(\beta_\infty - 1)(\beta_\infty + 1)^{-2}(f_\infty'' + f_\infty f_\infty' + \alpha_0 + \eta\beta_\infty),$$
$$F_1(0) = F_1'(0) = F'(\infty) = 0. \tag{5.60}$$

$$L_3(M_1, \Lambda^*_{B_1};\ \beta_\infty) \equiv M_1''' + f_\infty M_1'' + (\lambda_1 - 2\beta_\infty - \Lambda^*_{1_0})\ f_\infty' M_1'$$
$$+ (1+\Lambda^*_{1_0} - \lambda_1) f_\infty'' M_1 + (1+\Lambda^*_{1_0})\ N_1'' F_\infty - (2\beta_\infty + \Lambda^*_{1_0} - \lambda_1)$$
$$N_1' F_\infty' + (1-\lambda_1)\ N_1 F_\infty'' = -\eta N_1''' - 2(\beta_\infty - 1)(\beta_\infty + 1)^{-1}(1-\lambda_1)$$
$$[\lim_{\eta\to\infty} N_1(\eta)] + (\beta_\infty - 3)(\beta_\infty + 1)^{-1}\ [N_1'' + (1-\lambda_1) f_\infty' N_1$$
$$+ f_\infty N_1' + \lambda_1(1+\beta_\infty - \lambda_1)^{-1}\{ N_1'' + f_\infty N_1' + (1-\lambda_1) f_\infty' N_1$$
$$+ (1-\lambda_1)\ (\lim_{\eta\to\infty} N_1(\eta)\}],$$
$$M_1(0) = M_1'(0) = M_1'(\infty) = 0. \tag{5.61}$$

$$L_4(P_1, \Lambda^*_{B_1};\ \beta_\infty) \equiv P_1''' + f_\infty P_1'' + (\gamma_1 - 2\beta_\infty - \Lambda^*_{1_o})\ f_\infty' P_1'$$
$$+ (1 + \Lambda^*_{1_o} - \gamma_1)\ f_\infty'' P_1 = 0,$$
$$P_1(0) = P_1'(0) = P_1'(\infty). \qquad (5.62)$$

Here

$$\alpha_o = \lim_{\eta \to \infty} [\eta - f_\infty(\eta)],$$
$$\alpha_1 = \lim_{\eta \to \infty} [\ - f_1(\eta)],$$
$$\Lambda^*_{1_o} = -2,$$
$$\Lambda^*_{1_1} = 1 - \beta_\infty.$$

The second-order boundary-layer equation for the displacement effect is given by (5.26) and is repeated here (superscript d is dropped) for convenience,

$$L^+(F, \Lambda_{B_d}) = -\Lambda_{B_d} - 2\Lambda_{U_1},$$
$$(1 + \Lambda_{B_d})\ F(\sigma, 0) + 2\sigma F_\sigma(\sigma, 0) = 0. \qquad (5.63)$$
$$F'(\sigma, 0) = 0, \quad F'(\sigma, \eta) = 1 \quad \text{as} \quad \eta \to \infty. \qquad (5.64)$$

The initial condition:

$$B_d\ F''^{(d)}(\sigma_i, 0) = \tau_2^{(d)}$$

Here $\tau_2^{(d)}$ is given by (4.79) and represents the Eulerized series solution of the displacement problem, obtained in Chapter 4. The quantity B_d [$= U_2(s, 0)/U_1(s, 0)$], defined by (4.31), is expanded for large σ to yield the following expression, denoted by B_d^*:

$$B_d^* = -(1 - \beta_\infty)(2\sigma)^{-1/2} [B_o + B_1 \sigma^{-1} + \ldots .]$$

where

$$B_o = (2a_1 - a_o)/2$$

$$B_1 = (1 - \beta_\infty)(6a_1 - 7a_o)/8. \qquad (5.65)$$

Here a_o, a_1 etc. are same as those defined by (4.30). Using (4.32), we obtain the following expression of the displacement speed parameter Λ_{B_d} for large σ:

$$\Lambda^*_{B_d} = -1 + (1-\beta_\infty)\,[(6a_1-7a_o)/2(2a_1-a_o)]\,\sigma^{-1} + \ldots.$$

$$= \Lambda^*_{d_o} + \Lambda^*_{d_1}\sigma^{-1} + \ldots. \text{ say} \qquad (5.66)$$

The five term series (4.31) of B_d was obtained starting from the stagnation point and has been utilized above to obtain its asymptotic form ($\sigma \to \infty$) with the hope that the factor $(1+\xi_s^2)^{-1/2}$ extracted from the series gives the correct behaviour of B_d [and, therefore, of $U_2(s,0)$] as $\sigma \to \infty$. In the strict sense, we should find the required expansion for large σ, starting from $1/\sigma = 0$. However, it is still instructive to use the expansion (5.66) and obtain useful estimates of the solution of the displacement speed problem for large σ.

The solution to the displacement speed problem for large σ is assumed to be of the following form:

$$F(\sigma,\eta) = F_\infty(\eta) + \bar{F}_1(\eta)\sigma^{-1} + B_1P_1(\eta)\,\sigma^{-\gamma_1/2}$$

$$+ A_1M_1(\eta)\sigma^{-\lambda_1/2} + B_2P_2(\eta)\sigma^{-\gamma_2/2}$$

$$+ \bar{F}_2(\eta)\sigma^{-2} + A_2M_2(\eta)\sigma^{-\lambda_2/2} + \ldots. \qquad (5.67)$$

Here the terms of the type $\bar{F}_n(\eta)\sigma^{-n}$ arise due to variation of Λ_{B_d} with σ, given by (5.66). The relative position of the various terms in (5.67) are shown correctly for $\beta_\infty = 1/2$. The value of γ_n is to be determined using (5.48) with $\Lambda_d = \Lambda^*_{d_o}$.

Substituting (5.67) in (5.63) and collecting the coefficients of the like powers of σ, we obtain the following system of equations (again, bar on F_n's is dropped):

$$L_1(F_\infty, \Lambda^*_{B_d};\ \beta_\infty) = 1-2\beta_\infty,$$
$$F_\infty(0) = 0 = F'_\infty(0),\ F'_\infty(\infty) = 1. \qquad (5.68)$$

$$L_2(F_1, \Lambda^*_{B_d};\ \beta_\infty) = -(1-\beta_\infty)(6a_1-7a_0)(2a_1-a_0)^{-1}/2-(\beta_\infty-1)^2,$$
$$F_1(0) = F'_1(0) = F'_1(\infty) = 0. \qquad (5.69)$$

$$L_3(M_1, \Lambda_{B_d};\ \beta_\infty) = 0,$$
$$M_1(0) = M'_1(0) = M'_1(\infty) = 0. \qquad (5.70)$$

$$L_4(P_1, \Lambda_{B_d};\ \beta_\infty) = 0,$$
$$P_1(0) = P'_1(0) = P'_1(\infty) = 0. \qquad (5.71)$$

Here

$$\Lambda_{d_o} = -1,$$
$$\Lambda_{d_1} = (1-\beta_\infty)(6a_1-7a_0)(2a_1-a_2)^{-1}/2. \qquad (5.72)$$

The operators L_1, L_2, L_3 and L_4 are same as defined earlier for the longitudinal curvature problem.

5.7 Numerical Solutions and Discussion:

In order to examine how the skin friction will approach the limiting similar solution value as $\bar{\sigma} \to \infty$, we now evaluate the asymptotic expansions (5.52), (5.58) and (5.67) and estimate the multiplicative constant of the first eigenfunctions. The procedure will be illustrated for one typical value of β_∞, namely $\beta_\infty = 1/2$.

The first-order problem has been studied by Chen et.al. (1969) and numerical solutions are provided for $\beta_\infty = 1/2$; for completeness, we mention briefly their main results. For $\beta_\infty = 1/2$, the first five terms of (5.52) have been calculated to yield the following asymptotic expansion for the first-order skin friction:

$$f''(\bar{\sigma}, 0) \sim 0.927680 + 0.115960\ \bar{\sigma}^{-1} + A_1\ \bar{\sigma}^{-1.546} - 0.02615\ \bar{\sigma}^{-2} + A_2 \bar{\sigma}^{-2.46} + \ldots . \qquad (5.73)$$

The value of A_1 is determined by fitting (5.73) to the Eulerized Görtler series solution, given by

$$\hat{T}_1 = 1.232588 - 0.246920z - 0.033951z^2 - 0.010816z^3 - 0.004753z^4 - 0.002510z^5. \qquad (5.74)$$

This leads to $A_1 = -.026$. Chen et.al.(1969) have also used an alternate approach whereby they utilize the orthogonal properties of the eigenfunctions and find the value of $A_1 = -.027$ which is close to the value obtained by the first method. Substituting the value of A_1 in the series (5.73), we can find how the skin-friction approaches the limiting Falkner-Skan value as $\bar{\sigma} \to \infty$.

We now proceed to determine the multiplicative constant of the first eigenfunction corresponding to the second-order problem. Let us first consider the displacement speed problem. Equation (5.71) is solved subject to the normalizing condition $P_n''(0) = 1$. The first set of eigenvalues is given by $\gamma_n = \lambda_n + \Lambda_{d_o}^*$; for $\beta_\infty = 1/2$ and $n = 1$; it leads to the value $\gamma_1 = 2.092$. Equations (5.68), (5.69) and (5.70) are numerically integrated and we obtain the following solutions:

$$F_\infty''(0) = 0.5389, \quad M_1''(0) = -2.7668, \quad F_1''(0) = -9.0579.$$

Substituting the above values along with $P_1''(0) = 1$ in (5.67), we obtain the following asymptotic expansion of $F''(\bar{\sigma}, 0)$ for $\beta_\infty = 1/2$:

$$F''(\bar{\sigma}, 0) \sim 0.5389 - 9.0579\,\bar{\sigma}^{-1} + B_1\bar{\sigma}^{-1.046} + O(\bar{\sigma}^{-1.546}). \tag{5.75}$$

The multiplicative constant B_1 can be determined by using the initial condition (5.64). However, as the asymptotic expansion of B_d starting from $\bar{\sigma}^{-1} = 0$ is not available, we have used for the asymptotic expansion the same series of B_d as in the case of the Görtler series for small $\bar{\sigma}$. We, therefore, use the initial condition in terms of the Eulerized Görtler series of $F''(\bar{\sigma}_i, 0)$ equated to asymptotic form of $F''(\bar{\sigma}, 0)$ given by (5.75). For $\beta_\infty = 1/2$, the Eulerized Görtler series of $F''(\bar{\sigma}_i, 0)$, obtained in Chapter 4, has the following form:

$$F''(\bar{\sigma}, 0) = 1.8488 - 1.7322z - 0.7194z^2 - 0.4978z^3 - 0.4567z^4 - \ldots. \tag{5.76}$$

where $z = \sigma^{-}[\sigma^{-} + (1-\beta_{\infty})/2]^{-1}$

The outline of the procedure for obtaining B_1 is as follows: We rewrite the first three terms of (5.75) as a series in $(1-z)$, thus

$$F''(\sigma, 0) = -35.6926 + 36.2316\ z + B_1[4(1-z)]^{1.046} + O[(1-z)^{1.546}]. \qquad (5.77)$$

Equating right hand sides of (5.76) and (5.77), we obtain the following equation for B_1:

$$\begin{aligned} B_1[4(1-z)]^{1.046} &= 37.5415 - 37.9638\ z - 0.7194\ z^2 \\ &\quad -0.4978\ z^3 - 0.4567\ z^4 \\ &= 37.5415\ (1-1.011\ z - .0191\ z^2 \\ &\quad -.0132\ z^3 - .0122\ z^4). \end{aligned}$$

Raising both sides to the power (1/1.046) and using the binomial expansion for the right hand side, we obtain the following series for B_1:

$$(B_1)^{1/1.046}\ 4(1-z) = (37.5415)^{1/1.046}\ (1-.966\ z - .0183\ z^2 - .0126\ z^3 - .0115\ z^4) \qquad (5.78b)$$

Again, the right hand side of (5.78b) is rewritten in powers of $(1-z)$. Thus,

$$\begin{aligned} (B_1)^{1/1.046}\ 4(1-z) &= (37.5415)^{1/1.046}\ [(1-0.9660-0.0183 \\ &\quad -0.0126-0.0115) + (0.966+0.0366 \\ &\quad +0.0380+0.0463)(1-z)+O(1-z)^2]. \qquad (5,79) \end{aligned}$$

As it is, the two sides of the above equation do not match.

But on the right hand side of (5.79), the first coefficient in the square bracket has the last partial sum equal to the value -.0095 and as we would expect, it seems to approach zero. Therefore, we put the first coefficient equal to zero so that the coefficient of (1-z) can be matched. The second coefficient has the last partial sum equal to 1.087. Thus, equating the coefficients of (1-z) on the two sides of the equation (5.79) we obtain,

$$B_1 = (37.5415)\ (1.087/4)^{1.046}$$

$$= 9.57$$

Substituting the value of B_1 in (5.75), we obtain the following series for $F^{''(d)}(\sigma, 0)$:

$$F^{''(d)}(\sigma, 0) \sim .5389 - 9.059\ \sigma^{-1} + 9.575\ \sigma^{-1.046} + O(\sigma^{-1.546}). \qquad (5.80)$$

To obtain the asymptotic series for the overall displacement speed contribution to the skin friction, we multiply (5.80) by the asymptotic form of B_d (5.65) to yield the following series:

$$B_d^* F^{''(d)}(\sigma, 0) \sim -0.017\ \sigma^{-0.5} + 0.289\ \sigma^{-1.5} + O(\sigma^{-1.546}). \qquad (5.81)$$

The above asymptotic series for the overall contribution of the displacement speed to the skin friction shows that as $\sigma \to \infty$, the contribution is zero; thus it confirms what was predicted earlier (see Figure 4.11) by the Eulerized Görtler series solution and, in addition, gives the rate of approach of $\hat{\tau}_2(d)$ to zero as $\sigma \to \infty$ $(z \to 1)$.

Now we shall determine the multiplicative constant of the first eigenfunction of the longitudinal curvature problem. Again, the equation (5.62) is solved subject to the normalizing condition $P_n''(0) = 1$. The first eigenvalue is $\gamma_1 = \lambda_1 + \Lambda_{1_o}^* = 1.092$. Equations (5.59), (5.60) and (5.61) are numerically integrated to yield the following solutions:

$$F_\infty''(0) = .4371,\ M_1''(0) = 56.416,\ F_1''(0) = -1.2344. \quad (5.82)$$

Using (5.57a) and (5.58) along with the values obtained above, the left hand side of the equation (5.56a) is expressed in the following form for $\beta_\infty = 1/2$:

$$B_1^* F''(\sigma, 0) \sim .077\sigma^{-1} + B_1(2)^{-5/2}\ \sigma^{-1.546} + O(\sigma^{-2}). \quad (5.83)$$

The Eulerized Görtler series of the total skin friction due to longitudinal curvature $\tau_2^{(1)}$ as obtained in Chapter 4, is given by,

$$\tau_2^{(1)} = -1.352 + 2.014\ Z - 0.3750\ Z^2 - 0.1302\ Z^3 - 0.0600\ Z^4. \quad (5.84)$$

We determine B_1 by fitting (5.85) to (5.84). Since the procedure adopted is similar to the one outlined for the displacement speed problem, no details are given here. The value of the coefficient B_1 is found to be -0.22. Substituting the value of B_1 in (5.83), we obtain the following asymptotic series for the contribution of the longitudinal curvature to the skin friction for large values of σ:

$$B_1^* F''^{(1)}(\sigma, 0) \sim .077\ \sigma^{-1} - .039\ \sigma^{-1.546} + O(\sigma^{-2}). \quad (5.8$$

The above series expansion shows that for large values of

$\sigma^{-}(Z \simeq 1)$, the contribution of the longitudinal curvature to the skin friction is positive. Further, as $\sigma^{-} \to \infty (Z \to 1)$, the contribution becomes zero. These observations are consistent with the earlier results obtained via Eulerized Görtler series shown in Figure 4.18.

Combining (5.73), (5.81) and (5.85), we obtain the asymptotic series for the total skin friction coefficient, thus,

$$C_f = 0.92768 + 0.11598\,\sigma^{-1} - 0.026\,\sigma^{-1.546} + \ldots + R^{-1/2}\,(-0.017\,\sigma^{-.5} + 0.077\,\sigma^{-1} + 0.289\,\sigma^{-1.5} - .039\,\sigma^{-1.546} + \ldots). \tag{5.86}$$

The above asymptotic form of C_f shows that the total skin friction for $\rho_\infty = 1/2$ approaches a value equal to 0.92768 as $\sigma^{-} \to \infty$ $(z \to 1)$; this behaviour was exhibited by the improved Eulerized Gortler series obtained in Chapter 4 and shown in Figure 4.22b. Thus, the asymptotic series (5.86) provides, in some sense, a proof of convergence of the Eulerized Görtler series solutions obtained in Chapter 4 and consequently establish the validity of the latter for the complete range of σ^{-}.

We, thus, conclude that the power series solution obtained for the nose region with the range of validity extended by employing the Euler transformation, and the asymptotic solution for large streamwise distance from the nose region provide means for assessing the accuracy of the corresponding results obtained via numerical or approximate methods having unknown and/or uncertain error bounds.

REFERENCES

1. Afzal, N.
   1969 Studies of heat transfer in the first and the second-order boundary-layer flows, Ph.D.Thesis, I.I.T. Kanpur.

2. Afzal, N. and Oberai, M.M.
   1972 Self-similar solutions of the second-order boundary-layer of an incompressible fluid with heat transfer. Int. J. Heat Mass Transfer 15, 99-113.

3. Afzal, N. and Raisinghani, S.C.
   1973 Heat transfer in liquids due to second-order boundary-layer flows with dissipation. J. Aero. Society India, (To appear).

4. Afzal, N. and Raisinghani, S.C.
   Effects of dissipation on heat transfer due to second-order boundary-layer flows. Warme Und Stroffiibertragung (To appear).

5. Bellman, R.
   1955 J. Appl. Mech. 22, 500.

6. Botta, E.F.F., Dijkstra, D. and Veldman, A.E.P.
   1972 The numerical solution of the Navier-Stokes equations for laminar, incompressible flow past a parabolic cylinder. J. Eng. Math. 6, 63-81.

7. Bush, W.B.
   1964 Local similarity concept of the boundary-layer equations. AIAA Journal 2, 1857.

8. Chen, K.K.
   1970 Laminar heat transfer to a blunted wedge. Int. J. Heat Mass Transfer 13, 573-581.

9. Chen, K.K. and Libby, P.A.
   1968 Boundary-layers with small departures from the Falkner-Skan profile. J. Fluid Mech. 33, 273-282.

10. Chen, K.K., Libby, P.A., Rott, N. and Van Dyke, M.
    1969 The laminar boundary-layer on a blunted wedge. Z. Angew. Math. Phys. 20, 619-627.

11. Cole, J.D.
    1968 Perturbation Methods in applied mathematics, Blaisdell Publishing Co., New York.

12. Courant, R. and Hilbert, D.
1953 Methods of mathematical physics. Interscience Publishers Ltd., London.

13. Davis, R.T.
1972 Numerical solution of the Navier-Stokes equations for symmetric laminar incompressible flow past a parabola, J.Fluid Mech. 51, 417-433.

14. Davis, R.T. and Flügge-Lotz, I.
1964 Second-order boundary-layer effects in hypersonic flow past axisymmetric blunt bodies, J. Fluid Mech. 20, 593-623.

15. Davis, R.T., Worle, M.J. and Wornom, S.F.
1970 A consistent formulation of compressible boundary-layer theory with second-order curvature and displacement effects.AIAA Journal 8, 1701-1703 (Technical note).

16. Davis, R.T., Whitehead, R.E. and Wornom, S.F.
1971 The development of an incompressible boundary-layer theory valid to second-order. Warme Und Stroffiibertragung 4, 167-177.

17. Dennis, S.C.R. and Walsh, J.D.
1971 Numerical solutions for steady symmetric viscous flow past a parabolic cylinder in a uniform stream. J. Fluid Mech. 50, 801-814.

18. Evans, H.L.
1967 Laminar boundary-layer theory. Addison-Wesley Publishing Co. London.

19. Görtler, H.
1957 A new series for the calculation of steady laminar boundary-layer flows. J. Math. Mech. 6, 1-66.

20. Honda, M. and Kiyokawa, Y.
1969 An analysis of second-order effect on laminar boundary-layer flow. J. Fluid Mech. 35, 145-169.

21. Kaplun,S.
1967 Singular perturbation and fluid mechanics. Editors: Lagerstrom, P.A., Howarth, L.N. and Lin, C.S. Academic Press, New York.

22. Lagerstrom, P.A.
1964 Laminar flow theory. In theory of laminar flows (High Speed Aerodynamics and Jet Propulsion Vol.4) edited by K.F. Moore. Princeton University Press.

23. Lagerstrom, P.A. and Cole, J.D.
1955 Examples illustrating expansion procedures for Navier-Stokes equations. J. Ral. Mech. Anal.4, 817-882.

24. Lenard, M.
1961 Stagnation point of a variable property fluid at low Reynolds numbers, Ph.D. thesis, Cornell University.

25. Libby, P.A.
1970 A review of some perturbation methods in boundary-layer theory, Int. J.Engng Sci. 8, 289-306.

26. Libby, P.A. and Chen, K.K.
Application of quasilinearization to an eigenvalue problem arising in boundary-layer theory. J.Comp.Phys. 2, 356-

27. Libby, P.A. and Fox, H.
1963 Some perturbation solutions in laminar boundary-layer theory. Part I. The momentum equation. J.Fluid Mech. 17, 433-499.

28. Maslen, S.H.
1963 Second-order effects in laminar boundary-layers. AIAA Journal 1, 33.

29. Meksyn, D.
1961 New methods in laminar boundary-layer theory. Pergamon Press, Oxford.

30. Merk, H.J.
1959 Rapid calculations for boundary-layer transfer using wedge solutions and asymptotic expansions. J. Fluid Mech. 5, 460-480.

31. Murphy, J.S.
1965 Extensions of the Falkner-Skan similar solutions to flows with surface curvature. AIAA Journal 3, 2043-2049.

32. Narsimha, R.
1968 Non-linear vibration of an elastic string. J. Sound Vib. 8, 134-146.

33. Narasimha, R. and Ojha, S.K.
1967 Effect of longitudinal surface curvature on boundary-layer, J. Fluid Mech.29, 187-199.

34. Rott, N. and Lenard, M.
1959 Vorticity effect on the stagnation point flow of a viscous incompressible fluid. J. Aero/Space Sci. 26, 452.

35. Schlichting, H.
1968 Boundary-layer theory. Sixth edition. McGraw-Hill Book Co. New York.

36. Shanks, D.
Nonlinear transformations of divergent and slowly convergent sequences. J. Math. Phys. 34, 1.

37. Smith, A.M.O.
1954 Improved solutions of the Falkner-Skan boundary-layer equations. IAS Fairchild Fund preprint FF-10.

38. Van Dyke, M.
1962 Higher approximations in boundary-layer theory. Part I: General analysis. J. Fluid Mech. 14, 161-177.

39. Van Dyke M.
1964a Higher approximations in boundary-layer theory. Part III: Parabola in uniform stream. J. Fluid Mech. 19, 145-159.

40. Van Dyke, M.
1964b Perturbation methods in Fluid Mechanics. Academic Press, London.

41. Van Dyke, M.
1969 Higher order boundary-layer theory. Annual Review of Fluid Mechanics, Vol. 1, edited by Sears, W.R. and Van Dyke, M., 265-277.

42. Werle, M.J. and Davis, R.T.
1970 Self-similar solutions to second-order incompressible boundary-layer equations. J. Fluid Mech. 40, 343-360.

43. Werle, M.J. and Wornom, S.F.
1972 Longitudinal curvature and displacement speed effects on incompressible laminar boundary-layers. Int. J. Engng. Sci. 10, 875-888.

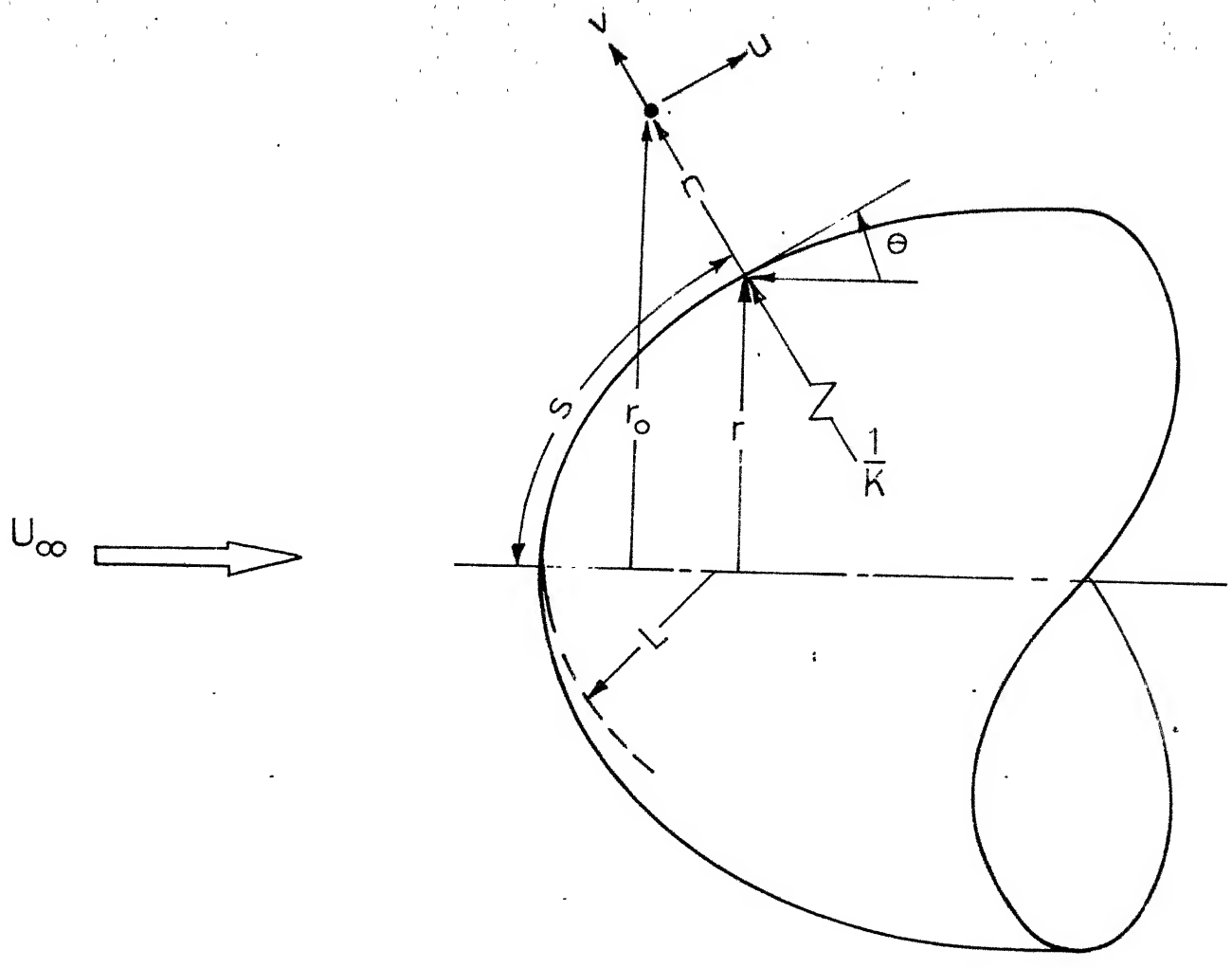

Fig. 2.1 _ Coordinate system

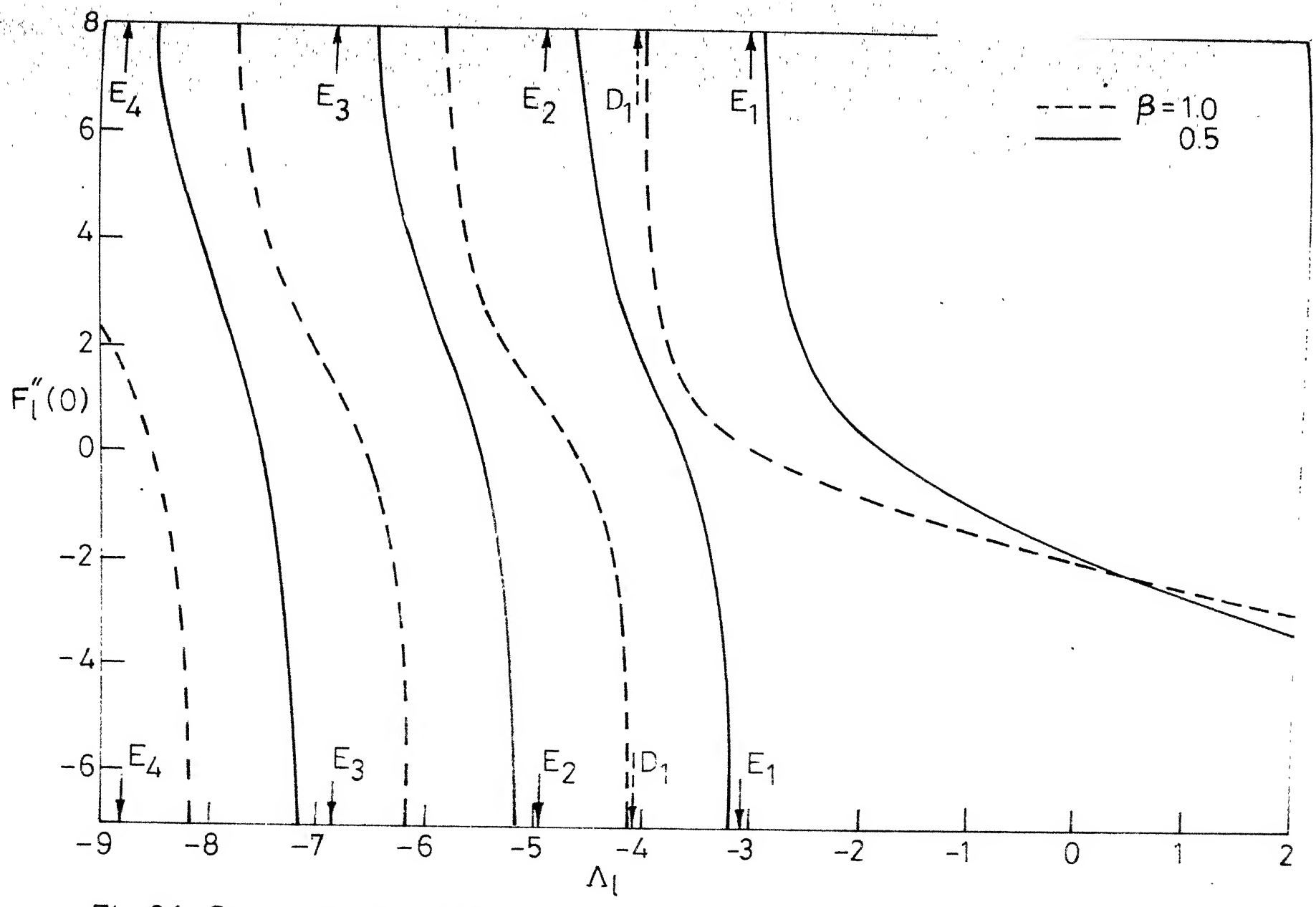

Fig. 3.1 _ Solutions to longitudinal curvature momentum transfer problem (3.14). $E_n, n = 1-4$ denote the first four eigenvalues of the operator (3.16) for $\beta = 0.5$ and D_1, the first eigenvalue for $\beta = 1.0$.

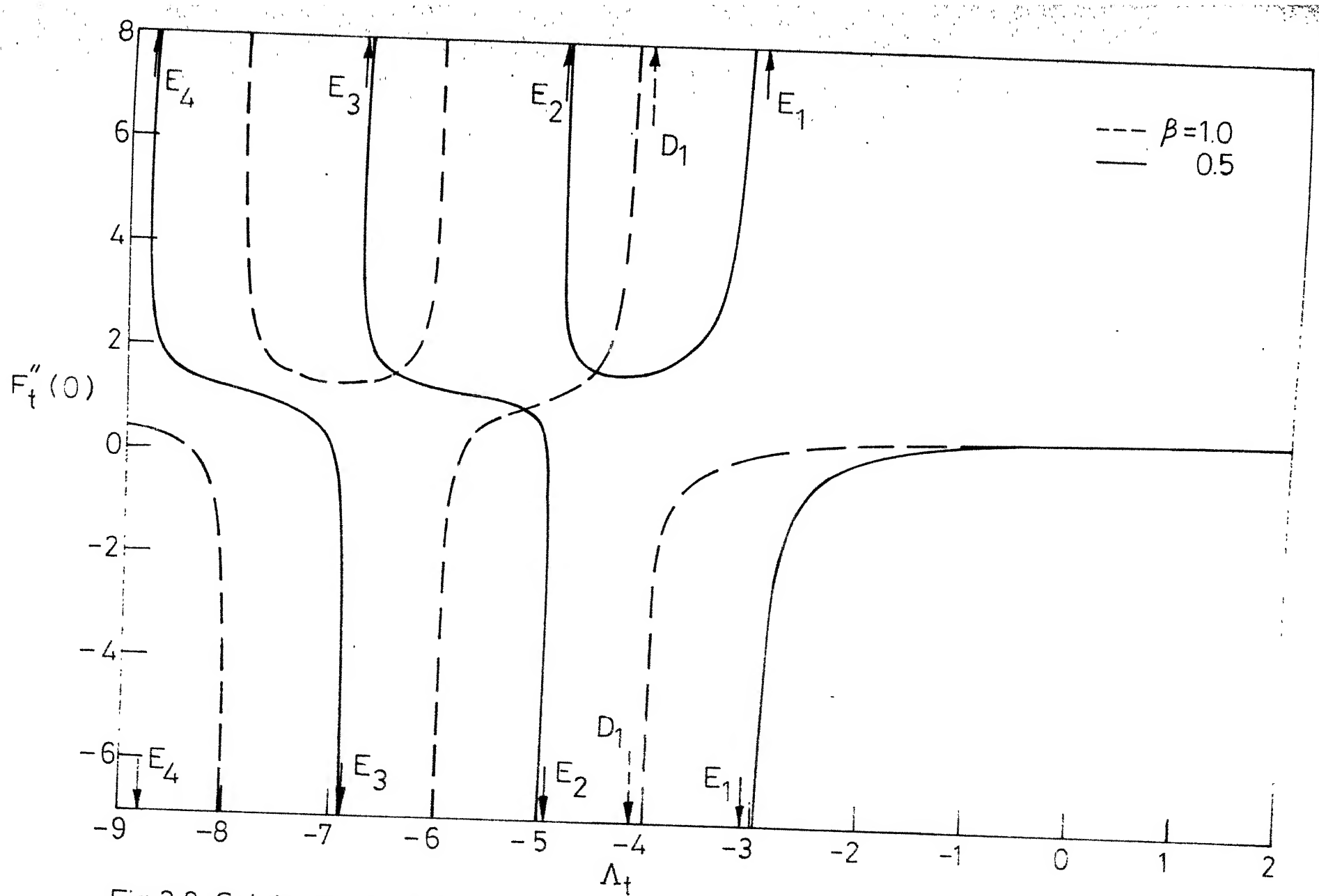

Fig.3.2_Solutions to transverse curvature problem (3.15). E_n, n = 1-4 denote the first four eigenvalves of the operator (3.18) for β =0.5 and D_1 , the first eigenvalve for β =1.0 .

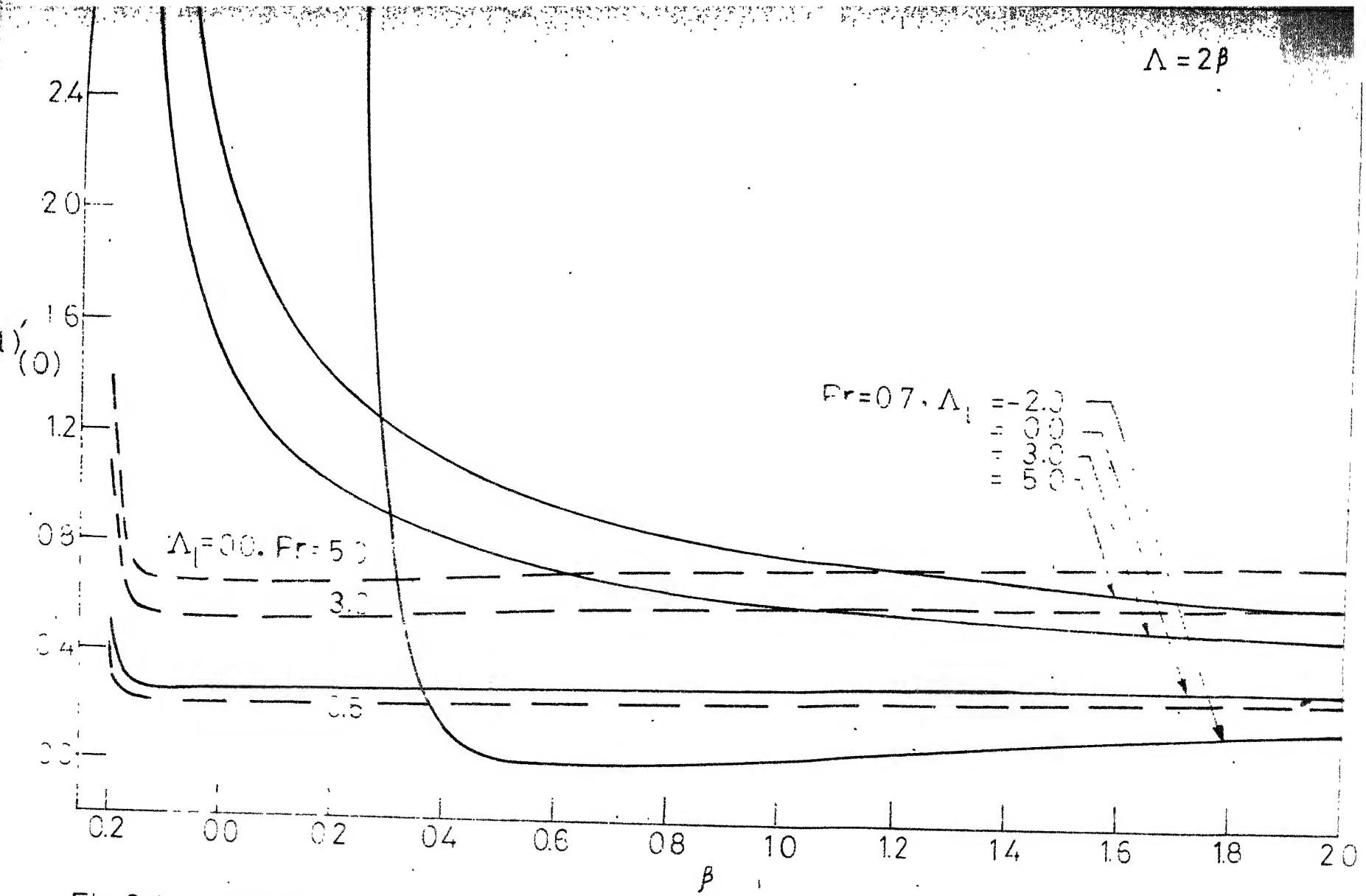

Fig.3.4 – Effect of longitudinal curvature on heat transfer due to the prescribed wall temperature .

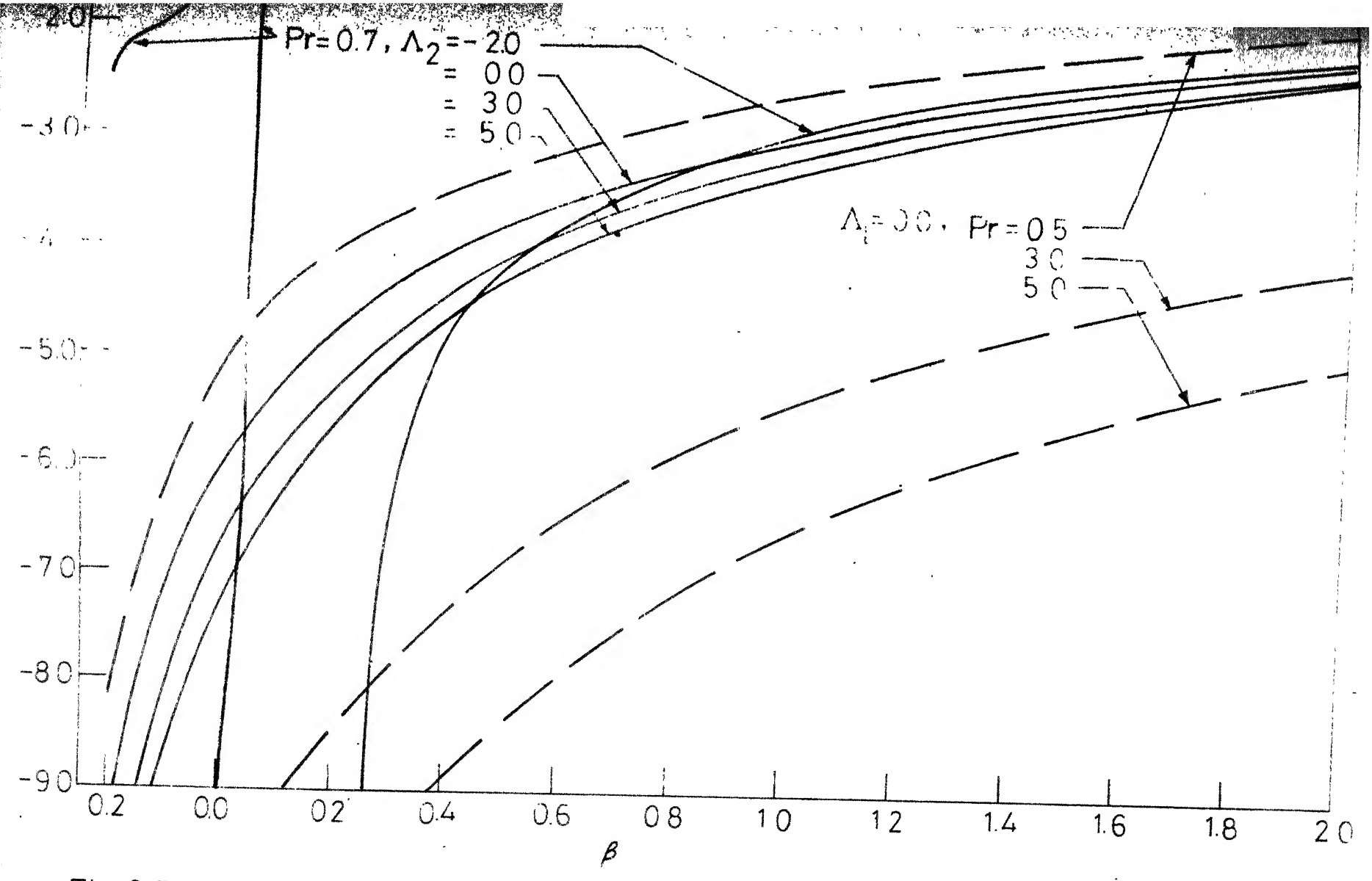

Fig. 3.5_ Second – order recovery factor due to longitudinal curvature : Liquids.

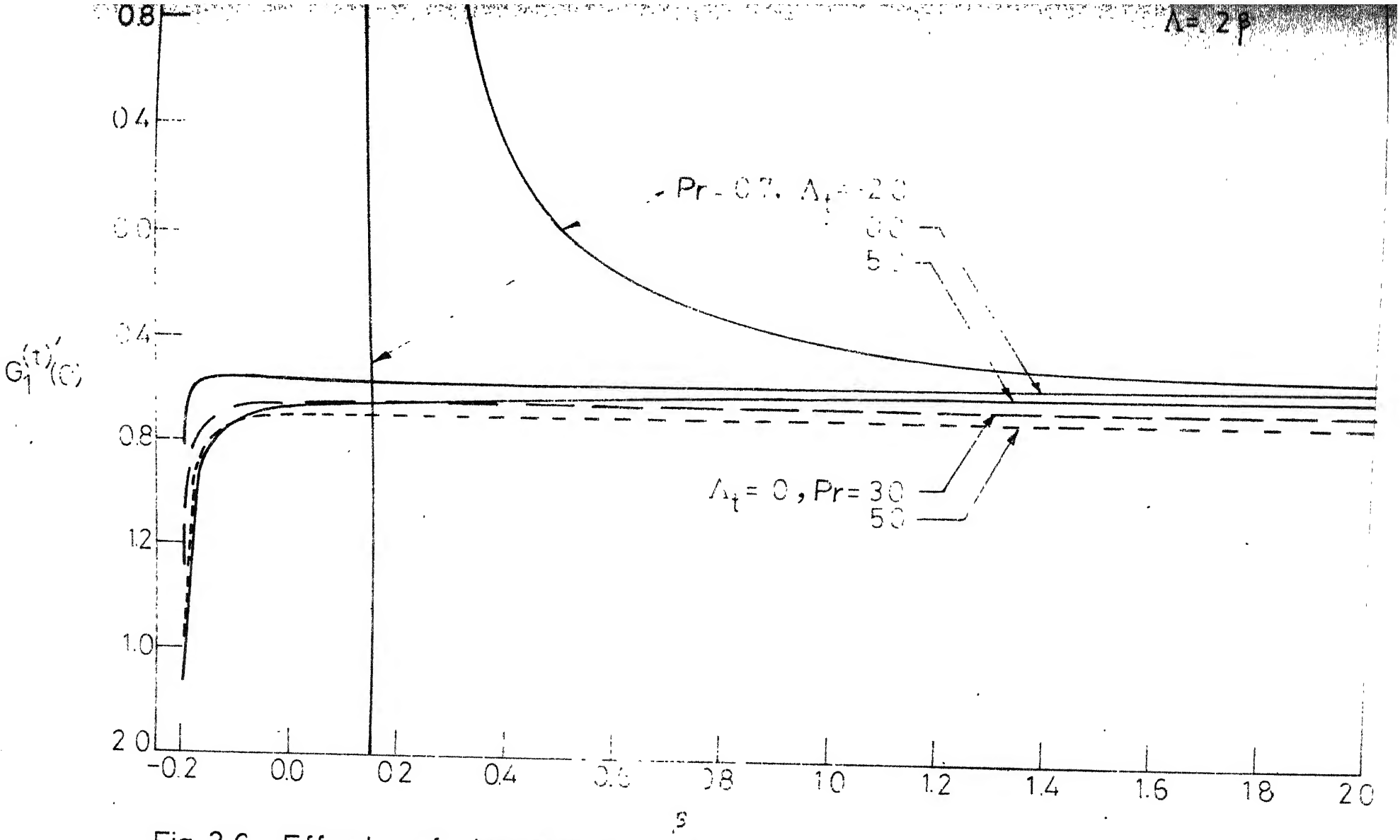

Fig. 3.6 – Effect of transverse curvature on heat transfer due to the prescribed wall temperature

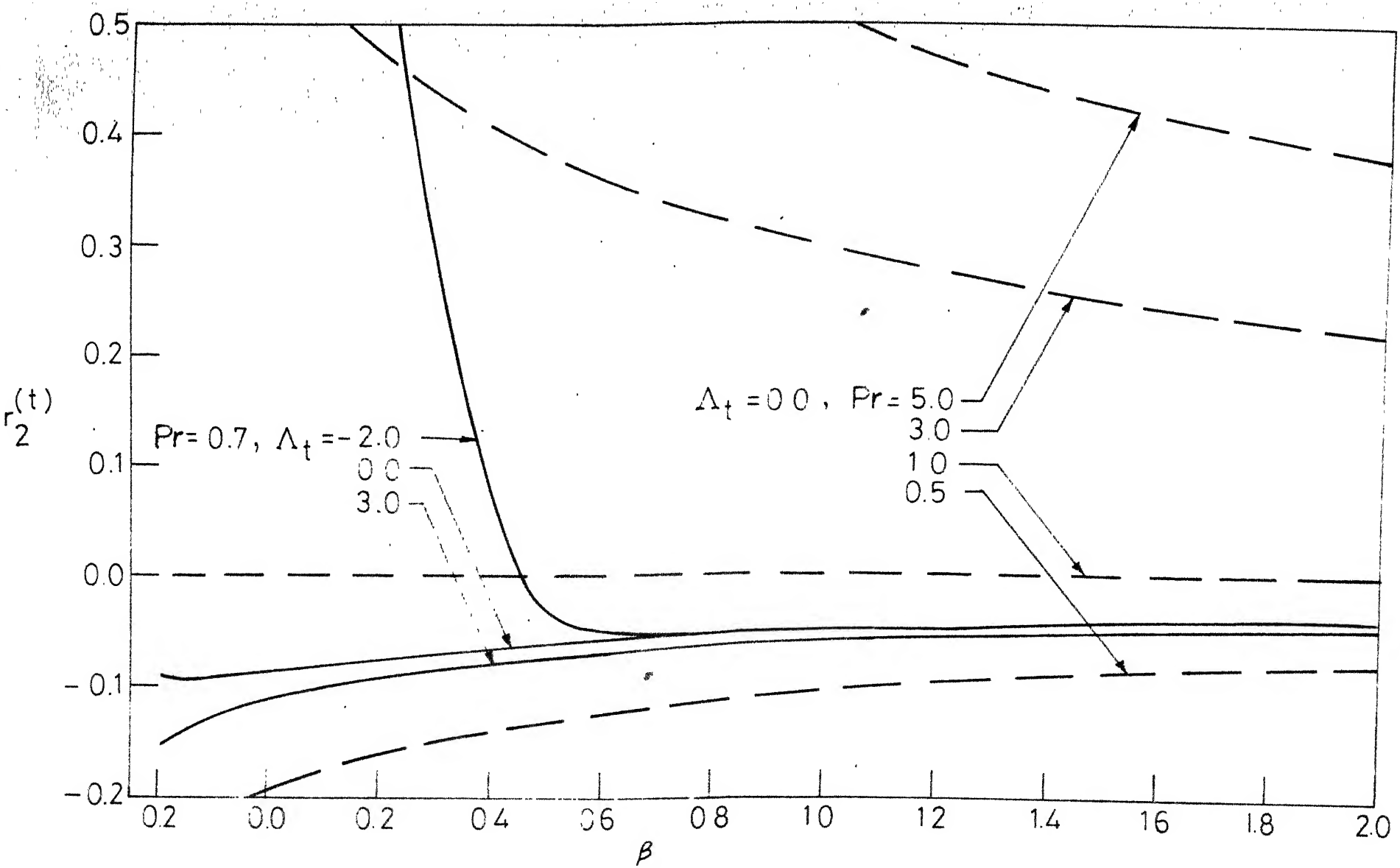

Fig. 3.7_ Second – order recovery factor due to transverse curvature: Liquids.

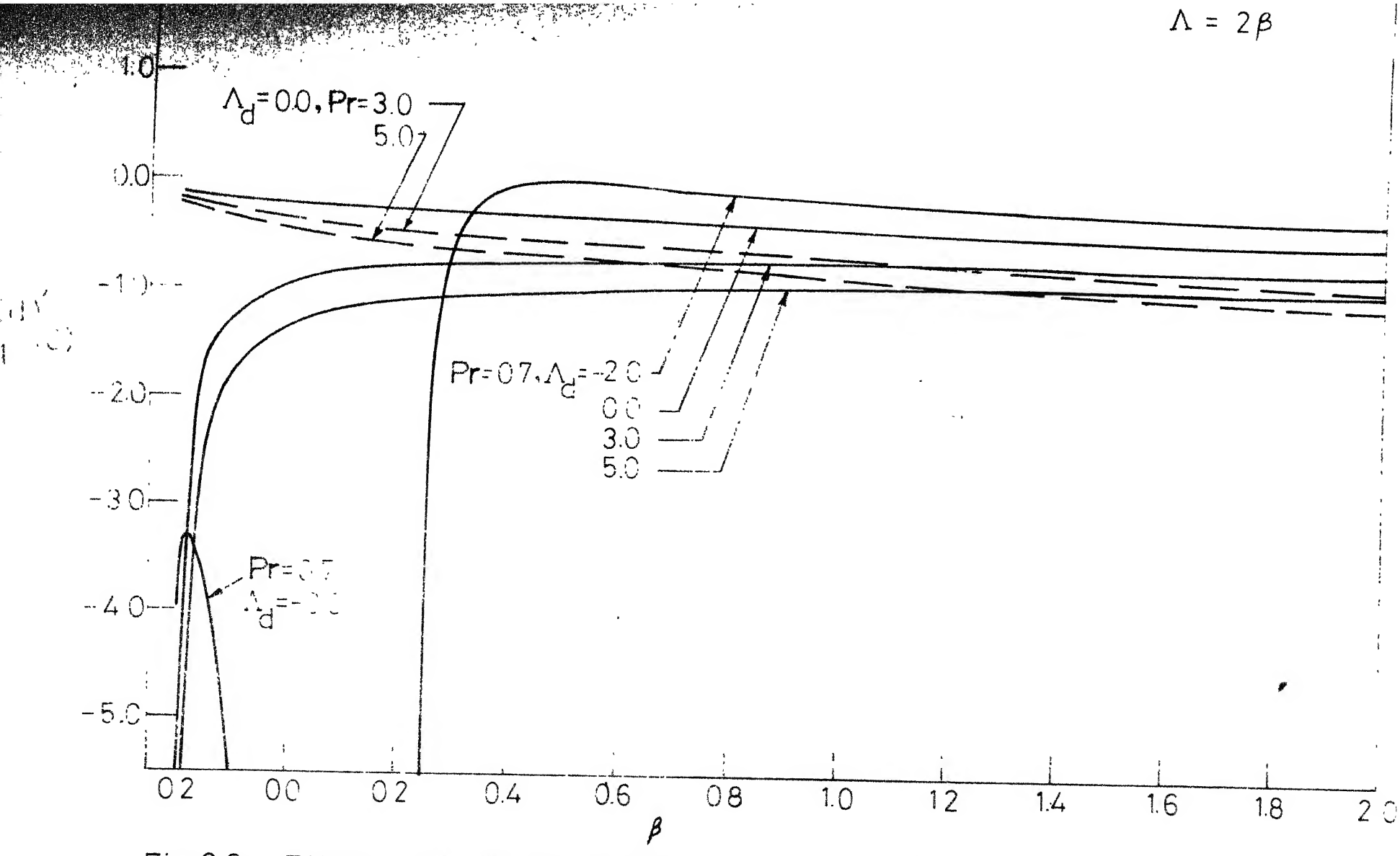

Fig 3.8 – Effect of displacement speed on heat transfer due to the prescribed wall temperature.

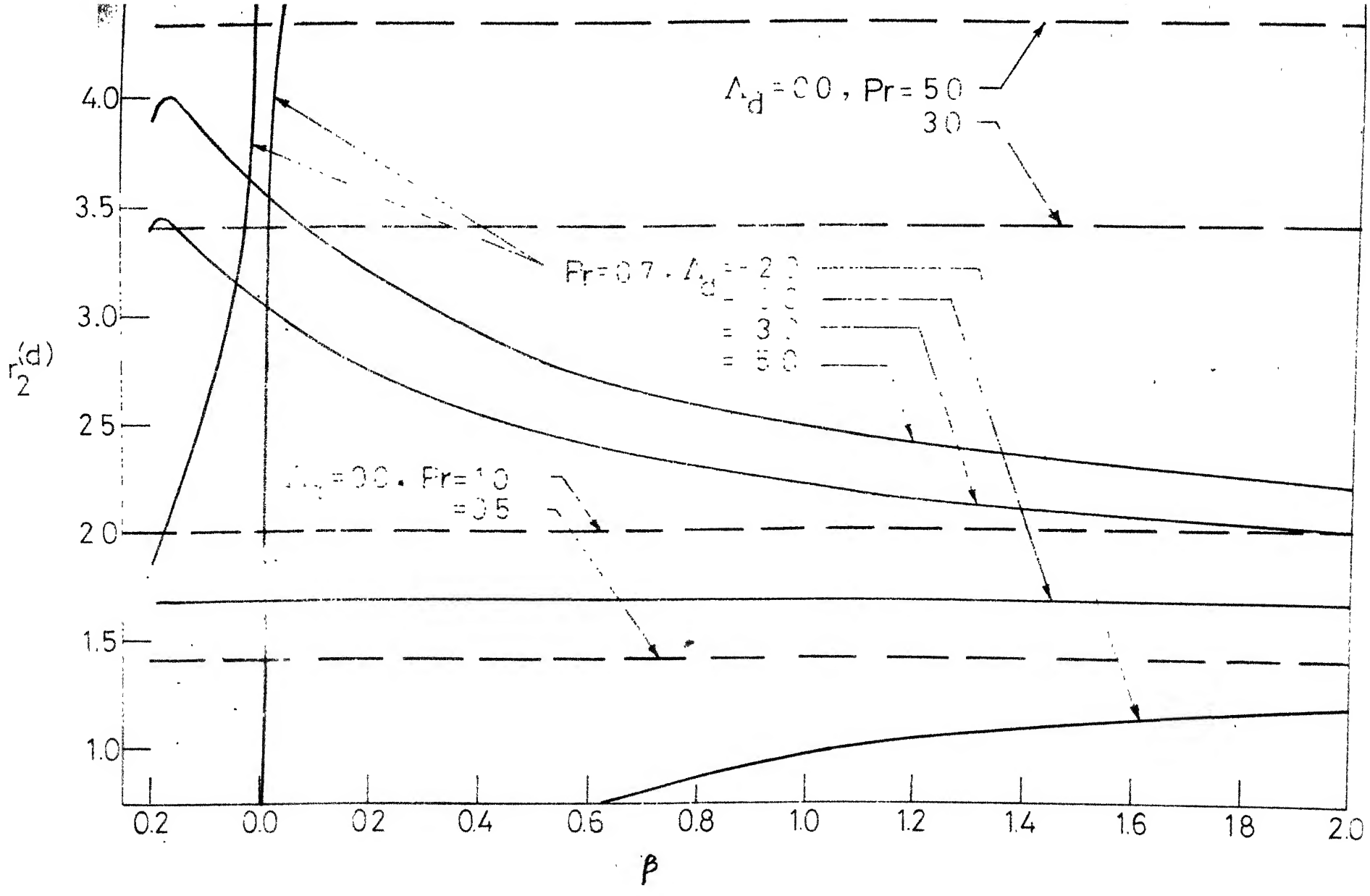

Fig.3.9_ Second – order recovery factor due to displacement speed : Liquids.

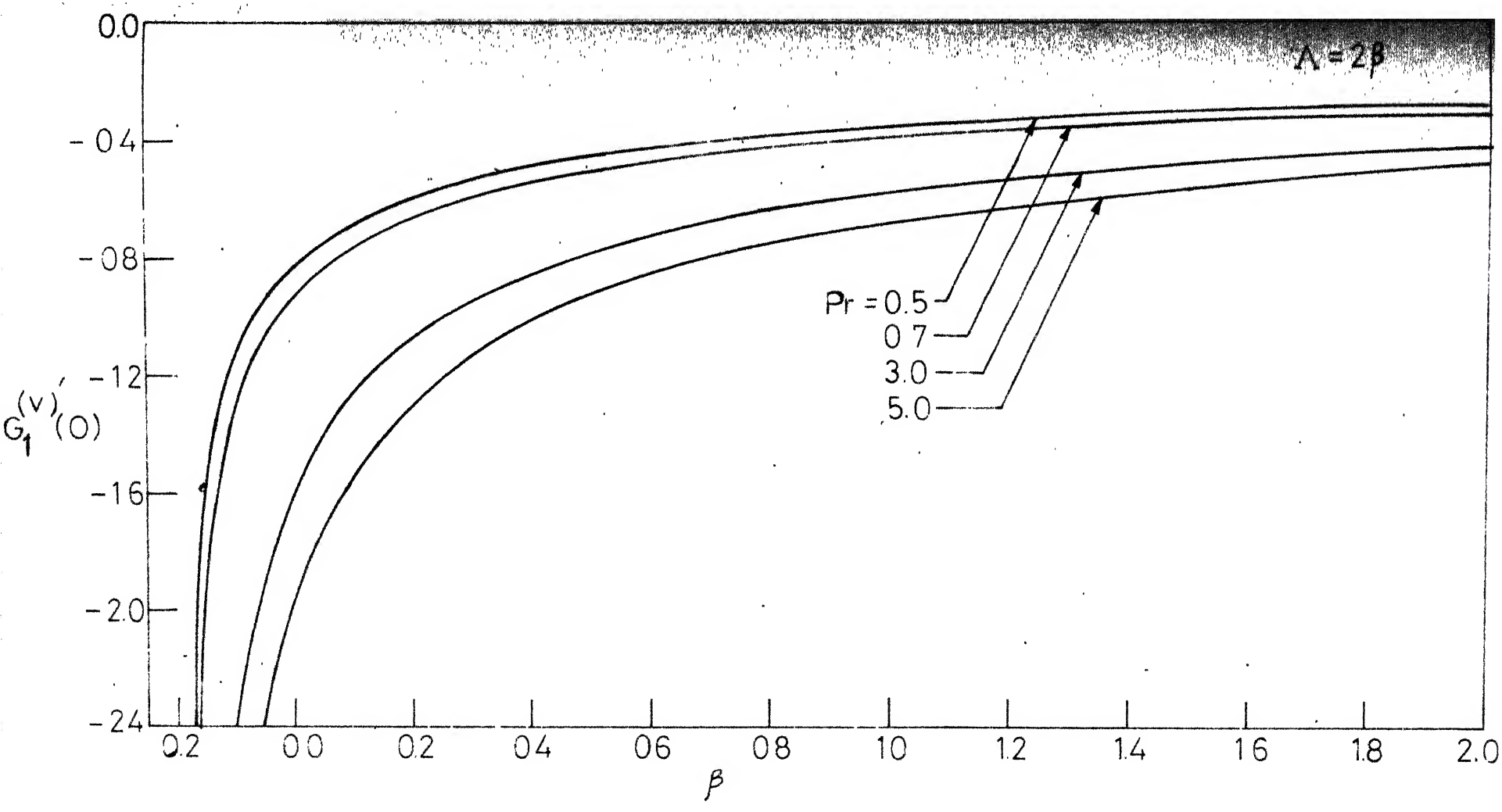

FIG. 3.10 - Effect of vorticity interaction on heat transfer due to the prescribed wall temperature .

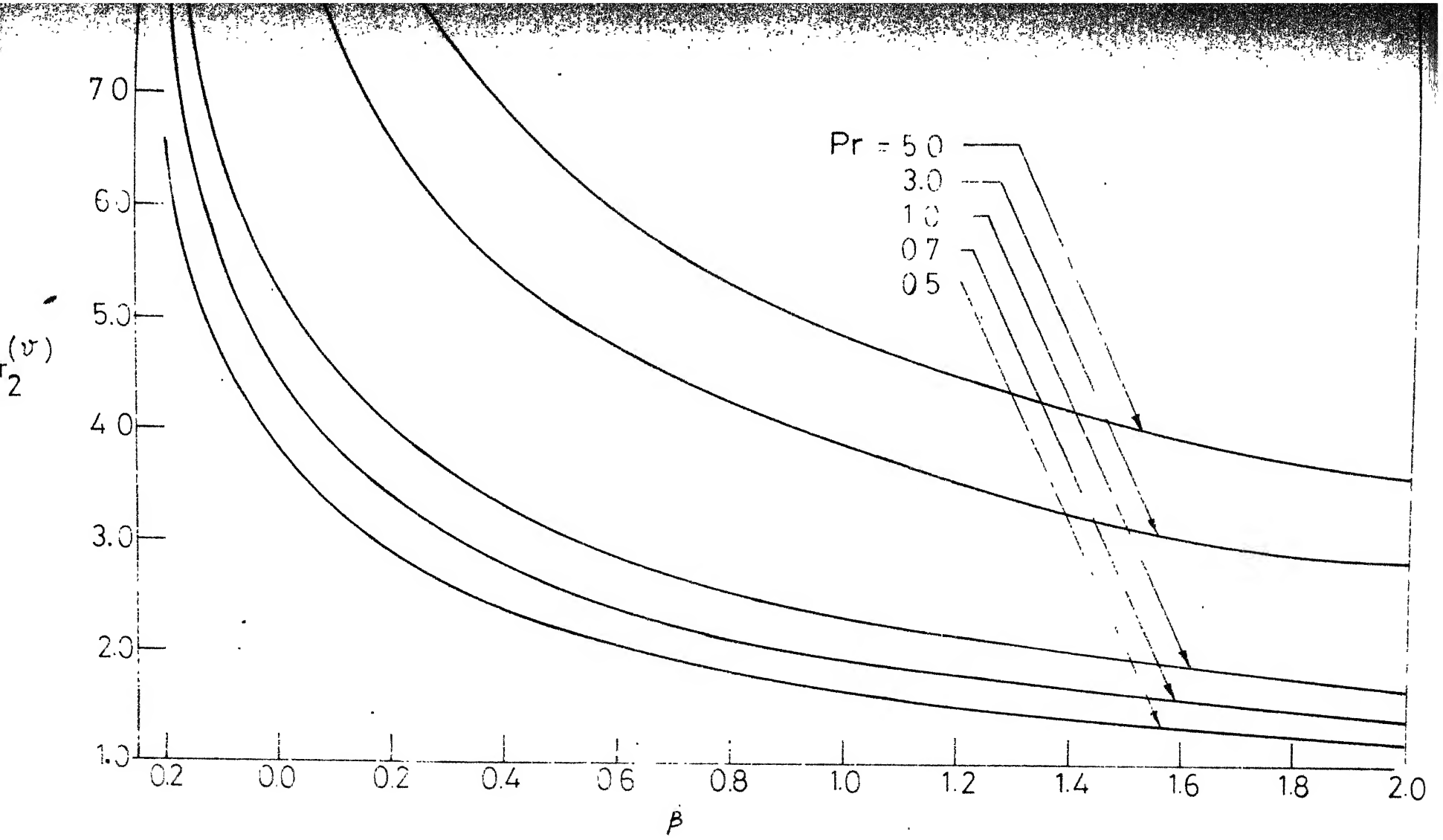

Fig. 3.11 – Second – order recovery factor due to vorticity interaction : Liquids.

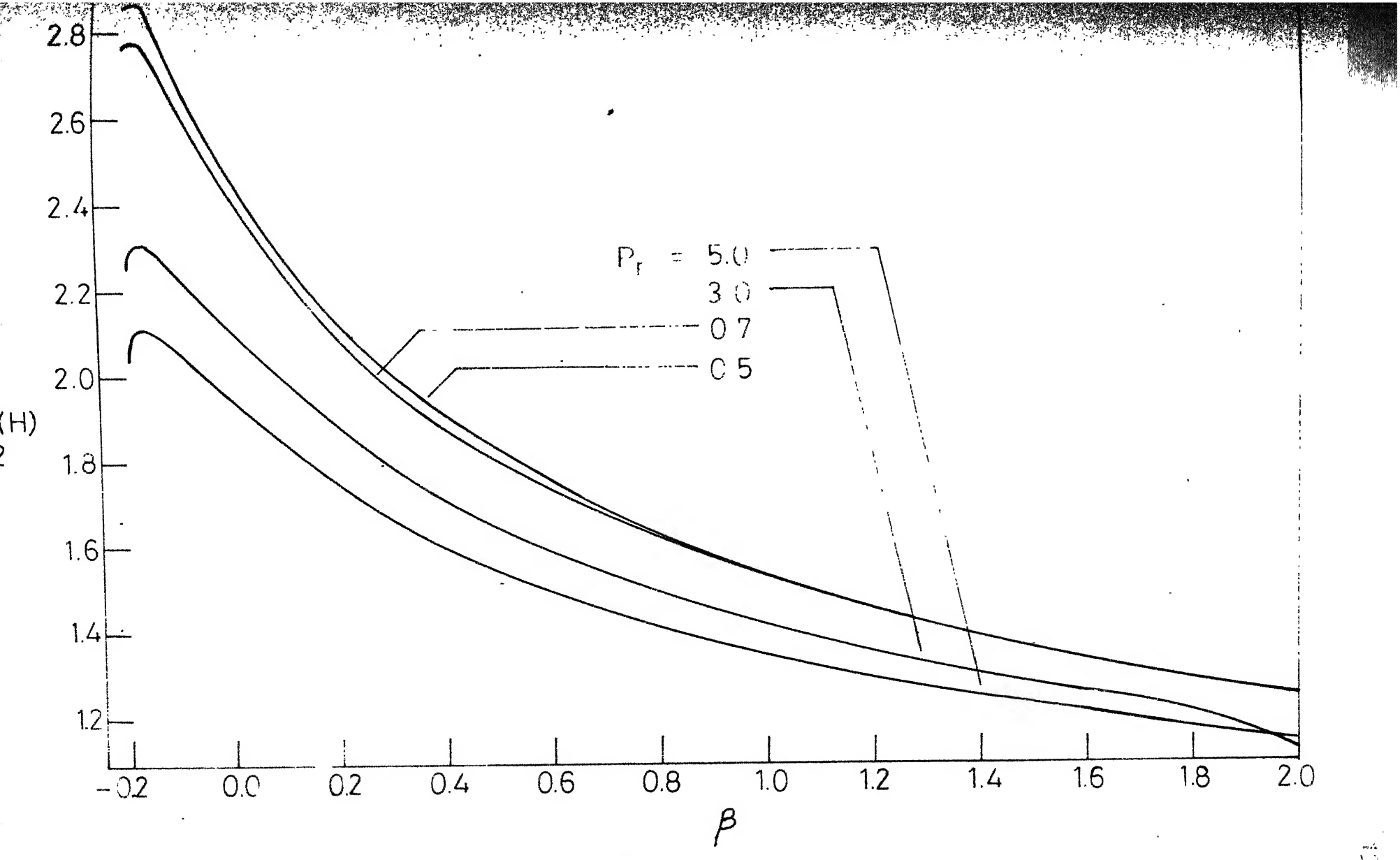

Fig. 3.12 _ Second – order recovery factor due to the temperature gradient in the on coming stream: Liquids.

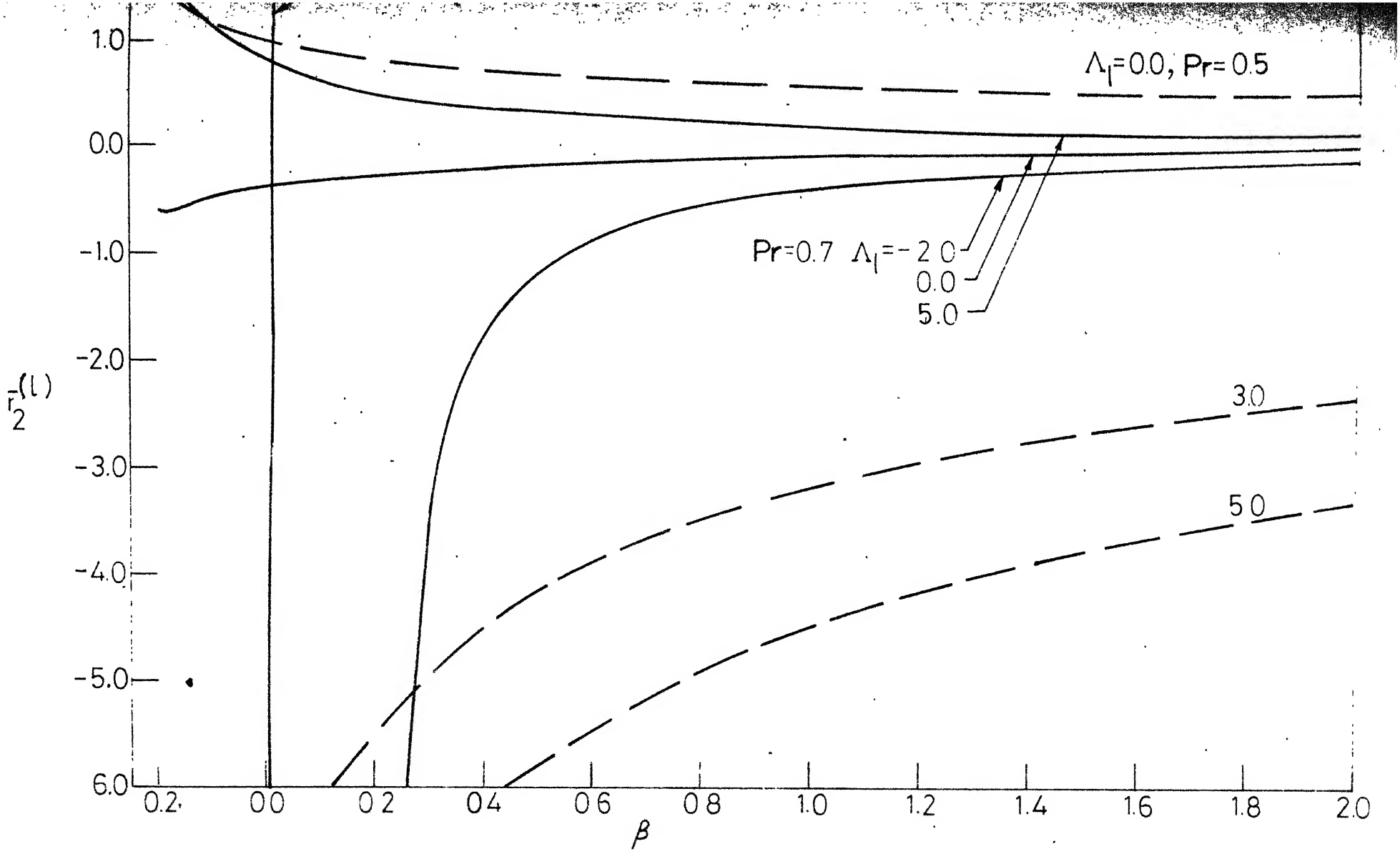

Fig.3.13_ Second-order recovery factor due to the longitudinal curvature : Gases.

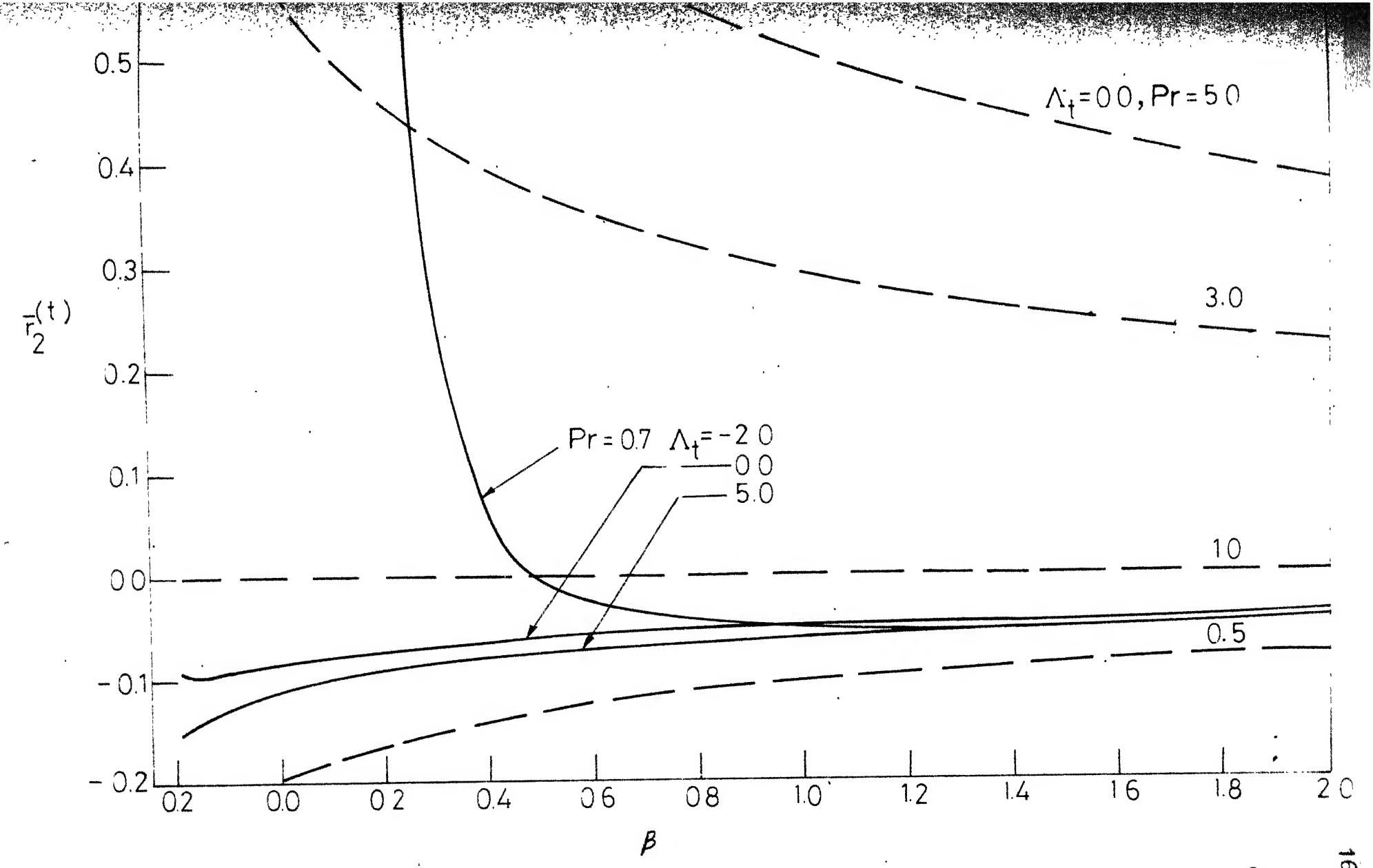

Fig. 3.14 _ Second – order recovery factor due to transverse curvature: Gases.

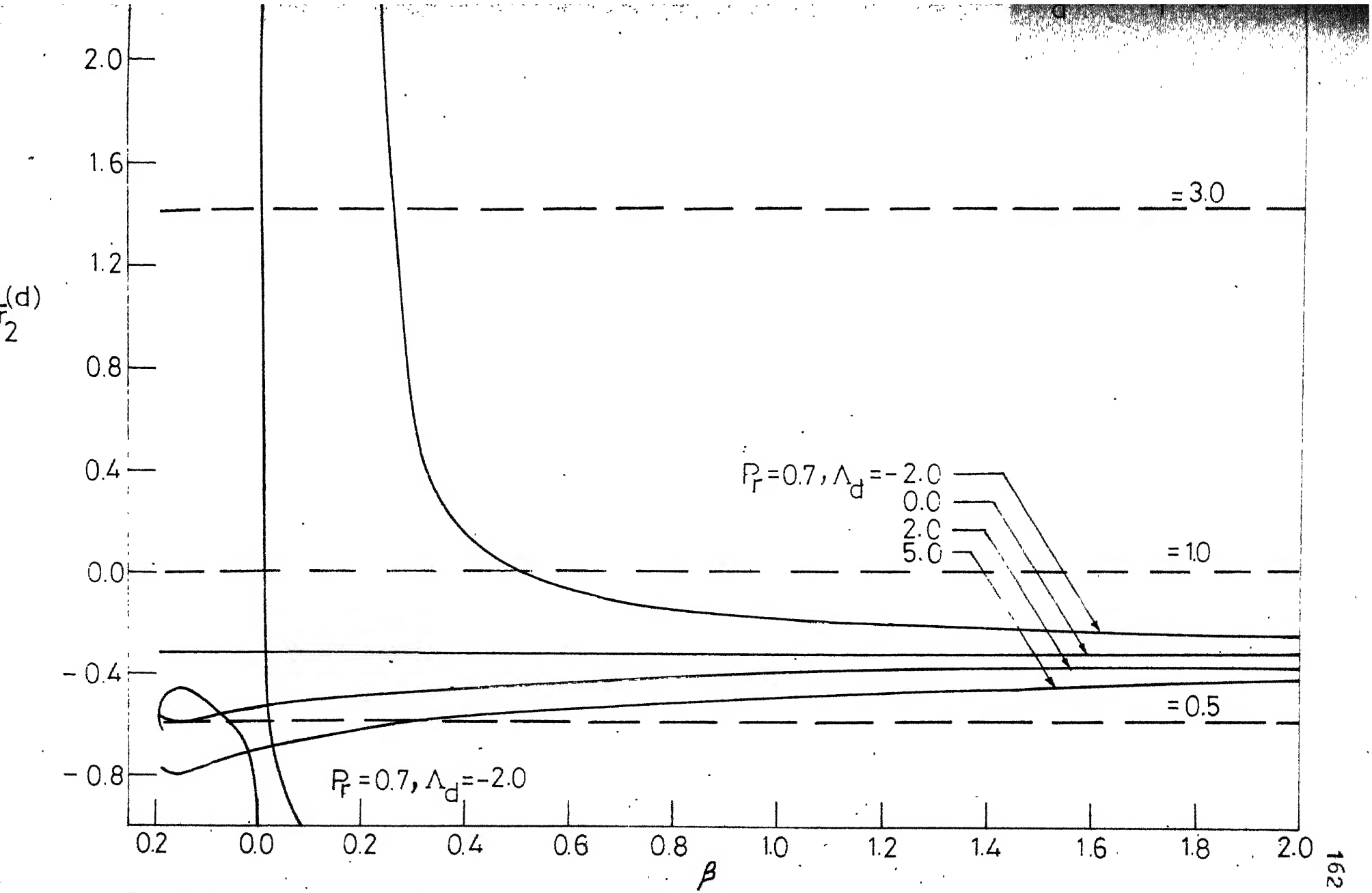

Fig. 3.15_ Second - order recovery factor due to displacement speed : Gases.

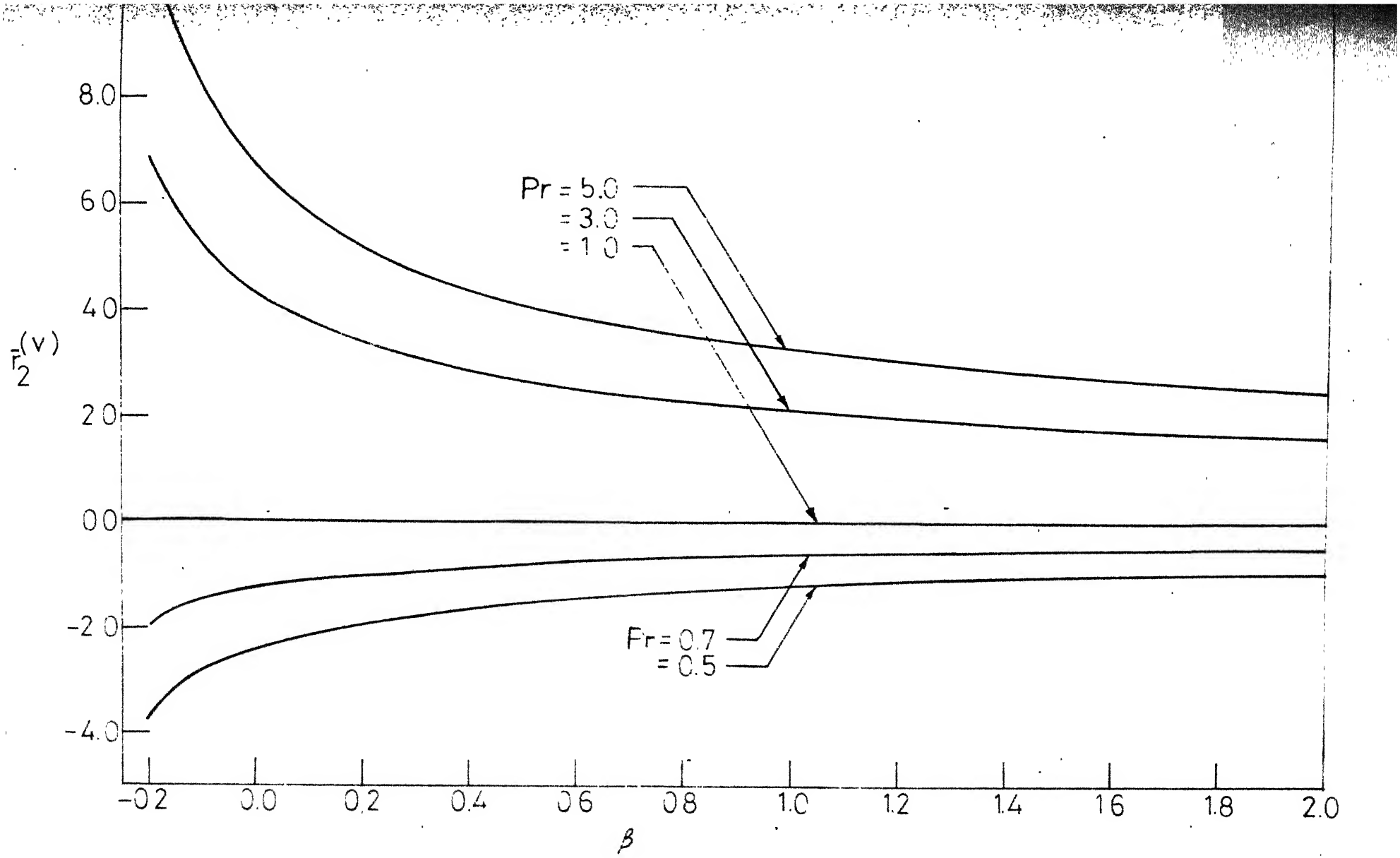

Fig. 3.16 - Second-order recovery factor due to vorticity interaction : Gases.

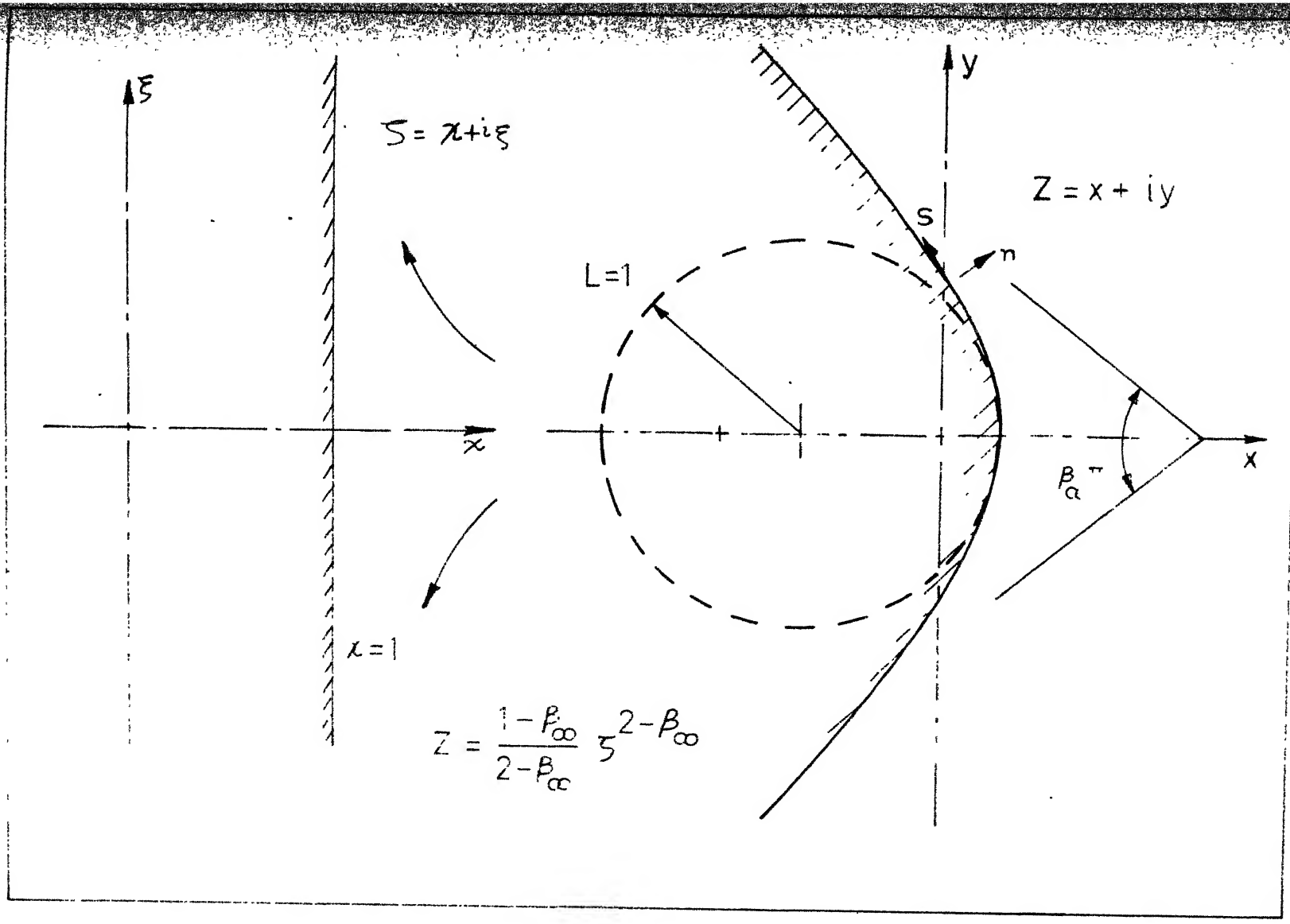

Fig.4.1_A blunted wedge configuration with conformal mapping used to obtain the inviscid flow velocity.

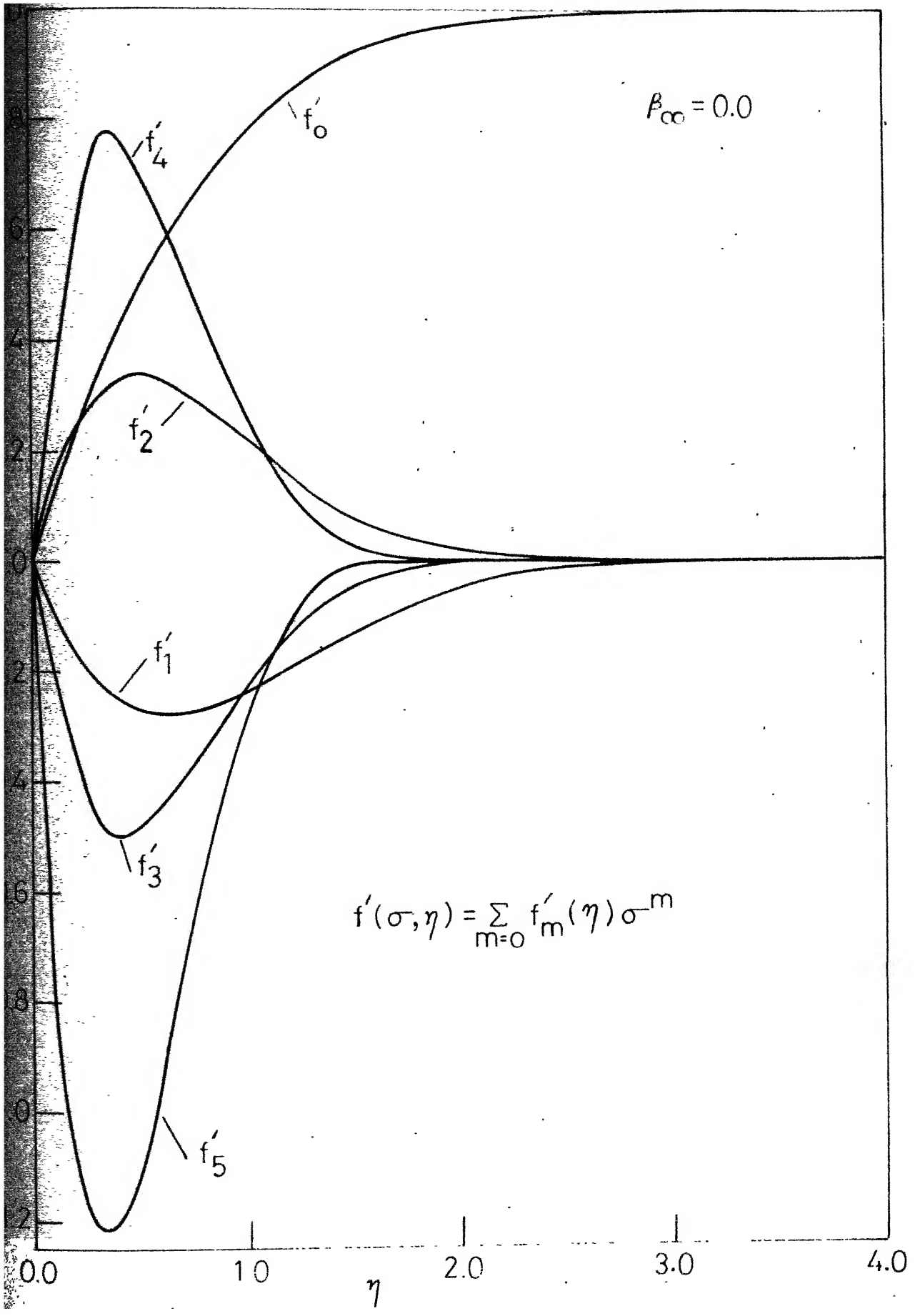
$\beta_\infty = 0.0$
f'_0
f'_4
f'_2
f'_1
f'_3
f'_5
$f'(\sigma,\eta) = \sum_{m=0} f'_m(\eta)\,\sigma^{-m}$
0.0
1.0
2.0
3.0
4.0
η

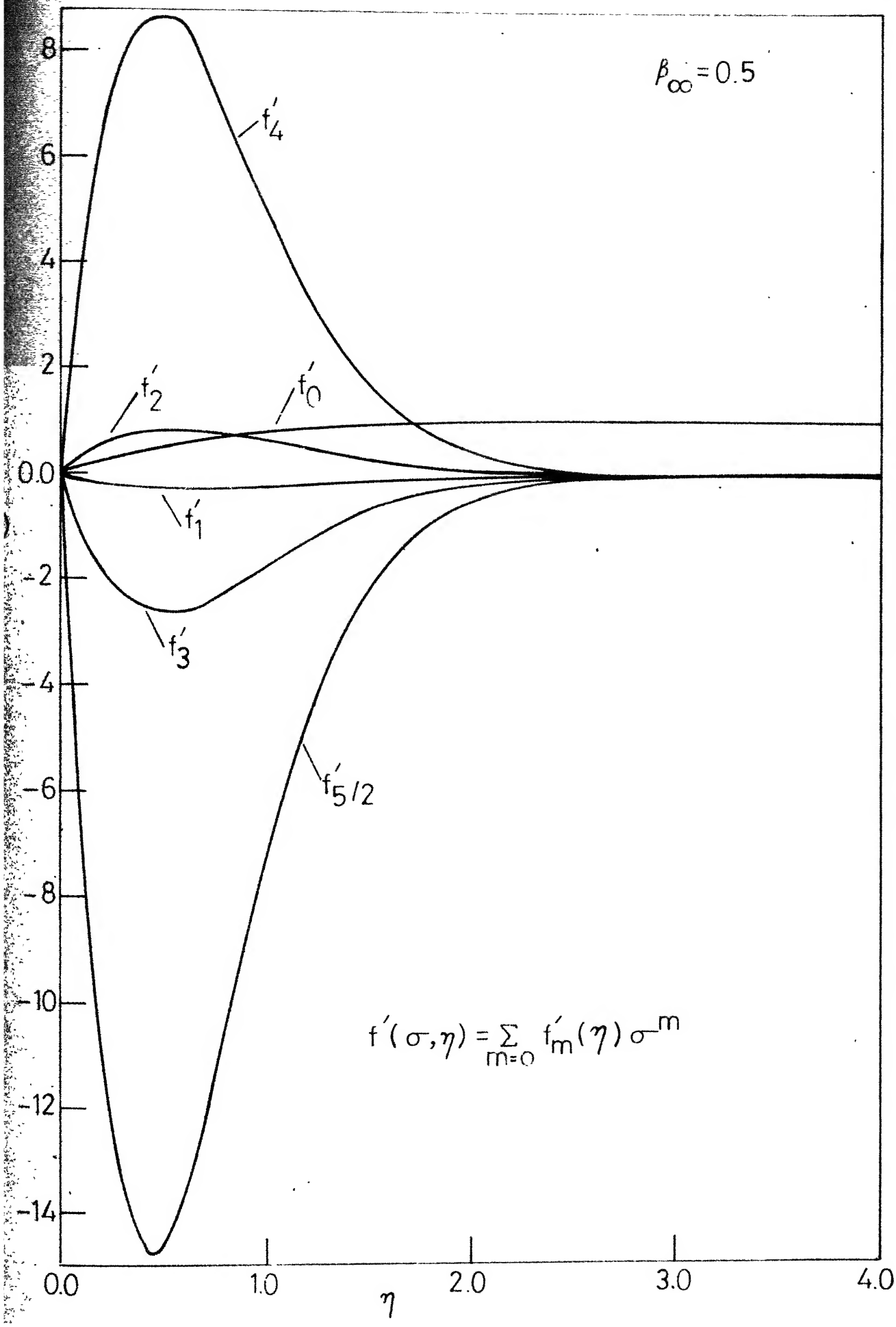
$\beta_\infty = 0.5$
f'_4
f'_2
f'_0
f'_1
f'_3
$f'_{5/2}$
$f'(\sigma,\eta) = \sum_{m=0} f'_m(\eta)\,\sigma^{-m}$
8
6
4
2
0.0
-2
-4
-6
-8
-10
-12
-14
0.0
1.0
2.0
3.0
4.0
η

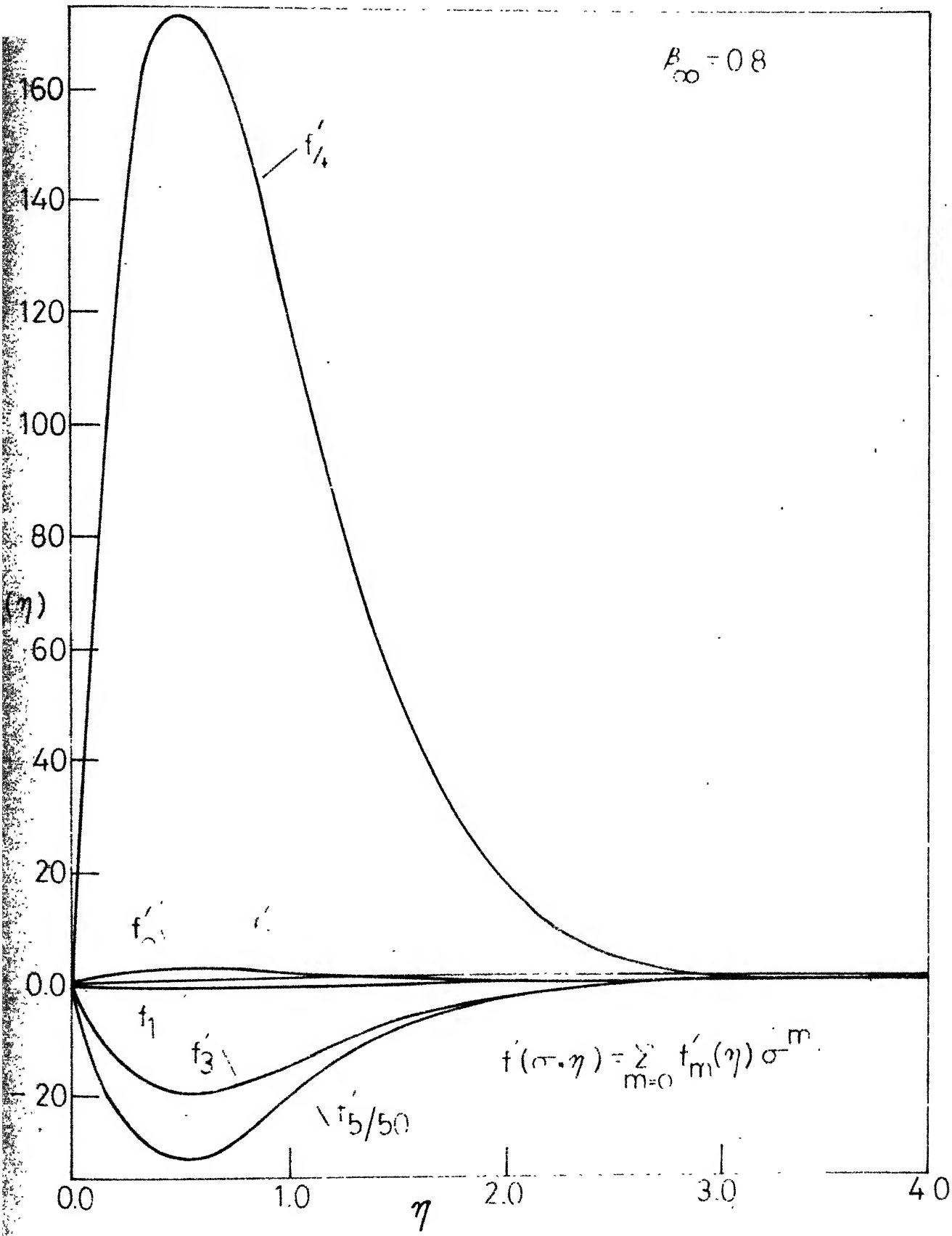

Fig. 4.2c – First-order velocity profile on a blunted wedge ($\beta_\infty = 0.8$)

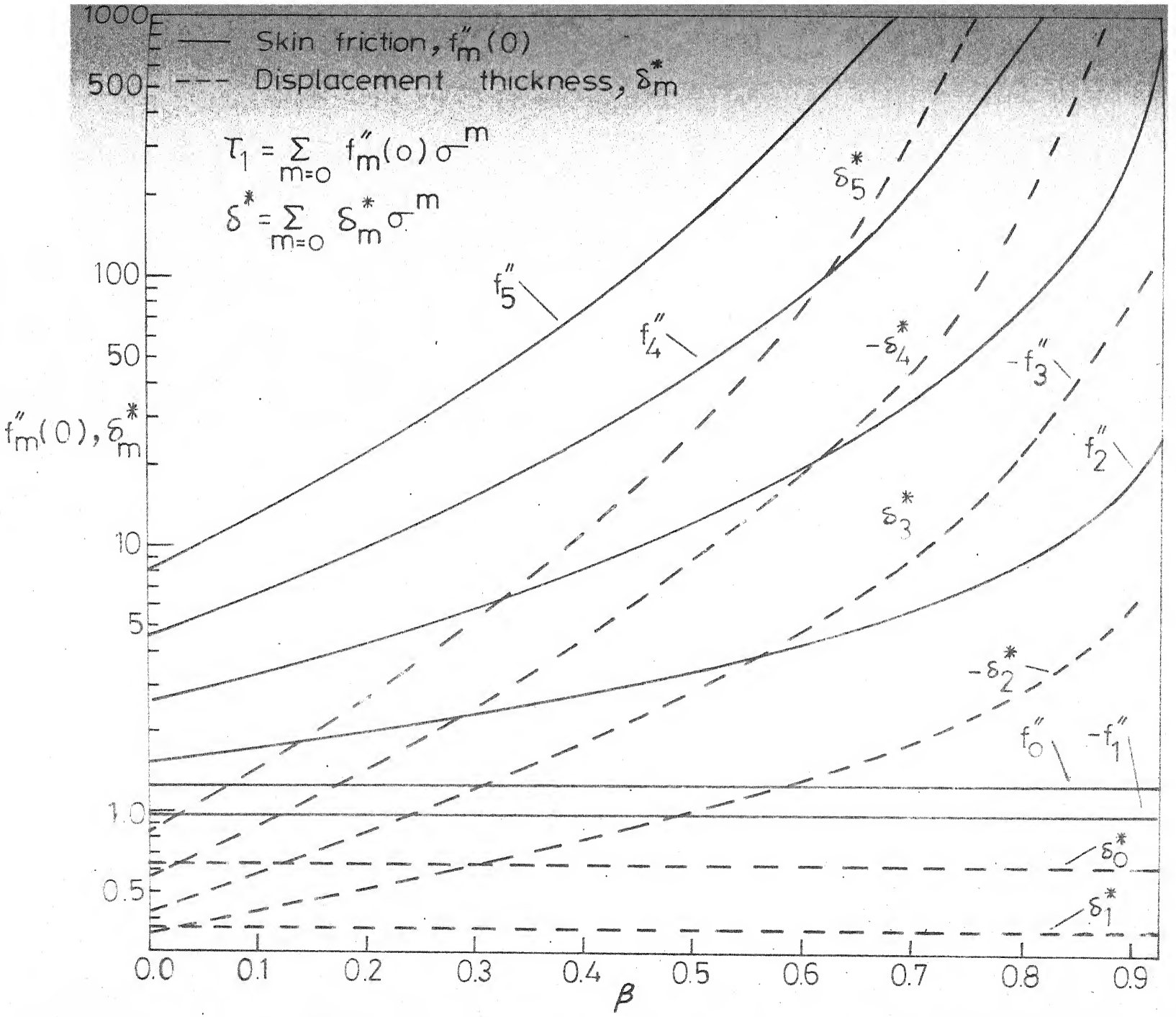

Fig. 4.3_First-order skin friction and displacement thickness

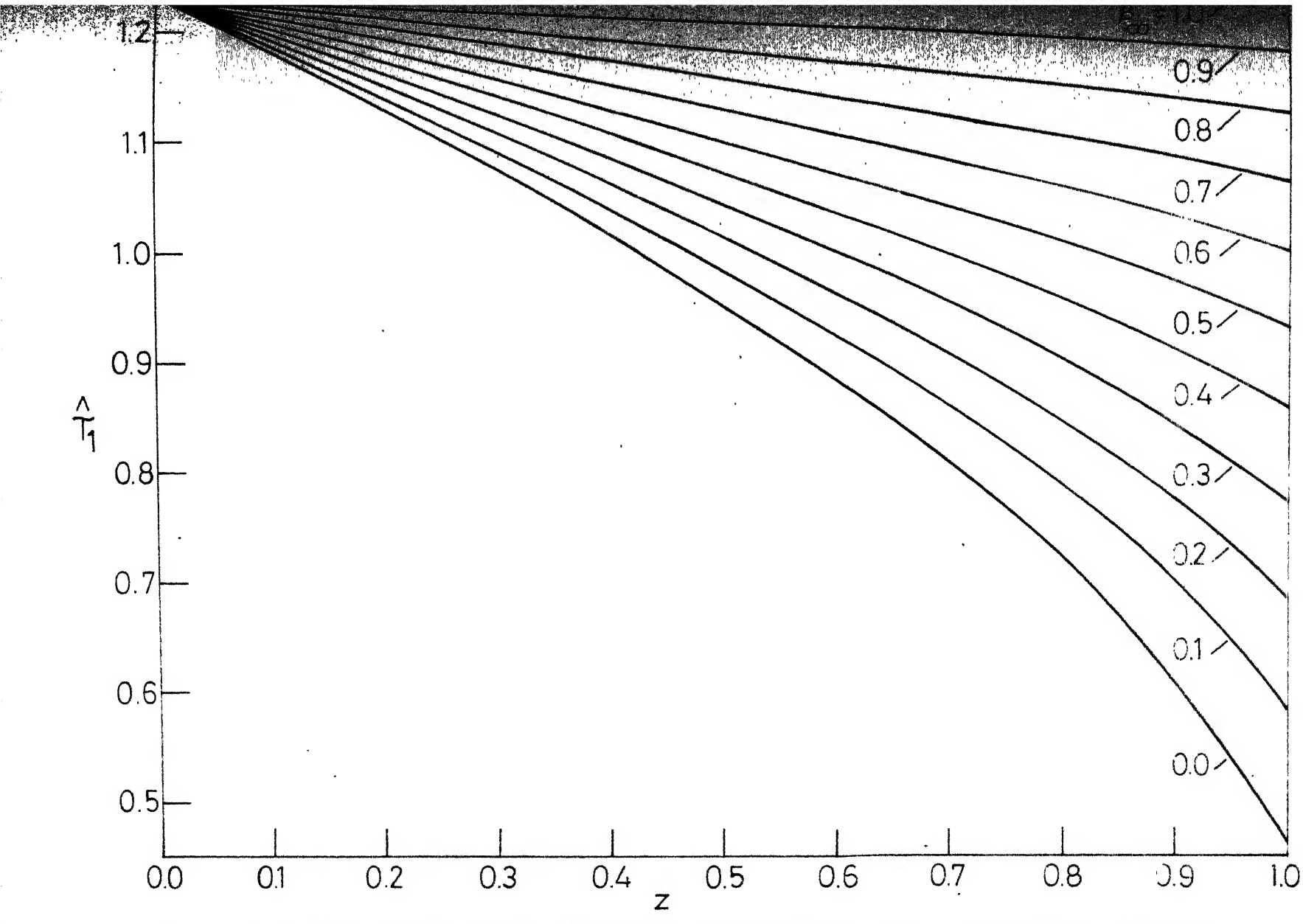

Fig. 4.4 - First-order skin friction distribution on a blunted wedge.

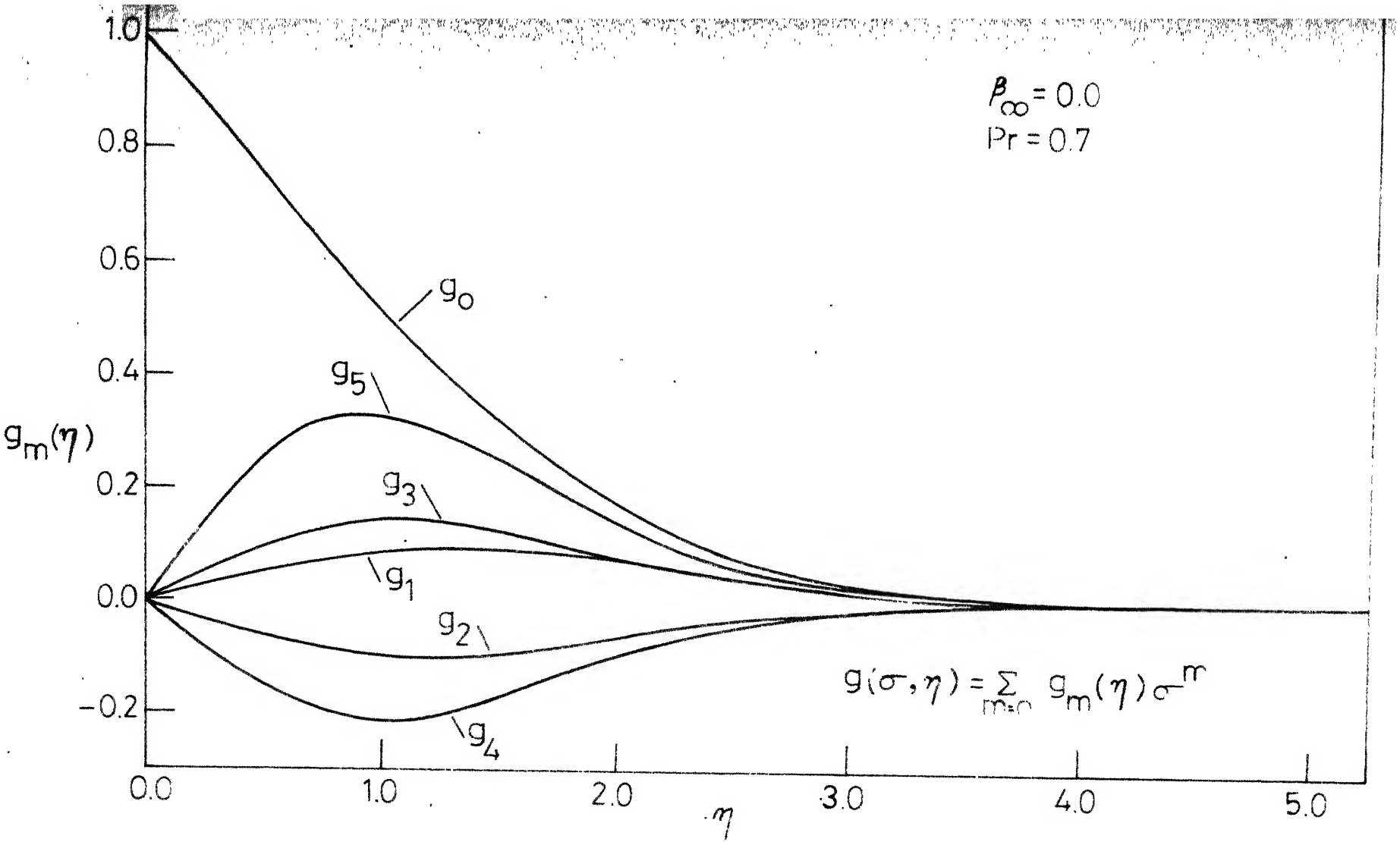

Fig 4.5a - First-order temperature profile on a parabola ($\beta_\infty = 0$).

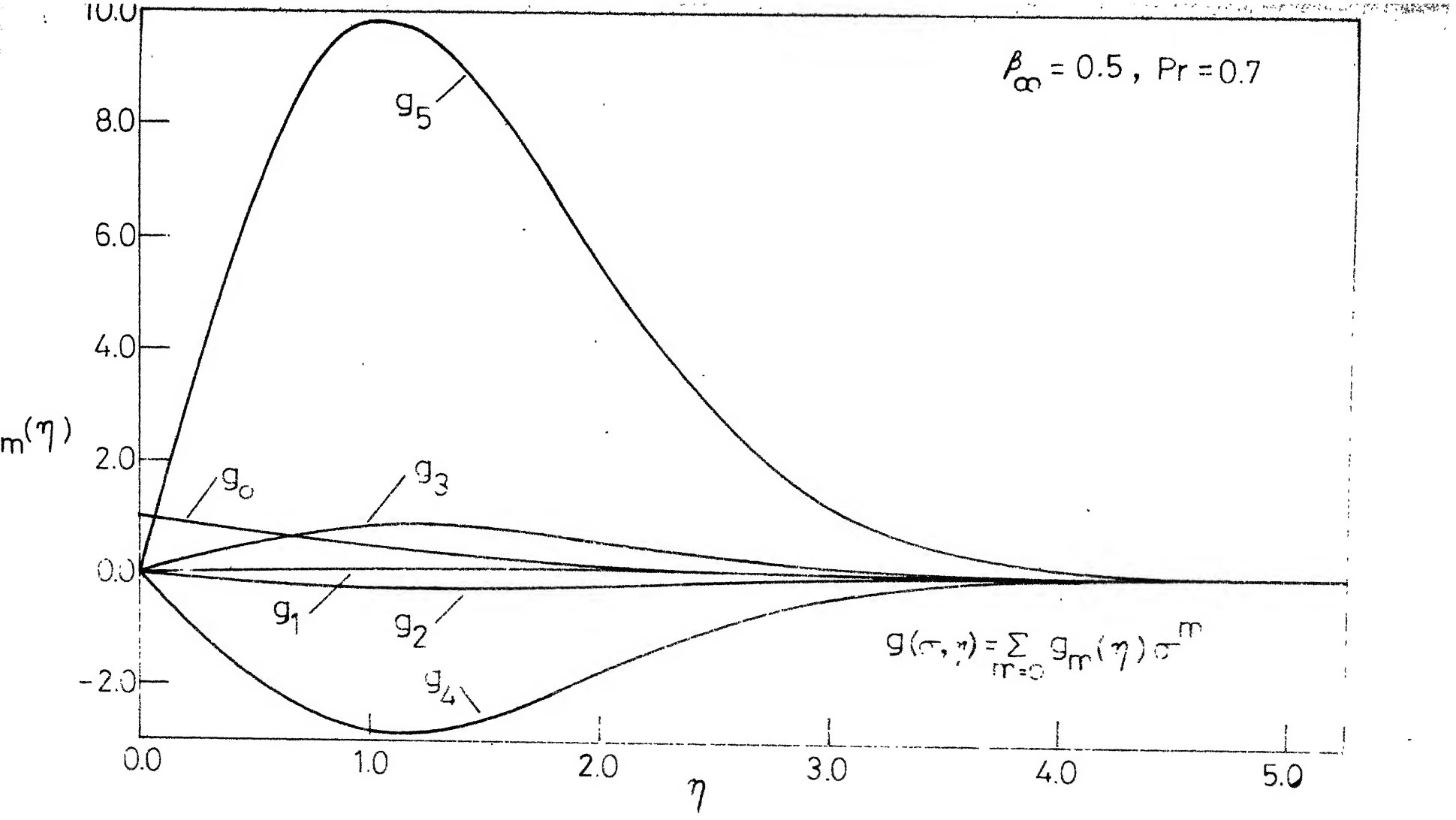

Fig. 4.5 b – First-order temperature profile on a blunted wedge (β_∞=0.5).

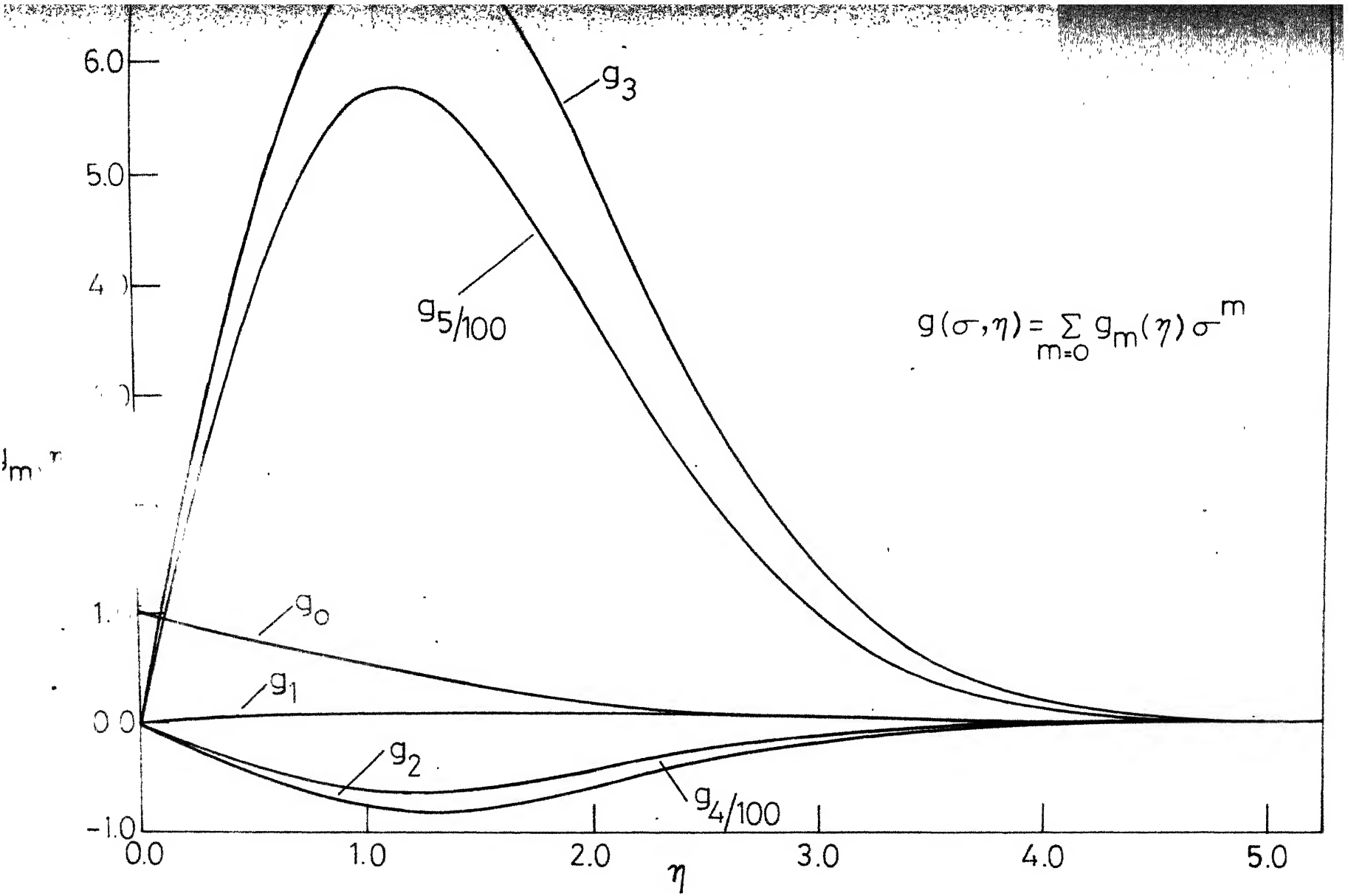

Fig. 4.5 c _ First-order temperature profile on a blunted wedge ($\beta_\infty = 0.8$).

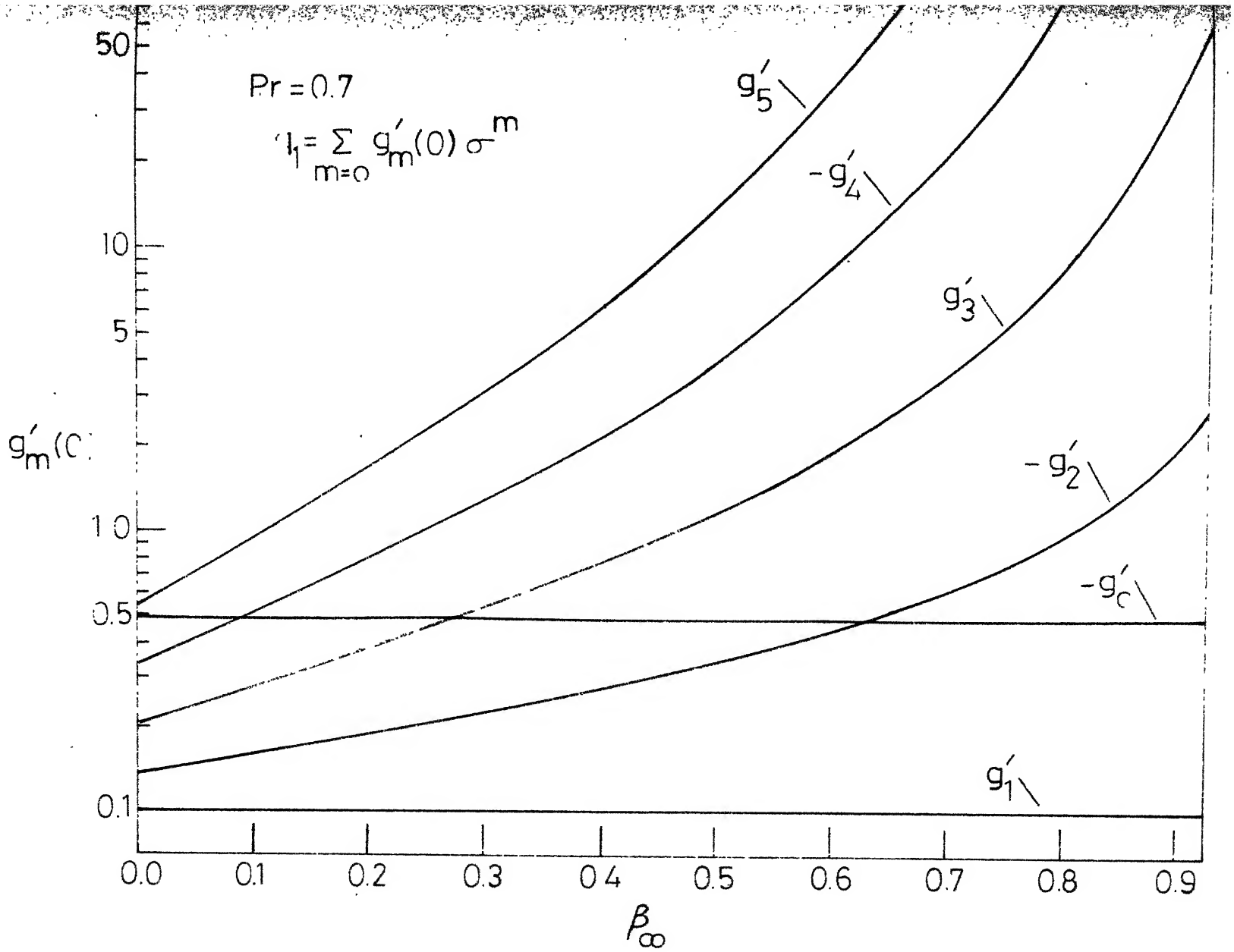

Fig. 4.6 – First – order, heat transfer on a blunted wedge.

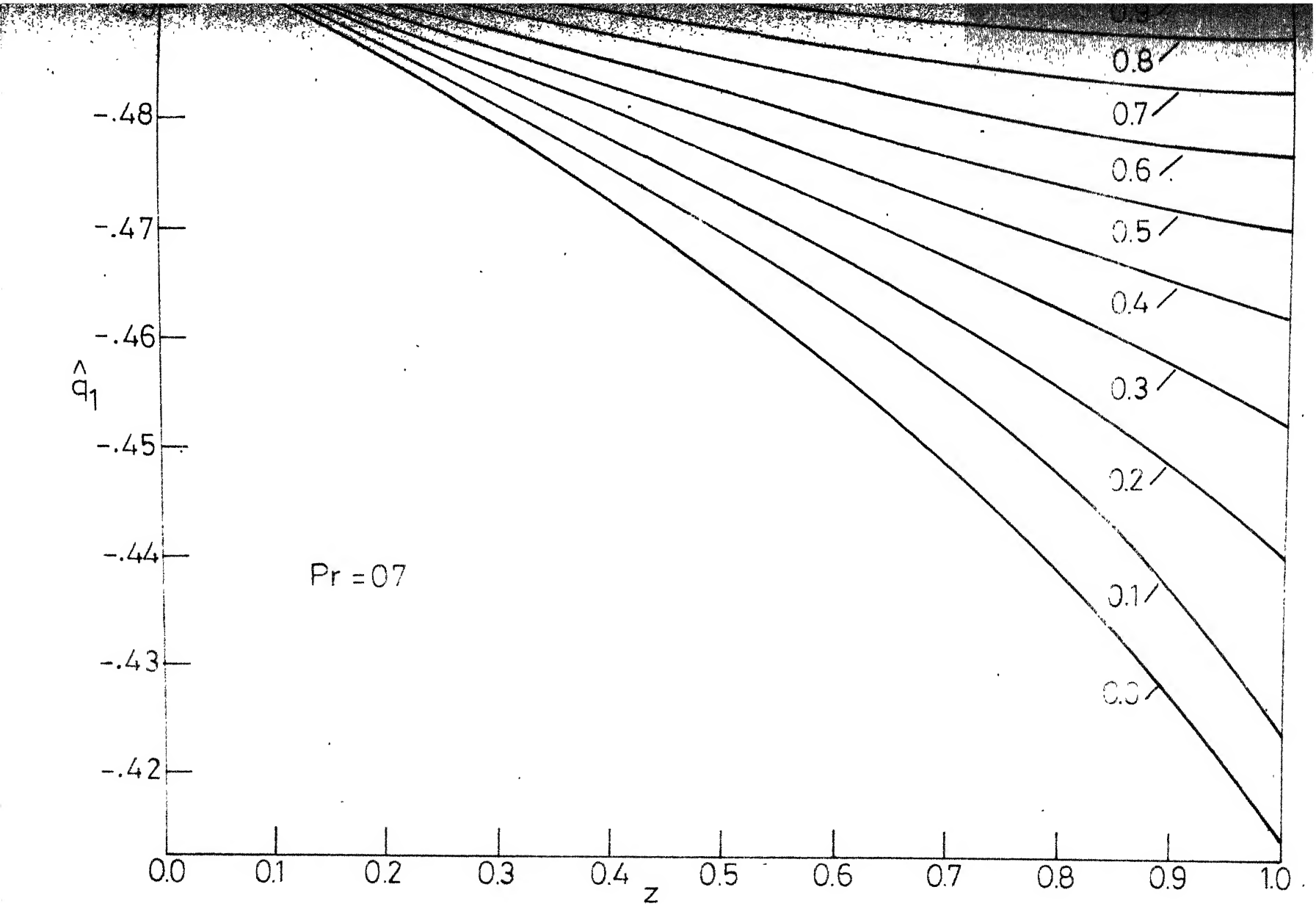

Fig.4.7_First-order heat transfer distribution on a blunted wedge.

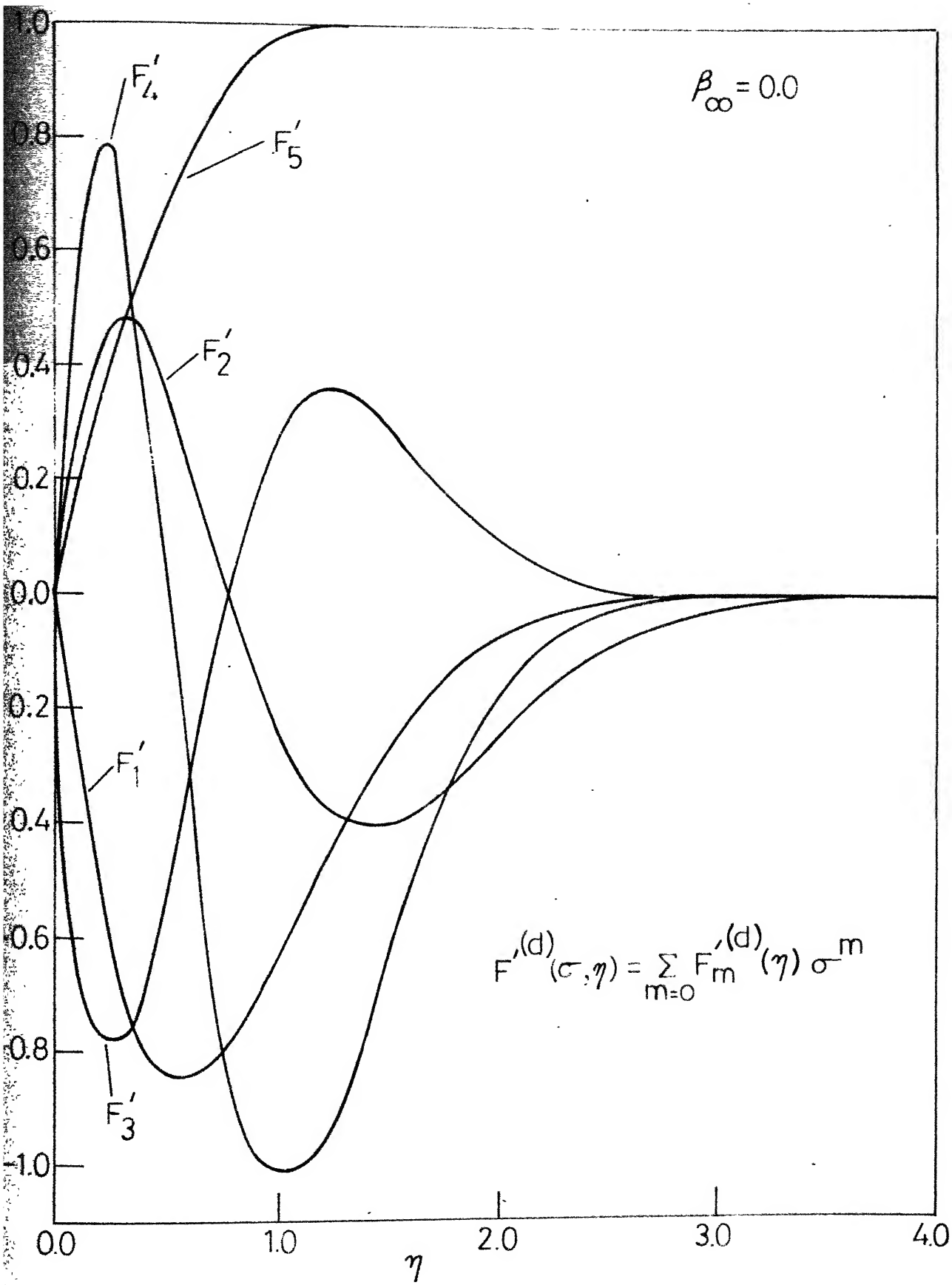

Fig.4.8a - Second-order velocity profile on a parabola ($\beta_\infty = 0$) due to displacement effect.

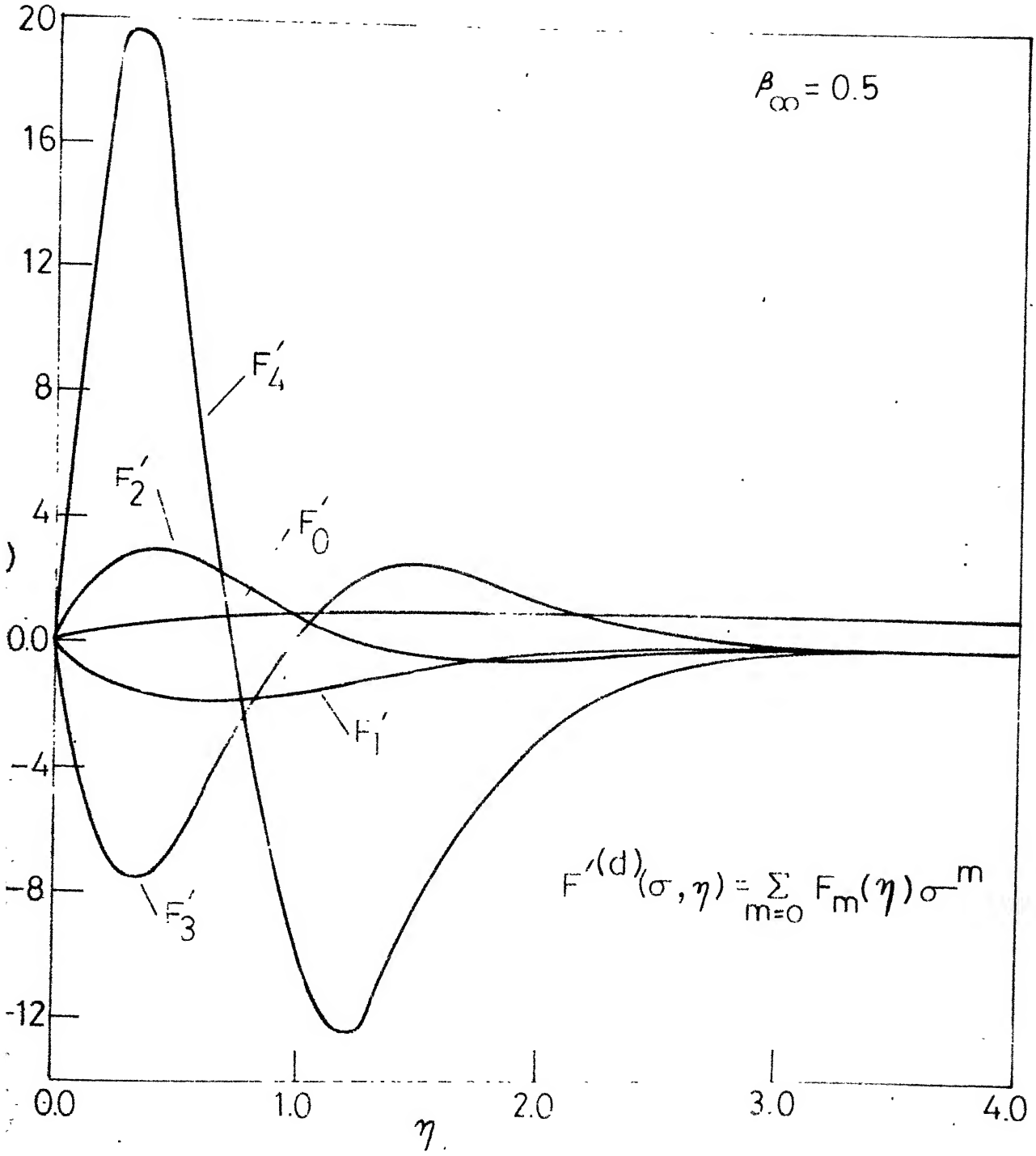

Fig. 4.8b – Second – order velocity profile on a blunted wedg (β_∞=0.5) due to displacement effects.

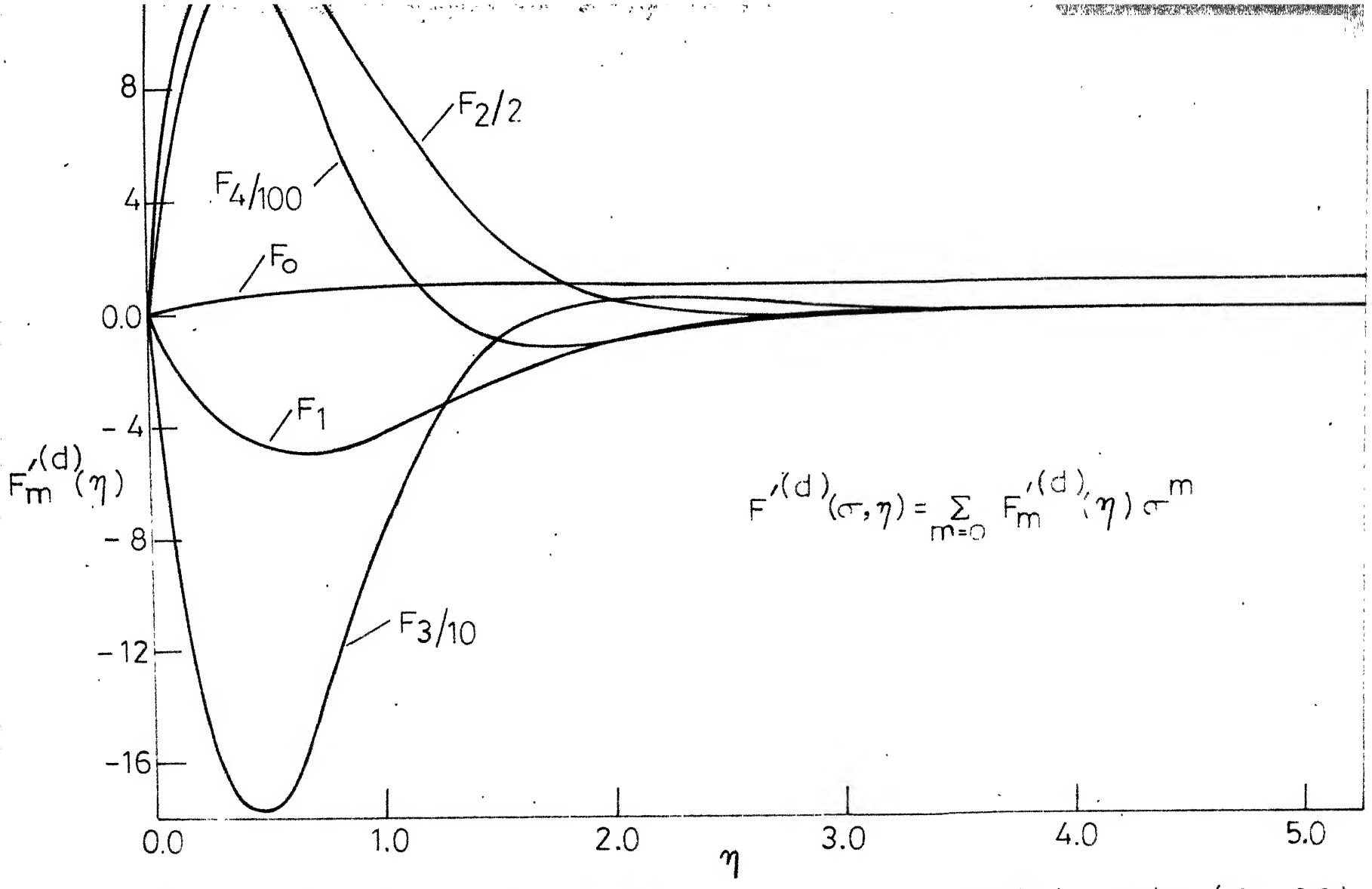

Fig. 4.8c – Second-order velocity profile on a blunted wedge ($\beta_\infty = 0.8$) due to displacement effect.

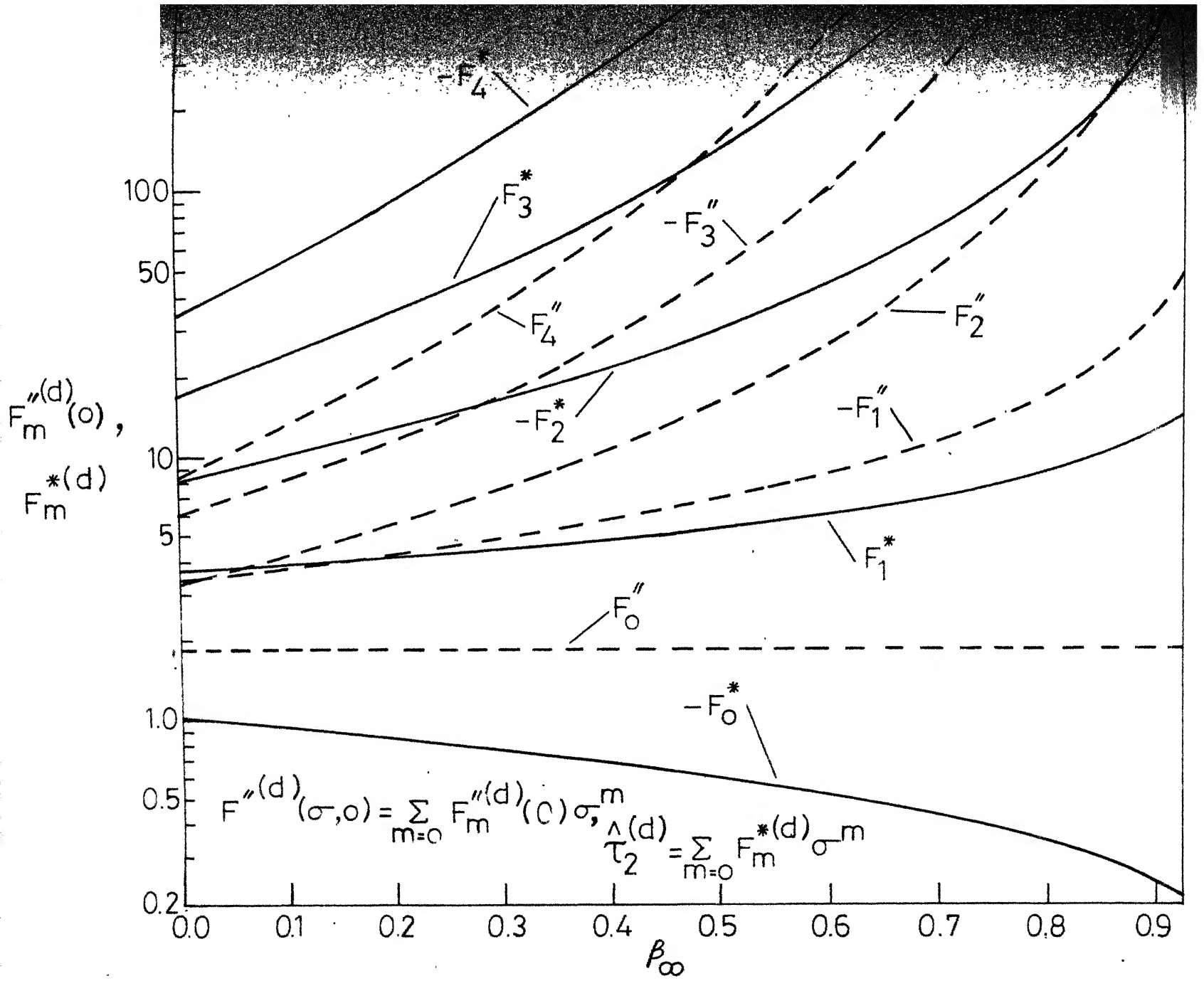

Fig. 4.9_Contribution of displacement speed to skin friction on a blunted wedge.

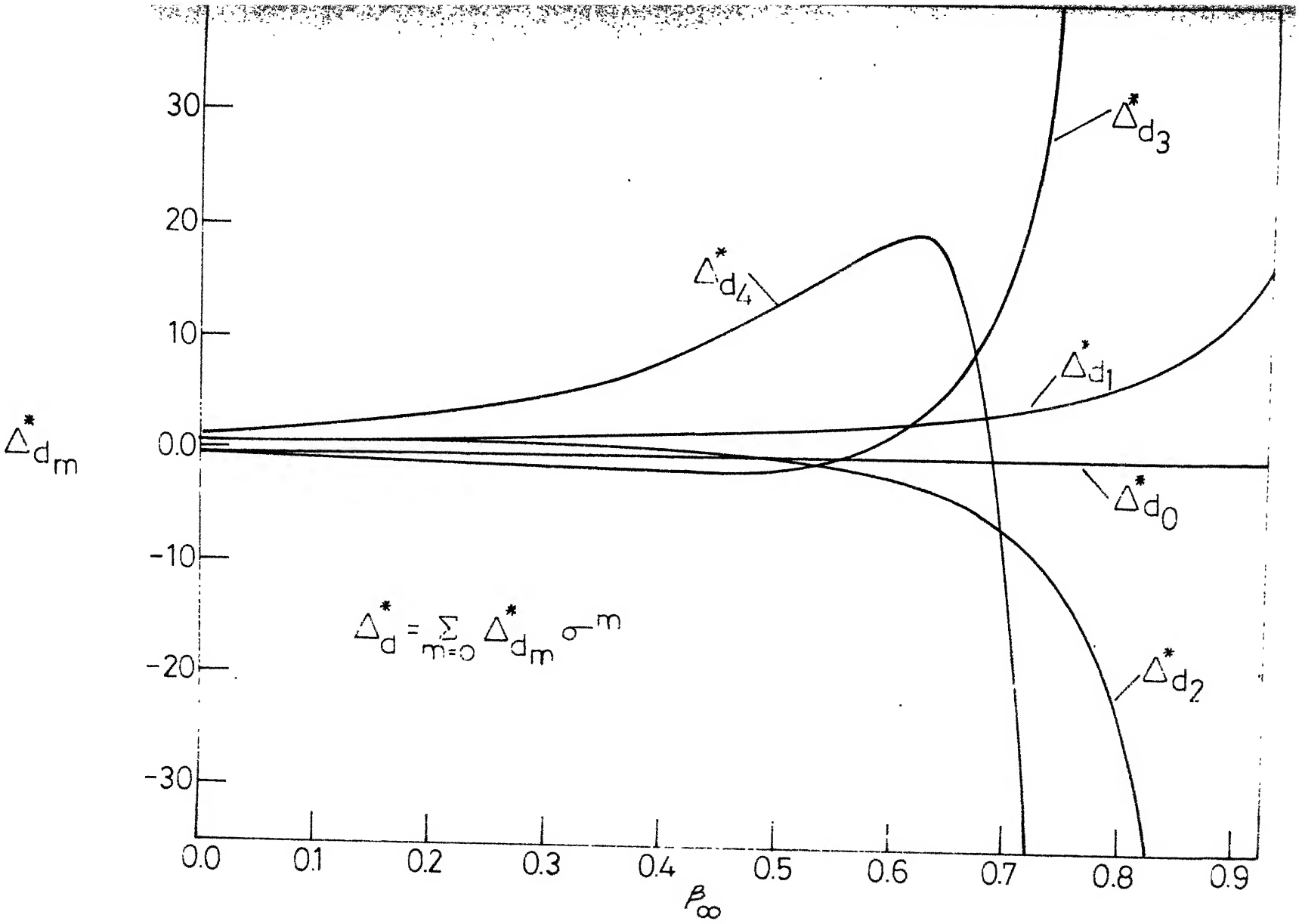

Fig. 4.10 _Contribution of displacement speed to displacement thickness on a blunted wedge.

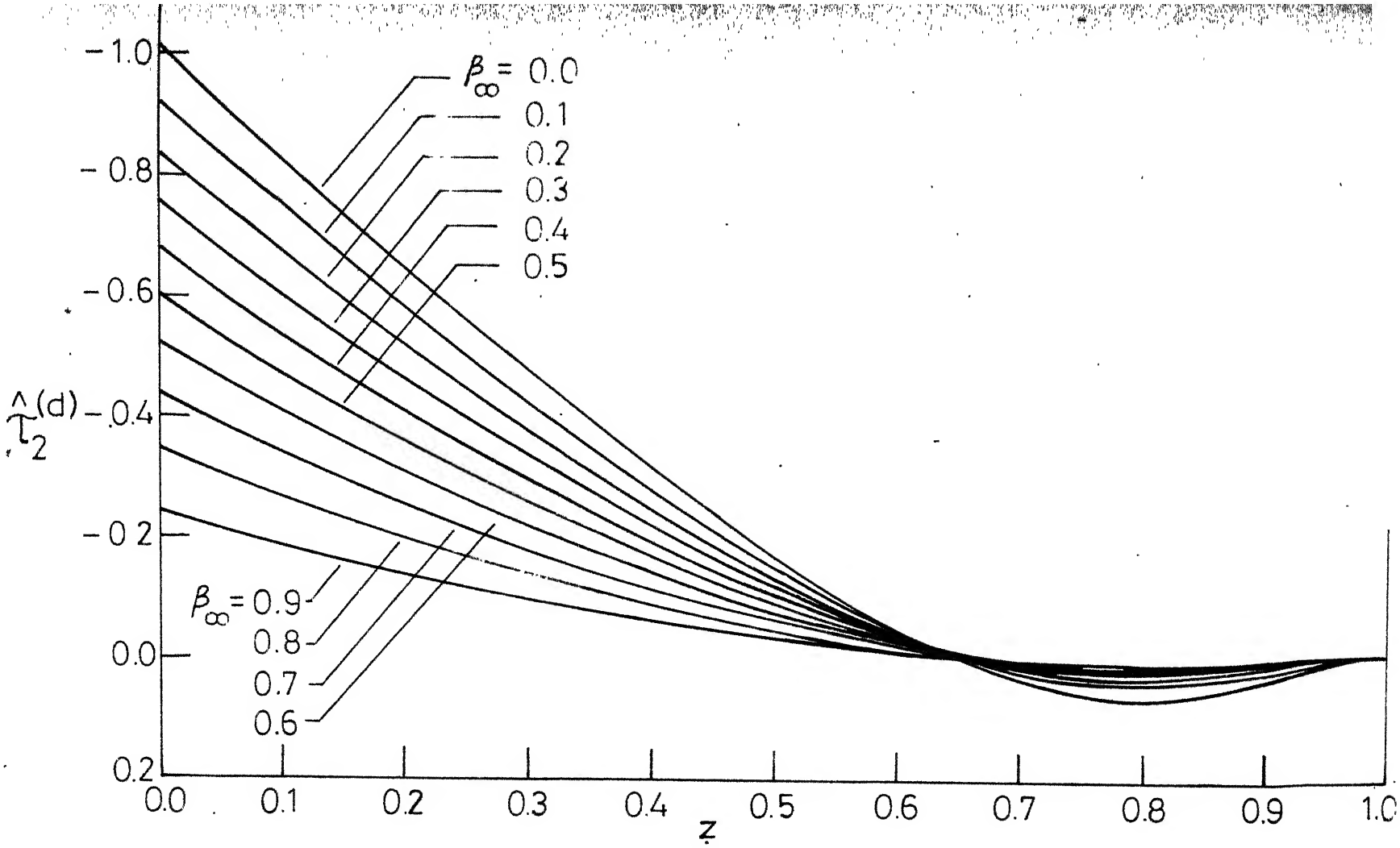

Fig. 4.11 _ Displacement speed contribution to skin friction distribution on a blunted wedge .

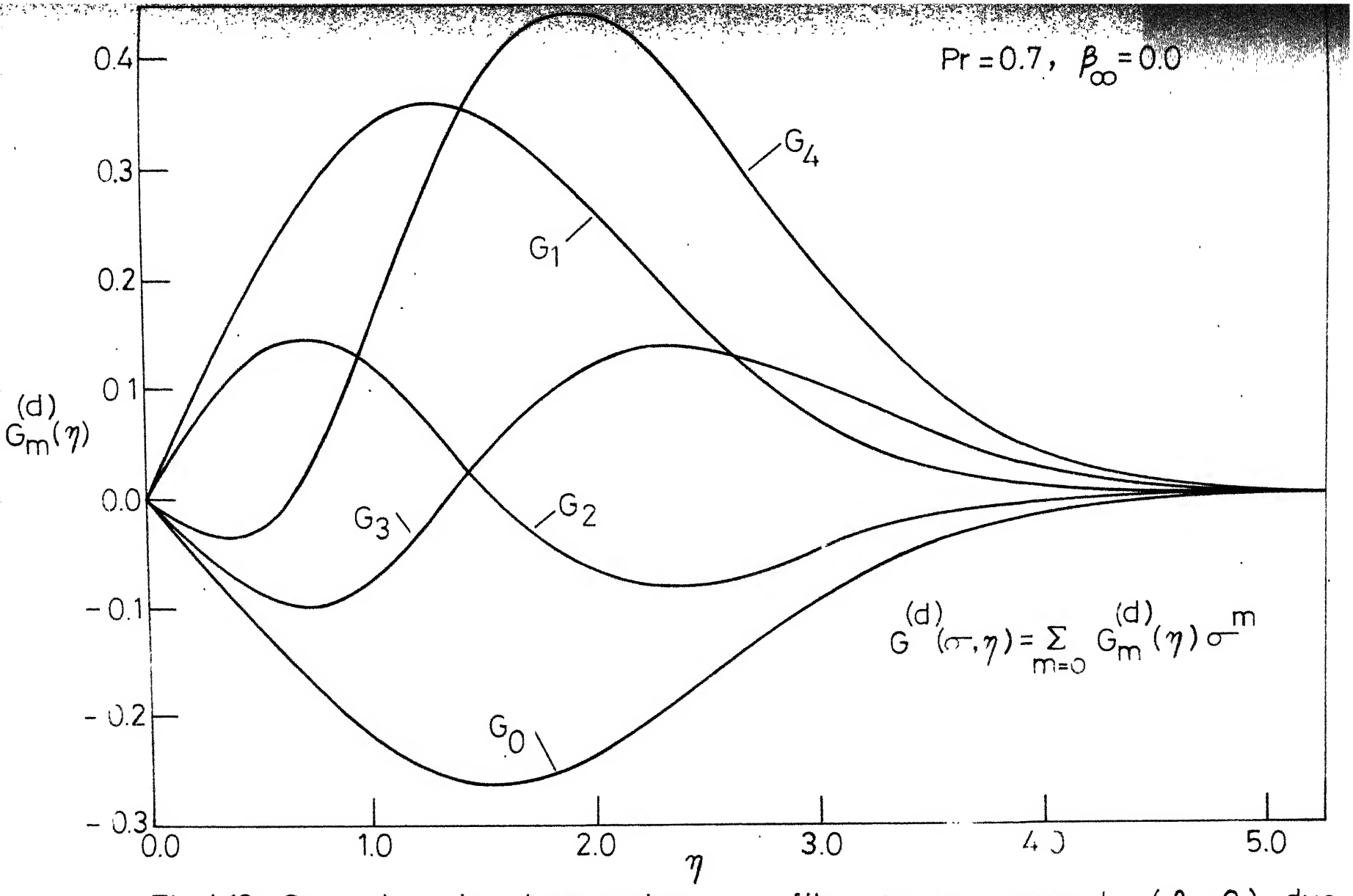

Fig. 4.12a. Second - order temperature profile on a parabola ($\beta_\infty = 0$) due to displacement effect.

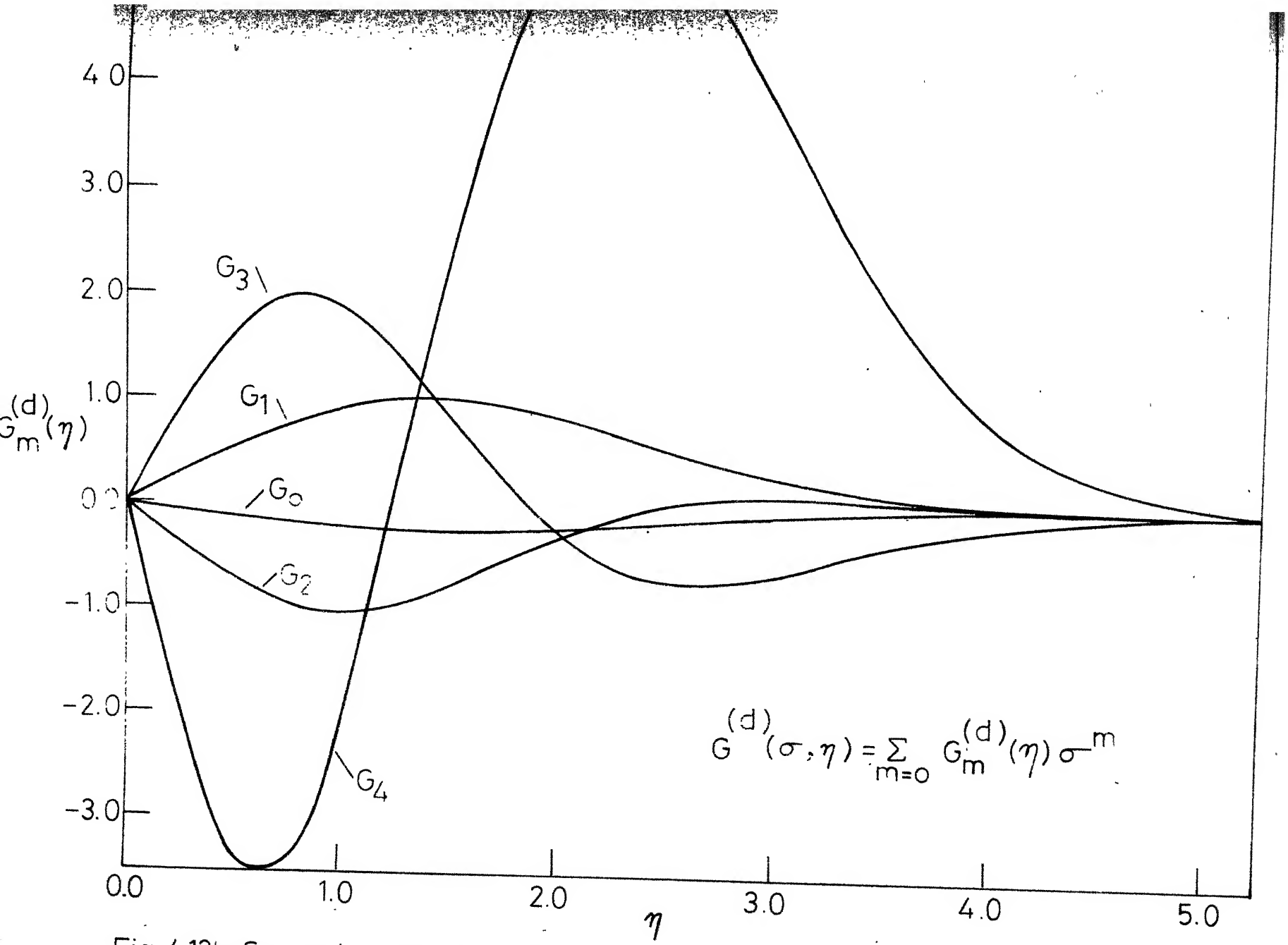

Fig. 4.12b-Second-order temperature profile on a blunted wedge (β =0.5) due to displacement effect

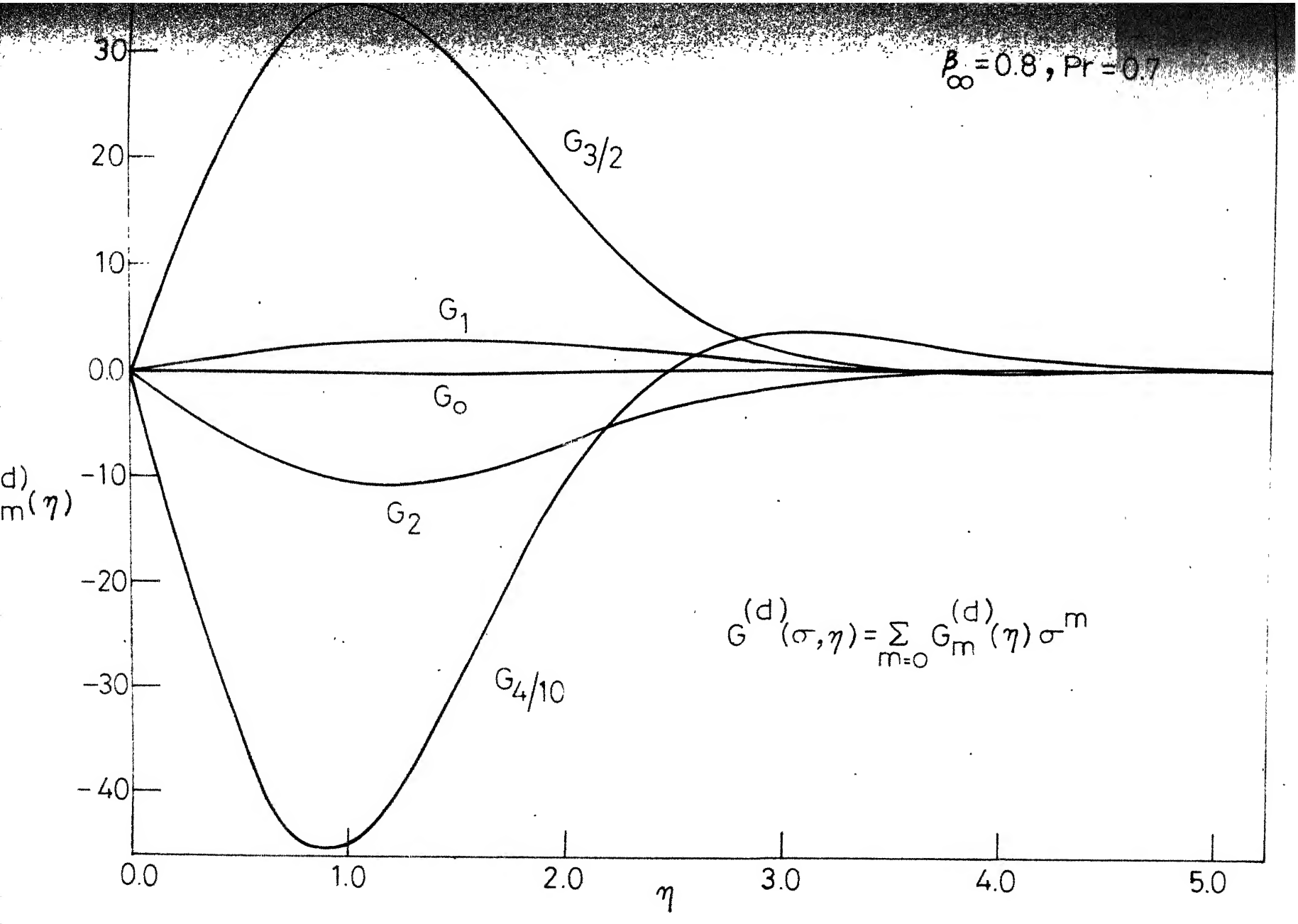

Fig. 4.12c – Second – order temperature profile on a blunted wedge (β_∞=0.8) due to displacement effect.

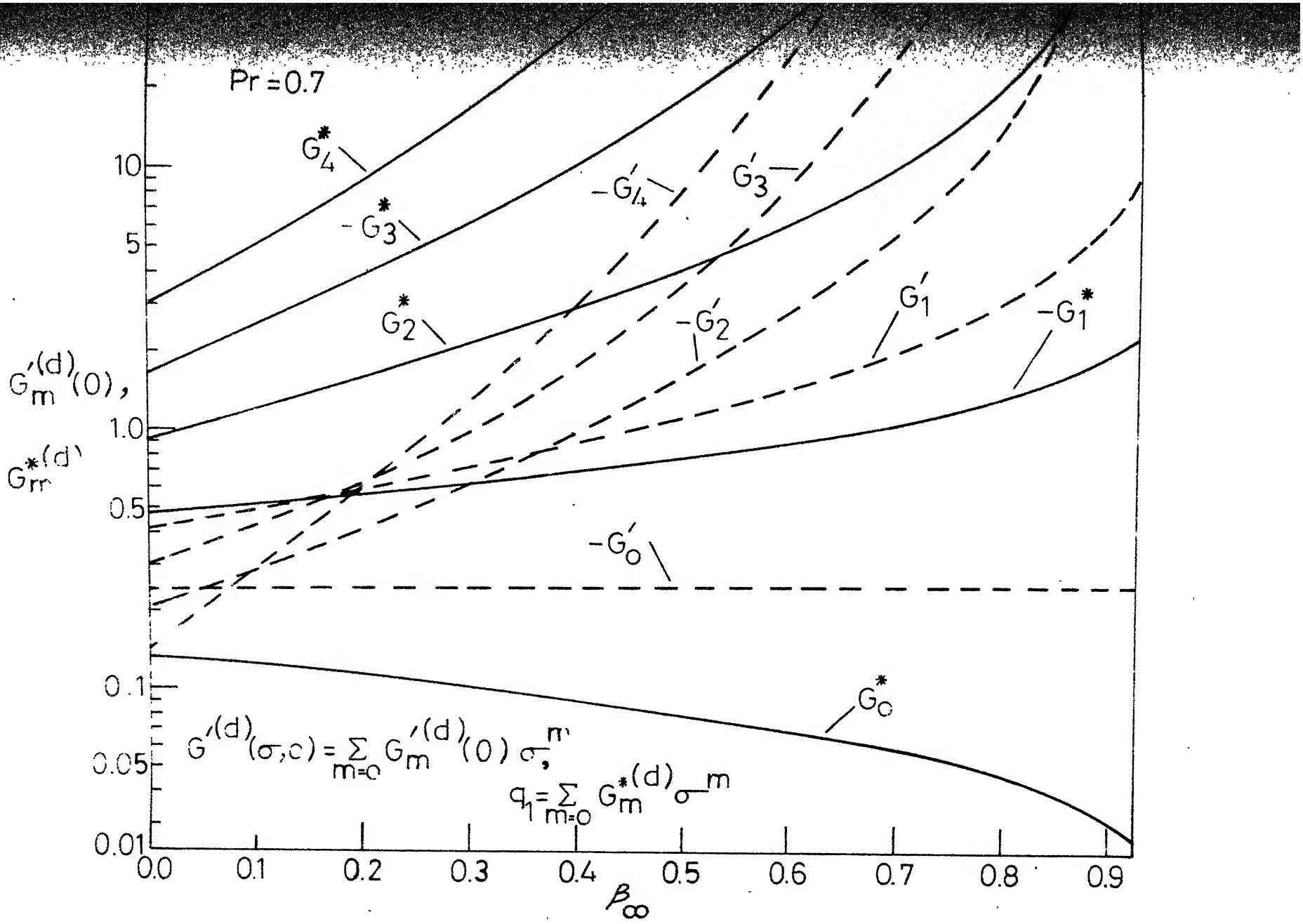

Fig. 4.13 – Contribution of displacement speed to heat transfer on a blunted wedge.

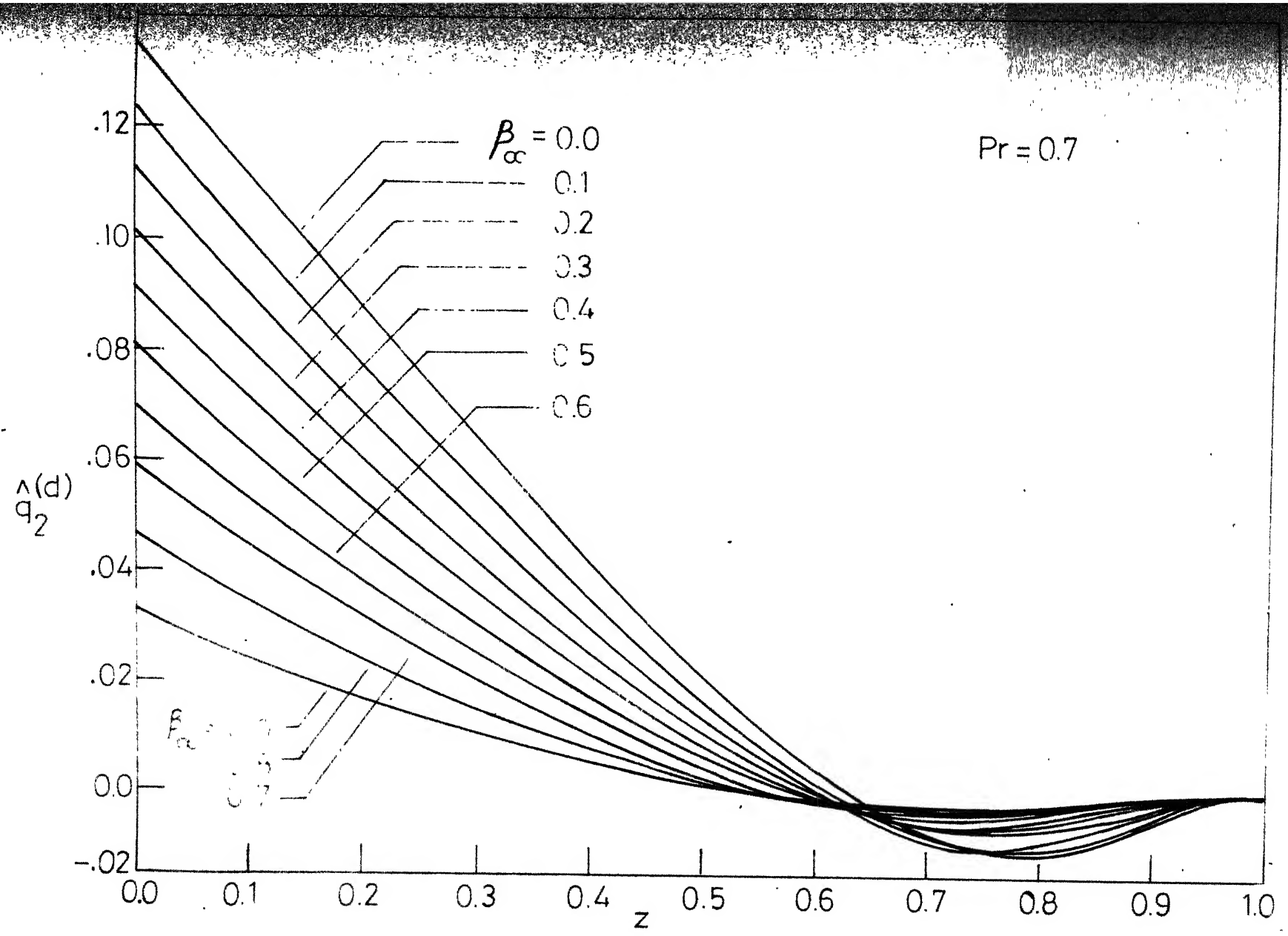

Fig. 4.14 _ Displacement speed contribution to heat transfer distribution on a blunted wedge .

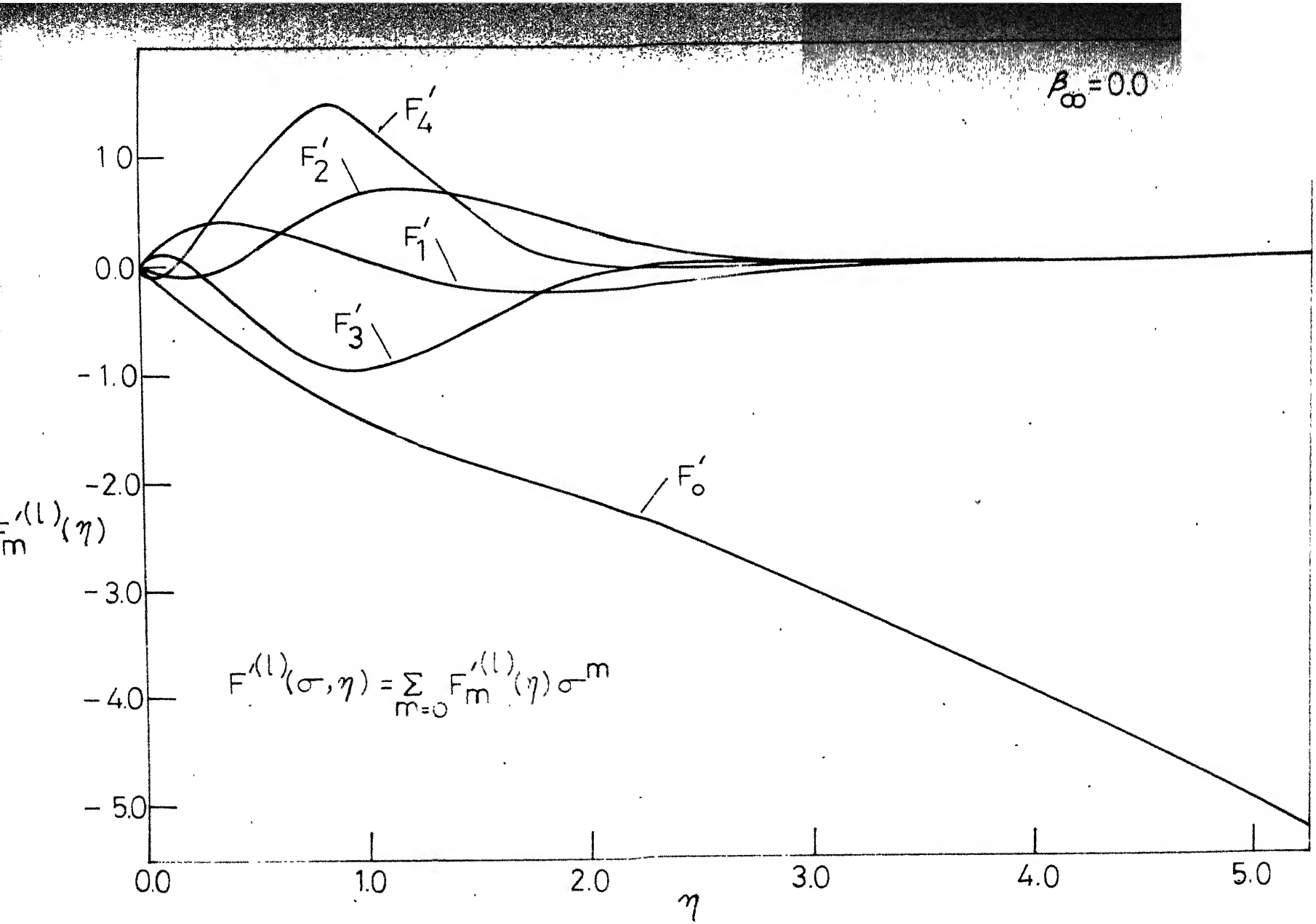

Fig.4.15a - Second-order velocity profile on a parabola (β_∞=0) due to longitudinal curvature.

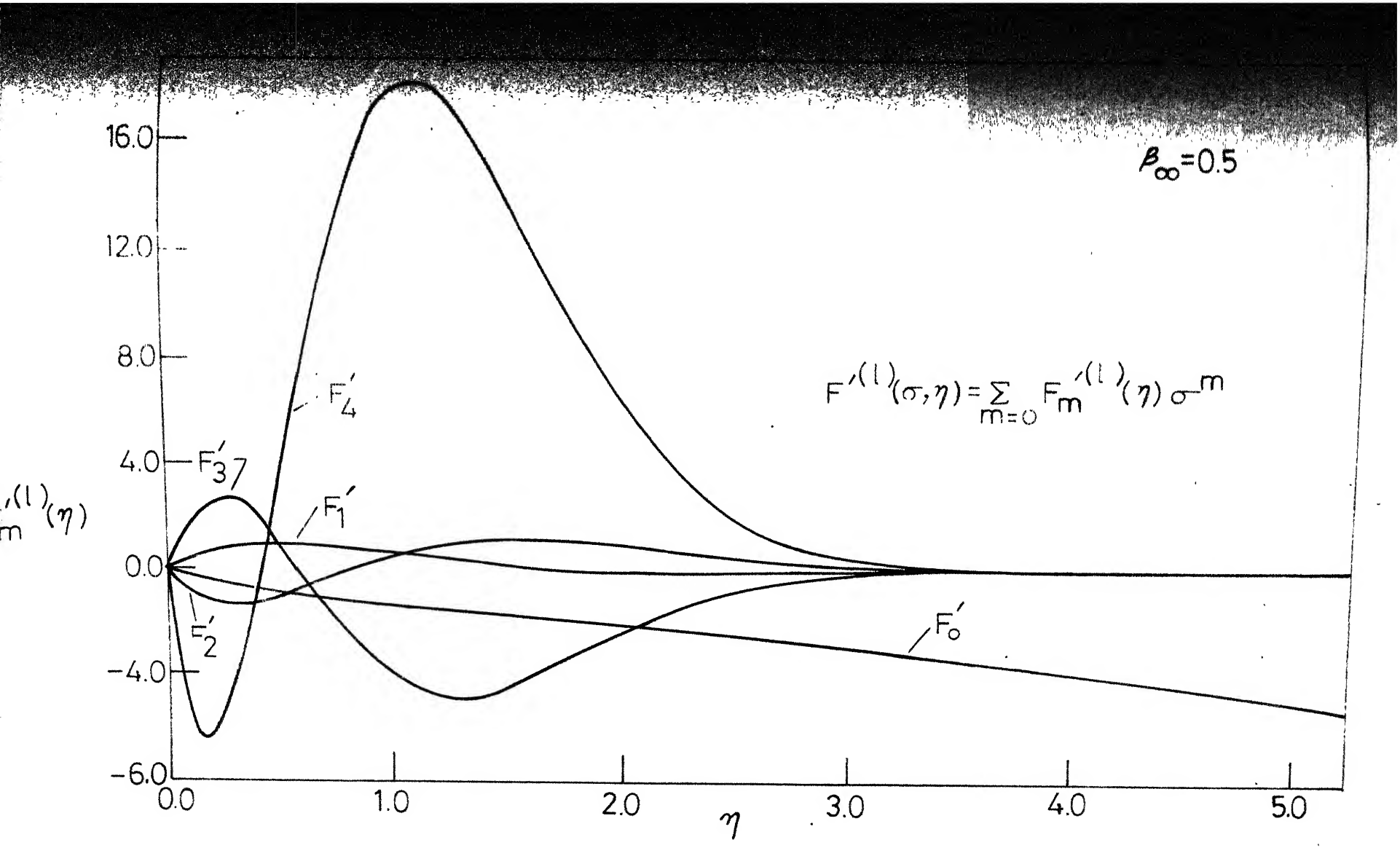

Fig. 4.15b_ Second-order velocity profile on a blunted wedge (β_∞ =0.5) due to longitudinal curvature

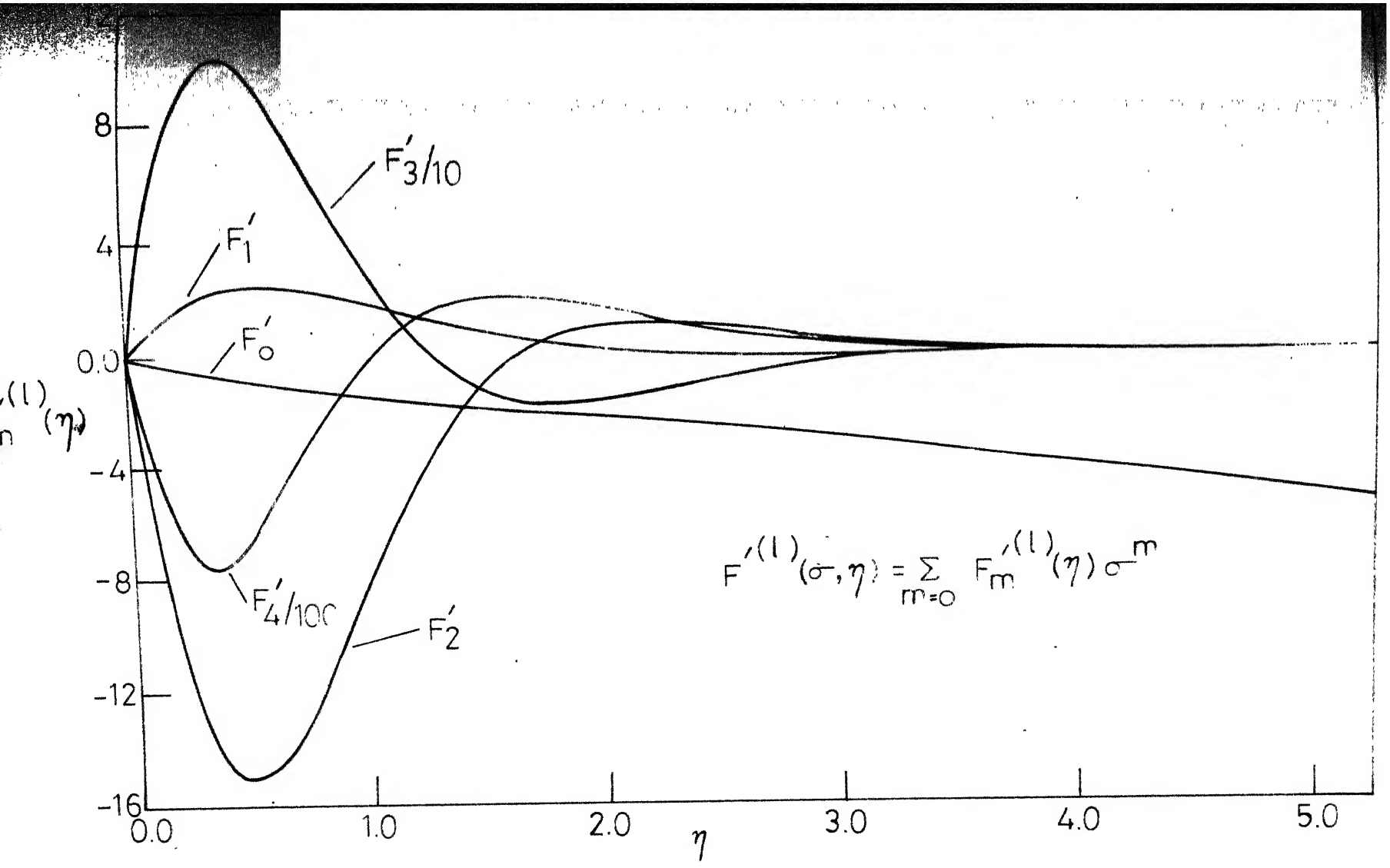

Fig. 4.15 c – Second - order velocity profile on a blunted wedge (β_∞=0.8) due to longitudinal curvature.

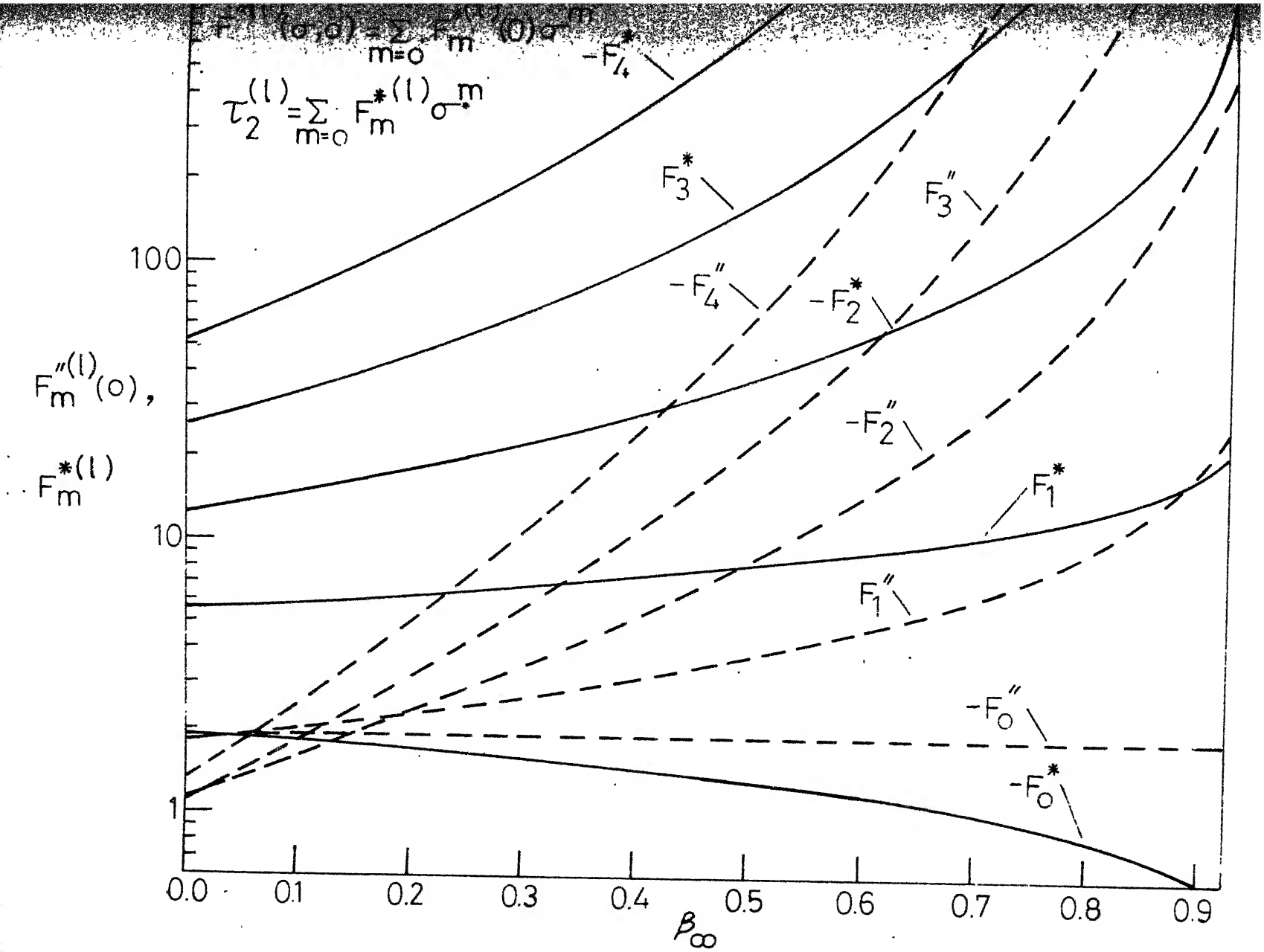

Fig. 4.16 – Contribution of longitudinal curvature to skin friction on a blunted wedge.

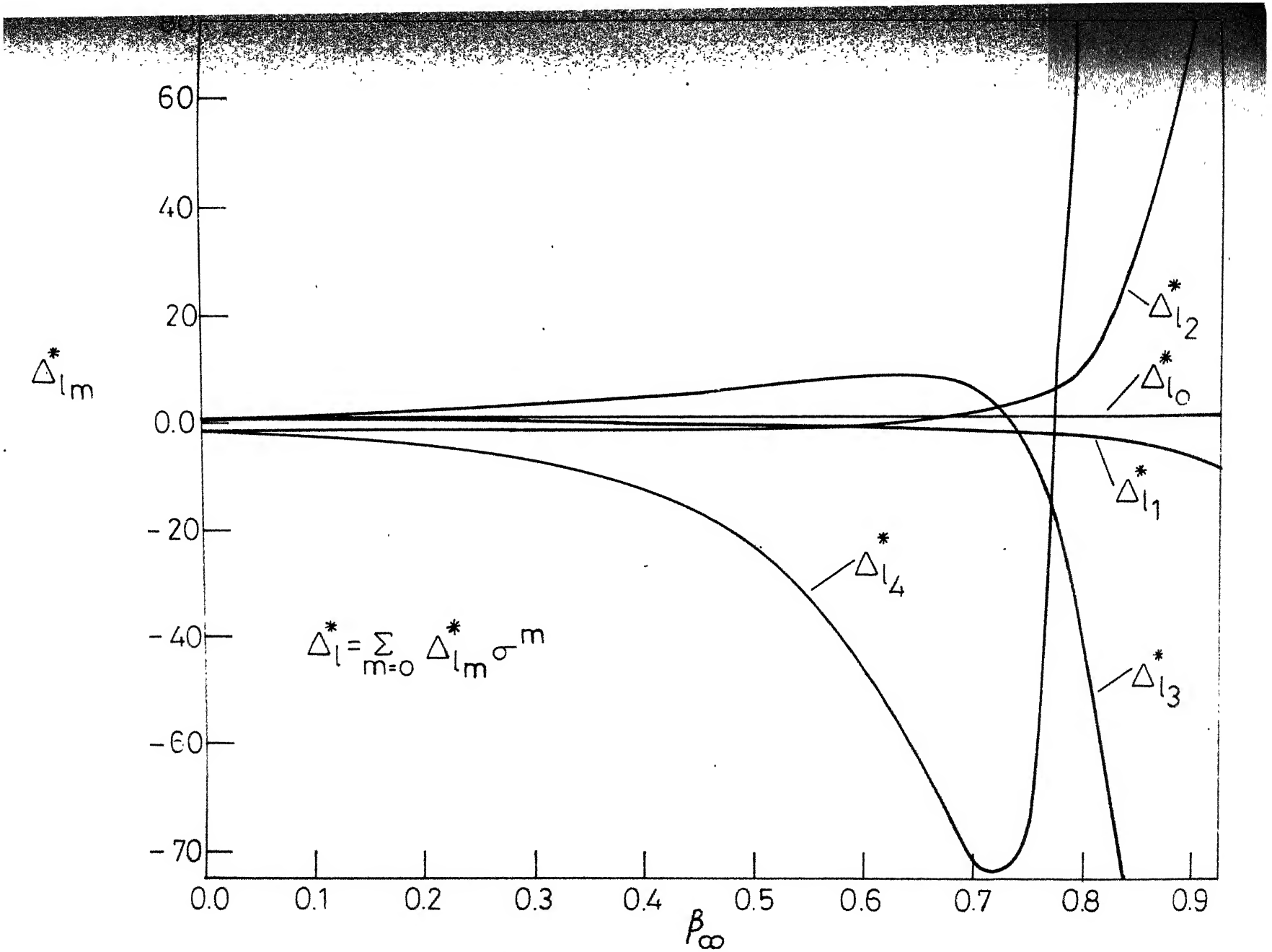

Fig. 4.17 _ Contribution of longitudinal curvature to displacement thickness on blunted wedge.

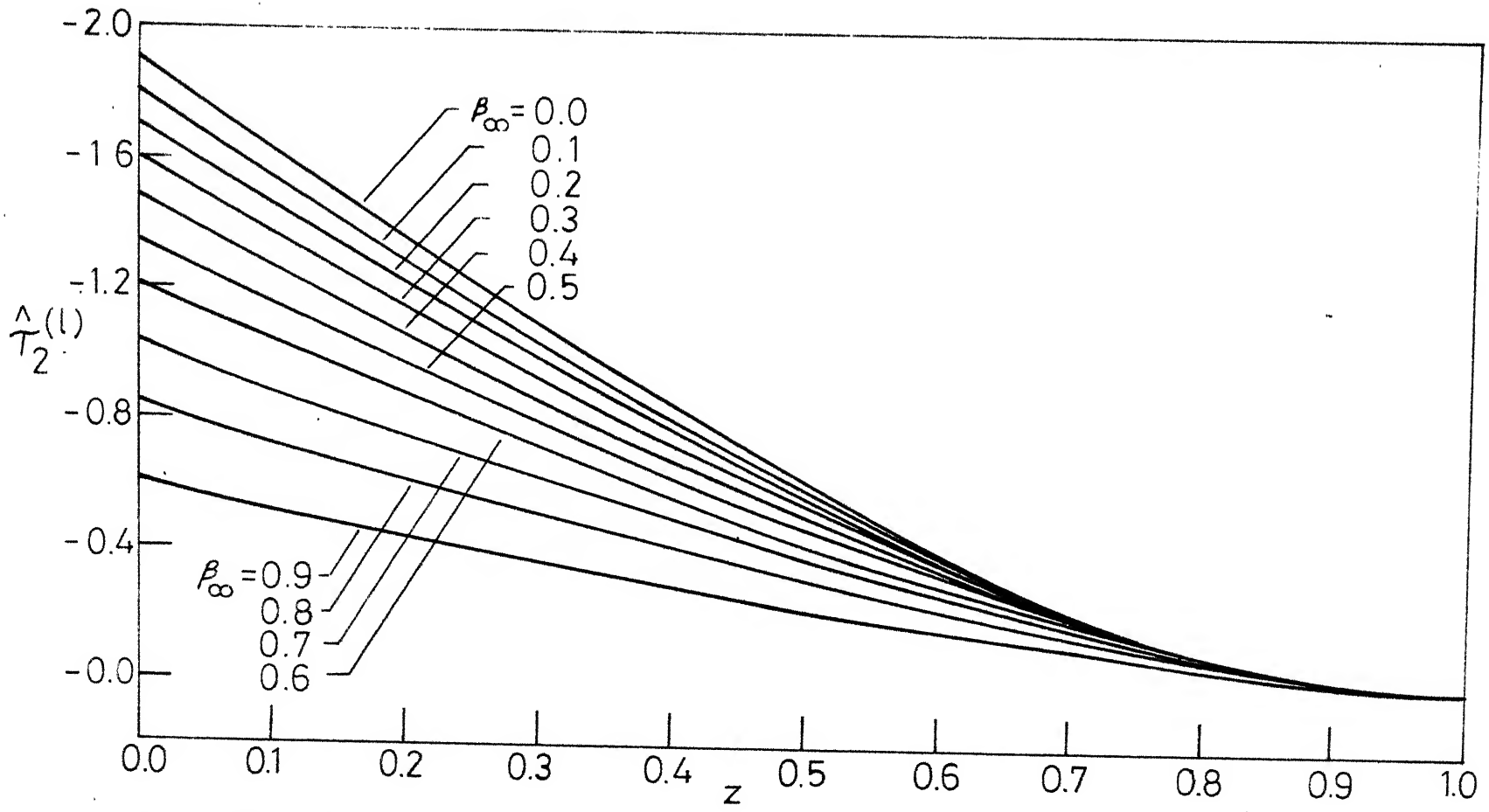

Fig. 4.18 - Longitudinal curvature contribution to skin friction distribution on a blunted wedge .

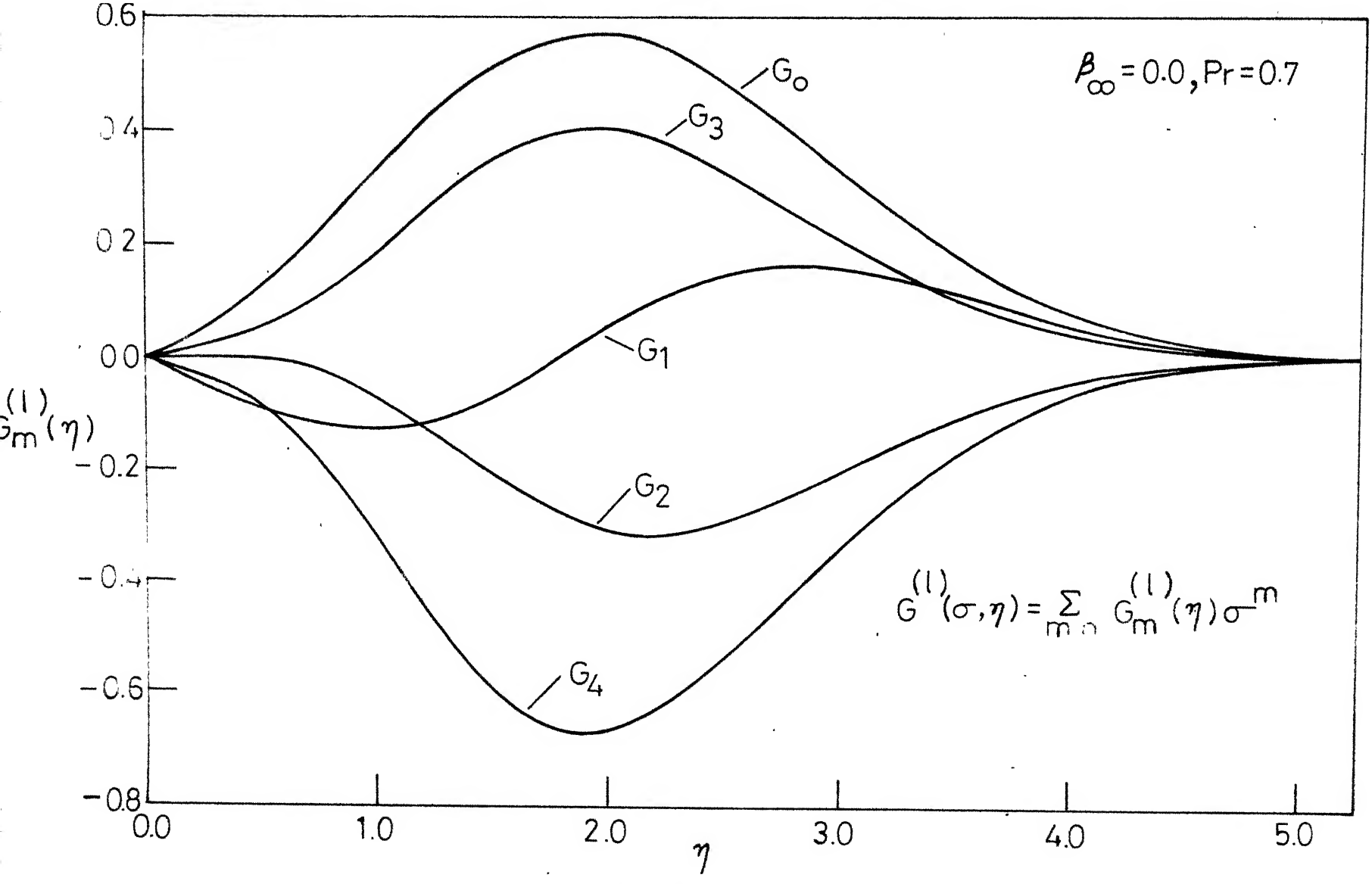

Fig. 4.19 a - Second-order temperature profile on a parabola ($\beta_\infty = 0$) due to longitudinal curvature .

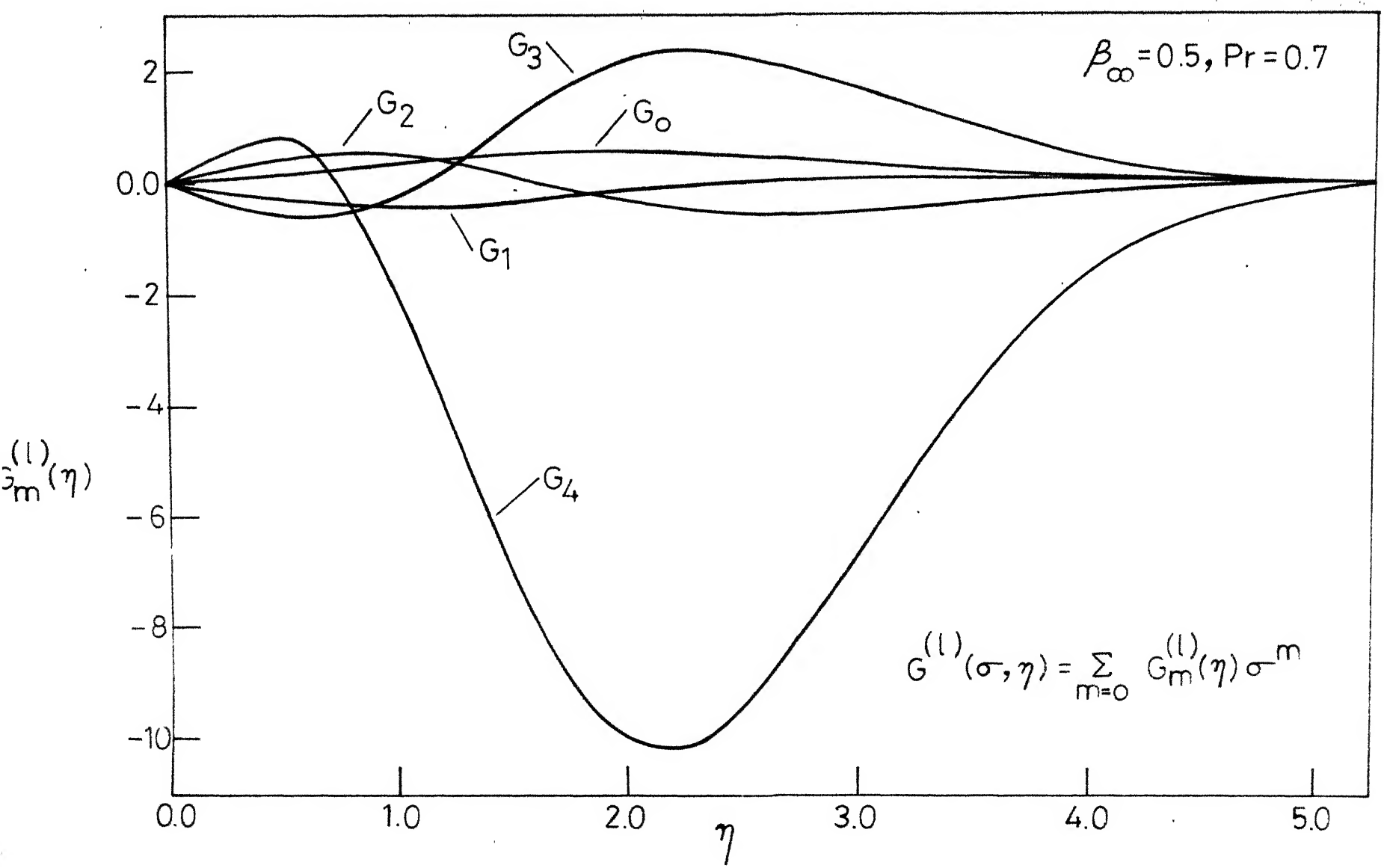

Fig. 4.19b – Second – order temperature profile on a blunted wedge ($\beta_\infty = 0.5$) due to longitudinal curvature.

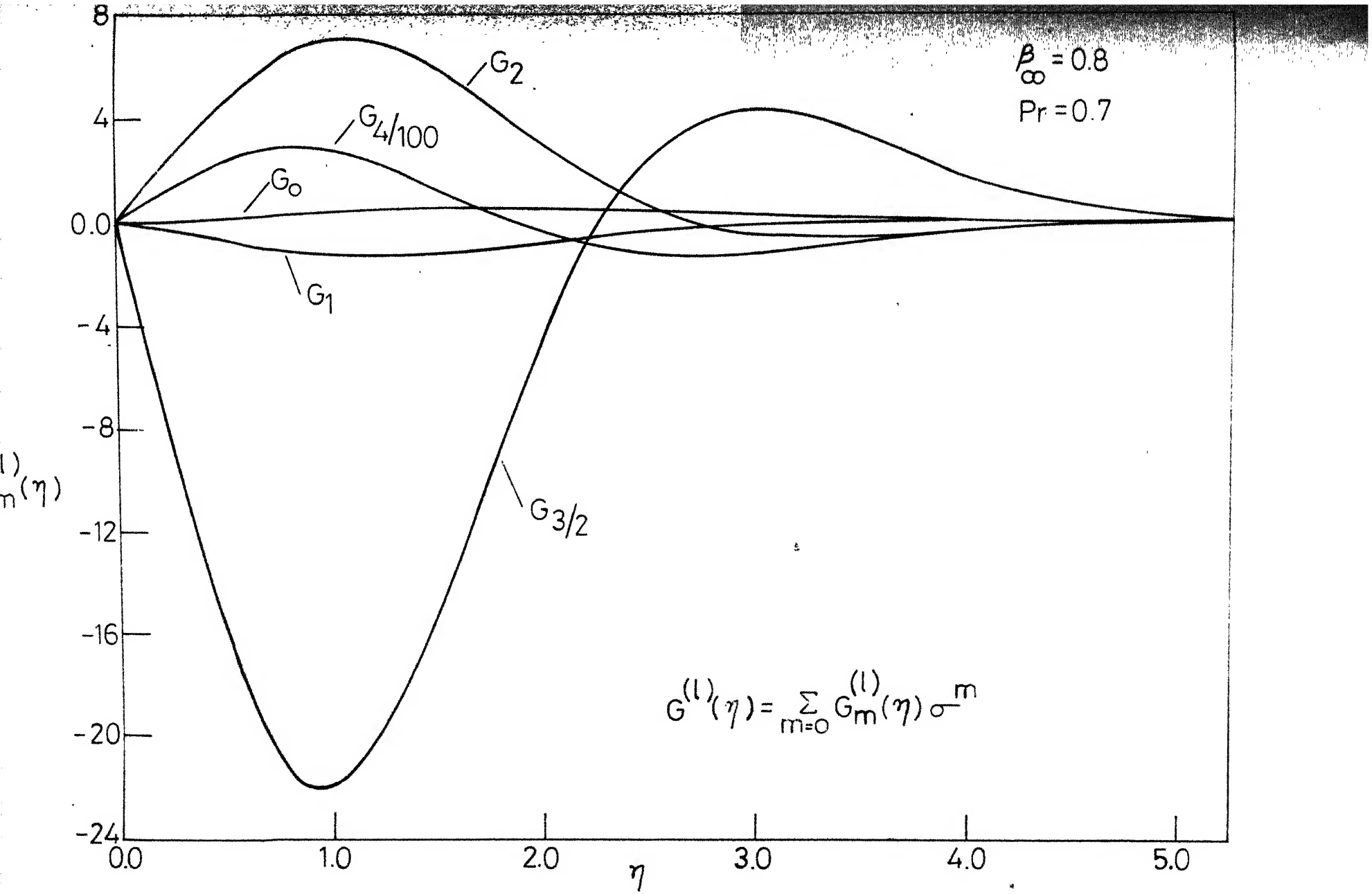

Fig. 4.19 c – Second-order temperature profile on a blunted wedge (β_∞=0.8) due to longitudinal curvature .

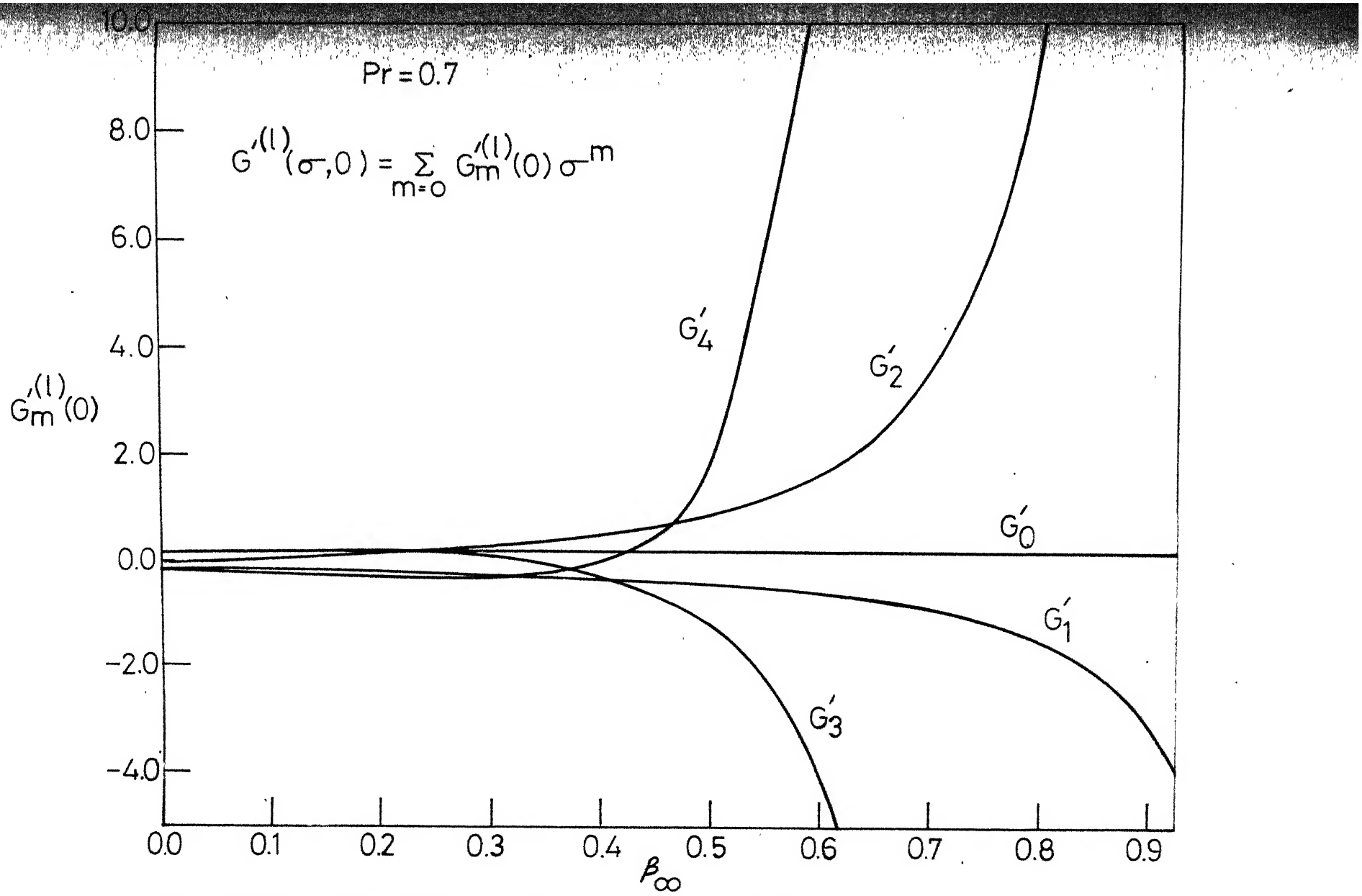

Fig. 4.20 a – Contribution of longitudinal curvature to heat transfer on a blunted wedge.

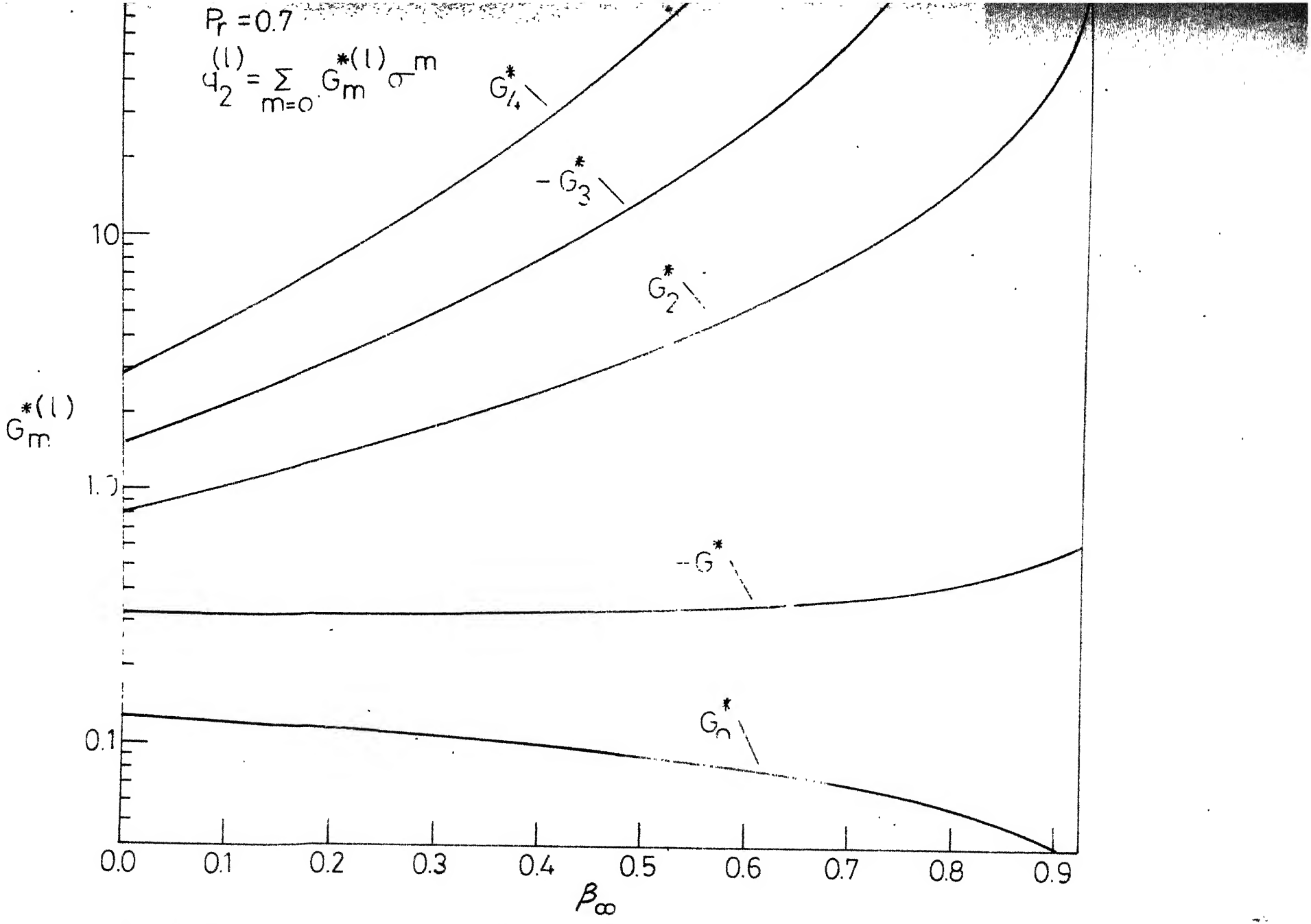

Fig. 4.20b – Contribution of longitudinal curvature to heat transfer

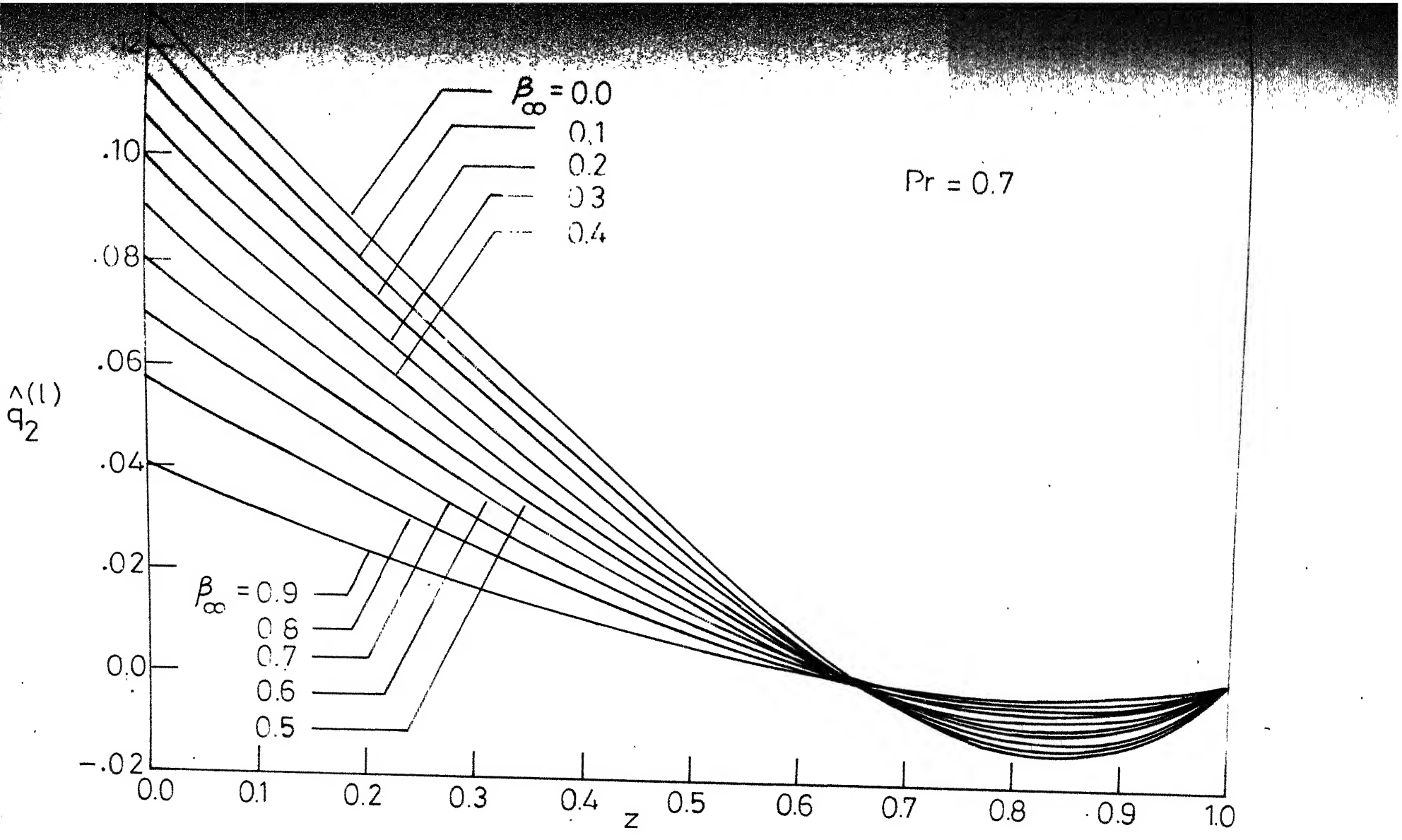

Fig. 4.21_ Longitudinal curvature contribution to heat transfer distribution on a blunted wedge.

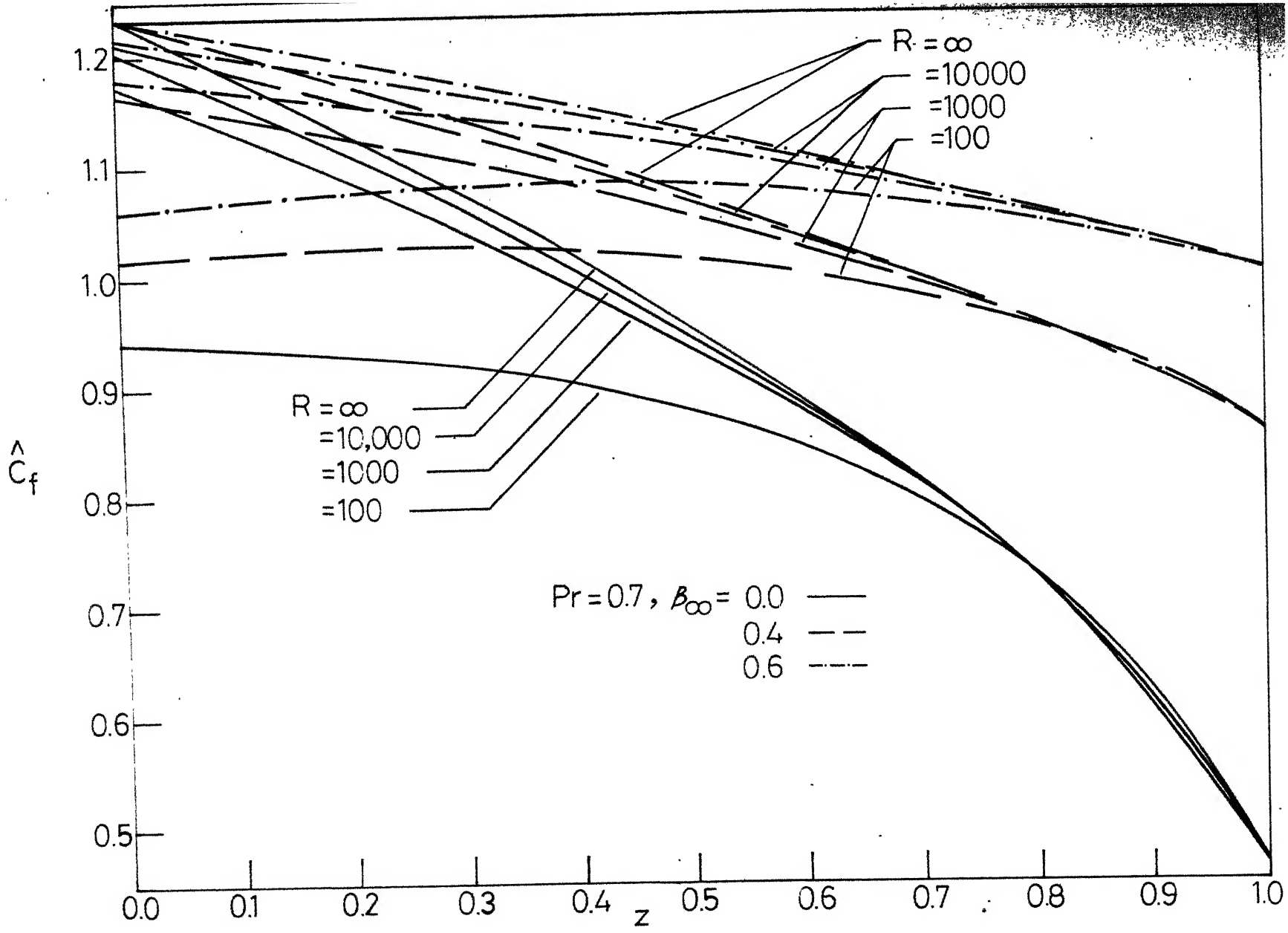

Fig. 4.22a – Skin friction distribution on a blunted wedge .

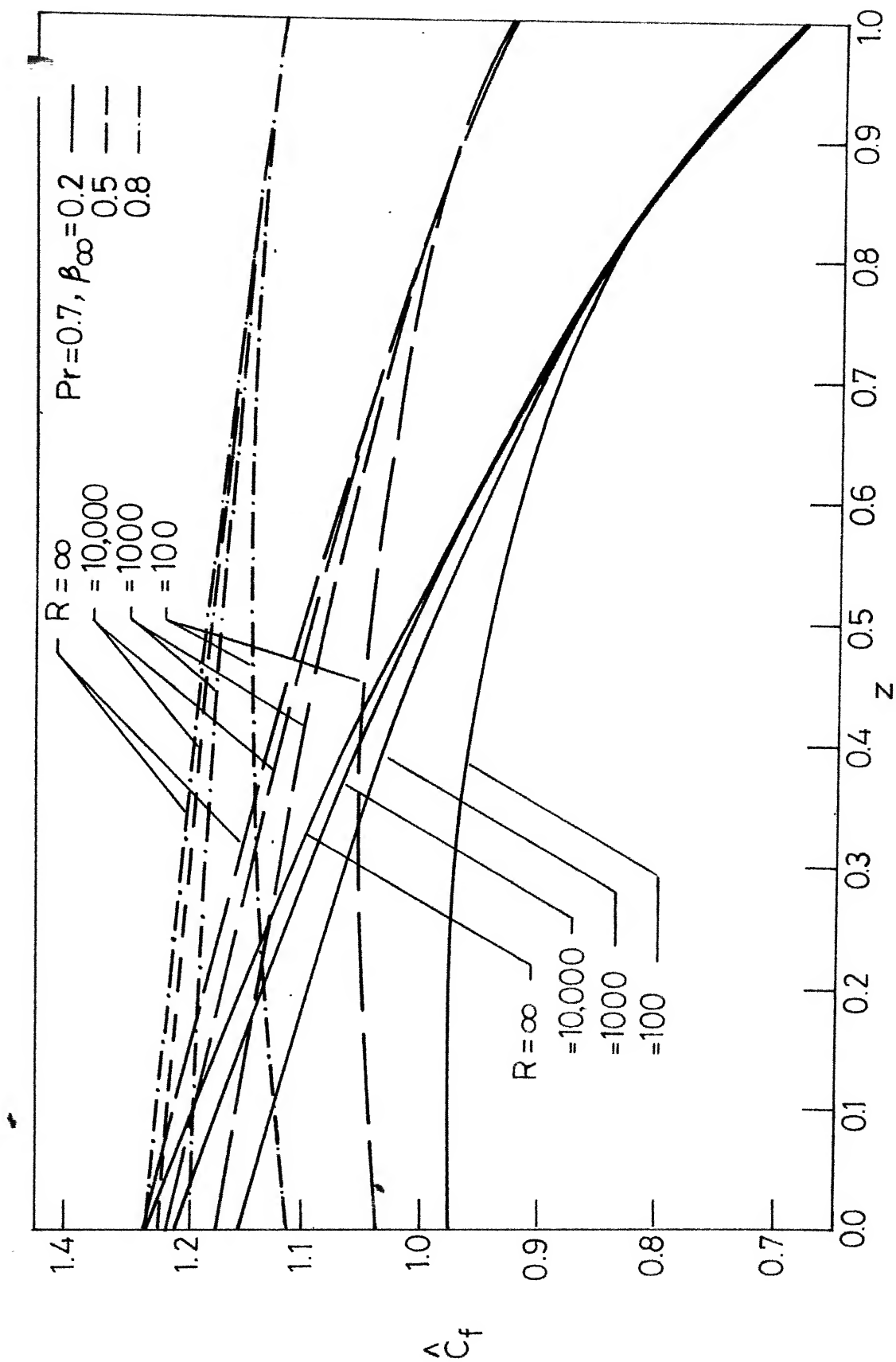

Fig.4.22b-Skin friction distribution on a blunted wedge.

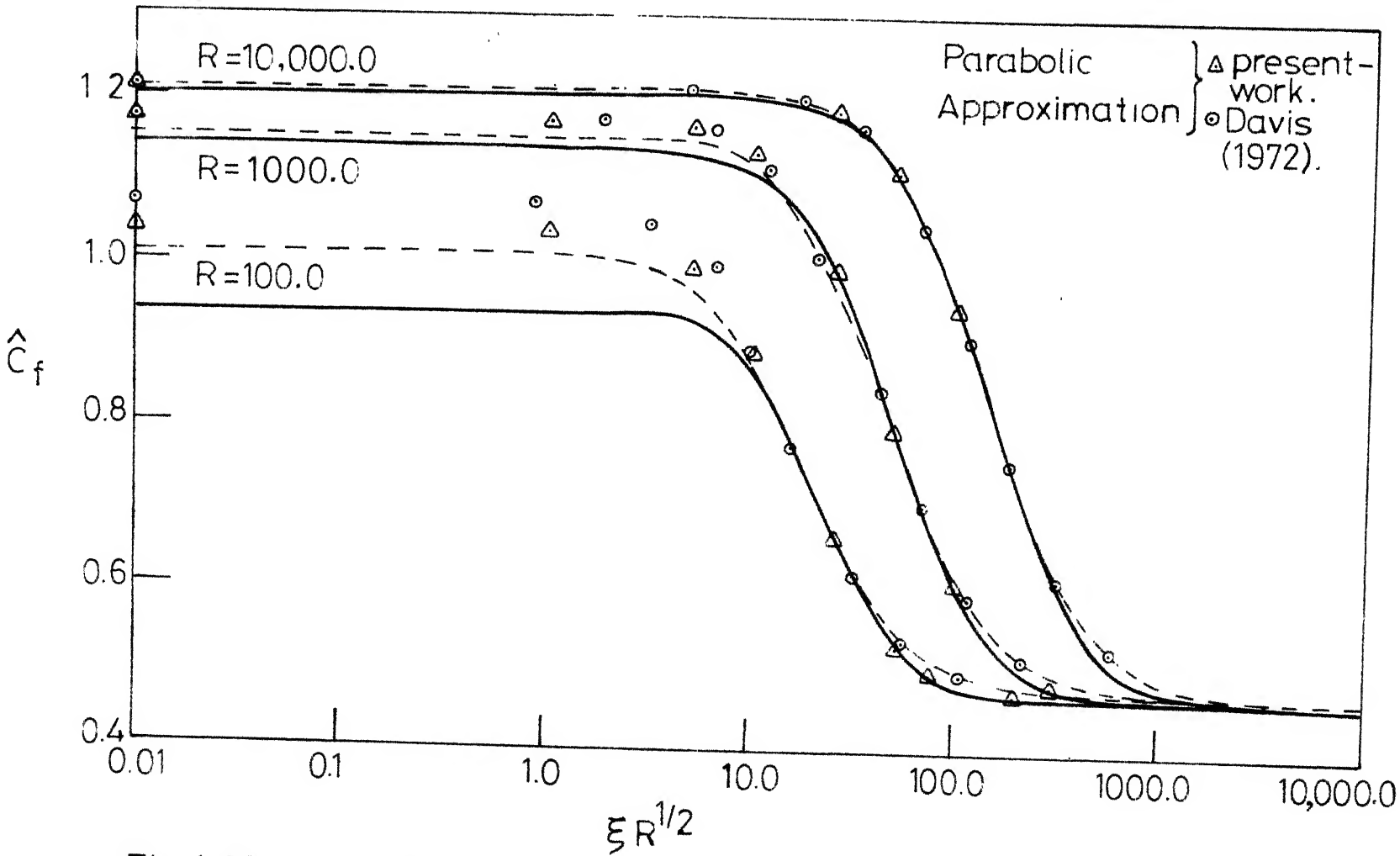

Fig. 4.23 - Comparison of present results of skin friction on a parabola ($\beta_\infty = 0$) with exact solution of the Navier-stokes equations: ——, Present results; - - -, Davis (1972).

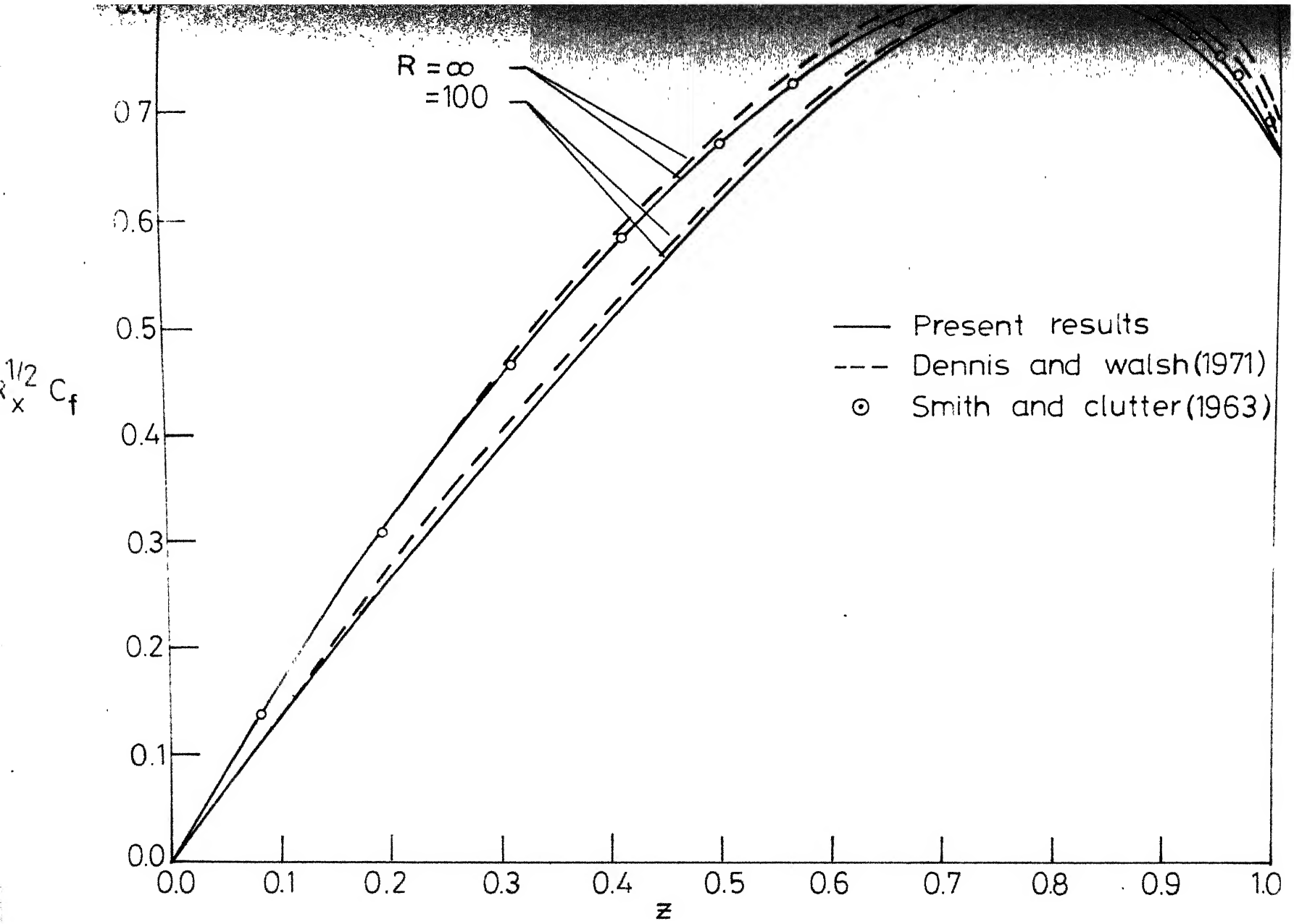

Fig.4.24_Comparison of present results of skin friction on a parabola ($\beta_\infty = 0$) with exact solution of the Navier-Stokes equations.

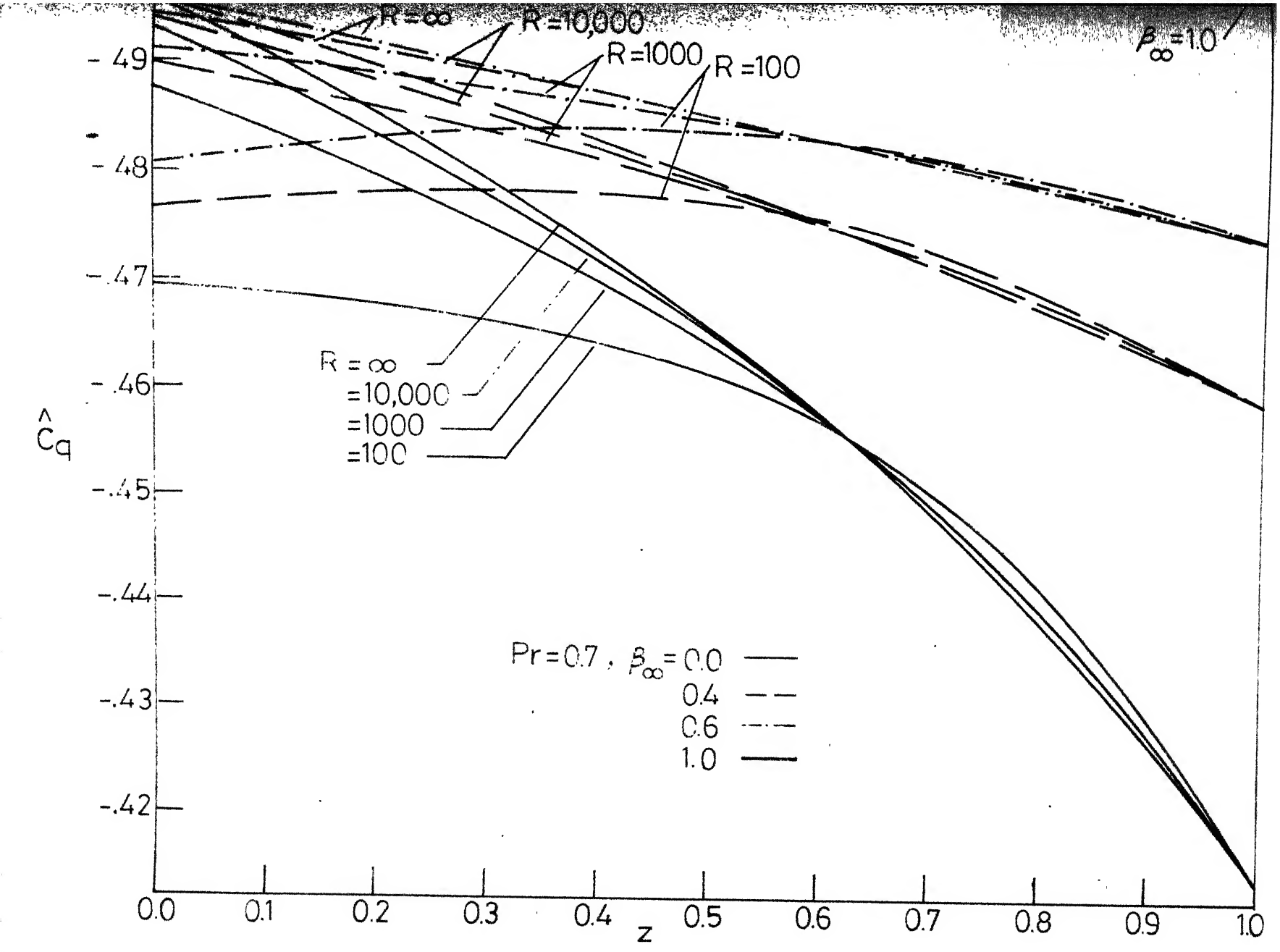

Fig. 4.25a - Heat transfer distribution on a blunted wedge.

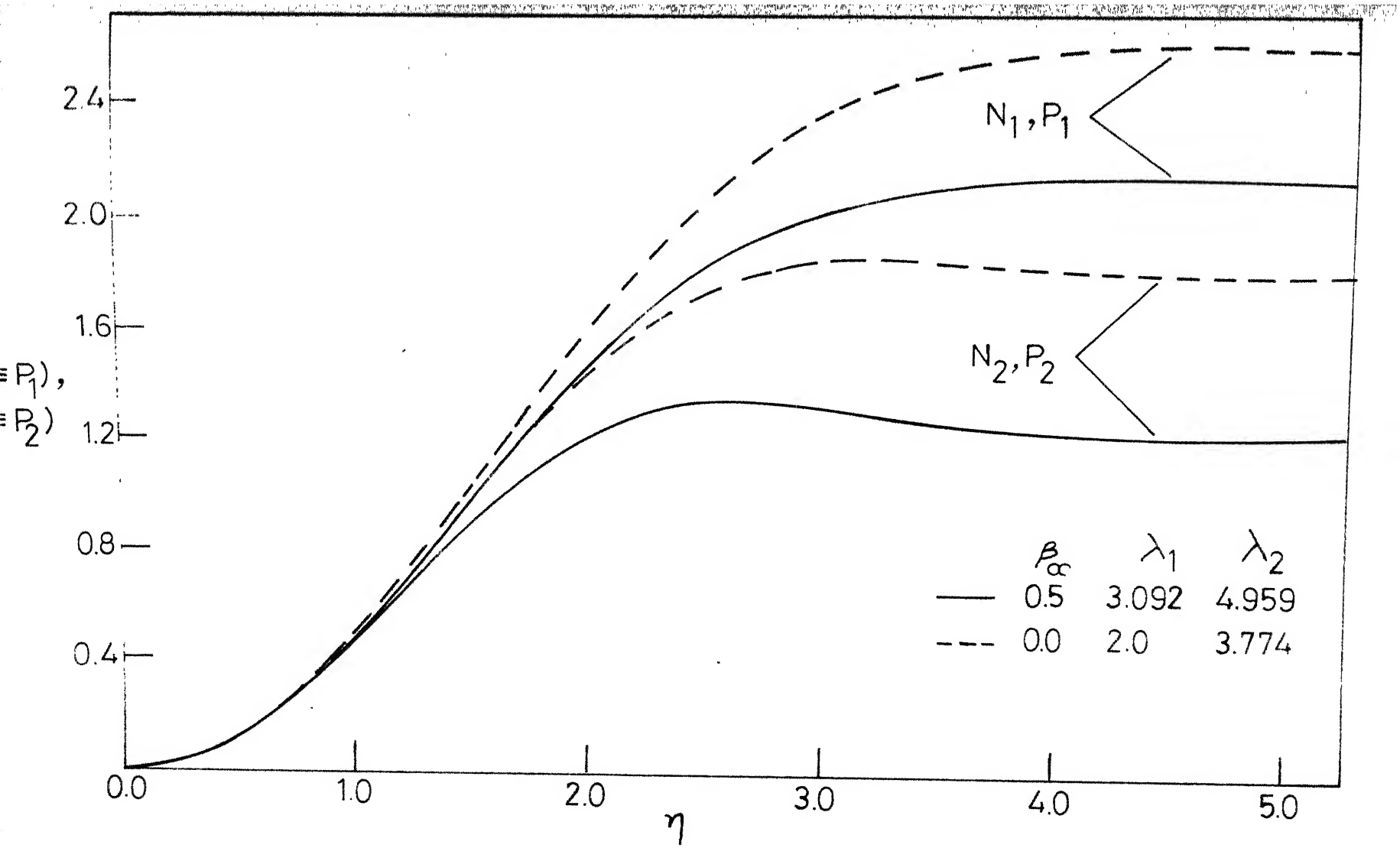

Fig. 5.1 – The first and the second – order eigenfunctions: initial value problem.

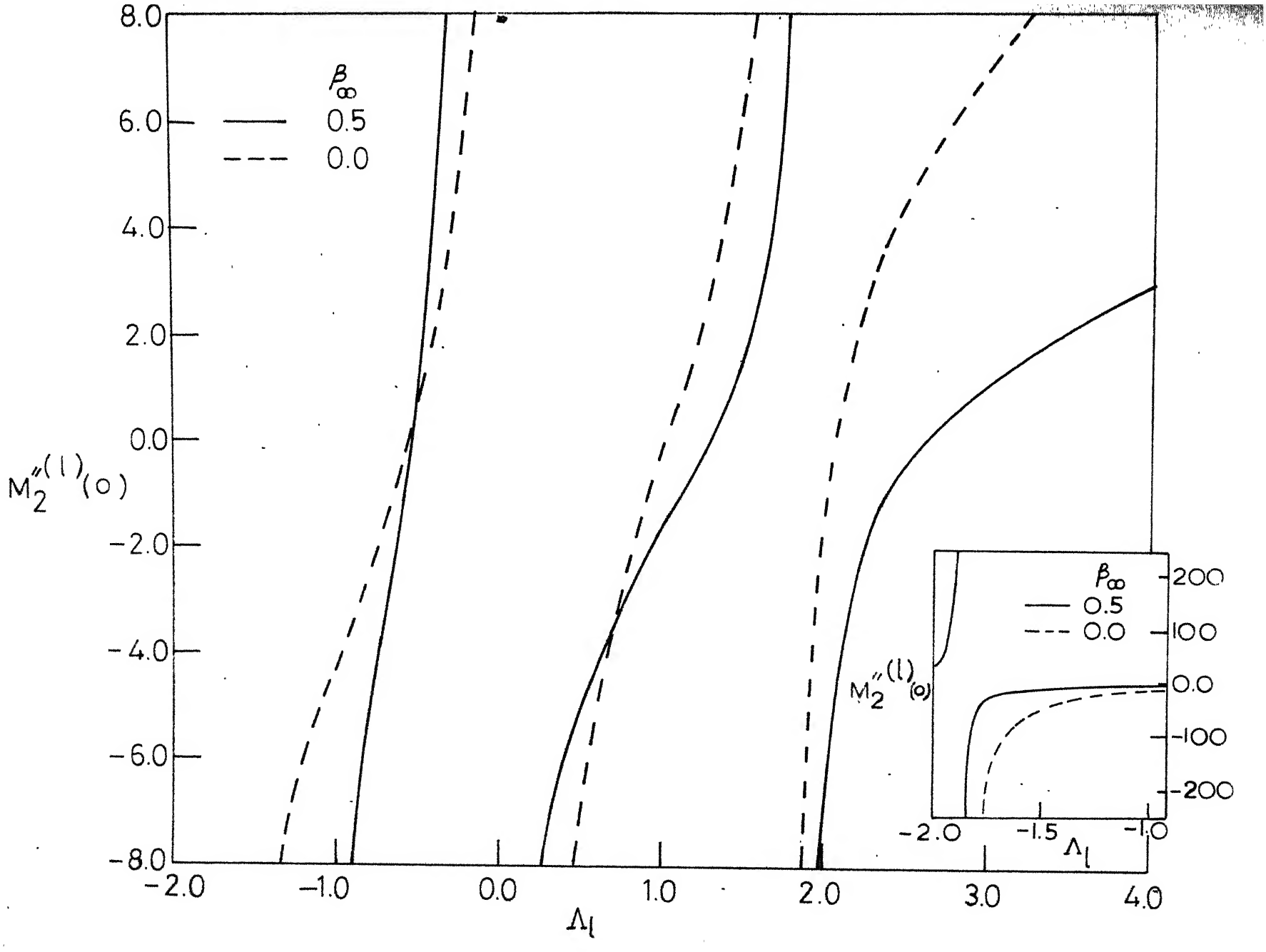
8.0
6.0
4.0
2.0
0.0
-2.0
-4.0
-6.0
-8.0
$M_2''^{(1)}(0)$
β_∞
0.5
0.0
-2.0
-1.0
0.0
1.0
2.0
3.0
4.0
Λ_1
β_∞
0.5
0.0
$M_2''^{(1)}(0)$
200
100
0.0
-100
-200
-2.0
-1.5
-1.0
Λ_1

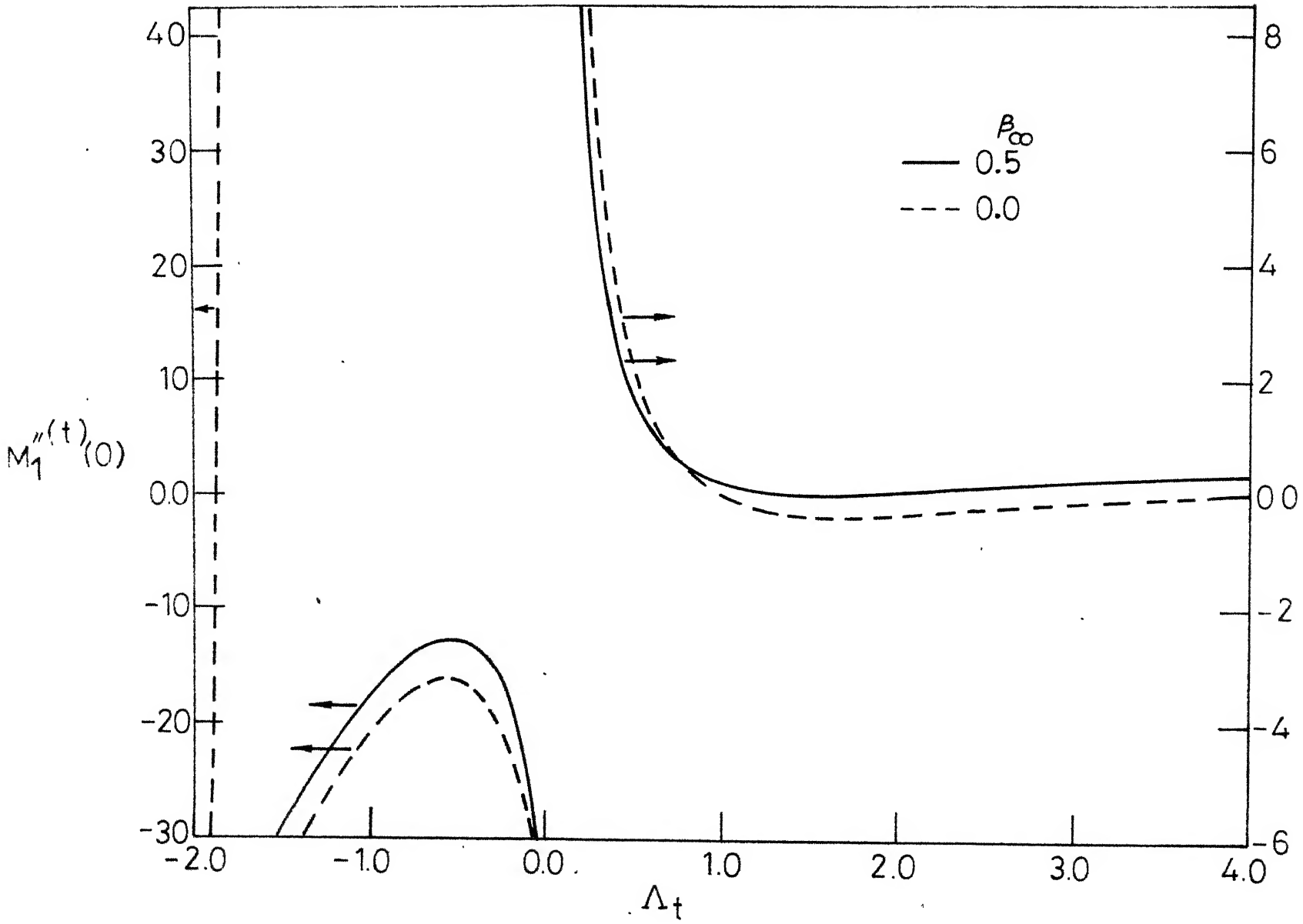

Fig. 5.4 – Solutions of equation (5.24) for n = 1.

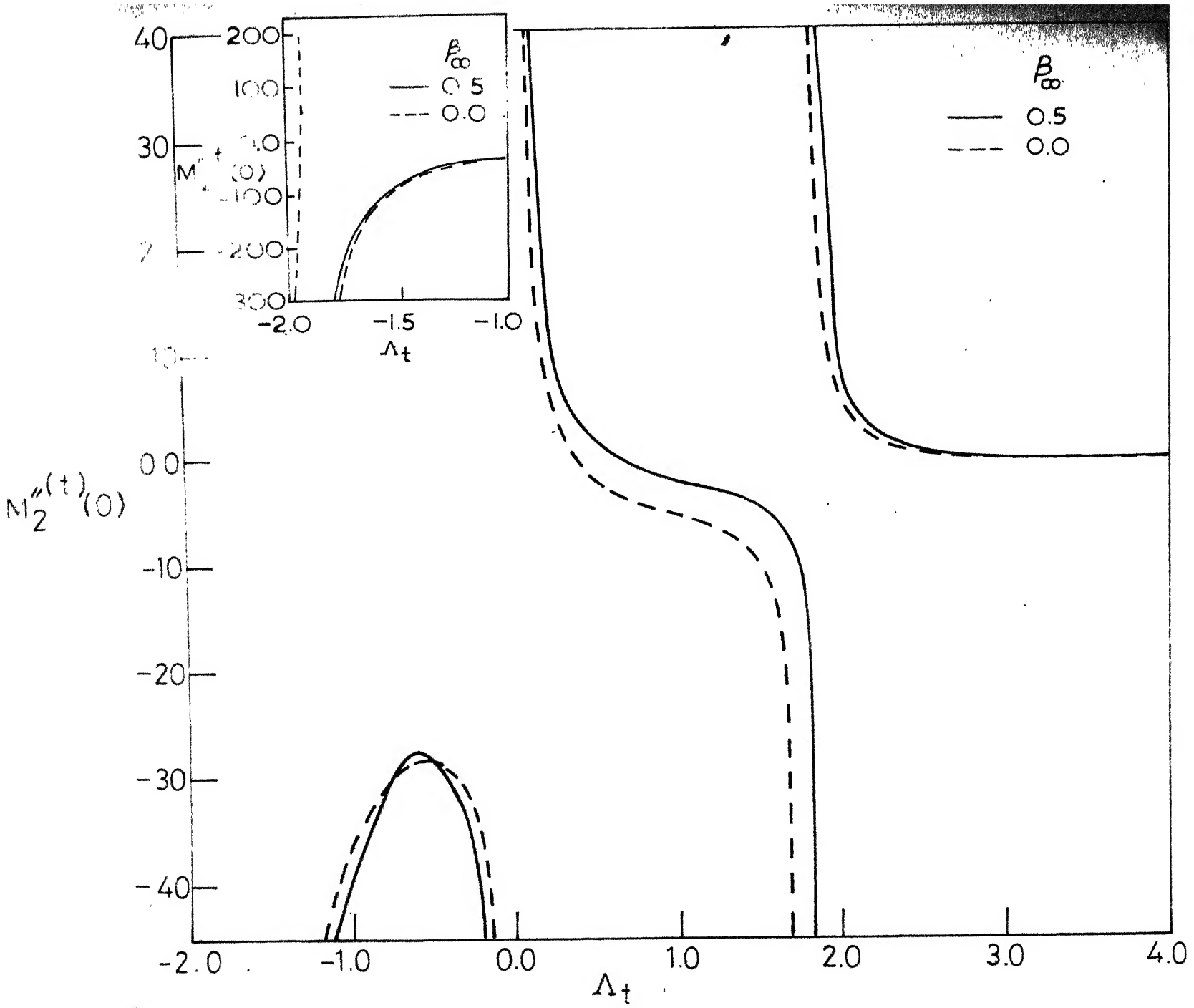
$M_2''^{(t)}(0)$
Λ_t
β_∞
0.5
0.0
40
30
20
10
0.0
-10
-20
-30
-40
-2.0
-1.0
0.0
1.0
2.0
3.0
4.0
200
100
-100
-200
-300
-1.5

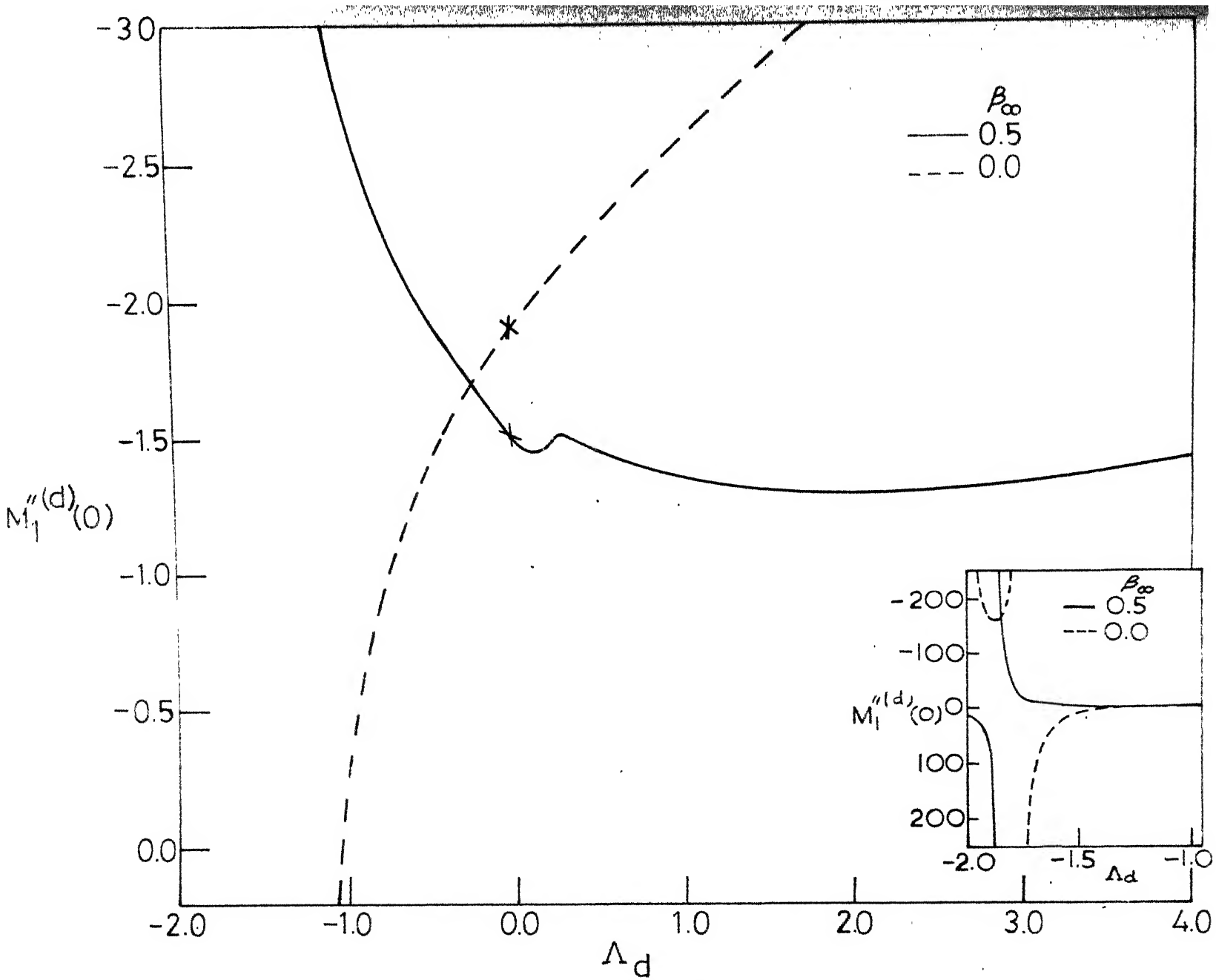

Fig. 5.6 _ Solutions of equation (5.30) for n=1.

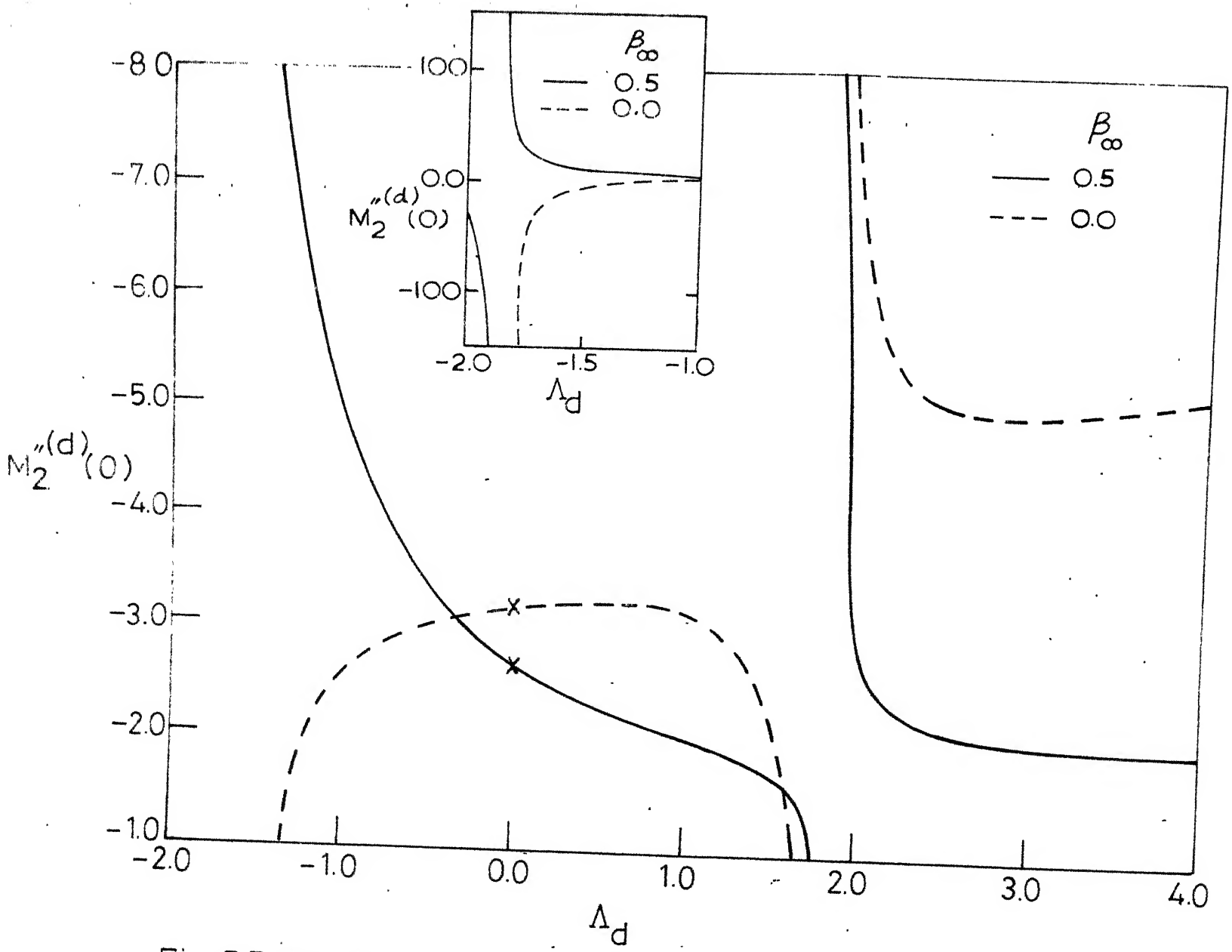

Fig. 5.7_Solutions of equation (5.30) for n=2.